

Right Ventricular Assessment by Real-time Three-dimensional Echocardiography in Congenital Heart Disease

Heleen B. van der Zwaan



ISBN: 978-94-6169-077-7

Text cover: Louisa Young, in *The Heart* 2007.

Layout and printing: Optima Grafische Communicatie, Rotterdam.

Copyright 2011 H.B. van der Zwaan

All rights reserved. No part of this publication may be reproduced, stored, or transmitted by any form or by any means, without written permission of the holder of the copyright. Several chapters of this thesis are based on published papers, which are reproduced with permission of the co-authors and the publishers. Copyright of these papers remains with the publishers.

Right Ventricular Assessment by Real-time Three-dimensional Echocardiography in Congenital Heart Disease

**Rechter ventrikel analyse middels real-time driedimensionale
echocardiografie bij congenitale hartziekten**

Proefschrift

ter verkrijging van de graad van doctor aan de
Erasmus Universiteit Rotterdam
op gezag van de
rector magnificus

Prof.dr. H.G. Schmidt

en volgens besluit van het College voor Promoties.

De openbare verdediging zal plaatsvinden op
woensdag 15 juni 2011 om 11:30 uur

door

Heleen Berdina van der Zwaan
geboren te Alkmaar



PROMOTIECOMMISSIE

Promotor:	Prof.dr. J.W. Roos-Hesselink Prof.dr. W.A. Helbing
Overige leden:	Prof.dr. M.L. Simoons Prof.dr. L. Mertens Prof.dr.ir. A.F.W. van der Steen
Copromotor:	Dr. F.J. Meijboom

Financial support by the Netherlands Heart Foundation for the publication of this thesis is gratefully acknowledged.

Aan de liefste moeder die ik ooit ken

Aan Seb, Gijs en Len

CONTENTS

PART 1. ECHOCARDIOGRAPHY IN CONGENITAL HEART DISEASE

Chapter 1.	General introduction and outline of the thesis	13
Chapter 2.	Right ventricular assessment in congenital heart disease: a systematic review on conventional and new echocardiographic techniques	29
Chapter 3.	Three-dimensional echocardiography in adult congenital heart disease	51

PART 2. RIGHT VENTRICULAR ACQUISITION, ANALYSIS, AND CLINICAL APPLICATIONS

Chapter 4.	Right ventricular quantification in clinical practice: two-dimensional versus three-dimensional echocardiography compared with cardiac magnetic resonance imaging	85
Chapter 5.	Test-retest variability of volumetric right ventricular measurements using real-time three-dimensional echocardiography	103
Chapter 6.	Clinical value of real-time three-dimensional echocardiography for right ventricular quantification in congenital heart disease: validation with cardiac magnetic resonance imaging	119
Chapter 7.	Usefulness of real-time three-dimensional echocardiography to identify right ventricular dysfunction in patients with congenital heart disease	137

PART 3. TROUBLESHOOTING FOR RIGHT VENTRICULAR ASSESSMENT

Chapter 8.	Sources of differences in volumetric right ventricular estimation: real-time three-dimensional echocardiography and cardiac magnetic resonance imaging in patients with tetralogy of Fallot	155
Chapter 9.	Right ventricular visualization and quantification using contrast-enhanced real-time three-dimensional echocardiography	171

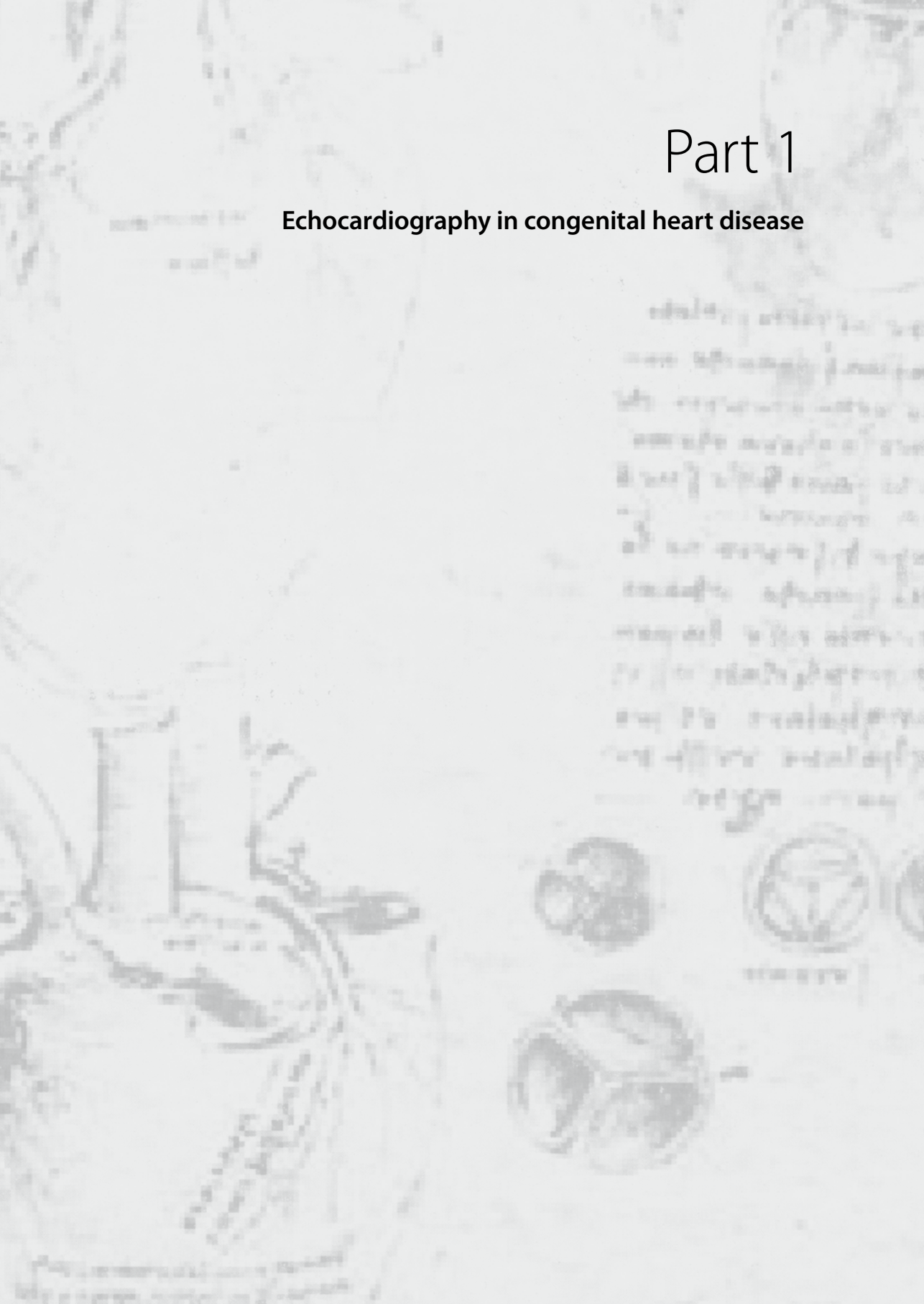
PART 4. GENERAL DISCUSSION AND SUMMARY

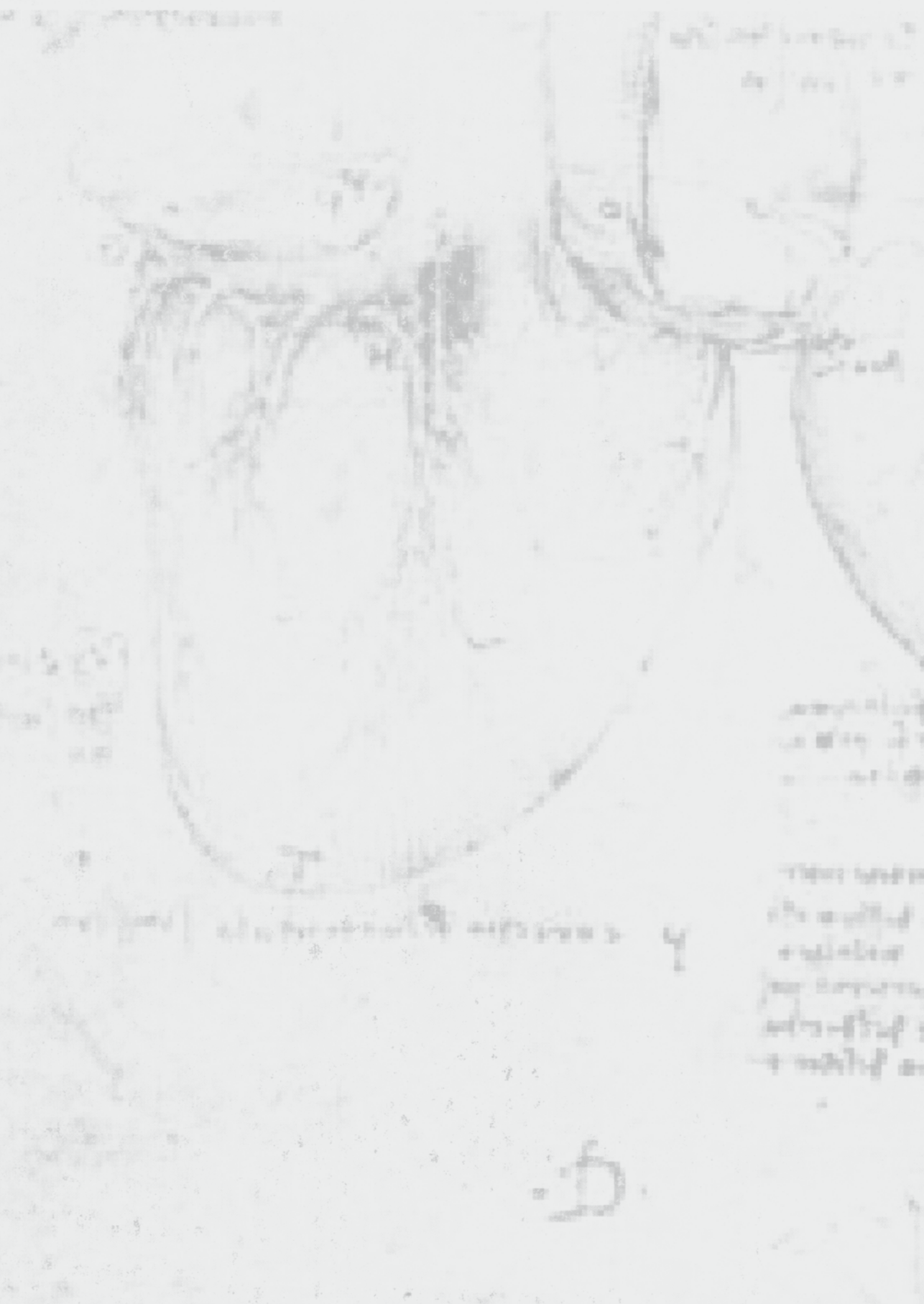
Chapter 10.	General discussion	189
Chapter 11.	Summary - Samenvatting	213
	List of publications	225
	PhD portfolio	231
	About the author	237
	Dankwoord	237



Part 1

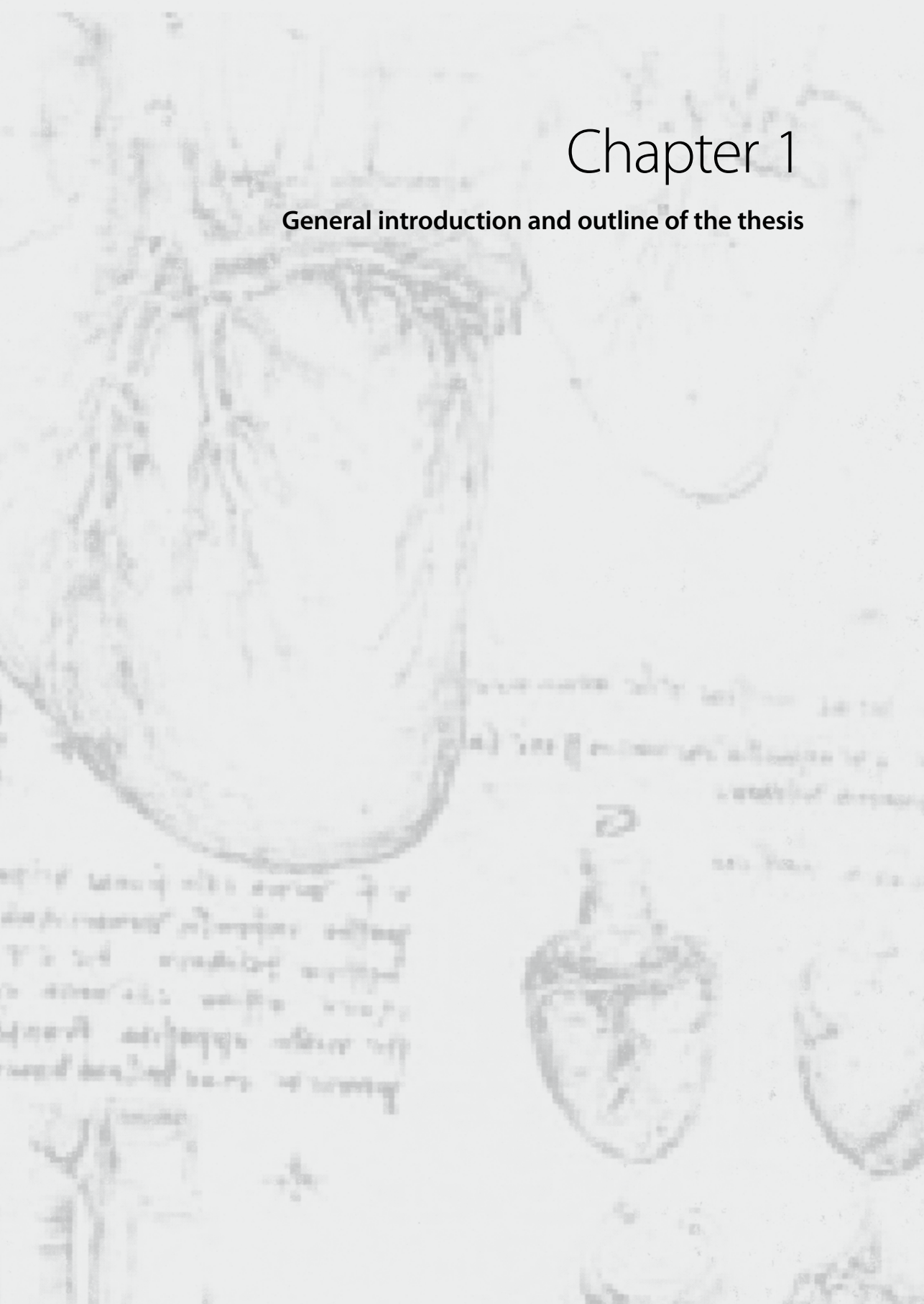
Echocardiography in congenital heart disease





Chapter 1

General introduction and outline of the thesis



1. The remarkable improvement in survival of patients with congenital heart disease has led to a
2. growing number of adult patients. In particular, patients with more complex disease showed
3. favorable outcomes in the last decades.¹⁻³ In addition, some defects (e.g. atrial septal defect,
4. Ebstein's anomaly, and congenitally corrected transposition of the great arteries) may be
5. diagnosed for the first time in adult life. A wide range of birth prevalence estimates has been
6. reported, and therefore complicates the evaluation of the number of patients with congenital
7. heart disease.⁴ In the Netherlands, every year approximately 1400 children are born with a
8. congenital heart defect. At present, it is estimated that there are over 40.000 adults with con-
9. genital heart disease⁵ and this group is annually growing with ~5%. Besides, there are about
10. 25.000 children with a congenital heart defect. The 32nd Bethesda Conference report in 2000⁶
11. estimated that there were ~2800 adults with congenital heart disease per 1 million population
12. in the United States, with more than half of them having moderate or high complexity of their
13. defect.⁷ The reported birth prevalence of congenital heart disease varied from four to fifty per
14. 1000 live births.⁸

15. The prognosis of patients with congenital heart disease has increased over the last decades,
16. because of improved surgical techniques and pediatric care. Now that operative mortality of
17. the early repair has fallen to low levels, attention has turned to improvement of longer-term
18. outcomes and preservation of cardiac function. A substantial proportion of infants and adults
19. with congenital heart disease develop ventricular dysfunction and clinical symptoms of heart
20. failure.⁹ Patients with a single or systemic right ventricle are particularly at risk.^{2, 10} Up to 40%
21. of adult patients who underwent a Fontan procedure and > 20% of those who underwent a
22. Mustard repair for transposition of the great arteries were estimated to develop moderate
23. to severe heart failure at young adult age.^{10, 11} Heart failure in patients with congenital heart
24. disease is often predominantly a problem of the right ventricle and can be caused by pressure
25. or volume overload, ischemia, intrinsic myocardial disease, or pericardial constraint.¹² Because
26. of the unique hemodynamics associated with right ventricular (RV) dysfunction, its impact and
27. overt failure may only become apparent clinically after decades of follow-up.¹³ The timing of
28. re-interventions or the initiation of medical therapy is difficult and is preferably done before RV
29. failure is manifest. Therefore, regular assessment of RV function in these patients is essential for
30. clinical management. Accurate and accessible tools are needed to monitor RV function which
31. may lead to a better timing of surgical re-interventions and medical therapy with ultimately a
32. better survival and quality of life.

33. Since the future is based on the past, in this chapter we will provide an overview on the
34. knowledge gained over the years on RV anatomy and function. Various imaging modalities
35. that are, and were, used for RV assessment will be discussed. Finally, the outline of this thesis
36. will be presented.

37.
38.
39.

THE RIGHT VENTRICLE THROUGH THE YEARS

Leonardo da Vinci (1452-1519) was the first to correctly describe the heart as a four-chambered structure.¹⁴ He illustrated the moderator band, and rightly ascribed it as a muscular bridge between the walls of the right ventricle (Figure 1). Characteristic of the ideas of Da Vinci was the inseparable combination of structure and function: he believed that every structure in nature is as it is for a reason. While Da Vinci's description of cardiac function remained rooted in the Galenic tradition, his drawings of the right ventricle and the tricuspid valve were accurate.¹⁵ Da Vinci's drawings were hidden for centuries and therefore, did not cause a revolutionary anatomical breakthrough in his time.



Figure 1 Dissection of the heart by Leonardo da Vinci displaying the right atrium and the right ventricle with the moderator band.

Until the 1950s, the interest in RV hemodynamics was centered mainly in the laboratories of small groups of investigators, who were intrigued by the hypothesis that the human circulation could work without a functional right ventricle. For cardiac surgeons in the 1950s, RV function became important, because they evaluated procedures to palliate congenital heart defects associated with right heart hypoplasia. Partial RV venous bypass was successfully implemented by anastomosis of the superior caval vein to the right pulmonary artery.¹⁶ Dr. William Glenn at Yale, for whom the shunt was later named, reported the first clinical application in 1958.¹⁷ After diversion of approximately one third of the venous blood directly to the right pulmonary circulation, superior vena caval pressure rose on average to 10 mmHg, which was well tolerated. Severely cyanotic infants benefited from more fully oxygenated blood. This first successful technique for partial venous bypass of the right side of the heart is still employed today for the palliation of cyanotic congenital heart disease.¹⁸

In the early 1970s, surgeons began to perform more sophisticated procedures to repair right-sided congenital heart defects. In 1971, Fontan and Bandet reported the surgical correction

1. of tricuspid atresia by full RV venous bypass.¹⁹ They first constructed a Glenn shunt and then
 2. inserted an allograft conduit to shunt flow from the right atrium to the left pulmonary circula-
 3. tion. After RV bypass, systemic venous pressures stabilized between 10 and 15 mmHg. Since
 4. then, continuous updates²⁰ and changes in the surgical techniques have been carried out with
 5. good long-term outcome.

6. A rise in publications followed, addressing problems of RV hemodynamics. Meanwhile, pul-
 7. monologists and cardiologists acquired new tools to explore old problems of RV dysfunction
 8. in pulmonary disease²¹ and to address new problems of right-sided cardiac dysfunction during
 9. treatment of adult respiratory distress syndrome with positive airway mechanical ventilation.²²
 10. ²³ Even up to this very day, new techniques are developed to investigate RV dysfunction,
 11. especially in patients with pulmonary hypertension, congenital heart defects, coronary artery
 12. disease, and left-sided heart failure, or valvular heart disease.¹²

13.

14.

15.

16.

17.

18.

19.

20.

21.

22.

23.

24.

25.

26.

27.

28.

29.

30.

31.

32.

33.

34.

35.

36.

37.

38.

39.

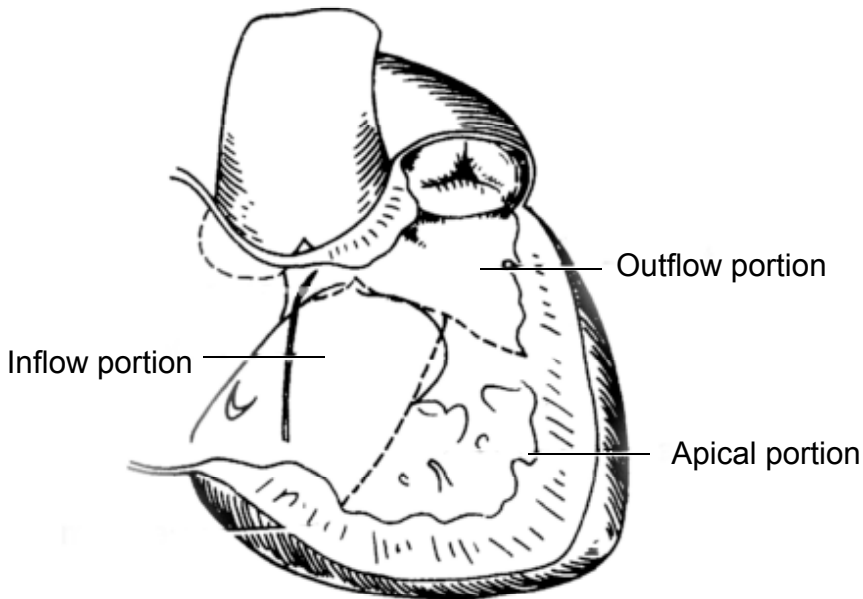


Figure 2 The right ventricle consists of three regions, being the inflow, apical, and outflow portions.

RIGHT VENTRICULAR ANATOMY

The right ventricle has a complex geometric shape that is composed of three basic regions referred to as the inlet-, apical- and outflow portion (Figure 2). The inlet portion consists of the tricuspid valve, chordae tendineae, and papillary muscles. The apical myocardium is coarsely

trabeculated. The outflow portion, or the infundibulum, is composed of smooth walled myocardium and contains the pulmonary valve. Whereas the left ventricular inlet and outlet portions are directly in continuity with each other, in the right ventricle these two tracts are actually separated by a muscular band which is referred to as the crista supraventricularis. This crista is made up of the infundibular septum and the parietal band. Two other muscular bands are present in the right ventricle: the septal band, and the moderator band. The septal band extends apically to become continuous with the moderator band.²⁴ The moderator band is an important landmark of the right ventricle that is well visible by echocardiography.

When ventricular function and loading conditions are normal, the right ventricle is triangular when viewed from the side and crescent-shaped when viewed in cross section (Figure 3). The left ventricle is ellipsoidal in shape and the interventricular septum bows into the right ventricle throughout the cardiac cycle. Multiple muscle layers encircle both ventricles in a complex interlacing fashion. The RV wall is composed primarily of superficial and deep muscle layers. The superficial layer is arranged circumferentially and is continuous with the superficial myofibers of the left ventricle. The deep layer of muscle fibers runs longitudinally from base to apex and is continuous of those of the interventricular septum.²⁵

The blood supply of the right ventricle is derived predominantly from the right coronary artery. In less than 10% of hearts, posterolateral branches from the left circumflex coronary artery supply a segment of the posterior right ventricle. The posterior part of the right ventricle receives blood from the posterior descending coronary artery, usually a branch of the right coronary artery. The moderator band artery, a branch of the first septal perforator of the left anterior descending artery, and the conus artery, a branch of the right coronary artery or arising as a separate ostium from the right sinus of Valsalva (40%), supply the anterior wall of the right ventricle. Acute marginal branches of the right coronary artery supply the lateral wall of the RV.²⁴

The atrioventricular node is located on the right atrial wall within the triangle of Koch, defined by the coronary sinus posteriorly, the tricuspid valve annulus inferiorly, and the tendon of Todero superiorly. The tendon of Todero is the continuation of the Eustachian valve (valve of the inferior vena cava) that runs to the central fibrous body near the membranous septum.²⁴

RIGHT VENTRICULAR FUNCTION

The right ventricle is essential for the maintenance of normal cardiovascular function. However, the importance and precise role of the right ventricle in normal cardiovascular physiology has been debated. Because the right ventricle is positioned between the systemic venous circulation and the pulmonary circulation, the most obvious function is the delivery of oxygen deficient venous blood to the gas exchange membranes of the pulmonary circulation. The right ventricle carries out this function under widely varying states of cardiovascular stress.¹⁸ Another function of the right ventricle is to maintain low systemic venous pressures.²⁶

- 1.
- 2.
- 3.
- 4.
- 5.
- 6.
- 7.
- 8.
- 9.
- 10.
- 11.
- 12.
- 13.
- 14.
- 15.
- 16.
- 17.
- 18.
- 19.
- 20.
- 21.
- 22.
- 23.
- 24.
- 25.
- 26.
- 27.
- 28.
- 29.
- 30.
- 31.
- 32.
- 33.
- 34.
- 35.
- 36.
- 37.
- 38.
- 39.

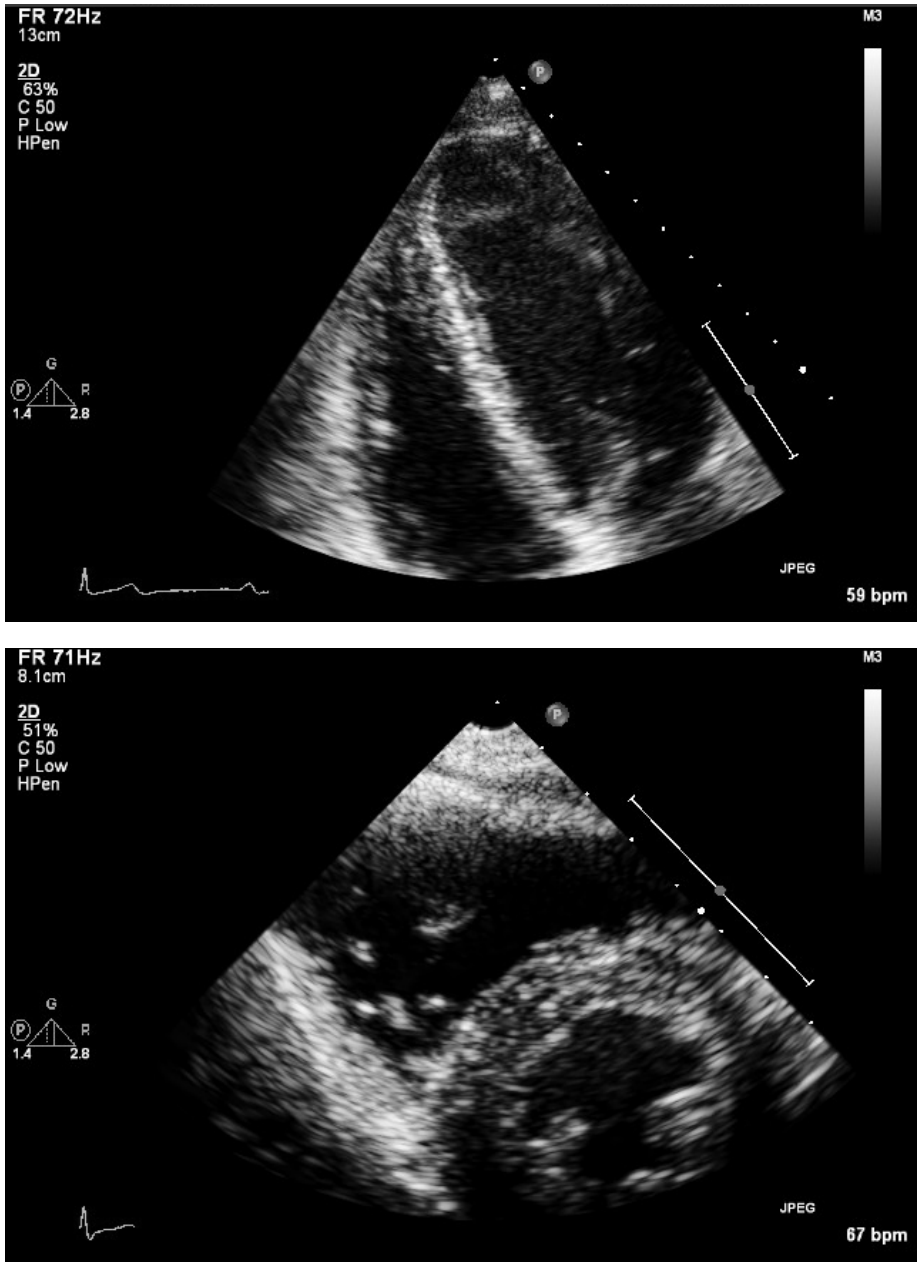


Figure 3 An apical four-chamber view and a short-axis view derived from two-dimensional echocardiography. The upper panel shows the triangular shape of the right ventricle when viewed from the side. The lower panel shows the crescent shape when viewed in cross section.

The right ventricle contracts in a peristaltic like manner, beginning with contraction of the inlet portion, followed by the apex, and ending with contraction of the infundibulum. With contraction of the circumferential fibers, the RV wall moves inward and causes the short-axis to shorten. The contraction of the longitudinal fibers causes the long-axis to shorten. In between the RV free wall and the interventricular septum serves a contractile strut that, with left ventricular contraction, further reduces the septal-to-free-wall distance.²⁷

RV function is dependent on several intrinsic and extrinsic factors. The most important intrinsic factor is the contractile state of the RV myocardium. The extrinsic determinants of RV performance include heart rate, preload, afterload, ventricular interaction, and neurohormonal influences. Because the right ventricle is connected in series with the left ventricle, it pumps on average the same stroke volume in steady state conditions. The right ventricle generates only ~25% of the stroke work, because the impedance in the pulmonary circulation is approximately one tenth that of the systemic circulation, and a 5 mmHg perfusion gradient is sufficient to drive blood across the pulmonary circuit.¹⁸ As a result, the muscle mass of the right ventricle is one sixth that of the left ventricle and it makes the right ventricle also more compliant. On the other hand, the right ventricle has much less contractile reserve than the left ventricle and is, therefore, much more sensitive to increases in afterload. The functional unit of contraction, the sarcomere, is the same for both ventricles; the difference in ventricular performance results from differences in muscle mass as well as the chamber geometry and the orientation of muscle fibers.²⁸ The RV free wall fibers are oriented transversely and simply squeeze blood by circumferential compression. In contrast, the left ventricular free wall and septum have predominantly obliquely oriented fibers, which twist and shorten to eject blood and, in doing so, generate an ejection fraction (EF) greater than for the right ventricle.^{28, 29}

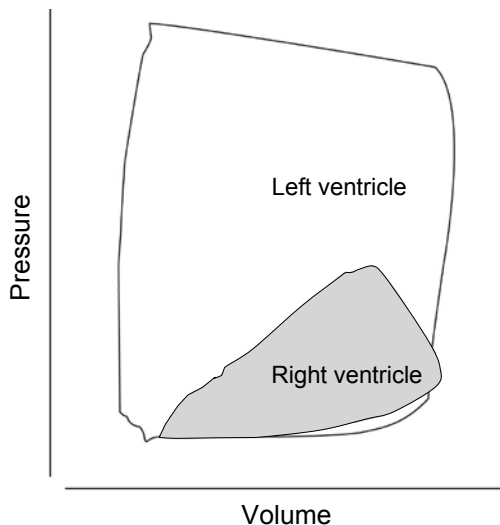


Figure 4 Figure showing the normal human left and right ventricular pressure–volume relationships.

1. The dissimilarity in ventricular afterload is responsible for the difference in ventricular
2. pressure-volume loops between the two ventricles (Figure 4). The left ventricle has a square-
3. shaped pressure-volume loop, whereas the RV pressure-volume loop is triangular in shape.
4. The triangular shape depicts the shorter pre-ejection period that is caused by the RV systolic
5. pressure that rapidly exceeds pulmonary artery diastolic pressure. If RV afterload increases, the
6. RV pressure-volume loop becomes more square-shaped. In addition, RV volumes and pressures
7. increase, altering the orientation of the interventricular septum and changing the geometry of
8. the ventricles. In cross section, the RV now appears spherical in shape whereas the left ventricle
9. becomes crescent-shaped in appearance when RV pressure exceeds the left ventricular pres-
10. sure.²⁵

11.

12. Right ventricular-left ventricular interaction

13. As mentioned before, besides contractility, heart rate, and loading conditions, the interdepen-
14. dence of both ventricles is a determinant of ventricular performance. Ventricular interaction
15. was first noted at the beginning of the 20th century when observations in isolated hearts
16. suggested that alteration in left ventricular geometry (i.e. ventricular hypertrophy and dilata-
17. tion) could decrease RV function which was referred to as the “Bernheim effect”.¹⁸ Ventricular
18. interdependence is a result of the close anatomic association between the two ventricles: they
19. are encircled by common epicardial muscle fibers, share a common interventricular septum,
20. and are enclosed within a pericardial sac. Interdependence can be distinguished into three
21. different components which include direct (or parallel-) interaction via the interventricular
22. septum, indirect (or series-) interaction via the pulmonary artery and systemic circulation, and
23. finally the effect of the pericardium.¹⁸ Ventricular interaction is present on a beat-to-beat basis
24. and influences both the diastolic and systolic part of the cardiac cycle. In addition, ventricular
25. interaction occurs in both directions, although it has been reported that this interaction during
26. diastole appears to be of lesser magnitude in left-to-right direction compared with right-to-left
27. direction.²⁷ So, the size, shape and function of one ventricle can directly influence the normal
28. function of the other and is mainly affected by loading conditions.

29.

30.

31. **IMAGING THE RIGHT VENTRICLE**

32.

33. The ideal measure of RV function would be a load independent measure of contractility,
34. assessing both global and regional function independent of the cardiac shape or mass, easy
35. and safe to apply and proven to be useful in clinical practice.³⁰ In addition, the ideal measure
36. of RV function should be accurate to assess the complex RV geometry and contraction pattern,
37. be reproducible, and not expensive. Adequate RV function assessment is more difficult than
38. that of the left ventricle. While the ellipsoid shape of the left ventricle lends itself to geometric
39. assumptions and mathematical interpretation, the shape, geometry, and anatomical location

of the right ventricle all make precise assessment difficult. Various imaging modalities are or have been used for RV assessment, with echocardiography and cardiac magnetic resonance (CMR) imaging being the most frequently applied techniques in clinical practice.

Cardiac catheterization

Cardiac catheterization using single- or bi-plane geometric algorithms, is no longer applied in everyday practice for the calculation of RV volumes. This technique is not only invasive, but also time consuming, and conceptually imperfect and inaccurate.¹³ Thus, diagnostic right heart catheterization in clinical practice used for the assessment of hemodynamics (e.g., RV end-diastolic pressure or complex gradients), the initial evaluation of pulmonary hypertension, or increasingly frequent, as an introduction to trans-catheter therapy of structural abnormalities (e.g., atrial septal defect closure, relieve of a pulmonary artery stenosis). For dynamic RV volume assessment, conductance catheter assessment can be considered state of the art although it remains an experimental tool. The strength of the technique is its ability to measure beat-to-beat changes in pressure-volume relationships during interventions. It is only with such measurements that intrinsic myocardial dysfunction can be separated from the sometimes complex load-dependent changes that are seen in adults after repair of congenital heart lesions.

Radionuclide studies

Equilibrium and first pass radio-nuclide assessments of RV volumes and EF have been used for many years. Radionuclide techniques have the advantage of relying on a count-based method that is independent of RV geometry. Three methods are available: first-pass radionuclide angiography, gated equilibrium radionuclide angiography, and gated first-pass techniques. Each technique had certain advantages as well as limitations. First-pass radionuclide angiography allows a good separation of the right ventricle from the other cardiac structures, at the cost of less activity and thus the need of newer-generation cameras or multicrystal cameras. Gated equilibrium radionuclide angiography does not allow a clear distinction of the pulmonary valve plane or of the right ventricle from the other cardiac structures, particularly the right atrium. The gating of gated first-pass radionuclide angiography allows the summation of data from several cycles and can be done with standard cameras.³¹ The choice of any method largely depended on the clinical setting and the availability of specific instrumentation.³² The validity of such techniques has been established in the normal biventricular heart.¹³ With the introduction of accurate measurements based on echocardiography and CMR imaging, radio-nuclide studies are now less often used.

Echocardiography

The right ventricle is less approachable for echocardiography than the left ventricle, because of its crescent shape, retrosternal position, and thin, coarsely trabeculated wall.³³ Nevertheless, echocardiography is the most used technique in clinical practice for RV size and function

1. assessment. Both qualitative and quantitative indices of RV size and function can be obtained.
2. Various imaging planes should be used to measure dimensions, areas, and the tricuspid annular plane systolic excursion.³⁴ There is no single M-mode-derived or two-dimensional echocardiography-derived measurement of RV dimension that adequately describes overall RV size.
3. Individual measurements of the RV inflow and outflow dimensions and RV areas can be derived
4. from apical four-chamber views and parasternal short-axis views, respectively.³⁴ The accuracy
5. of these M-mode and two-dimensional echocardiography-derived measurements has been
6. investigated compared with CMR imaging,³⁵⁻³⁷ and resulted in moderate to poor agreement. It
7. has been suggested that two-dimensional echocardiography-derived measurements were less
8. accurate in patients with congenital heart disease and enlarged right ventricles than in healthy
9. controls.³⁸ Up to now, no accurate, simple geometric models based on two-dimensional echocardiography have been found to calculate RV volumes and EF, because they were impossible to fit onto the complex shaped right ventricle.³⁹ These measurements may be used for serial follow-up, although their accuracy as compared with RV volumes or EF is limited.³⁸

10.

11. Cardiac magnetic resonance imaging

12. CMR techniques are established as an important diagnostic modality in adults with congenital
13. heart disease. CMR imaging is considered the clinical standard for the assessment of RV volumes,
14. and volume-based indices of function. The calculation of RV volumes and EF is based on the
15. disc summation method (Figure 5). A stack of short-axis images are acquired from the tricuspid
16. valve down to the apex. Manual tracing of contours in each end-diastolic and end-systolic slice,
17. results in end-diastolic and end-systolic volumes from which EF can be calculated. Besides RV
18. volumes and EF, flow and shunt measurements can be obtained. All these measurements are
19. unaffected by the geometric and spatial constraints of the other imaging techniques, and are
20. reproducible^{40, 41} making them applicable for sequential assessment of longitudinal change.
21. While much of the enthusiasm for CMR imaging is justified, because this technique is the most
22. accurate of the different techniques currently available to quantify RV volumes and mass,⁴²
23. there are some caveats. CMR imaging has is limited accessible, expensive, and time-consuming
24. for RV analysis and acquisition. Furthermore, claustrophobia, poor patient compliance and
25. pacemakers or cardioverterdefibrillators restrict the use of CMR imaging. CMR imaging is only
26. reliable when adequately standardized.⁴⁰ An alternative imaging modality has been searched
27. for to overcome the aforementioned limitations and has resulted in increased attention for
28. using three-dimensional echocardiography.

29.

30.

31. **OUTLINE OF THE THESIS**

32.

33. The ideal RV imaging modality should be easily applicable, real-time and a three-dimensional
34. assessment of RV volumes.¹³ This has come on the horizon with the availability of real-time

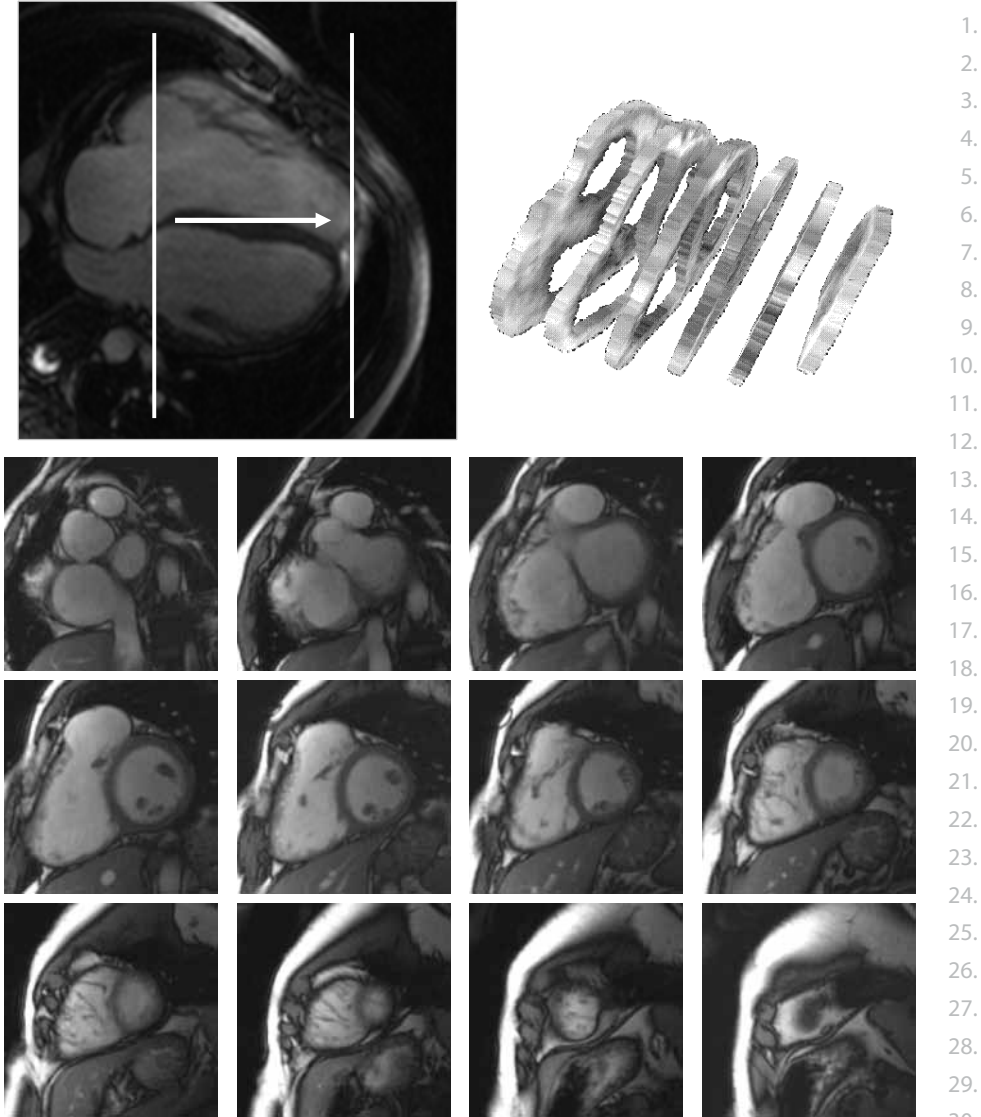


Figure 5 The disc summation method is used for the calculation of right ventricular volumes and ejection fraction by cardiac magnetic resonance imaging.

three-dimensional echocardiography (real-time 3D echo) combined with dedicated software, the four-dimensional RV Function program. The aim of this thesis was to investigate the clinical use of real-time 3D echo for RV assessment in patients with congenital heart disease and healthy controls. The thesis is divided into three parts.

1. Part 1: Echocardiography in congenital heart disease

2. An overview on echocardiographic techniques and measurements used for RV quantification
3. is provided. A systematic review of the clinical value of these echocardiographic modalities in
4. patients with congenital heart disease is presented. In addition, current applications of real-
5. time 3D echo in adult congenital heart disease are discussed. Not only using real-time 3D echo
6. for RV volume and EF assessment is outlined, but also the added value of real-time 3D echo for
7. cardiac morphology.

8.

9. Part 2: Right ventricular acquisition, analysis, and clinical applications

10. The supplementary value of real-time 3D echo versus two-dimensional echocardiography for
11. RV assessment is studied. The acquisition related variability – test-retest variability – of real-time
12. 3D echo-derived RV volumes and EF is examined. Furthermore, the clinical value of real-time
13. 3D echo for RV assessment is explored in terms of feasibility, accuracy, reproducibility, and time
14. consumption. The usefulness of real-time 3D echo to identify RV dysfunction in patients with
15. congenital heart disease is described.

16.

17. Part 3: Troubleshooting for right ventricular assessment

18. Proper endocardial border definition is a prerequisite for reliable RV assessment using real-time
19. 3D echo. The sources of RV volume differences between real-time 3D echo and CMR imaging
20. are described. Furthermore, the value of using contrast-enhanced real-time 3D echo on both
21. RV visualization and quantification of RV volumes and EF is presented.

22.

23. By reading this thesis, we hope that the reader will appreciate the unique features that real-
24. time 3D echo offers for the assessment of RV volumes and EF in patients with congenital heart
25. defects.

26.

27.

28.

29.

30.

31.

32.

33.

34.

35.

36.

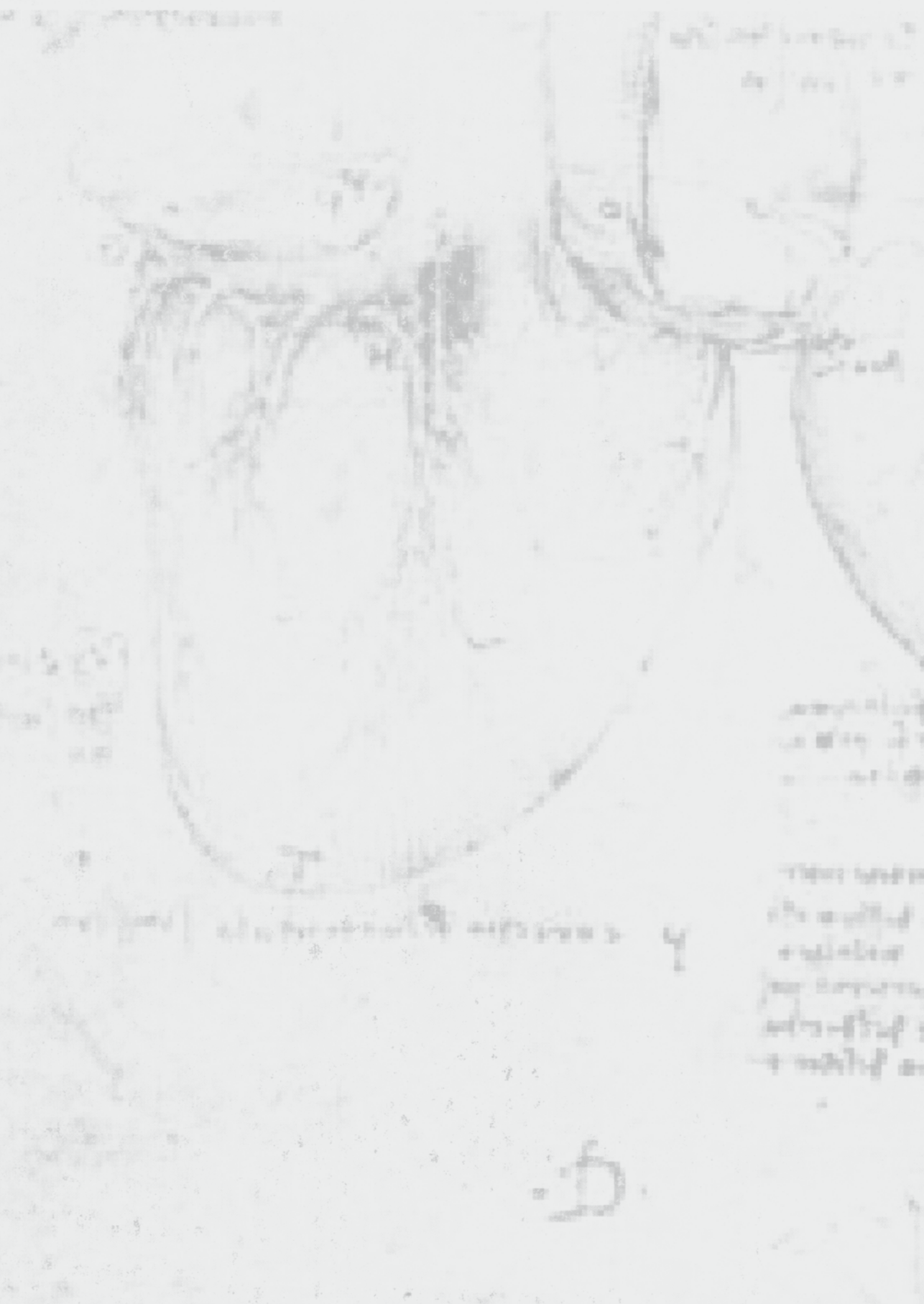
37.

38.

39.

1. Roos-Hesselink JW, Meijboom FJ, Spitaels SE, van Domburg R, van Rijen EH, Utens EM, et al. Decline in ventricular function and clinical condition after Mustard repair for transposition of the great arteries (a prospective study of 22-29 years). *Eur Heart J*. 2004;25:1264-70. 1.
2. Graham TP, Jr., Bernard YD, Mellen BG, Celermajer D, Baumgartner H, Cetta F, et al. Long-term outcome in congenitally corrected transposition of the great arteries: a multi-institutional study. *J Am Coll Cardiol*. 2000;36:255-61. 2.
3. Murphy JG, Gersh BJ, Mair DD, Fuster V, McGoon MD, Ilstrup DM, et al. Long-term outcome in patients undergoing surgical repair of tetralogy of Fallot. *N Engl J Med*. 1993;329:593-9. 3.
4. van der Bom T, Zomer AC, Zwinderman AH, Meijboom FJ, Bouma BJ, Mulder BJ. The changing epidemiology of congenital heart disease. *Nat Rev Cardiol*. 2011;8:50-60. 4.
5. Meijboom F, Mulder B. Problems in the organization of care for patients with adult congenital heart disease. *Arch Cardiovasc Dis*. 2010;103:411-5. 5.
6. Warnes CA, Liberthson R, Danielson GK, Dore A, Harris L, Hoffman JI, et al. Task force 1: the changing profile of congenital heart disease in adult life. *J Am Coll Cardiol*. 2001;37:1170-5. 6.
7. Baumgartner H, Bonhoeffer P, De Groot NM, de Haan F, Deanfield JE, Galie N, et al. ESC Guidelines for the management of grown-up congenital heart disease (new version 2010). *Eur Heart J*. 2010;31:2915-57. 7.
8. Hoffman JI, Kaplan S. The incidence of congenital heart disease. *J Am Coll Cardiol*. 2002;39:1890-900. 8.
9. Kantor PF, Redington AN. Pathophysiology and management of heart failure in repaired congenital heart disease. *Heart Fail Clin*. 2010;6:497-506, ix. 9.
10. Norozi K, Wessel A, Alpers V, Arnhold JO, Geyer S, Zoege M, et al. Incidence and risk distribution of heart failure in adolescents and adults with congenital heart disease after cardiac surgery. *Am J Cardiol*. 2006;97:1238-43. 10.
11. Piran S, Veldtman G, Siu S, Webb GD, Liu PP. Heart failure and ventricular dysfunction in patients with single or systemic right ventricles. *Circulation*. 2002;105:1189-94. 11.
12. Haddad F, Doyle R, Murphy DJ, Hunt SA. Right ventricular function in cardiovascular disease, part II: pathophysiology, clinical importance, and management of right ventricular failure. *Circulation*. 2008;117:1717-31. 12.
13. Redington AN. Right ventricular function. *Cardiol Clin*. 2002;20:341-9, v. 13.
14. Keele KD. Leonardo da Vinci, and the movement of the heart. *Proc R Soc Med*. 1951;44:209-13. 14.
15. Wells F. The renaissance heart, the drawings of Leonardo da Vinci. In: Peto J, ed. *The Heart*. Vol 1. New Haven and London: Yale University Press; 2007:70-94. 15.
16. Carlon CA, Mondini PG, De Marchi R. Surgical treatment of some cardiovascular diseases. *J Int Coll Surg*. 1951;16:1-11. 16.
17. Glenn WW. Circulatory bypass of the right side of the heart. IV. Shunt between superior vena cava and distal right pulmonary artery; report of clinical application. *N Engl J Med*. 1958;259:117-20. 17.
18. Lee FA. Hemodynamics of the right ventricle in normal and disease states. *Cardiol Clin*. 1992;10:59-67. 18.
19. Fontan F, Baudet E. Surgical repair of tricuspid atresia. *Thorax*. 1971;26:240-8. 19.
20. Fixler DE, Monroe GA, Wheeler JM. Hemodynamic alterations during septal or right ventricular ischemia in dogs. *Am Heart J*. 1977;93:210-5. 20.
21. Berger HJ, Matthay RA, Loke J, Marshall RC, Gottschalk A, Zaret BL. Assessment of cardiac performance with quantitative radionuclide angiocardiology: right ventricular ejection fraction with reference to findings in chronic obstructive pulmonary disease. *Am J Cardiol*. 1978;41:897-905. 21.
22. Fewell JE, Abendschein DR, Carlson CJ, Murray JF, Rapaport E. Continuous positive-pressure ventilation decreases right and left ventricular end-diastolic volumes in the dog. *Circ Res*. 1980;46:125-32. 22.
23. Jardin F, Farcot JC, Boisante L, Curien N, Margairaz A, Bourdarias JP. Influence of positive end-expiratory pressure on left ventricular performance. *N Engl J Med*. 1981;304:387-92. 23.
24. Farb A, Burke AP, Virmani R. Anatomy and pathology of the right ventricle (including acquired tricuspid and pulmonic valve disease). *Cardiol Clin*. 1992;10:1-21. 24.

1. 25. Bronicki RA, Baden HP. Pathophysiology of right ventricular failure in pulmonary hypertension. *Pediatr Crit Care Med*. 2010;11:S15-22.
2. 26. Furey SA, 3rd, Zieske HA, Levy MN. The essential function of the right ventricle. *Am Heart J*. 1984;107:404-10.
3. 27. Haddad F, Hunt SA, Rosenthal DN, Murphy DJ. Right ventricular function in cardiovascular disease, part I: Anatomy, physiology, aging, and functional assessment of the right ventricle. *Circulation*. 2008;117:1436-48.
4. 28. Anderson RH, Sanchez-Quintana D, Niederer P, Lunkenheimer PP. Structural-functional correlates of the 3-dimensional arrangement of the myocytes making up the ventricular walls. *J Thorac Cardiovasc Surg*. 2008;136:10-8.
5. 29. Saleh S, Liakopoulos OJ, Buckberg GD. The septal motor of biventricular function. *Eur J Cardiothorac Surg*. 2006;29 Suppl 1:S126-38.
6. 30. Carabello BA. Evolution of the study of left ventricular function: everything old is new again. *Circulation*. 2002;105:2701-3.
7. 31. Schulman DS. Assessment of the right ventricle with radionuclide techniques. *J Nucl Cardiol*. 1996;3:253-64.
8. 32. Jain D, Zaret BL. Assessment of right ventricular function. Role of nuclear imaging techniques. *Cardiol Clin*. 1992;10:23-39.
9. 33. Jaffe CC, Weltin G. Echocardiography of the right side of the heart. *Cardiol Clin*. 1992;10:41-57.
10. 34. Rudski LG, Lai WW, Afilalo J, Hua L, Handschumacher MD, Chandrasekaran K, et al. Guidelines for the echocardiographic assessment of the right heart in adults: a report from the American Society of Echocardiography endorsed by the European Association of Echocardiography, a registered branch of the European Society of Cardiology, and the Canadian Society of Echocardiography. *J Am Soc Echocardiogr*. 2010;23:685-713; quiz 86-8.
11. 35. Hui W, Abd El Rahman MY, Dsebissowa F, Gutberlet M, Alexi-Meskishvili V, Hetzer R, et al. Comparison of modified short axis view and apical four chamber view in evaluating right ventricular function after repair of tetralogy of Fallot. *Int J Cardiol*. 2005;105:256-61.
12. 36. Koestenberger M, Nagel B, Ravekes W, Everett AD, Stueger HP, Heinzl B, et al. Systolic right ventricular function in pediatric and adolescent patients with tetralogy of Fallot: echocardiography versus magnetic resonance imaging. *J Am Soc Echocardiogr*. 2011;24:45-52.
13. 37. Puchalski MD, Williams RV, Askovich B, Minich LL, Mart C, Tani LY. Assessment of right ventricular size and function: echo versus magnetic resonance imaging. *Congenit Heart Dis*. 2007;2:27-31.
14. 38. Lai WW, Gauvreau K, Rivera ES, Saleeb S, Powell AJ, Geva T. Accuracy of guideline recommendations for two-dimensional quantification of the right ventricle by echocardiography. *Int J Cardiovasc Imaging*. 2008;24:691-8.
15. 39. Jiang L, Levine RA, Weyman AE. Echocardiographic Assessment of Right Ventricular Volume and Function. *Echocardiography*. 1997;14:189-206.
16. 40. Beerbaum P, Barth P, Kropf S, Sarikouch S, Kelter-Kloepping A, Franke D, et al. Cardiac function by MRI in congenital heart disease: impact of consensus training on interinstitutional variance. *J Magn Reson Imaging*. 2009;30:956-66.
17. 41. Luijnenburg SE, Robbers-Visser D, Moelker A, Vliegen HW, Mulder BJ, Helbing WA. Intra-observer and interobserver variability of biventricular function, volumes and mass in patients with congenital heart disease measured by CMR imaging. *Int J Cardiovasc Imaging*. 2010;26:57-64.
18. 42. Mertens LL, Friedberg MK. Imaging the right ventricle-current state of the art. *Nat Rev Cardiol*. 2010.
19. 35.
20. 36.
21. 37.
22. 38.
23. 39.



Chapter 2

Right ventricular quantification in congenital heart disease: a systematic review on conventional and new echocardiographic techniques

H.B. van der Zwaan
J.W. Roos-Hesselink
E. Boersma
W.A. Helbing
O.I.I. Soliman
M.L. Geleijnse
F.J. Meijboom

Submitted for publication

ABSTRACT

Background. Repeated assessment of right ventricular (RV) size and function is essential for clinical management of patients with congenital heart disease (CHD). For quantification of RV volumes and ejection fraction, cardiac magnetic resonance (CMR) imaging is considered the reference technique. Yet, various new echocardiographic techniques are available and their value in clinical practice remains to be established. We systematically reviewed articles on the clinical value of echocardiographic techniques for RV function assessment in patients with CHD.

Methods. We executed a search of PubMed and Embase databases and included 34 studies (in total 1114 patients with CHD and 478 healthy controls) in which RV size and/ or function were assessed by tricuspid annular plane systolic excursion (TAPSE), two-dimensional (2D) echocardiography, three-dimensional (3D) echocardiography, Doppler- or speckle tracking echocardiography. Data on accuracy of echocardiography compared with CMR imaging and/ or data on reproducibility of echocardiography were extracted.

Results. 3D echocardiography-derived measurements correlated better with CMR imaging for RV quantification (R 0.73-0.99) than conventional 2D echocardiography-derived measurements (R 0.33-0.87) in patients with tetralogy of Fallot, atrial septal defect, or systemic right ventricles. Doppler-based techniques measuring regional RV wall motion velocities, strain, and strain rate showed a wide range of correlations (R 0.29 - 0.87) compared with RV ejection fraction by CMR imaging.

Conclusions. Besides the by guidelines recommended RV echocardiographic measurements, the accumulated data in this review indicate that 3D echocardiography should be used for serial follow-up in patients with CHD. In case of poor acoustic windows or if deterioration of RV function is suspected based on echocardiographic measurements, CMR imaging remains the indicated technique.

1.
2.
3.
4.
5.
6.
7.
8.
9.
10.
11.
12.
13.
14.
15.
16.
17.
18.
19.
20.
21.
22.
23.
24.
25.
26.
27.
28.
29.
30.
31.
32.
33.
34.
35.
36.
37.
38.
39.

1. INTRODUCTION

2.

3. Repeated assessment of right ventricular (RV) size and function represents a crucial step in
4. the initiation and guiding of therapy, follow-up and prediction of outcome in patients with
5. certain congenital heart diseases (CHD).¹⁻⁶ Therefore, accurate and reproducible RV measure-
6. ments are mandatory. The right ventricle has a complex geometric shape that consists of three
7. basic regions referred to as the inlet, apex and outflow. For clinicians, an ideal parameter for
8. RV quantification should be simple, accurate to assess its complex geometry and contraction
9. pattern, reproducible and not expensive.

10. Cardiac magnetic resonance (CMR) imaging is the reference technique to assess RV volumes
11. and ejection fraction (EF) due to its high accuracy and reproducibility. On the other hand echo-
12. cardiography is the most widely used tool for RV assessment due to high versatility and the ease
13. of use. Latest guidelines on echocardiographic RV quantification addressed the use of tricuspid
14. annular systolic excursion (TAPSE), 2-dimensional echocardiography (2D echo) and Doppler
15. imaging.⁷ The accuracy of 2D- and Doppler echo for RV assessment is limited, either due to the
16. need of geometric assumptions^{8,9} or because these techniques only assess a limited region
17. of function which cannot be extrapolated to global RV function. More recently, RV assessment
18. using 3-dimensional echocardiography (3D echo), tissue Doppler imaging (TDI) and speckle
19. tracking echocardiography has been investigated in several studies that included various
20. patient populations.¹⁰⁻¹² The additional value of the latter techniques above conventional RV
21. measurements in terms of accuracy and reproducibility in patients with CHD is unknown.

22. The purpose of this paper was to provide an overview of the conventional and newer
23. echocardiographic techniques and variables used for RV quantification based on a systematic
24. review of published literature in children and adults with CHD.

25.

26.

27. METHODS

28.

29. Search strategy, selection criteria, and data extraction

30. We conducted a search of Medline (source PubMed, 1966 to 1st December 2010) and Embase
31. (1980 to December 2010). The following combination of keywords was used: "echocardiogra-
32. phy", "right ventricle" and "CHD". We repeated the search substituting "CHD" with specific CHD
33. such as "tetralogy of Fallot", "atrial septal defect", "transposition of the great arteries", "systemic
34. right ventricle" or "Fontan". The search strategy was limited to articles concerning human sub-
35. jects that were published in the English language and accompanied by an abstract. By screen-
36. ing of titles and abstracts we identified potentially relevant studies. In addition, we searched
37. the reference lists of the included studies and review articles on RV function assessment to
38. identify studies missed by the search strategy applied.

39.

The following selection criteria were used. The only assessment of methodology quality used was the study design. The study's main purpose was 1) the validation of echocardiography against the CMR reference to quantify RV dimensions or function in patients with CHD; 2) to study the reproducibility of echocardiography for RV assessment in these patients. Articles solely reporting on RV pressures or right sided valvular function, i.e. not measuring RV function, were excluded. We extracted data on the type of CHD studied, the echo parameters measured, the feasibility, the agreement with CMR imaging, the reproducibility of the parameters and the authors' conclusion concerning agreement between both techniques and applicability in clinical practice. Unless otherwise indicated by the authors, we concluded that the patient numbers studied for reproducibility were equal to the total number studied.

All potentially relevant articles were independently reviewed by two investigators (H.B.Z., J.W.R.H.) to establish eligibility. Disagreements (n = 5) were resolved by discussion.

RESULTS

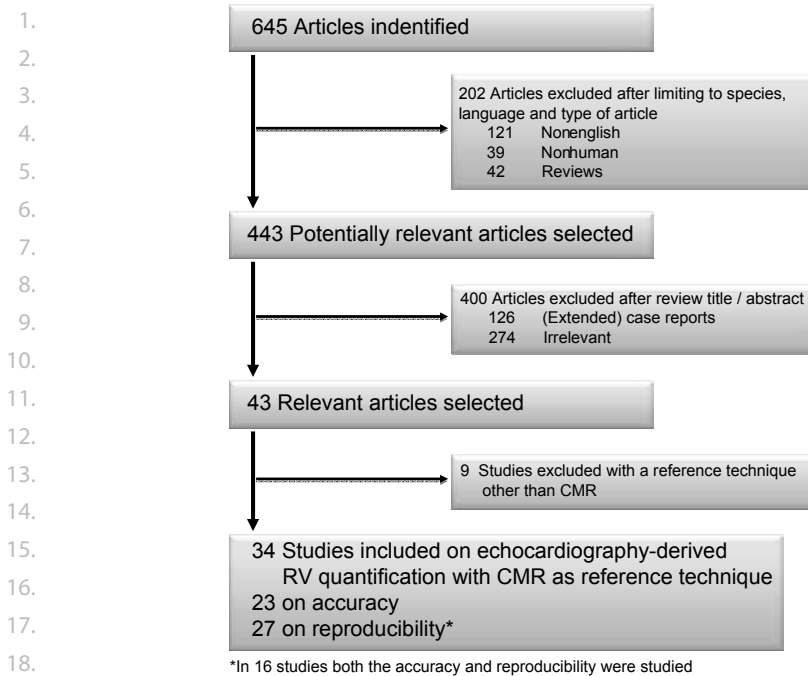
The electronic search resulted in 643 potentially applicable references (Figure 1). We included 34 in this review, whereas most articles were excluded because echocardiography was not the main topic. In 9 articles a reference technique different from CMR imaging was used (biplane cine angiography,^{13, 14} volumes obtained by conventional angiography,¹⁵⁻¹⁷ radionuclide angiography¹⁸⁻²⁰ and intra-operative RV volumes (Figure 1).²¹ These 9 articles were excluded for analysis of accuracy, because CMR imaging was not used as the reference technique. In 5 included articles data were collected retrospectively.²²⁻²⁶

Table 1. Echocardiographic measurements used for right ventricular assessment

Right ventricular dimensions	Right ventricular function
<i>Qualitative assessment</i>	<i>Qualitative assessment</i>
2D eyeballing: size relative to left ventricle	2D eyeballing: contractility
<i>Quantitative assessment</i>	<i>Quantitative assessment</i>
2D diameters in AP4C and PSAX view	Tricuspid annular plane systolic excursion
2D areas in end-diastole and end-systole	2D fractional area change / ejection fraction
Volumes: 2D biplane	Myocardial performance index
3D	Myocardial velocities
	Myocardial strain and strain rate
	3D ejection fraction

2D denotes 2-dimensional, AP4C apical four-chamber, PSAX parasternal short-axis, 3D 3-dimensional.

The total number of patients with CHD studied for accuracy was 1114 and the total number of healthy controls 478. The 12 echocardiographic measurements which were used by articles included in this review, either on RV size or function, are summarized in Table 1. These



19. **Figure 1** Flow chart of the search strategy and the selection of studies.

20. 21. measurements were based on M-mode (Figure 2), 2D echo (Figure 3), 3D echo (Figure 4), tissue
22. Doppler imaging, and 2D speckle tracking (Figure 5). The time interval between echocardiogra-
23. phy and CMR imaging ranged from within one hour up to six months (Tables 2-4). In 27 studies
24. ^{10, 11, 20-24, 26-45} the intra- and/or inter-observer values of echocardiography were judged (mean
25. 22 patients per study). Various statistical methods for reproducibility were used including linear
26. regression with Pearson's correlation coefficient, interclass correlation, the coefficient of varia-
27. tion and limits of agreement by Bland-Altman analysis (Table 5).

28. Either a mixed population of patients with CHD or one of the following specific diseases was
29. studied: tetralogy of Fallot (ToF), atrial septal defect (ASD), systemic right ventricle or Fontan
30. circulation. The youngest patient population included was 6 ± 2 years, while the oldest was 45
31. ± 19 years.

32. 33. Various congenital heart diseases

34. In 9 articles accuracy and/ or reproducibility were reported on echocardiography in various
35. CHD ^{9, 10, 23, 26, 30-33, 42} Since these patients were included consecutively, numbers on feasibility
36. were derived: 52% for 2D echo-derived volumes, 52-100% for 3D-echo-derived volumes and EF
37. and 91-100% for color tissue Doppler-derived measurements (Tables 2-4). Helbing et al⁹ com-
38. pared RV volumes based on a 2D echo bi-plane method and found of -14 ± 16 for end-diastolic
39. volume, 4 ± 7 for end-systolic volume, and -11 ± 5 for EF. They concluded that the volumetric

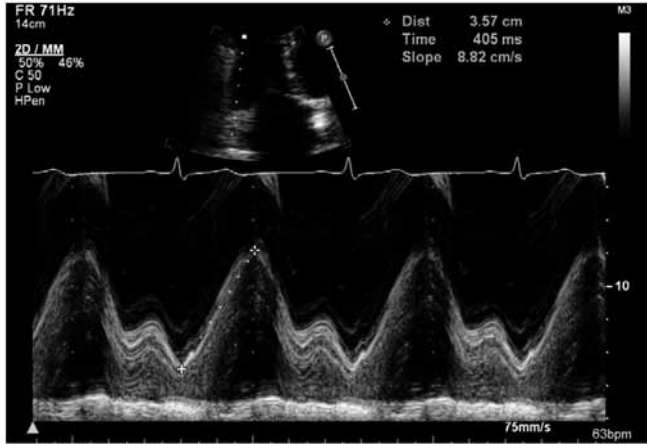


Figure 2 Tricuspid annular systolic plane excursion by M-mode at the lateral tricuspid valve annulus to obtain information on the longitudinal right ventricular function from an apparently healthy 37 years-old female.

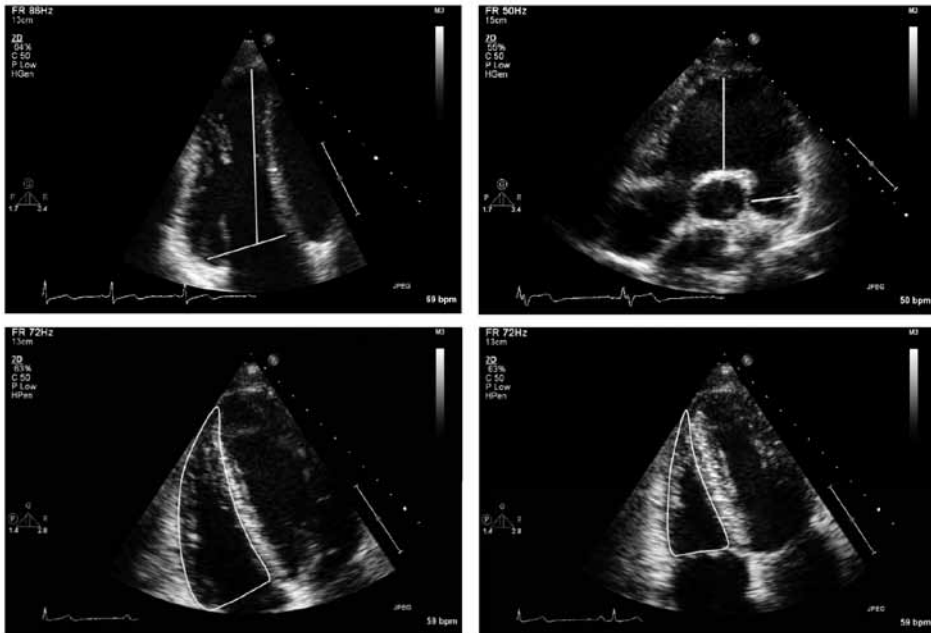
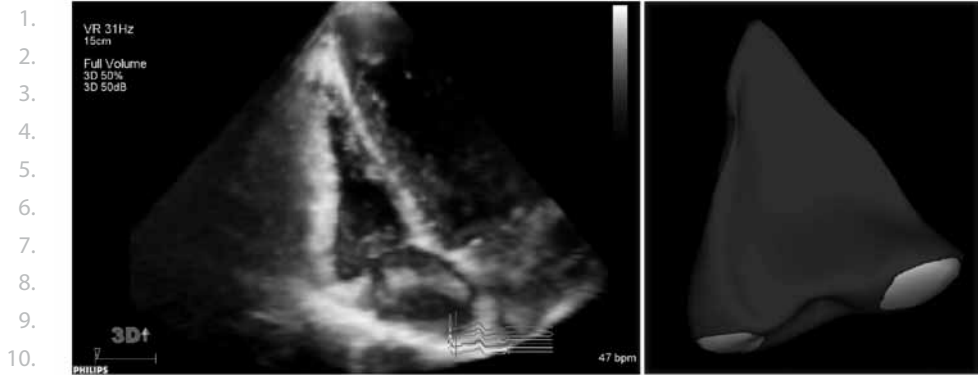
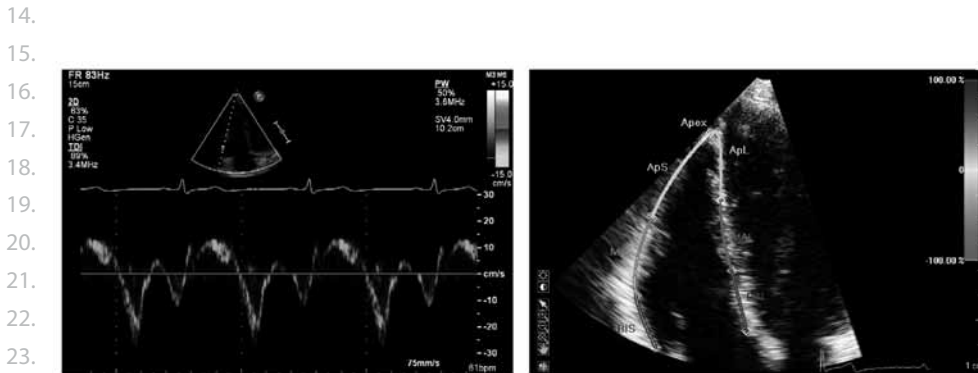


Figure 3 Inlet and longitudinal right ventricular dimensions measured onto a 2-dimensional echocardiographic apical four-chamber view from a 14 years-old male with a pulmonary auto transplantation according to Ross (a). Dimensions of the right ventricular outflow tract from a 22 years-old male with a tetralogy of Fallot (b). Right ventricular end-diastolic area (c) and end-systolic area (d) from which the area change can be measured as the end-diastolic area minus the end-systolic area divided by the end-diastolic area, from an apparently healthy 35 years-old male.



11. **Figure 4** Right ventricular full-volume acquisition by real-time 3-dimensional echocardiography from
12. an apparently healthy 29 years-old female (left) and the surface geometry obtained from analysis of the
13. dataset (right).



24. **Figure 5** Regional right ventricular function measured by color Doppler Imaging of the basal
25. right ventricular free wall from an apparently healthy 37 years-old female (left) and speckle tracking
26. echocardiography from an apparently healthy 35 years-old male (right) measuring deformation.

27.
28. area-length method was as accurate as more complex methods (Table 2). The best agreement
29. between 3D echo and CMR imaging was obtained by Niemann et al³⁰ who used a prototype
30. software package that enables analysis of both real-time 3D echo and CMR images with the
31. same rotational approach. Despite good to excellent correlations between 3D echo and CMR
32. imaging in all studies, significant biases in RV volumes by 3D echo and CMR imaging have been
33. found (Table 3, Figure 6). Concerning reproducibility, Lytrivi et al²⁶ studied 27 patients and
34. found low inter-observer values (0.3 ± 0.4 and -0.1 ± 0.2) for velocities based on color tissue
35. Doppler imaging (Table 5).

36. Tetralogy of Fallot

38. We identified 14 articles,^{22,24,25,27,29,33,36,38-40,44-47} in which RV size and/or function were judged
39. in patients with ToF. In the largest study, TAPSE was assessed in 88 pediatric and adolescent

Table 2. Right ventricular size and function by M-mode and two-dimensional echocardiography

Author	No.	Patients	Age (y)	Time interval	Echo parameters	Feasibility in consecutive patients	Statistical method inter-technique difference	r	Mean value echo, ml or %	Mean value ml difference, ml (%)	Limits of agreement
Puchalski ²³	22	Various CHD	17 ± 7	49 ± 54 days	Eyeballing: RV size RV function	-	Kendall's tau correlation	0.63	-	-	-
Salehian ²⁴	11	Systemic RV	32 ± 10	66 ± 51 days	Eyeballing: RV function	-	Spearman's correlation	0.71	-	-	-
Lai ²²	31	ToF	21 (4-57)	0 - 6 months	RV basal dimension	-	Pearson's correlation	0.33/0.52/0.51*	-	-	-
	33	ASD	14 (0-60)	months	RV fractional area change	-	Pearson's correlation	0.54/0.70/0.39*	-	-	-
	23	Healthy ctrls	16 (4-46)								
Greutmann ⁴⁴	67	ToF	33 ± 12	0 - 6 months	RV dimensions RV EDV based on model	100%	Pearson's correlation	0.35 - 0.84	154 ± 42	157 ± 51	- 3 ± 25
Hui ²⁷	30	ToF	21 ± 10	-	RV fractional area change	-	Bland and Altman	0.51	43 ± 10	46 ± 13	- 3 (7) -
Lissin ⁴⁸	18	Systemic RV	25 ± 5	<48 hours	RV basal dimension TAPSE	-	Pearson's correlation	0.60	-	-	-
Koestenberger ⁴⁵	88	ToF	0 - 28	76 ± 44 days	TAPSE	-	Spearman's correlation	0.47	-	-	-
Helbing ⁹	16	Various CHD	11 ± 3	<2 hours	Bi-plane EDV	52%	Systematic difference: mean of the paired difference	0.86	72 ± 29	92 ± 27	-14 (15) ± 16
	17	Healthy ctrls	11 ± 2		Bi-plane ESV EF			0.82	32 ± 14	33 ± 13	4 (12) ± 7
								0.66	-	65 ± 8	-11 (17) ± 5
Margossian ²⁸	124	Fontan	12 ± 3	<3 months	Bi-plane EDV Bi-plane ESV EF	-	Bland and Altman	-	72 ± 39	102 ± 44	-30 (29) ± 27
									32 ± 24	44 ± 25	-13 (30) ± 19
									57 ± 11	57 ± 10	0 (0) ± 12

Accuracy of echocardiography as compared with cardiac magnetic resonance imaging-derived volumes and/or ejection fraction.

* R-value for tetralogy of Fallot patients, atrial septal defect patients and healthy controls respectively. No. indicates number of participants; age is either indicated as mean ± standard deviation or median with (range). CHD indicates congenital heart disease, RV right ventricle, ToF tetralogy of Fallot, ASD atrial septal defect, ctrls controls, TAPSE tricuspid annular plane systolic excursion, EDV end-systolic volume, ESV end-diastolic volume, EF ejection fraction.

1.
2.
3.
4.
5.
6.
7.
8.
9.
10.
11.
12.
13.
14.
15.
16.
17.
18.
19.
20.
21.
22.
23.
24.
25.
26.
27.
28.
29.
30.
31.
32.
33.
34.
35.
36.
37.
38.
39.

Table 3. Right ventricular assessment by three-dimensional echocardiography

Author	No.	Patients	Age (y)	Time interval	3D echo technique	Echo parameters	Feasibility in consecutive patients	Statistical method inter-technique difference	r	Mean value echo, ml or %	Mean value CMR, ml or %	Mean difference, ml (%)	Limits of agreement, ml
Vogel ³²	13 3	Various CHD Healthy ctrls	10 ± 6	<24 hours	Rotational scanning	EDV ESV EF	100%	Bland and Altman	0.95 0.87	-	-	-	± 4 ± 5 ± 5
Papavassiliou ³¹	13	Various CHD	6 ± 3	<1 hour	Rotational scanning	EDV ESV EF	88%	Bland and Altman	0.95 0.95 0.80	58 ± 27 36 ± 22 42 ± 12	68 ± 39 40 ± 33 46 ± 12	-10 (15) -4 (10) -4 (9)	± 16 ± 14 ± 7
Abd el Rahman ⁴⁶	21	ToF	14 (3-44)	<24 hours	Rotational scanning	EDV _{indexed} ESV _{indexed} EF	100%	Bland and Altman	0.95 0.93	80 (20) 38 (14)	-	-	± 28 ± 21
Niemann ³⁰	14 16	Various CHD Healthy ctrls	9 ± 6 39 ± 22	Same visit	Real-time	EDV ESV EF	100%	Bland and Altman	0.99 0.98 0.97	71 ± 15 40 ± 10 44 ± 7	71 ± 15 39 ± 10 44 ± 8	-1 (1) -1 (3) 0 (0)	± 2 ± 2 ± 3
Iriart ²⁹	20 14	ToF Healthy ctrls	31 ± 14	<24 hours	Real-time	EDV ESV EF	92%	Bland and Altman	0.93 0.92 0.73	144 ± 52 77 ± 36 48 ± 8	163 ± 55 86 ± 38 48 ± 7	-19 (12) -9 (11) 0 (0)	± 21 ± 15 ± 6
Khoo ⁴²	28	Various CHD	17 (12-25)	<2 hours	Real-time	EDV ESV EF	52%	Bland and Altman	0.91 0.89 0.78	182 ± 71 96 ± 49 49 ± 9	237 ± 95 128 ± 70 48 ± 10	-55 (23) -32 (25) 1 (7)	- - -
Grewal ³³	25	ToF	35 ± 14	<24 hours	Real-time	EDV ESV EF	86%	Bland and Altman	0.88 0.89 0.89	249 ± 66 147 ± 50 42 ± 8	274 ± 82 159 ± 60 44 ± 7	-25 (9) -14 (9) -2 (5)	- - -
Van der Zwaan ¹⁰	50	Various CHD	27 ± 10	<2 hours	Real-time	EDV ESV EF	81%	Bland and Altman	0.93 0.91 0.74	185 ± 71 103 ± 48 46 ± 8	219 ± 86 114 ± 62 49 ± 10	-34 (16) -11 (10) -4 (8)	± 32 ± 27 ± 6

Abbreviations see Table 2.

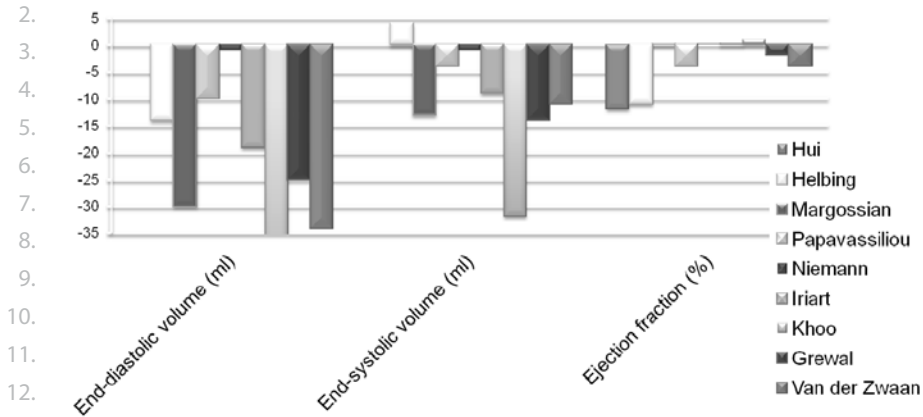
Table 4. Right ventricular function by Doppler and speckle tracking echocardiography

Author	No.	Patients	Age (y)	Time interval	Echo technique	Echo parameters	Feasibility in consecutive patients	r
Lissin ⁴⁸	18	Systemic RV	25 ± 5	<48 hours	Spectral Doppler	Myocardial performance index	-	NS
Schwerzmann ²⁵	57	ToF	37 ± 12	<6 months	Spectral Doppler	Myocardial performance index	-	0.73
Cheung ⁴⁷	30	ToF	16 ± 3	-	Spectral tissue Doppler	Myocardial performance index	-	0.40
Salehian ³⁷	29	Systemic RV	32 ± 10	66 ± 51 days	Spectral tissue Doppler	Myocardial performance index	-	0.82
Lytrivi ²⁶	35	Various CHD	15 (6-42)	<24 hours	Color tissue Doppler	Peak systolic tricuspid annular velocity Acceleration during isovolumic contraction Peak velocity during isovolumic contraction Myocardial performance index	100% 91% 97%	0.29 0.37 0.25 0.33
Eyskens ⁴³	20 30	Systemic RV Healthy ctrls	14 ± 3	<24 hours	Color tissue Doppler	Longitudinal strain	88%	0.87
Chow ¹¹	26 27	Systemic RV Healthy ctrls	21 ± 4 19 ± 4	-	2D speckle tracking	Longitudinal strain Strain rate	-	0.35 0.62
Pettersen ¹²	14 14	Systemic RV Other CHD Healthy ctrls	18 ± 1 18 ± 5 27 ± 1	-	Color tissue Doppler	Circumferential strain	-	0.82

Abbreviations see Table 2.

1.
2.
3.
4.
5.
6.
7.
8.
9.
10.
11.
12.
13.
14.
15.
16.
17.
18.
19.
20.
21.
22.
23.
24.
25.
26.
27.
28.
29.
30.
31.
32.
33.
34.
35.
36.
37.
38.
39.

1. Right Ventricular Volume Differences: echocardiography versus cardiac magnetic resonance imaging



13. **Figure 6** The right ventricular volume differences measured by 2-dimensional echocardiography and
 14. 3-dimensional echocardiography compared with cardiac magnetic resonance imaging.

15.
 16. patients with ToF and compared with CMR imaging resulting in modest correlations.⁴⁵ Grewal
 17. et al³³ compared 3D echo-derived volumes and EF with CMR imaging and found correlation
 18. coefficients ranging from 0.88-0.89 with mean differences between 5 to 9% (Table 3). Iriart et
 19. al²⁹ studied 34 patients and healthy controls for reproducibility and reported high correlation
 20. coefficients, 0.86 to 0.99, for RV volumes with small mean differences, 0.1 ± 4 to 0.4 ± 14 ml
 21. (Table 5).

22. Atrial septal defect

24. Lai et al²² performed a retrospective study in 33 patients with ASD, 31 with ToF and 23 healthy
 25. controls. They found the RV basal dimension to correlate with a coefficient of 0.52 with CMR-
 26. derived end-diastolic volume, and the RV fractional area change with a coefficient of 0.70 with
 27. CMR-derived EF. They concluded that patients with CHD had worse correlations compared with
 28. healthy controls (Table 2). In 5 articles data on reproducibility were reported, the largest group
 29. being performed by Jategaonkar et al⁴¹ in 33 ASD patients by 2D speckle tracking. They found
 30. inter- and intra-observer values of respectively $5 \pm 3\%$ and $6 \pm 4\%$ for longitudinal strain and 7
 31. $\pm 4\%$ and $10 \pm 8\%$ for strain rate (Table 5).

32. Systemic right ventricle

34. In 8 articles accuracy and reproducibility data on patients with systemic right ventricles were
 35. given.^{11, 12, 20, 24, 34, 35, 43, 48} TAPSE was compared with CMR-derived EF and resulted in a correla-
 36. tion coefficient of 0.63 (Table 2).⁴⁸ Interestingly, accuracy of the myocardial performance index
 37. ranged from a non-significant correlation up to a correlation coefficient of 0.82 in comparable
 38. patient populations. Pettersen et al¹² were the only ones to give a mean difference between
 39. circumferential strain measured by color tissue Doppler imaging and the reference technique

Table 5. Reproducibility of echocardiographic techniques for right ventricular size and function assessment

Author	Patients	Age (y)	Echo technique	Echo parameters	No.	Intra-observer values		Inter-observer values	
						r	Difference	r	Difference
Puchalski ²³	Various CHD	17 ± 7	2D echo	Eyeballing: global RV function	22*	-	-	0.07 #	-
Lai ²²	ToF	21 (4-57)	2D echo	RV basal dimension	10	-	-	0.12 #	0.1-0.5
	ASD	14 (0-60)		RV diastolic area	10	-	-	-	0.2-4
	Healthy ctrls	16 (4-46)		RV systolic area	10	-	-	-	0.3-2
Hui ²⁷	ToF	21 ± 10	2D echo	RV diastolic area	10	-	-	-	6 ± 3%
				RV systolic area	10	-	-	-	6 ± 4%
				RV fractional area change	10	-	-	-	4 ± 3%
Koestenberger ⁴⁵	ToF	0 - 28	2D echo	TAPSE	16	0.98	-	0.97	-
	ToF	33 ± 12		2D echo EDV based on model	20	-	1 ± 4	-	0.1 ± 4
Greutmann ⁴⁴	ToF	33 ± 12	2D echo	Bi-plane EDV	20	0.88 #	14 (20%) ^o	0.85 #	20 (26%) ^o
				EF	46	0.86 #	7 (21%) ^o	0.82 #	10 (28%) ^o
				EF	46	0.35 #	9 (15%) ^o	0.43 #	8 (15%) ^o
Margossian ²⁸	Fontan	12 ± 3	2D echo	Single-plane EF	22	0.81	-	0.73	-
Wilson ²⁰	Systemic RV	19 (11-29)	2D echo	EDV	5	-	-	-	4%
Vogel ³²	Various CHD	10 ± 6	Rotational 3D echo	ESV	5	-	-	-	5%
	Healthy ctrls			5	-	-	-	-	-
Papavassiliou ³¹	Various CHD	6 ± 3	Rotational 3D echo	EDV	12	-	-	0.96	1 ± 9
				ESV	12	-	-	-	-
Grison ²¹	ASD	18 + 5	Rotational 3D echo	EDV	14	0.99	0.03 [^]	-	-
				ESV	14	0.99	0.03 [^]	-	-
Niemann ³⁰	Various CHD	9 ± 6	Real-time 3D echo	-	14	-	3%	-	< 10%
				Healthy ctrls	16	-	-	-	-
Iriart ²⁹	ToF	26 (17-54)	Real-time 3D echo	EDV	34	0.99	1 ± 8	0.96	0.4 ± 14
	Healthy ctrls	32 (22-44)		ESV	34	0.98	1 ± 8	0.98	0.5 ± 7
	Healthy ctrls	32 (22-44)		EF	34	0.86	0.1 ± 4	0.87	0.2 ± 4
Khoo ⁴²	Various CHD	17 (12-25)	Real-time 3D echo	EDV	10	-	-	0.84	21 ± 27
				ESV	10	-	-	0.58	16 ± 18
				EF	10	-	-	-	4 ± 3

1.
2.
3.
4.
5.
6.
7.
8.
9.
10.
11.
12.
13.
14.
15.
16.
17.
18.
19.
20.
21.
22.
23.
24.
25.
26.
27.
28.
29.
30.
31.
32.
33.
34.
35.
36.
37.
38.
39.

Table 5. Continued

Author	Patients	Age (y)	Echo technique	Echo parameters	No.	Intra-observer values	Inter-observer values
						Difference	r
						Difference	r
Grewal ³³	ToF	35 ± 14	Real-time 3D echo	EDV	15	8.7%	0.97
				EF		5.4%	
Van der Zwaan ¹⁰	Various CHD	27 ± 10	Real-time 3D echo	EDV	25	1 ± 12%	1 ± 15%
				ESV		7 ± 14%	6 ± 17%
				EF		6 ± 9%	8 ± 13%
Ishij ³⁴	ASD	8 ± 6		Myocardial performance index	-	-	0 ± 0.01
	Systemic RV	13 ± 2	Spectral Doppler				
	Healthy ctrls	5 ± 6					
Norozi ³⁵	Systemic RV Shunt defects	23 ± 7	Spectral Doppler	Myocardial performance index	20	-	0 ± 0.1
		22 ± 7					
Salehian ³⁷	Systemic RV	32 ± 10	Spectral tissue Doppler	Myocardial performance index	10	3 ± 2%	0.70 [†]
Yasuoka ³⁸	ToF	6 ± 2	Spectral tissue Doppler	Peak systolic tricuspid annular velocity	10	6 ± 3%	0.92
	Healthy ctrls	7 ± 3		Myocardial performance index		6 ± 4%	0.96
Harada ³⁶	ToF	10 ± 3	Spectral tissue Doppler	Peak systolic tricuspid annular velocity	18	-0.1 ± 1	0.94
	Healthy ctrls	11 ± 2		Peak systolic tricuspid annular velocity			
Salehian ³⁷	ToF	36 ± 13	Spectral tissue Doppler	Peak velocity during isovolumic contraction	10	2 ± 2%	3 ± 2%
	Healthy ctrls	Matched		Acceleration during isovolumic contraction		2 ± 2%	3 ± 2%
						4 ± 2%	5 ± 3%

Table 5. Continued

Author	Patients	Age (y)	Echo technique	Echo parameters		No.	Intra-observer values		Inter-observer values	
							r	Difference	r	Difference
Toyono ⁴⁰	ToF	8 ± 3	Spectral tissue	Peak velocity during isovolumic contraction		10	-	0.94	5 ± 3%	
	Healthy ctrls	9 ± 3	Doppler	Acceleration during isovolumic contraction				0.97	6 ± 3%	
Lytrivi ²⁶	Various CHD	15 (6-42)	Color tissue Doppler	Peak systolic tricuspid annular velocity		14, 27**	0.97	0.95	0.1 ± 1	
				Acceleration during isovolumic contraction			0.85	0.93	0.01 ± 0.2	
Eyskens ⁴³	ASD	8 ± 5	Color tissue Doppler	Longitudinal strain		51	-	-	12 ± 5%	
	Healthy ctrls	9 ± 7		Longitudinal strain rate				-	14 ± 6%	
Solarz ³⁹	ToF	7 ± 4 (2-15)	Color tissue Doppler	Longitudinal strain		40	-	-	14%	
	Healthy ctrls	10 ± 5 (3-16)		Longitudinal strain rate				-	15%	
Chow ¹¹	Systemic RV	21 (4)	2D speckle tracking	Longitudinal strain		20	-	-	0.2 (2%)	
	Healthy ctrls	19 (4)		Longitudinal strain				-	0.1 (1%)	
Jategaonkar ⁴¹	ASD	45 ± 19	2D speckle tracking	Longitudinal strain		33	-	-	6 ± 4%	
	Healthy ctrls			Longitudinal strain rate		34	-	-	10 ± 8%	

* Four raters judged the images. # Fleiss Kappa coefficient: non significant. # Intraclass correlation coefficients. ° Within-subject SD (% mean). ^ Coefficient of variability. † Data expressed by Cohen's K correlation. ** 14 patients were studied for intra-observer values and 27 for inter-observer values. Abbreviations see Table 2.

1.
2.
3.
4.
5.
6.
7.
8.
9.
10.
11.
12.
13.
14.
15.
16.
17.
18.
19.
20.
21.
22.
23.
24.
25.
26.
27.
28.
29.
30.
31.
32.
33.
34.
35.
36.
37.
38.
39.

1. of choice, CMR tagging. They found no difference between the two techniques (Table 4). Chow
 2. et al¹¹ found low inter- and intra-observer values of 0.1 (1%) to 0.2 (2%) for longitudinal strain
 3. measurements based on 2D speckle tracking (Table 5).

4.

5.

6. **DISCUSSION**

7.

8. In this systematic review we compared data on the accuracy and reproducibility of echocar-
 9. diography with CMR imaging, for RV assessment in patients with CHD. A first surprising finding
 10. of this review was that only a few studies tested the agreement between echocardiography and
 11. CMR imaging and the sample sizes of all studies were rather small. A second finding was that
 12. newer echocardiographic techniques such as 3D echo were more accurate for RV quantification
 13. than the conventional 2D echo-derived measurements. Doppler based techniques measuring
 14. regional RV wall motion velocities, strain, and strain rate showed a wide range of correlations
 15. compared with RV EF by CMR imaging. The differences in agreements seen between both tech-
 16. niques between the various studies may firstly be caused by the time-interval between echo-
 17. cardiography and CMR imaging. Measurements on RV volumes and EF are load dependent, so
 18. time intervals of more than a few hours or days may be a potential confounder in the volume
 19. differences found between the two techniques.⁴⁹ Secondly, the earliest study that we included,
 20. dates from 1995 when multiphase gradient echo CMR imaging was applied. Volumes and EF
 21. estimated by this CMR technique are underestimated compared with the currently used cine
 22. steady-state free precession sequences due to the difference in endocardial border definition.⁵⁰
 23. ⁵¹ Thirdly, RV assessment by CMR imaging is effected by the choice of slices used for analysis,
 24. and the inclusion or exclusion of trabeculae that will affect the calculation of RV volumes. The
 25. choice of the basal slice containing the tricuspid valve and the choice to take into account the
 26. RV outflow tract will significantly influence RV volumes. Fourthly, different ultrasound systems
 27. and at last the differences in the underlying pathologies studied may account for the variation
 28. in agreements.

29. The comparison of reproducibility data was complex, since various statistical methods were
 30. used. Nevertheless, several studies concluded that 2D- and 3D echo based volumes and color
 31. TDI-derived velocities have shown a reproducibility that is considered acceptable for clinical
 32. practice.^{26, 28, 29} The best way to consider reproducibility is the test-retest variability, which
 33. has not been studied by any of the included studies. Test-retest variability comprises not only
 34. analysis-based differences but also differences that are caused by different acquisitions. There-
 35. fore it more closely reflects the everyday clinical use of a technique.⁵²

36. The differences in agreement between the various studies using 3D echo, may be caused by
 37. the following factors. RV size will influence the ability to include the entire endocardial surface:
 38. the larger the right ventricle is, the more difficult it will be to include both the apex and the RV
 39. outflow tract into one dataset. In addition, previous cardiac surgery, age, and gender all influence

image quality, and image quality is an essential element for accurate measurements. Surprisingly, 3D echo was found to be applicable in a high percentage of consecutive patients in all studies included in this review. It is unlikely that these results obtained by very experienced centres can directly be translated into everyday clinical practice; initially a lower feasibility may be expected.

Validation of Doppler- and speckle tracking-based measurements is complicated, because the most accurate reference technique, CMR tagging, is difficult to apply onto the thin RV wall. In normal hearts, a good regional function may reflect the function of the entire right ventricle, but in abnormal hearts, e.g. with non-contracting patch material in the interventricular septum and RV outflow tract (tetralogy of Fallot), a good regional function of the inlet of the right ventricle can co-exist with a poor EF. It is debatable what a better reflector of RV function is in this respect. The RV myocardial performance index (Tei index) has been used as a measurement for RV function²⁵ but it is only in the systemic right ventricle that a good correlation with CMR imaging was described.²⁴ The index is much debated, since it includes an isovolumic contraction and relaxation time which on the pressure-volume analysis of the normal subpulmonary right ventricle are not present,^{53, 54} and consequently, the relevance of the index is unclear. Specific use of this index in the subpulmonary right ventricle is not recommended based on the findings of this literature review.

TDI measuring velocities can be used to assess RV longitudinal motion, but this measure is affected by the overall heart motion. Therefore, strain and strain rate imaging methods were developed, measuring the degree of myocardial deformation (strain) or rate of deformation over time (strain rate). Measurement of myocardial acceleration during isovolumic contraction is a load-independent index of systolic function, in contrast with the aforementioned measurements that are load-dependent.⁵⁵ The integration of TDI and speckle tracking in clinical practice remains limited so far, partly due to the complicated off-line analysis and partly because the role in clinical decision making remains to be delineated. The current ease of using speckle tracking echocardiography will result in limited post-processing times.

Clinical implications

The recently published guidelines on the management of grown-up CHD by the European Society of Cardiology state that, despite the fact that CMR imaging is considered superior to conventional echocardiography for the quantification of RV volumes and EF, echocardiography remains the first-line investigation and continues to evolve, with improved functional assessment using 3D echo.⁵⁶ The data from the studies included in this review indicate that centres following patients with congenital heart defects should use 3D echo, provided the technique has been mastered after an appropriate learning period for acquisition and analysis. Using 3D echo will result in accurate estimations of RV volumes and EF. Because 3D echo has practical advantages over CMR imaging, being its ease of use, patient comfort, portability, speed, and relative inexpensiveness, it may become the technique of choice for serial follow-up. Systematic different RV volumes will be found using 3D echo compared with CMR imaging, but normal

1. values have been defined for 3D echo.^{57,58} If patients have poor acoustic windows, CMR imaging
2. remains the indicated imaging technique. In case of contra-indications for CMR imaging, such
3. as implanted pacemakers or defibrillators, computed tomography provides an alternative.⁵⁹
4. Ventricular size and function can be assessed by computed tomography with inferior temporal
5. resolution compared with CMR imaging. Moreover, the ionizing radiation used in computed
6. tomography makes serial use unattractive.⁶⁰

7. In the articles included in this review three main patient groups have been studied: ToF,
8. ASD, and systemic right ventricles. In accordance with the guidelines,^{7, 56} we would suggest
9. using areas by 2D echo, TAPSE, tissue Doppler imaging of the RV lateral wall, and on top of
10. this 3D echo in patients with ToF or ASD. The first two measurements can be applied because
11. of their simplicity and reproducibility, but as their accuracy is limited, multiple views must be
12. used. In addition, in patients with systemic right ventricles, the RV myocardial performance
13. index may be used instead of TAPSE, since the function of these right ventricles is shifted from
14. longitudinal towards circumferential.¹² CMR imaging should be applied in case RV dysfunction
15. is suspected in patients with CHD with RV pressure- and/ or volume-overload or in case of
16. suboptimal acoustic windows.⁵⁹ If significant changes in echocardiographic measurements are
17. found over time, CMR imaging is the preferred method to confirm the echocardiographic data.

18.

19. Study limitations

20. Most of the included studies, except the study of Lai et al.²² did not report on agreement or
21. reproducibility in the various patient groups versus healthy controls, so we could not answer the
22. question whether certain echo based measurements are accurate in the normal right ventricle,
23. but not in patients with CHD. Possible differences in agreement or reproducibility between
24. abnormal and normal right ventricles remain undetected if they are analysed together. This
25. may also have influenced the strength of correlations and mean differences in many studies
26. and therefore the overall conclusion.

27. The sample size or the rank or impact factor of the journal were not used to assess the meth-
28. odology quality of the included articles, since mostly smaller studies were performed. Most
29. articles published on echocardiography of the right ventricle in congenital heart disease were
30. published in imaging journals.

31.

32.

33. CONCLUSIONS

34.

35. Besides the by guidelines recommended RV echocardiographic measurements, the accumu-
36. lated data in this review indicate that 3D echocardiography should be used for serial follow-up
37. in patients with CHD. In case of poor acoustic windows or if deterioration of RV function is
38. suspected based on echocardiographic measurements, CMR imaging remains the indicated
39. technique.

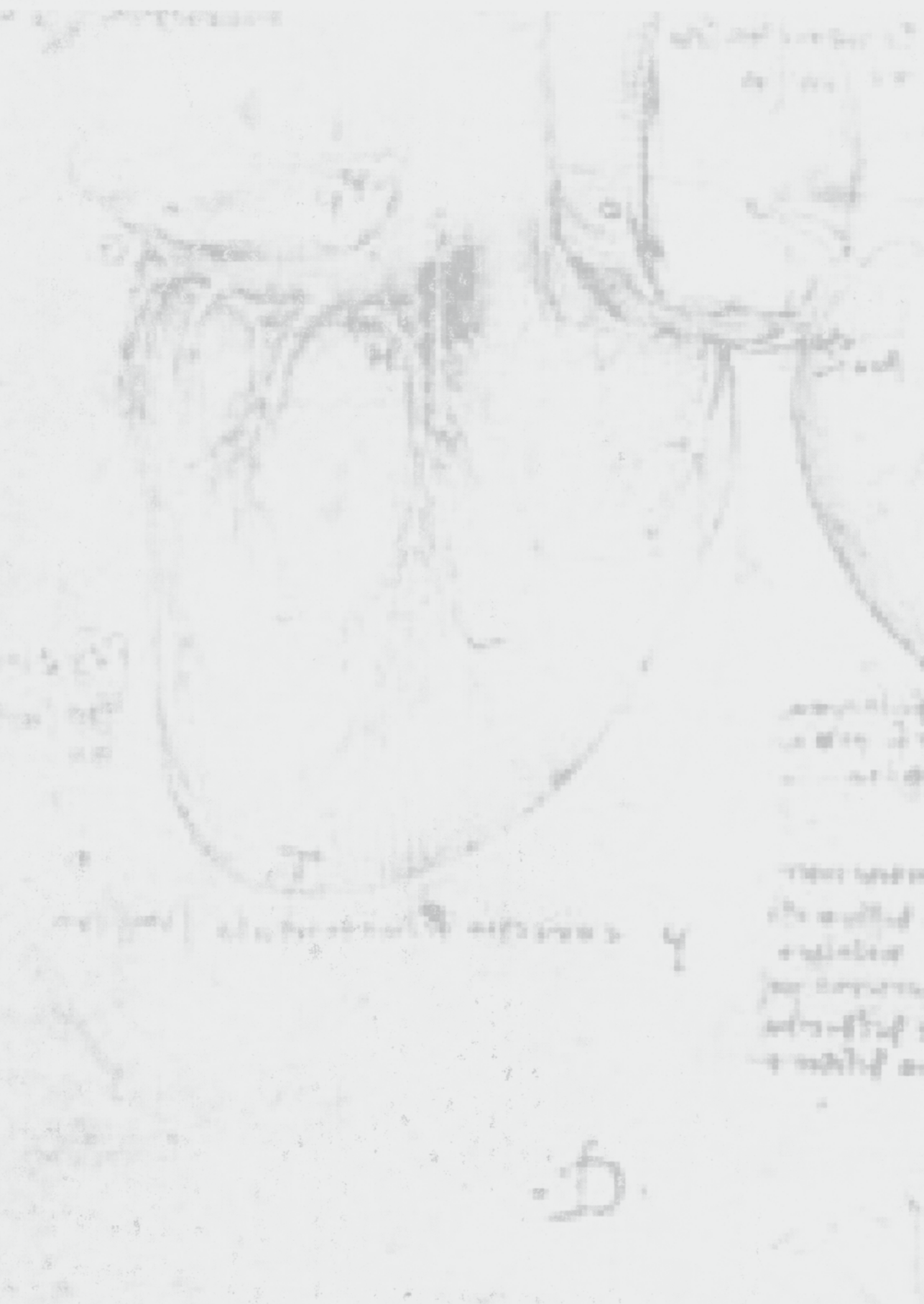
1. Davlouros PA, Niwa K, Webb G, Gatzoulis MA. The right ventricle in congenital heart disease. *Heart*. 2006;92 Suppl 1:i27-38. 1.
2. Voelkel NF, Quaife RA, Leinwand LA, Barst RJ, McGoon MD, Meldrum DR, et al. Right ventricular function and failure: report of a National Heart, Lung, and Blood Institute working group on cellular and molecular mechanisms of right heart failure. *Circulation*. 2006;114:1883-91. 2.
3. Knauth AL, Gauvreau K, Powell AJ, Landzberg MJ, Walsh EP, Lock JE, et al. Ventricular size and function assessed by cardiac MRI predict major adverse clinical outcomes late after tetralogy of Fallot repair. *Heart*. 2008;94:211-6. 3.
4. Piran S, Veldtman G, Siu S, Webb GD, Liu PP. Heart failure and ventricular dysfunction in patients with single or systemic right ventricles. *Circulation*. 2002;105:1189-94. 4.
5. Rutledge JM, Nihill MR, Fraser CD, Smith OE, McMahan CJ, Bezold LI. Outcome of 121 patients with congenitally corrected transposition of the great arteries. *Pediatr Cardiol*. 2002;23:137-45. 5.
6. van Wolferen SA, Marcus JT, Boonstra A, Marques KM, Bronzwaer JG, Spreeuwenberg MD, et al. Prognostic value of right ventricular mass, volume, and function in idiopathic pulmonary arterial hypertension. *Eur Heart J*. 2007;28:1250-7. 6.
7. Rudski LG, Lai WW, Afilalo J, Hua L, Handschumacher MD, Chandrasekaran K, et al. Guidelines for the echocardiographic assessment of the right heart in adults: a report from the American Society of Echocardiography endorsed by the European Association of Echocardiography, a registered branch of the European Society of Cardiology, and the Canadian Society of Echocardiography. *J Am Soc Echocardiogr*. 2010;23:685-713; quiz 86-8. 7.
8. Jiang L, Levine RA, Weyman AE. Echocardiographic Assessment of Right Ventricular Volume and Function. *Echocardiography*. 1997;14:189-206. 8.
9. Helbing WA, Bosch HG, Maliepaard C, Rebergen SA, van der Geest RJ, Hansen B, et al. Comparison of echocardiographic methods with magnetic resonance imaging for assessment of right ventricular function in children. *Am J Cardiol*. 1995;76:589-94. 9.
10. van der Zwaan HB, Helbing WA, McGhie JS, Geleijnse ML, Luijnenburg SE, Roos-Hesselink JW, et al. Clinical Value of Real-Time Three-Dimensional Echocardiography for Right Ventricular Quantification in Congenital Heart Disease: Validation With Cardiac Magnetic Resonance Imaging. *J Am Soc Echocardiogr*. 2010;23:134-40. 10.
11. Chow PC, Liang XC, Cheung EW, Lam WW, Cheung YF. New two-dimensional global longitudinal strain and strain rate imaging for assessment of systemic right ventricular function. *Heart*. 2008;94:855-9. 11.
12. Pettersen E, Helle-Valle T, Edvardsen T, Lindberg H, Smith HJ, Smevik B, et al. Contraction pattern of the systemic right ventricle shift from longitudinal to circumferential shortening and absent global ventricular torsion. *J Am Coll Cardiol*. 2007;49:2450-6. 12.
13. Hiraishi S, DiSessa TG, Jarmakani JM, Nakanishi T, Isabel-Jones JB, Friedman WF. Two-dimensional echocardiographic assessment of right ventricular volume in children with congenital heart disease. *Am J Cardiol*. 1982;50:1368-75. 13.
14. Watanabe T, Katsume H, Matsukubo H, Furukawa K, Ijichi H. Estimation of right ventricular volume with two dimensional echocardiography. *Am J Cardiol*. 1982;49:1946-53. 14.
15. Noori NM, Mehralizadeh S, Khaje A. Assessment of right ventricular function in children with congenital heart disease. Doppler tissue imaging. *Saudi Med J*. 2008;29:1168-72. 15.
16. Vogel M, Derrick G, White PA, Cullen S, Aichner H, Deanfield J, et al. Systemic ventricular function in patients with transposition of the great arteries after atrial repair: a tissue Doppler and conductance catheter study. *J Am Coll Cardiol*. 2004;43:100-6. 16.
17. Watanabe M, Ono S, Tomomasa T, Okada Y, Kobayashi T, Suzuki T, et al. Measurement of tricuspid annular diastolic velocities by Doppler tissue imaging to assess right ventricular function in patients with congenital heart disease. *Pediatr Cardiol*. 2003;24:463-7. 17.
18. Boneva R, Milanese O, Zucchetta P, Moreolo GS, Secchieri S, Gregianin M, et al. Comparison between echocardiographic subtraction method and first-pass radionuclide ventriculography for measuring 18.

- right ventricular volume after operative "repair" of patients with tetralogy of Fallot. *Am J Cardiol.* 1998;81:1258-62.
19. Hoffman P, Szymanski P, Lubiszewska B, Rozanski J. Echocardiographic evaluation of the systemic ventricle after atrial switch procedure. The usefulness of subcostal imaging. *Cardiol J.* 2008;15:156-61.
 20. Wilson NJ, Neutze JM, Rutland MD, Ramage MC. Transthoracic echocardiography for right ventricular function late after the Mustard operation. *Am Heart J.* 1996;131:360-7.
 21. Grison A, Maschietto N, Reffo E, Stellin G, Padalino M, Vida V, et al. Three-dimensional echocardiographic evaluation of right ventricular volume and function in pediatric patients: validation of the technique. *J Am Soc Echocardiogr.* 2007;20:921-9.
 22. Lai WW, Gauvreau K, Rivera ES, Saleeb S, Powell AJ, Geva T. Accuracy of guideline recommendations for two-dimensional quantification of the right ventricle by echocardiography. *Int J Cardiovasc Imaging.* 2008;24:691-8.
 23. Puchalski MD, Williams RV, Askovich B, Minich LL, Mart C, Tani LY. Assessment of right ventricular size and function: echo versus magnetic resonance imaging. *Congenit Heart Dis.* 2007;2:27-31.
 24. Salehian O, Schwerzmann M, Merchant N, Webb GD, Siu SC, Therrien J. Assessment of systemic right ventricular function in patients with transposition of the great arteries using the myocardial performance index: comparison with cardiac magnetic resonance imaging. *Circulation.* 2004;110:3229-33.
 25. Schwerzmann M, Samman AM, Salehian O, Holm J, Provost Y, Webb GD, et al. Comparison of echocardiographic and cardiac magnetic resonance imaging for assessing right ventricular function in adults with repaired tetralogy of fallot. *Am J Cardiol.* 2007;99:1593-7.
 26. Lytrivi ID, Lai WW, Ko HH, Nielsen JC, Parness IA, Srivastava S. Color Doppler tissue imaging for evaluation of right ventricular systolic function in patients with congenital heart disease. *J Am Soc Echocardiogr.* 2005;18:1099-104.
 27. Hui W, Abd El Rahman MY, Dsebissowa F, Gutberlet M, Alexi-Meskishvili V, Hetzer R, et al. Comparison of modified short axis view and apical four chamber view in evaluating right ventricular function after repair of tetralogy of Fallot. *Int J Cardiol.* 2005;105:256-61.
 28. Margossian R, Schwartz ML, Prakash A, Wruck L, Colan SD, Atz AM, et al. Comparison of echocardiographic and cardiac magnetic resonance imaging measurements of functional single ventricular volumes, mass, and ejection fraction (from the Pediatric Heart Network Fontan Cross-Sectional Study). *Am J Cardiol.* 2009;104:419-28.
 29. Iriart X, Montaudon M, Lafitte S, Chabaneix J, Reant P, Balbach T, et al. Right ventricle three-dimensional echography in corrected tetralogy of fallot: accuracy and variability. *Eur J Echocardiogr.* 2009.
 30. Niemann PS, Pinho L, Balbach T, Galuschky C, Blankenhagen M, Silberbach M, et al. Anatomically oriented right ventricular volume measurements with dynamic three-dimensional echocardiography validated by 3-Tesla magnetic resonance imaging. *J Am Coll Cardiol.* 2007;50:1668-76.
 31. Papavassiliou DP, Parks WJ, Hopkins KL, Fyfe DA. Three-dimensional echocardiographic measurement of right ventricular volume in children with congenital heart disease validated by magnetic resonance imaging. *J Am Soc Echocardiogr.* 1998;11:770-7.
 32. Vogel M, Gutberlet M, Dittrich S, Hosten N, Lange PE. Comparison of transthoracic three dimensional echocardiography with magnetic resonance imaging in the assessment of right ventricular volume and mass. *Heart.* 1997;78:127-30.
 33. Grewal J, Majdalany D, Syed I, Pellikka P, Warnes CA. Three-dimensional echocardiographic assessment of right ventricular volume and function in adult patients with congenital heart disease: comparison with magnetic resonance imaging. *J Am Soc Echocardiogr.* 2010;23:127-33.
 34. Ishii M, Eto G, Tei C, Tsutsumi T, Hashino K, Sugahara Y, et al. Quantitation of the global right ventricular function in children with normal heart and congenital heart disease: a right ventricular myocardial performance index. *Pediatr Cardiol.* 2000;21:416-21.
 35. Norozi K, Buchhorn R, Alpers V, Arnhold JO, Schoof S, Zoega M, et al. Relation of systemic ventricular function quantified by myocardial performance index (Tei) to cardiopulmonary exercise capacity in adults after Mustard procedure for transposition of the great arteries. *Am J Cardiol.* 2005;96:1721-5.

36. Harada K, Toyono M, Yamamoto F. Assessment of right ventricular function during exercise with quantitative Doppler tissue imaging in children late after repair of tetralogy of Fallot. *J Am Soc Echocardiogr.* 2004;17:863-9. 1.
37. Salehian O, Burwash IG, Chan KL, Beauchesne LM. Tricuspid annular systolic velocity predicts maximal oxygen consumption during exercise in adult patients with repaired tetralogy of Fallot. *J Am Soc Echocardiogr.* 2008;21:342-6. 2.
38. Yasuoka K, Harada K, Toyono M, Tamura M, Yamamoto F. Tei index determined by tissue Doppler imaging in patients with pulmonary regurgitation after repair of tetralogy of Fallot. *Pediatr Cardiol.* 2004;25:131-6. 3.
39. Solarz DE, Witt SA, Glascock BJ, Jones FD, Khoury PR, Kimball TR. Right ventricular strain rate and strain analysis in patients with repaired tetralogy of Fallot: possible interventricular septal compensation. *J Am Soc Echocardiogr.* 2004;17:338-44. 4.
40. Toyono M, Harada K, Tamura M, Yamamoto F, Takada G. Myocardial acceleration during isovolumic contraction as a new index of right ventricular contractile function and its relation to pulmonary regurgitation in patients after repair of tetralogy of Fallot. *J Am Soc Echocardiogr.* 2004;17:332-7. 5.
41. Jategaonkar SR, Scholtz W, Butz T, Bogunovic N, Faber L, Horstkotte D. Two-dimensional strain and strain rate imaging of the right ventricle in adult patients before and after percutaneous closure of atrial septal defects. *Eur J Echocardiogr.* 2009;10:499-502. 6.
42. Khoo NS, Young A, Occleshaw C, Cowan B, Zeng IS, Gentles TL. Assessments of right ventricular volume and function using three-dimensional echocardiography in older children and adults with congenital heart disease: comparison with cardiac magnetic resonance imaging. *J Am Soc Echocardiogr.* 2009;22:1279-88. 7.
43. Eyskens B, Weidemann F, Kowalski M, Bogaert J, Dymarkowski S, Bijmens B, et al. Regional right and left ventricular function after the Senning operation: an ultrasonic study of strain rate and strain. *Cardiol Young.* 2004;14:255-64. 8.
44. Greutmann M, Tobler D, Biaggi P, Mah ML, Crean A, Oechslin EN, et al. Echocardiography for assessment of right ventricular volumes revisited: a cardiac magnetic resonance comparison study in adults with repaired tetralogy of Fallot. *J Am Soc Echocardiogr.* 2010;23:905-11. 9.
45. Koestenberger M, Ravekes W, Everett AD, Stueger HP, Heinzl B, Gamillscheg A, et al. Right ventricular function in infants, children and adolescents: reference values of the tricuspid annular plane systolic excursion (TAPSE) in 640 healthy patients and calculation of z score values. *J Am Soc Echocardiogr.* 2009;22:715-9. 10.
46. Abd El Rahman MY, Abdul-Khaliq H, Vogel M, Alexi-Meskishvili V, Gutberlet M, Lange PE. Relation between right ventricular enlargement, QRS duration, and right ventricular function in patients with tetralogy of Fallot and pulmonary regurgitation after surgical repair. *Heart.* 2000;84:416-20. 11.
47. Cheung EW, Lam WW, Cheung SC, Cheung YF. Functional implications of the right ventricular myocardial performance index in patients after surgical repair of tetralogy of Fallot. *Heart Vessels.* 2008;23:112-7. 12.
48. Lissin LW, Li W, Murphy DJ, Jr., Hornung T, Swan L, Mullen M, et al. Comparison of transthoracic echocardiography versus cardiovascular magnetic resonance imaging for the assessment of ventricular function in adults after atrial switch procedures for complete transposition of the great arteries. *Am J Cardiol.* 2004;93:654-7. 13.
49. Carabello BA. Evolution of the study of left ventricular function: everything old is new again. *Circulation.* 2002;105:2701-3. 14.
50. Alfakih K, Plein S, Thiele H, Jones T, Ridgway JP, Sivananthan MU. Normal human left and right ventricular dimensions for MRI as assessed by turbo gradient echo and steady-state free precession imaging sequences. *J Magn Reson Imaging.* 2003;17:323-9. 15.
51. Alfakih K, Thiele H, Plein S, Bainbridge GJ, Ridgway JP, Sivananthan MU. Comparison of right ventricular volume measurement between segmented k-space gradient-echo and steady-state free precession magnetic resonance imaging. *J Magn Reson Imaging.* 2002;16:253-8. 16.

1.
2.
3.
4.
5.
6.
7.
8.
9.
10.
11.
12.
13.
14.
15.
16.
17.
18.
19.
20.
21.
22.
23.
24.
25.
26.
27.
28.
29.
30.
31.
32.
33.
34.
35.
36.
37.
38.
39.

1. 52. Jenkins C, Chan J, Bricknell K, Strudwick M, Marwick TH. Reproducibility of right ventricular volumes and ejection fraction using real-time three-dimensional echocardiography: comparison with cardiac MRI. *Chest*. 2007;131:1844-51.
- 2.
3. 53. Redington AN, Rigby ML, Shinebourne EA, Oldershaw PJ. Changes in the pressure-volume relation of the right ventricle when its loading conditions are modified. *Br Heart J*. 1990;63:45-9.
4. 54. Yoshifuku S, Otsuji Y, Takasaki K, Yuge K, Kisanuki A, Toyonaga K, et al. Pseudonormalized Doppler total ejection isovolume (Tei) index in patients with right ventricular acute myocardial infarction. *Am J Cardiol*. 2003;91:527-31.
5. 55. Mertens LL, Friedberg MK. Imaging the right ventricle-current state of the art. *Nat Rev Cardiol*. 2010.
6. 56. Endorsed by the Association for European Paediatric C, Authors/Task Force M, Baumgartner H, Bonhoeffer P, De Groot NM, de Haan F, et al. ESC Guidelines for the management of grown-up congenital heart disease (new version 2010): The Task Force on the Management of Grown-up Congenital Heart Disease of the European Society of Cardiology (ESC). *Eur Heart J*. 2010.
7. 57. Tamborini G, Marsan NA, Gripari P, Maffessanti F, Brusoni D, Muratori M, et al. Reference values for right ventricular volumes and ejection fraction with real-time three-dimensional echocardiography: evaluation in a large series of normal subjects. *J Am Soc Echocardiogr*. 2010;23:109-15.
8. 58. van der Zwaan HB, Helbing WA, Boersma E, Geleijnse ML, McGhie JS, Soliman OI, et al. Usefulness of real-time three-dimensional echocardiography to identify right ventricular dysfunction in patients with congenital heart disease. *Am J Cardiol*. 2010;106:843-50.
9. 59. Kilner PJ, Geva T, Kaemmerer H, Trindade PT, Schwitter J, Webb GD. Recommendations for cardiovascular magnetic resonance in adults with congenital heart disease from the respective working groups of the European Society of Cardiology. *Eur Heart J*. 2010;31:794-805.
10. 60. Savino G, Zwerner P, Herzog C, Politi M, Bonomo L, Costello P, et al. CT of cardiac function. *J Thorac Imaging*. 2007;22:86-100.
- 11.
- 12.
- 13.
- 14.
- 15.
- 16.
- 17.
- 18.
- 19.
- 20.
- 21.
- 22.
- 23.
- 24.
- 25.
- 26.
- 27.
- 28.
- 29.
- 30.
- 31.
- 32.
- 33.
- 34.
- 35.
- 36.
- 37.
- 38.
- 39.



Chapter 3

Three-dimensional echocardiography in adult congenital heart disease

F.J. Meijboom
H.B. van der Zwaan
J.S. McGhie

In: Buck T, Franke A, Monaghan M, ed. Three-dimensional Echocardiography. Berlin: Springer-Verlag Berlin and Heidelberg GmbH & Co, November 2010. p175-199.

1. Due to the success of cardiac surgery in infancy and childhood, starting some 40 years ago and
2. improving ever since, the survival for patients with congenital heart disease has improved dra-
3. matically. Over 85% of all patients born with a congenital cardiac defect now survive beyond
4. childhood, often well into adult life. Many of these patients have residual abnormalities, which
5. may be morphological, functional or (most often) both, and these residua tend to change
6. with time. As an example, the patient with repaired tetralogy of Fallot will require long-term
7. monitoring of problems such as pulmonary regurgitation with consequent volume loading of
8. the right ventricle, ventricular dysfunction, and associated arrhythmias. Patients with repaired
9. coarctation will require monitoring of associated lesions, such as bicuspid aortic valve, aortic
10. valve stenosis/regurgitation, recurrent aortic arch obstruction, and systemic arterial blood
11. pressure. The result is that the vast majority of patients, who had their congenital cardiac
12. malformation “repaired” or “corrected” at a young age, require follow-up throughout childhood
13. and adult life. Imaging plays a major role in this follow-up. In current clinical practice, more than
14. 90% of the imaging involves echocardiography.

15. Echocardiography of congenital heart disease is often considered to be one of the most
16. difficult aspects of the technique. The examination should be performed by cardiologists,
17. pediatric cardiologists, or sonographers with great expertise and skill in this specific domain.
18. Most of these professionals are content with two-dimensional (2D) echocardiography and
19. are confident that they can image and evaluate even the most complex congenital cardiac
20. malformation. However, even experienced operators are often challenged by the spatial inter-
21. pretation of complex congenital cardiac malformations.

22. This is where three-dimensional (3D) imaging comes in as a very helpful technique: it can
23. show the anatomy of the heart as it is, in its real 3D nature. Even if 3D imaging is broadly acces-
24. sible and its understanding is more intuitive to a wider audience, ranging from medical students
25. to electrophysiologists and cardiac surgeons, RT3DE scanning of congenital malformations is
26. demanding and should remain in the hands of the more experienced subspecialized echocar-
27. diographers. Current 3D platforms have lower spatial and temporal resolution compared with
28. 2D echocardiography, but the added dimension enhances the understanding of congenital
29. heart defects. Unique projections, such as en face views of intracardiac structures, including
30. not only the semilunar and atrioventricular valves but also the interatrial and interventricular
31. septums, can be created using 3D echocardiograms.

32. Another very useful feature of 3D echocardiography is the possibility to image the entire
33. heart in one full volume dataset.¹ Off-line analysis allows crosssections through the heart in any
34. desired plane. For beginners in 3D analysis, it is very useful to start with the preprogrammed
35. orthogonal cross-sections: sagittal (right-left), coronal (anterior-posterior) and transverse
36. (superior-inferior) orientation. In most current 3D analysis systems, like Philips Qlab and in the
37. Tomtec Cardio View, these three planes can be shown in the multiplane representation (MPR)
38. view, together with a fourth image, in which these planes are shown in a 3D rendered view
39. (Figure 1).

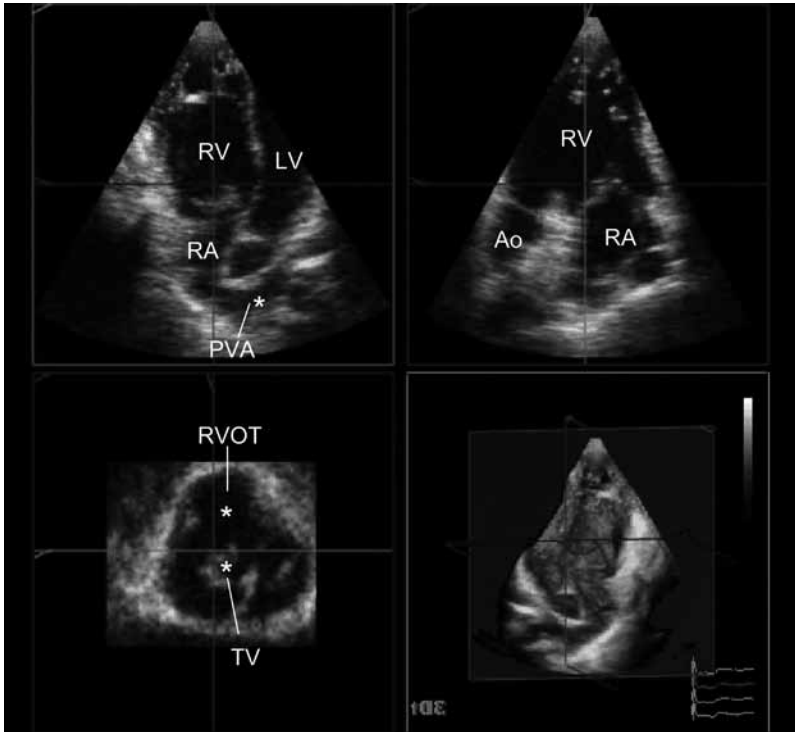


Figure 1 Example of multiplane representation (MPR) of three orthogonal cross-sectional planes from a full volume 3D dataset in a patient with transposition of the great arteries after a Mustard-type atrial switch. RV right ventricle, LV left ventricle, RA right atrium, PVA pulmonary venous atrium, RVOT right ventricular outflow tract, Ao aorta, TV tricuspid valve.

Apart from these three cross-sectional planes which can be moved and rotated in any direction, the anyplane mode allows cropping of the 3D image in any orientation or direction (Figure 2). It is no longer necessary to memorize or to mentally reconstruct the transducer position that was necessary to create the cross-section: this can be displayed visually.

Apart from the advantage that multiple 2D cross sections can be shown (and understood!) simultaneously in the 3D anatomy, the 3D hologram that can be produced (on the flat screen of the computer) allows visualization of the actual anatomy in its true 3D sense. For complex anatomy in particular, both the multiple 2D cross-sections visible in the 3D anatomy and the rendered 3D images have proven to be very useful to both expert users of 2D echocardiography as well as those having less experience. In current practice, real-time 3D echocardiography (RT3DE) has become an integral part of the analysis of congenital heart disease in many labs. If, in the future, 3D could match 2D echocardiography in terms of spatial and temporal resolution (which is mainly a matter of increased computing performance), then the role of 3D echocardiography is likely to increase further and the complementary nature of the techniques would be enhanced.

1.
2.
3.
4.
5.
6.
7.
8.
9.
10.
11.
12.
13.
14.
15.
16.
17.
18.
19.
20.
21.
22.

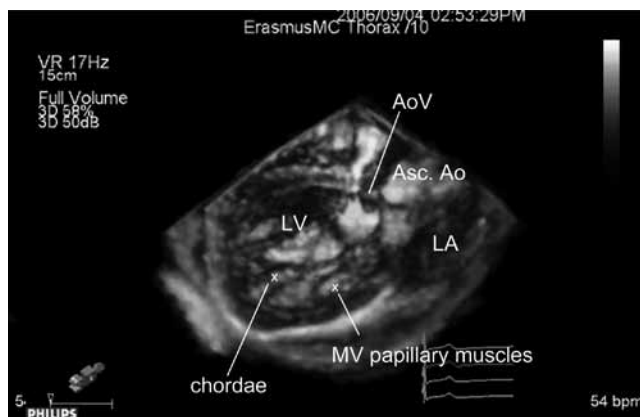
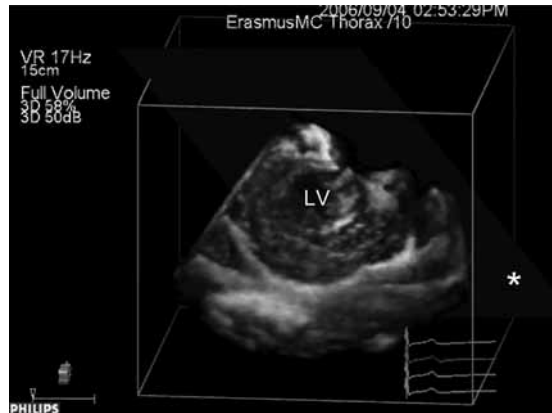


Figure 2 Example of cropping. Left The anyplane marked with an asterisk (*) – as seen in the crop box. Right The cross section that is made with this anyplane and the view into the heart from this anyplane is shown. LV left ventricle, LA left atrium, Asc Ao ascending aorta, AoV aortic valve, MV mitral valve.

26. Dedicated high-frequency pediatric probes are mandatory for transthoracic 3D echocardiographic studies in the pediatric age group, providing excellent results with image resolution
27. good enough to visualize even very thin and delicate intracardiac structures. High-frequency
28. 3D transducers (2–7 MHz) lack acoustic power and are not suitable for larger adult patients with
29. a congenital cardiac malformation. The image resolution of the lower frequency transducer,
30. mainly 1–3 MHz, sometimes 2–4 MHz, is certainly adequate for left ventricular (LV) volume
31. calculations. In congenital heart disease practice, reliable assessment of LV function by RT3DE
32. is important. The 2D analysis of LV function depends on assumptions about LV geometry, which
33. are not reliable in the often deformed left ventricles in patients with congenital heart disease.
34. Some have reported excellent correlation between RT3DE-derived LV volumes, ejection frac-
35. tion, and stroke volume with magnetic resonance imaging (MRI)-derived volumes.²⁻⁴ Reliable
36. measurement of right ventricular (RV) volumes and function would be of great help, since the
37. RV plays a more important role in congenital heart disease than in general cardiology. The last
38. section of this chapter will elaborate on RV analysis with 3D echocardiography. Application of
39.

transthoracic RT3DE for analysis of intracardiac morphology produces less spectacular images in adults than in the pediatric population due to the limited spatial resolution of the low-frequency transducers. Despite this limitation, it provides important additional information that cannot be obtained with 2D imaging, justifying its use to supplement 2D echocardiographic analysis. However, in all cases where a more detailed morphologic assessment is required a transesophageal RT3DE examination can be performed providing high quality 3D imaging.

Because of the enormous diversity of congenital heart disease (e.g., both unrepaired and repaired, with many different surgical techniques, creating different sequelae and residua) in adult patients, it is impossible to give a complete overview of the possibilities and added value of 3D echocardiography for all diagnostic categories. Instead, illustrative examples of congenital abnormalities that are common in adults are described in the following section with emphasis on the added value of 3D echocardiography in these cases.

PATENT FORAMEN OVALE

A patent foramen ovale (PFO) is present in approximately one third of the population and, therefore, is not considered as a congenital cardiac anomaly. Increasingly, it has become the focus of medical attention since transient ischemic attacks (TIAs), cerebral vascular accidents (CVAs), and migraine have been attributed to paradoxical embolization through a foramen ovale. The role of RT3DE is limited, since functional assessment, demonstration of right-to-left shunting through the foramen using echo contrast, is the essence of the diagnosis. However, the RT3D TEE en face view from the LA to the interatrial septum can be useful to detect the exact location of the shunt orifice. In selected cases, e.g., if an atrial septal aneurysm is present, RT3DE may contribute to assessing the exact anatomy of the interatrial septum and the extent of the fossa ovalis membranous aneurysm.

ATRIAL SEPTAL DEFECT

The nomenclature of atrial septal defects (ASD) has gradually changed over the past few decades. It used to be customary to differentiate between a primum and secundum type ASD, which is no longer done. The term primum ASD is considered obsolete and is classified as a partial atrioventricular septal defect (pAVSD) and is discussed always as such, because of the abnormality of the atrioventricular valves inherent to a partial AVSD. This section deals with secundum type ASD and sinus venosus defects.

The exact size and shape of ASDs and their exact position within the interatrial septum have become more important since transcatheter closure of ASDs has developed into a serious alternative to surgical closure. Not all defects are amenable for transcatheter closure: they should

1. not be too large, the rims should be sufficient to provide good anchoring of the device, and the
 2. defects should not be too close to important intracardiac structures, such as the mitral and tri-
 3. cuspid valves or orifices of veins that drain into the left or right atrium. In children, transthoracic
 4. 2D echocardiography is often diagnostic, because, in contrast to adult patients, the subcostal
 5. view can virtually always be used and it is this view that provides the most information. Without
 6. this view, 2D transesophageal echocardiography (TEE) is often indicated to identify all rims and
 7. the relation of the defect to relevant structures. Compared to this, transthoracic RT3DE provides
 8. an unlimited viewing perspective to the interatrial septum. The optimal 3D dataset is acquired
 9. from the subcostal position, but this is rarely feasible in adults. A foreshortened 4-chamber
 10. position or a parasternal long-axis view angulated to the right, with the ASD between the dot-
 11. ted lines and not further than 15 cm away from the transducer is next best option (Figure 3).

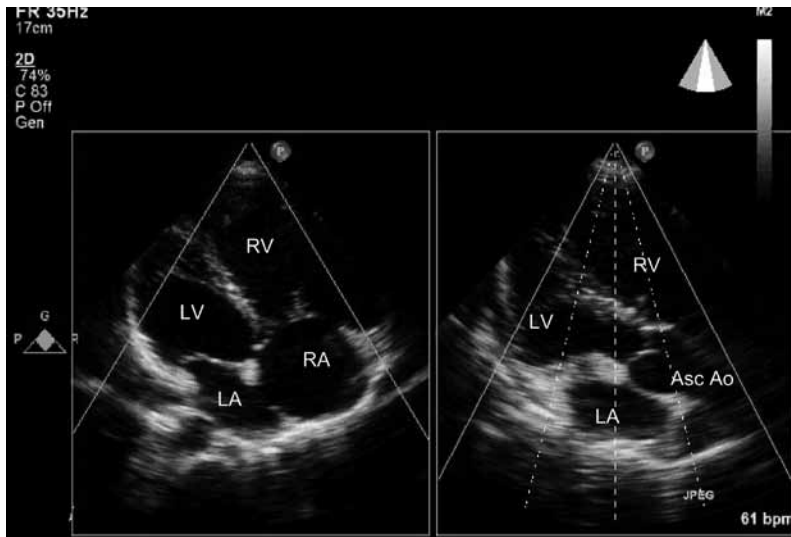


Figure 3 Left Foreshortened 4-chamber view. Right The dotted lines represent the subvolumes that will be acquired and stitched together to construct a full volume 3D dataset. RV right ventricle, LV left ventricle, RA right atrium, LA left atrium, RVOT right ventricular outflow tract, Asc Ao ascending aorta.

The added value that RT3DE has for analysis of an ASD is the possibility to create an en face view of the interatrial septum.^{5,6} The entire interatrial septum can be seen with the defect within it. It can be viewed and measured both from the left and right atrial side (Figure 4).

The rims around the defect can be seen in one view. From the right-sided view, distances to important anatomical landmarks (e.g., the tricuspid valve, the ostium of the coronary sinus, and the ostia of the caval veins) can be measured. Mathewson et al⁷ proposed a standardized orientation and nomenclature for the rims (Figure 5).

Something that is difficult to appreciate with 2D echocardiography – the change of the size of the ASD during the cardiac cycle – is easy to see in the en face view using RT3DE.^{6,8} The area

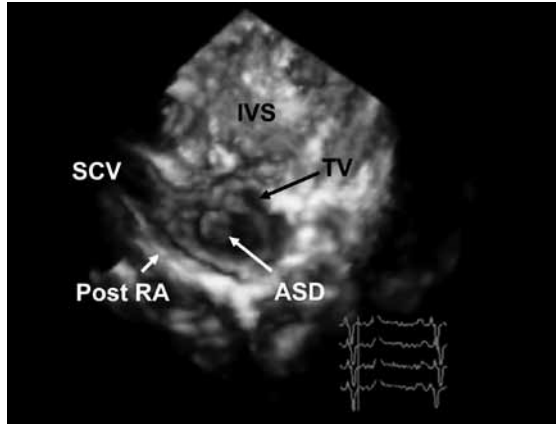


Figure 4 The right lateral view onto the interatrial septum reveals a large, centrally located ASD II with adequate rims around the defect. The patient is probably a good candidate for transcatheter closure. SCV superior vena cava, IVS interventricular septum, TV tricuspid valve, ASD atrial septal defect, Post RA posterior right atrial wall.

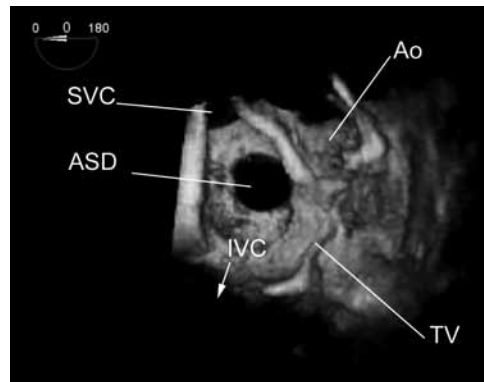
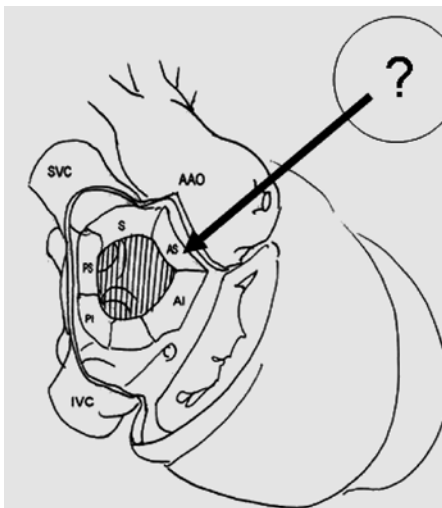


Figure 5 Right atrial view as proposed by Mathewson et al. Left In the schematic drawing, all rims can be identified, except the anterior-superior rim, indicated by the question mark. It is not possible to differentiate between the real anterior-superior rim and the wall of the aortic sinus. Copyright Elsevier. Right For comparison, the RT3DE image of the right atrial view is shown. SVC superior vena cava, AAO ascending aorta, IVC inferior vena cava, ASD atrial septal defect, Ao aorta, TV tricuspid valve.

of the defect is largest during atrial relaxation and is smallest during atrial contraction. During atrial contraction, the area was reported to >50% smaller than during atrial relaxation.⁹ This implies that the choice for the size of a closure device should be based on the measurement during atrial relaxation, when the ASD is at its largest.

In patients who have sufficient transthoracic echocardiographic (TTE) image quality, a RT3DE study might provide all the answers to the questions about feasibility of transcatheter closure

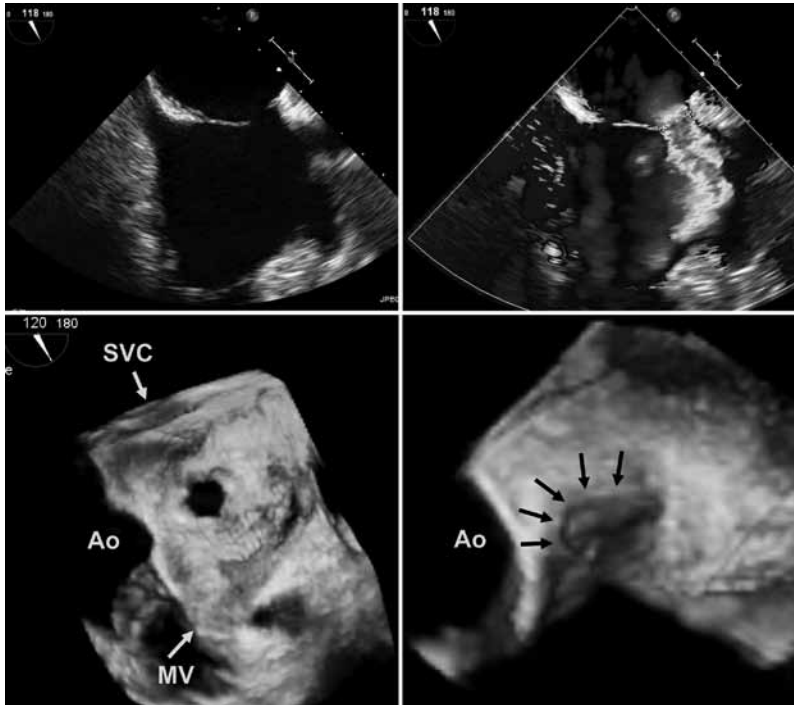


Figure 6 Comparison of transesophageal 2D versus live 3D representation of an ostium secundum ASD with a small rim towards the aortic wall (anterior-superior). The 3D en face view from the left atrium towards the interatrial septum (IAS) shows the exact shape and size of the defect and its anterior-superior location in the IAS (bottom left). The zoomed 3D representation allows exact detection of the extent and width of the anterior-superior rim and its relation to the aortic wall (bottom right). SVC superior vena cava, Ao aortic root, MV mitral valve.

and a TEE might be omitted.⁸ However, besides RT3D TTE with all its additive information, RT3D TEE provides far more detailed information about spatial relationships of atrial septal defects and surrounding structures (Figures 6, 7, and 8) as well as much higher spatial resolution for more accurate quantification of ASD size (Figure 11).

Because of the above stated additional information that 3D echocardiography provides, we believe that RT3DE should be included in all echocardiographic work-ups of ASDs, in addition to the standard modalities, especially when transcatheter closure is considered. RT3D TEE, apart from offering additional diagnostic accuracy because of its superior image resolution when compared with RT3D TTE, can be used as guidance for device closure of the defect.

VENTRICULAR SEPTAL DEFECT

The interventricular septum (IVS) has a complex, curved shape, which cannot be visualized in its entirety in a single 2D plane. It is again the en face view of the IVS that brings added value

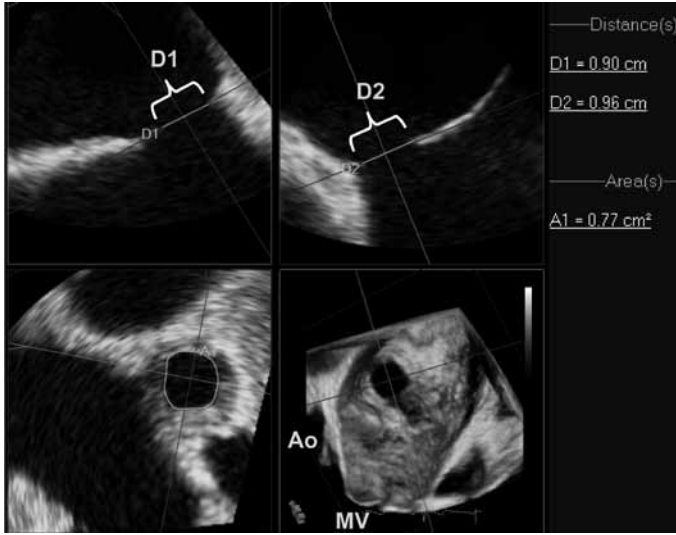


Figure 7 The 3D measurement of atrial septal defect (ASD) diameters and area in the same case as shown in Figure 6. Ao aortic root, MV mitral valve.

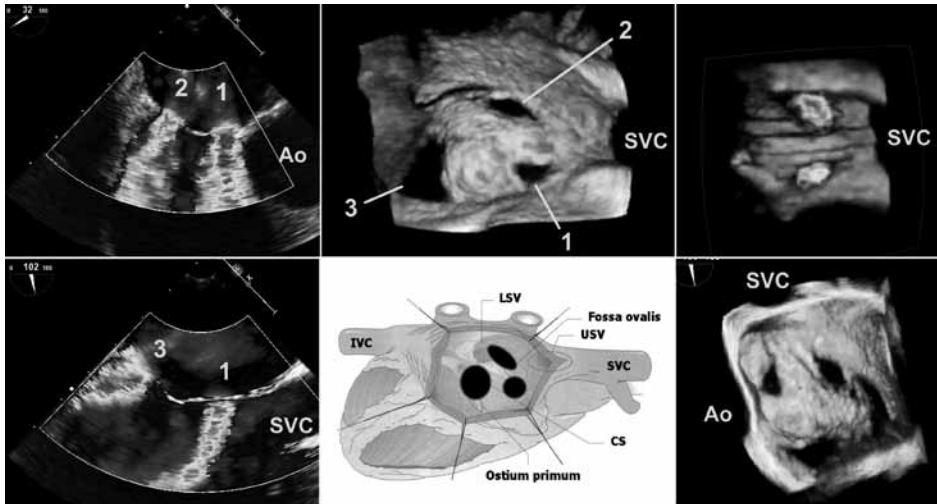


Figure 8 Example of 2D TEE and RT3D TEE representation of a multifenestrated ASD. Because 2D TEE showed two defects in the 32° rotation (top left) and two defects in the 102° rotation (bottom left), there had to be at least three defects that could not be visualized in one 2D image plane. The RT3DE en face view from the right atrium (top middle) and from the left atrium to the interatrial septum (IAS) (bottom right) clearly visualized the orientation of the three defects to each other as well as the location within the IAS and the spatial relation to surrounding cardiac structures. RT3D color Doppler en face view from the right atrium clearly identifies the flow passing through the three defects (top right). Defect 1 (1) is located anterior-superior, defect 2 (2) posterior-superior, and defect 3 (3) anterior-inferior. The RT3DE en face view from the right atrium to the IAS shows the location of the three defects on a nonplanar, domed IAS which makes 2D representation and planimetry of each defect very difficult (top middle). Ao aortic root, SVC superior vena cava, IVC inferior vena cava, LSV lower sinus venosus, USV upper sinus venosus, CS coronary sinus.

1.
2.
3.
4.
5.
6.
7.
8.
9.
10.
11.
12.
13.
14.
15.
16.
17.
18.
19.
20.
21.
22.
23.
24.
25.
26.
27.
28.
29.
30.
31.
32.
33.
34.
35.
36.
37.
38.
39.

- 1.
- 2.
- 3.
- 4.
- 5.
- 6.
- 7.
- 8.
- 9.
- 10.
- 11.
- 12.
- 13.
- 14.
- 15.
- 16.
- 17.
- 18.
- 19.
- 20.
- 21.
- 22.
- 23.
- 24.
- 25.
- 26.
- 27.
- 28.
- 29.
- 30.
- 31.
- 32.
- 33.
- 34.
- 35.
- 36.
- 37.
- 38.
- 39.



Figure 9 The 3D measurement of each of the three ASDs demonstrated in Figure 8 is shown. Note that the spatial orientation of the three cross-sectional planes must be individually adjusted for each defect.

by showing its curved structure, the ventricular septal defect (VSD) within it, and the relation to other intracardiac structures. The spatial relationship of the VSD to other parts of the intracardiac anatomy can directly be assessed during data acquisition or off-line in one 3D dataset.¹⁰⁻¹³

Transthoracic datasets are acquired from the apical 4-chamber position and from the parasternal long-axis view. The subcostal view is very rewarding, but can be challenging to obtain in adult patients.

During cropping of the 3D dataset, the images from the left ventricle onto the IVS and the VSD are easier to obtain than the images from the right side of the IVS. From the left side, the defect is directly visible, showing its exact location, size, and relation to landmark structures like the mitral and aortic valves (Figures 10, 11, and 17). The problem with the view from the right side of the

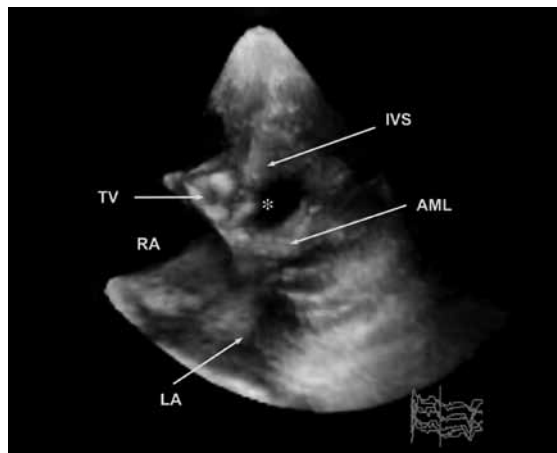


Figure 10 Example of transthoracic RT3DE representation of a large membranous VSD (*) in a non-operated 61-year-old woman with Eisenmenger's syndrome and severe right heart dilatation. TV tricuspid valve, RA right atrium, IVS interventricular septum, AML anterior mitral leaflet, LA left atrium.

heart for the most common form of the VSD, the perimembranous VSD, is the fact that the right side of the VSD is partially (if not entirely) covered by the septal leaflet of the tricuspid valve, its chordae, and papillary muscles. Only by digitally "cutting away" these structures that obscure the view can the VSD be visualized in a 3D fashion from the right side. In addition, muscular VSDs are usually better seen from the left side of the heart, where the IVS has a rather smooth wall, than from the right side of the heart. The many, coarse trabeculation on the right side of the IVS can obscure the defect (Figures 12 and 13). If the 3D en face view from the right side of the IVS does not provide the desired information, scrolling of a 2D cutting plane from right to left (and vice versa) through the IVS is helpful to find the delineation of the borders of the VSD.

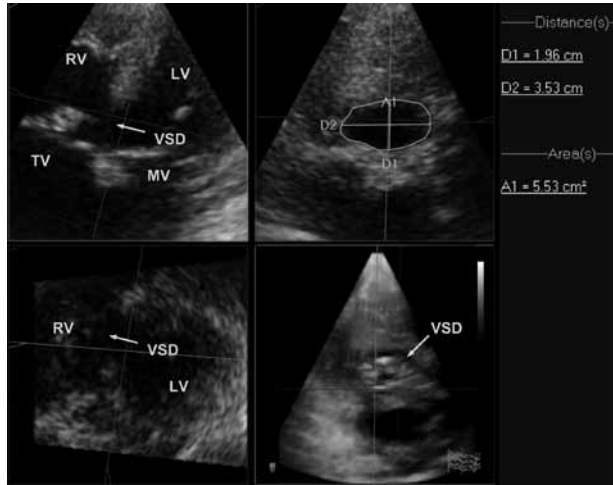


Figure 11 Representation of the same ventricular septal defect (VSD) shown in Figure 10 in three cross-sectional planes, allowing exact detection of the VSD and measurement of diameters and area. The RT3DE en face view from the left ventricle (LV) to the interventricular septum (IVS) shows the exact size, shape, and location of the VSD as well as a view through the VSD to the tricuspid valve (TV) behind it. RV right ventricle, MV mitral valve.

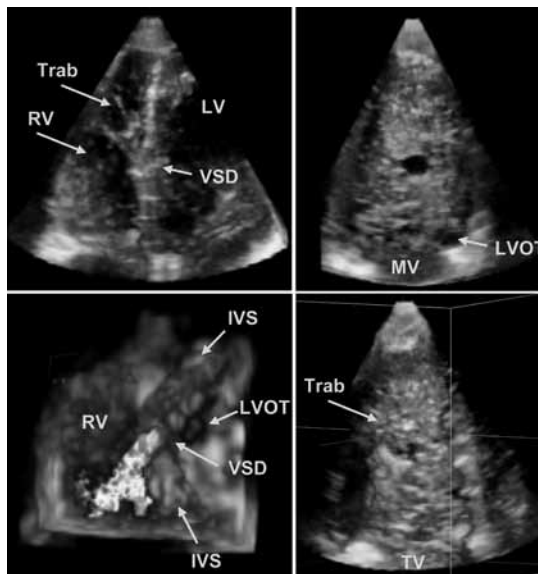


Figure 12 Example of transthoracic RT3DE representation of a small muscular ventricular septal defect (VSD) which is covered by marked trabeculation (Trab) on the right ventricular side of the interventricular septum (IVS; top left). The 3D en face view from the left ventricle (LV) to the IVS provides clear visualization of size, shape, and location of the VSD (top right), whereas the en face view from the right ventricle (RV) to the VSD is obscured by the trabeculation (bottom right). The 3D color Doppler short-axis view from the apex to the IVS shows the eccentric direction of shunt flow through the VSD (bottom left). LVOT left ventricular outflow tract, MV mitral valve, TV tricuspid valve.

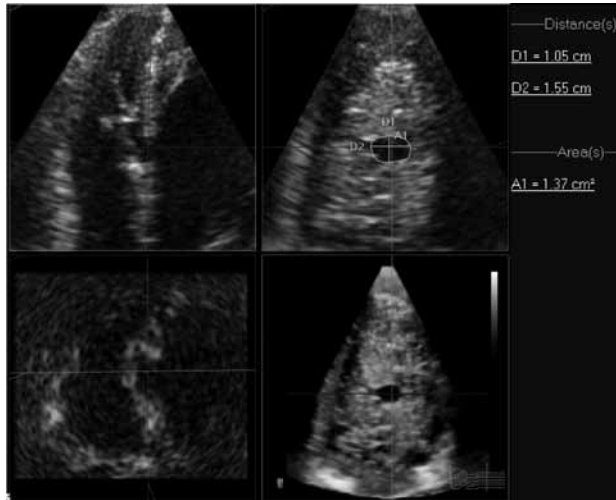


Figure 13 Multiplane representation of the same muscular VSD shown in Figure 12 with 3D measurement of the diameters and area.

ATRIOVENTRICULAR SEPTAL DEFECTS

RT3DE analysis of an atrioventricular septal defect (AVSD) is extremely rewarding.¹⁴⁻¹⁶ Adult patients with an AVSD can have a defect repaired in childhood or an unrepaired form of AVSD. Patients with an AVSD, repaired or unrepaired, either complete or incomplete, invariably have abnormalities at the level of the atrioventricular valves: the essence of an AVSD is that it has a common atrioventricular junction, guarded by five leaflets (right mural leaflet, anterior-superior leaflet, superior (or anterior) bridging leaflet, left mural leaflet, and inferior (or posterior) bridging leaflet). In the complete form, there is only one orifice between atria and ventricles (Figures 14 and 15). The septal defect of an AVSD is one large defect, extending both into the interatrial and into the interventricular septum, and should not be confused with separate atrial and ventricular septal defects that happen to be adjacent. This can occur in the presence of normal atrioventricular valves, but the anatomy is completely different from an AVSD. In partial AVSD, there is fusion of the anterior and posterior bridging leaflet in the midline, where these two leaflets are also attached to the intact interventricular septum. This creates a separate left and right valve opening, in what is anatomically still one common atrioventricular junction. An incomplete AVSD or a surgically repaired complete AVSD has two atrioventricular orifices, but these should not be confused with the mitral and tricuspid valves. The entirely different anatomy is difficult to appreciate with 2D echocardiography, but is unmistakable with the en face view of the valves that is only possible with 3D echocardiography. The en face view from the ventricular side is usually of a better quality than the view from atrial side. This is unfortunate, since a good surgical view can rarely be produced with adequate image quality. RT3D TEE is able to provide these images. The size and shape of the septal defects can be depicted in an excellent manner with transthoracic 3D echocardiography.

1.
2.
3.
4.
5.
6.
7.
8.
9.
10.
11.
12.
13.
14.
15.
16.
17.
18.
19.
20.
21.
22.
23.
24.
25.
26.
27.
28.
29.
30.
31.
32.
33.
34.
35.
36.
37.
38.
39.

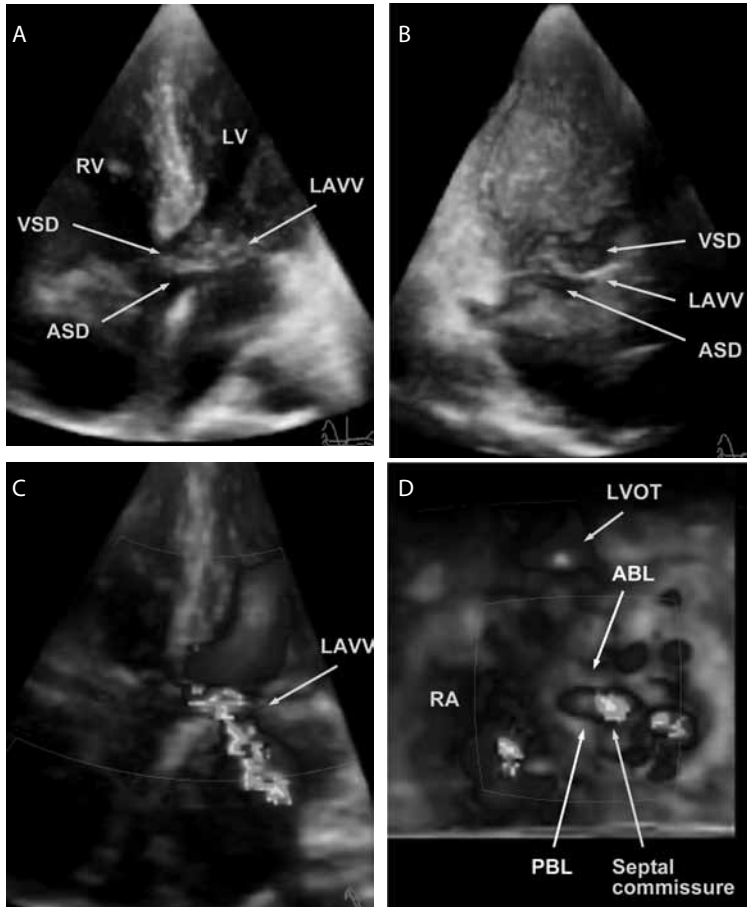


Figure 14 Example of a complete AVSD in a 46-year-old woman. The septal commissure, often (but actually erroneously) referred to as “cleft” in the left atrioventricular valve (LAVV) is indicated with an arrow. Top right The 3D en face view from left ventricle (LV) to the interventricular septum (IVS) shows clearly the atrial side of the AVSD below the LAVV and the ventricular side of the AVSD above the LAVV. Bottom left The 3D color Doppler 4-chamber view shows the regurgitant jet through the septal commissure in a typical location. Bottom right The 3D color Doppler short-axis en face view from the apex to the base shows the LAVV with a posterior bridging leaflet (PBL), an anterior bridging leaflet (ABL) and a septal commissure pointing to the ventricular septum. RV right ventricle, RA right atrium, ASD atrial septal defect, VSD ventricular septal defect, LVOT left ventricular outflow tract.

In patients with AVSD, a septal commissure can erroneously be described as a “cleft” (Figure 14). However, several characteristic differences between the two exist. In AVSD, the clues are (1) characteristic interatrial communication, (2) a common atrioventricular junction, (3) no differential insertion of AV valves, (4) the line of apposition between the superior and inferior bridging leaflets points to the ventricular septum, and (5) the mural leaflet of the left AV valve is typically small and relatively triangular in shape. Whereas in a real cleft mitral valve (Figure 16), characteristic clues include the following: (1) the cleft typically runs toward the aortic valve,

(2) there are separate AV valves and a normal morphology of the right (tricuspid) valve, (3) no “primum” atrial communication exists, (4) the cleft never crosses the ventricular septum, and (5) differential insertion of the AV valves is usually maintained.

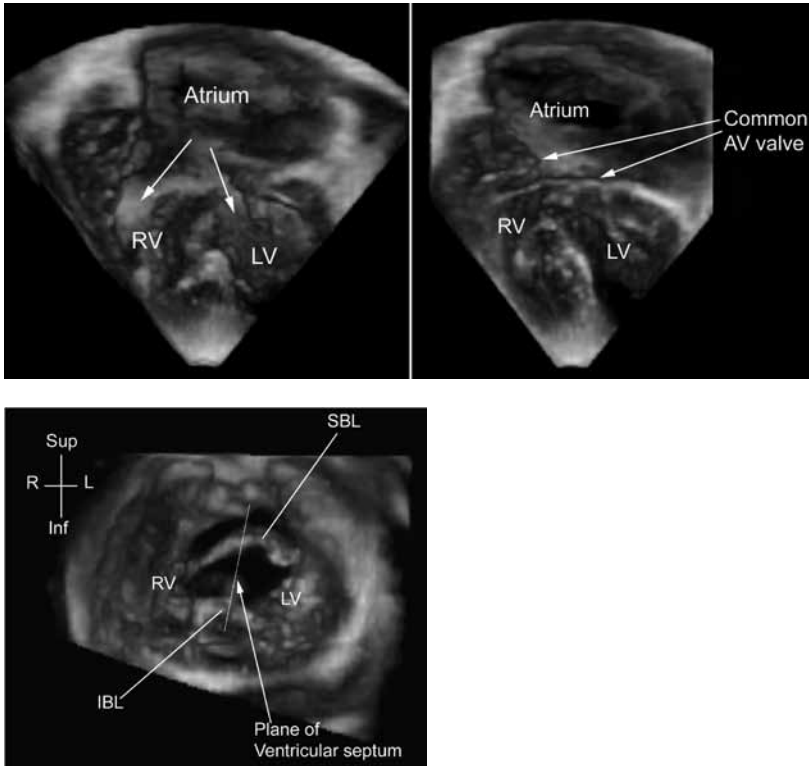


Figure 15 A Complete atrioventricular septal defect with a common atrium in an 11-year-old patient. Left The common atrioventricular valve is shown in an open position with the left and right ventricular components (arrows). Right The 4-chamber view demonstrates the common atrioventricular (AV) valve in the closed position. There is no differential insertion of left and right ventricular components. B The en face view of the common atrioventricular junction from the ventricular aspect of the common atrioventricular valve is shown. The superior bridging leaflet (SBL) and inferior bridging leaflet (IBL) are indicated. These leaflets “bridge” across the plane of the ventricular septum (marked by the line). LV left ventricle, RV right ventricle, L left, R right, Sup superior, Inf inferior.

EBSTEIN'S ANOMALY

Echocardiographic analysis of the tricuspid valve (TV) is notoriously difficult. In the standard 2D echocardiographic views, only two leaflets are visible and it can be difficult to differentiate between the septal and the postero-inferior leaflet.¹⁷ TEE is sometimes very helpful in the evaluation of the tricuspid valve, but since the TV is positioned anteriorly, away from the transducer located in the esophagus, the results can be disappointing. In adults, the transgastric

1.
2.
3.
4.
5.
6.
7.
8.
9.
10.
11.
12.
13.
14.
15.
16.
17.
18.
19.
20.
21.
22.
23.
24.
25.
26.
27.
28.
29.
30.
31.
32.
33.
34.
35.
36.
37.
38.
39.

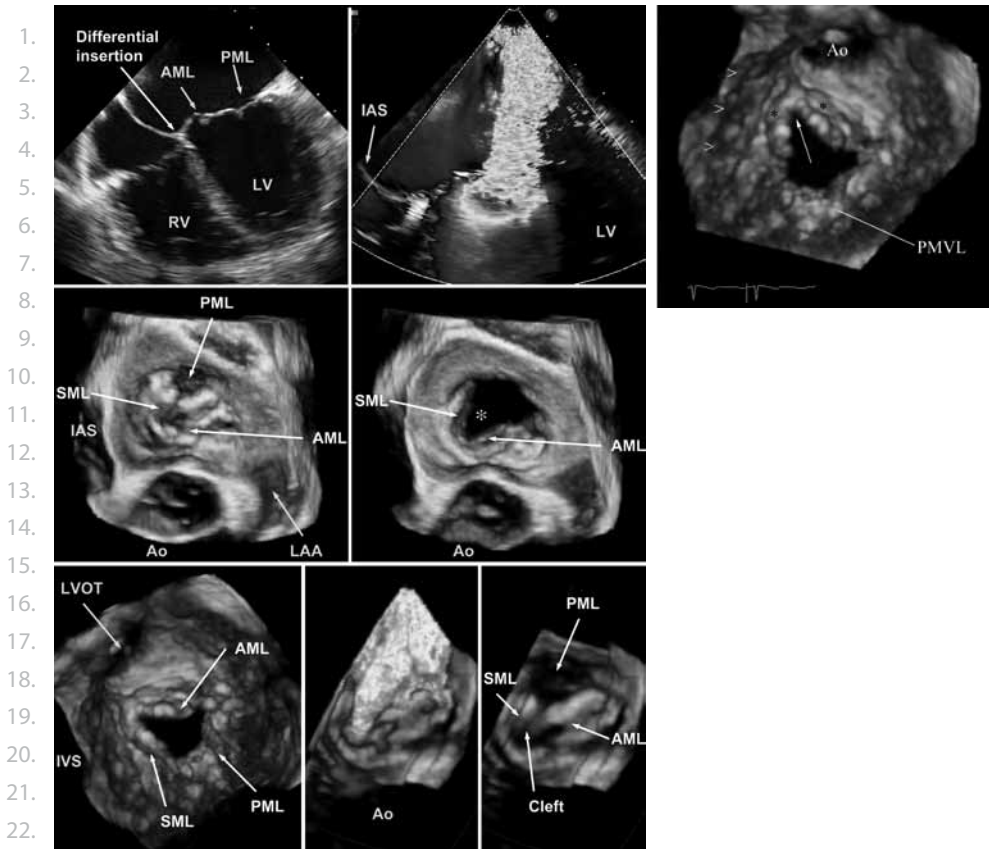


Figure 16 A Transesophageal 2D and RT3DE representation of a true cleft mitral valve with severe regurgitation in a 26-year-old woman. Top left The 2D image clearly depicts differential insertion of atrioventricular valves suggesting a real cleft. The RT3DE en face view from the left atrium to the mitral valve (middle row) shows the prolapsing mitral valve with the cleft (*), a septal (SML), anterior (AML) and posterior mitral leaflet (PML) in systole (middle left) and diastolic opening (middle right). The 3D en face view from the apex to the mitral valve clearly shows the cleft and the chordae attachment to the SML and AML (bottom left). The 3D en face view from the left atrium towards the cleft MV with color Doppler (bottom middle) and without color Doppler (bottom right) clearly depicts the anatomy of the regurgitant lesion. B Magnified view of the true cleft in the anterior leaflet of the mitral valve (arrow). Note that the cleft is orientated toward the aorta and does not extend to the ventricular septum (>). The posterior mitral valve leaflet (PMVL) is indicated. The asterisks (*) mark the two parts of the cleft anterior mitral valve leaflet. RV right ventricle, LV left ventricle, IAS interatrial septum, Ao aortic root, LAA left atrial appendage, LVOT left ventricular outflow tract.

view is helpful for the evaluation of the TV with TEE. If the tricuspid valve is abnormal, as in the case of Ebstein's anomaly, the most common congenital malformation of the tricuspid valve, it becomes even more difficult.

The transthoracic acquisition of 3D data with the TV as the region of interest is best achieved from the apical or foreshortened 4-chamber position. It will encompass the entire tricuspid valve. A high parasternal view with the transducer angulated to the right towards the right hip

can also provide a useable 3D dataset. In a 3D dataset acquired from these positions, Ebstein's malformation of the TV can be analyzed. The leaflets, their attachment to the septum and to the anterior wall, and the degree displacement of the functional TV orifice towards the pulmonary valve or the apex can be seen (Figures 17 and 18).

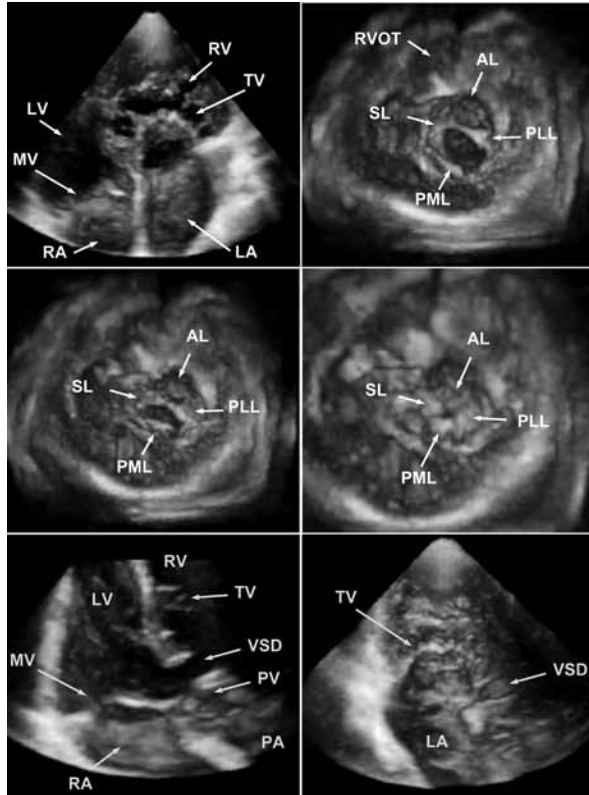
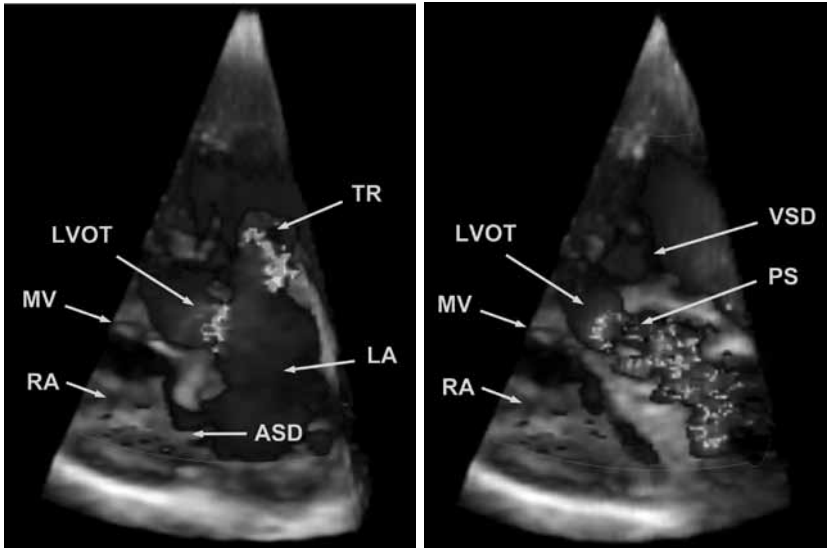


Figure 17 Example of transthoracic RT3DE representation of Ebstein's disease in a 22-year-old woman with congenitally corrected transposition of great arteries (ccTGA) in combination with a perimembranous ventricular septal defect (VSD) and pulmonary valve (PV) stenosis. The 3D en face view from the apex to the tricuspid valve (TV) reveals detailed information about TV leaflet anatomy during valve opening (top right), valve mid closure (middle left), and complete closure (middle right) showing four leaflets: a septal (SL), anterior (AL), posteromedial (PML) and postero-lateral (PLL) with the SL and the PLL connected by a bridge like a natural Alfieri stitch. A modified 3D 5-chamber view clearly shows the spatial relation between the VSD, the LVOT, and the stenotic PV (bottom left). The 3D en face view from the right ventricle (RV) to the interventricular septum shows the exact size, shape, and location of the VSD (bottom right). LV left ventricle, MV mitral valve, RA right atrium, LA left atrium, RVOT right ventricular outflow track, PA pulmonary artery.

To assess the size and (sometimes very irregular) shape of the actual TV orifice – often remote from the anatomic TV annulus – an en face view is very helpful (Figure 17).¹⁸ However, creating this en face view can be very challenging; there is no standardized approach due to the wide

1.
2.
3.
4.
5.
6.
7.
8.
9.
10.
11.
12.
13.
14.



15. **Figure 18** The RT3DE color Doppler information in the same patient with Ebstein's disease shown in
16. Figure 17. The 3D color Doppler reveals not only mild tricuspid regurgitation (TR) but also a secundum
17. type ASD in the same view (left). The flow propagation zone entering through the left ventricular outflow
18. tract (LVOT) into the LA is an illusion (left), with the flow propagation belonging to the pulmonary valve
19. stenosis (PS) as shown in the 3D view cropped more anteriorly (right) with depiction of flow through the
20. VSD. MV mitral valve, RA right atrium, LA left atrium, ASD atrial septal defect, VSD ventricular septal defect.

21. variety of the degree and direction of displacement of the TV opening. Once a good en face
22. view is obtained, not only the orifice can be seen but also the sail-like anterior-superior leaflet
23. is visualized. In the same view, the right ventricular anterior wall and the presence (or absence)
24. of attachment of the anterosuperior leaflet to the RV free wall can be judged. The en face view
25. can be used for planimetry of the orifice, which is relevant in case of TV stenosis.

26. Both the en face and the right lateral views will provide extra anatomical information in
27. addition to that from the 2D analysis. Combination of RT3DE with color Doppler provides more
28. insight into the mechanism of tricuspid regurgitation. In our experience, the TV and Ebstein's
29. disease are more difficult to assess (even with 3D echocardiography) than abnormalities situ-
30. ated on the left side of the heart. However, actually seeing, in one image, that a tricuspid valve
31. has three leaflets is already an improvement over 2D imaging.¹⁸

32.
33.

34. **TRANSPOSITION OF THE GREAT ARTERIES**

35.

36. In adult congenital heart disease, almost all patients with a simple transposition of the great
37. arteries (TGA) have had either a Mustard or a Senning atrial switch procedure. The LV sustains
38. the (low-resistance) pulmonary circulation and has, as a consequence, low systolic pressure.
39. The RV sustains the systemic circulation and has systemic ventricular pressures. Due to these

pressure differences, the ventricular septum bulges to the left and the LV is squashed behind the high-pressured RV. Assessment of LV ejection fraction by 2D echocardiography is not very reliable in these patients, because the assumptions underlying Simpson's biplane planimetry method (round shape and concentric contractions) are not valid in abnormally shaped, squashed LVs. It has been reported that RT3DE can measure LV function more reliably than 2D echocardiography in these circumstances.³ Assessment of RV function remains difficult. The systemic RV lies anteriorly in the chest and is, in adults, very often dilated. From an apical 4-chamber position, it is a challenge to encompass the entire RV in a 3D dataset. Analysis of RV function with dedicated software is difficult, but sometimes feasible (it is addressed separately at the end of this chapter).

The anatomy of atrioventricular and semilunar valves is usually normal and the interventricular septum is most often intact; RT3DE has nothing extra to offer in this respect. "Piece de resistance" in the echocardiographic analysis of a patient with a Mustard or Senning repair is the analysis of the systemic venous pathways that are created to connect the superior and inferior vena cava with the left atrium. These intraatrial tunnels are usually referred to as atrial baffles (Figure 19).

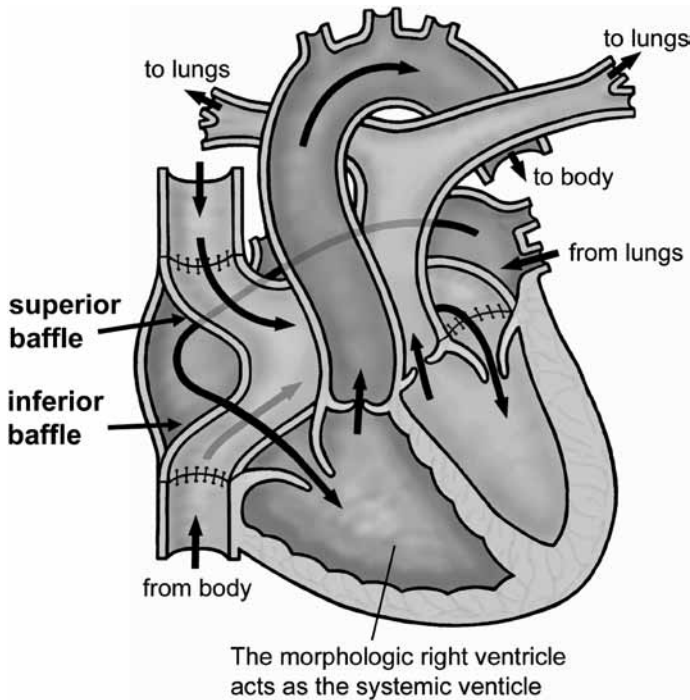
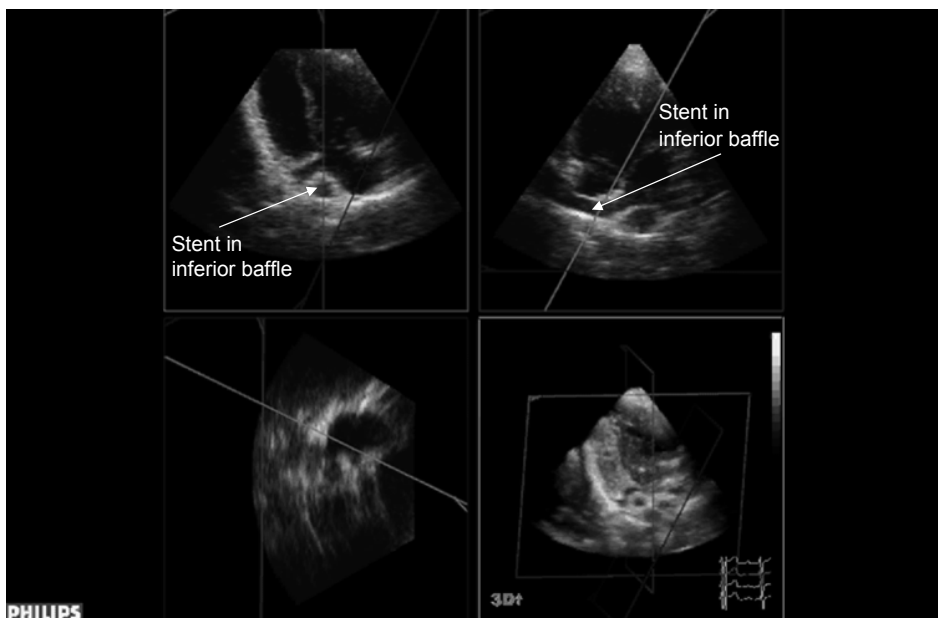


Figure 19 A schematic drawing of an atrial switch according to Mustard. The baffles are the intratunnels created by the surgeon to transport the systemic venous return from the superior and inferior vena cava towards the left atrium and the mitral valve in such a way that the pulmonary veins, which enter the posterior wall of the left atrium, have unobstructed communication with the right atrium.

1. Many (sometimes even very experienced sonographers and cardiologists) have difficulties
 2. in understanding how the atrial baffles actually run inside the right atrium, how they are related
 3. to each other, how they drain into the remains of the left atrium, and how they relate to the
 4. pulmonary veins. These pulmonary veins drain, unaltered and untouched by the surgical procedure,
 5. into the posterior wall of the left atrium. The pulmonary venous blood is directed toward
 6. the right atrium and should not be obstructed by the atrial baffles. RT3DE of an atrial switch
 7. repair is a good example how 3D echocardiography can be used in the analysis of complex
 8. anatomy. Analysis using the MPR mode in which the three orthogonal cross sections are shown
 9. together with the 3D dataset is the first very helpful step in the analysis of a transposition after
 10. atrial switch (Figure 20).



11.
 12.
 13.
 14.
 15.
 16.
 17.
 18.
 19.
 20.
 21.
 22.
 23.
 24.
 25.
 26.
 27. **Figure 20** TGA after Mustard type atrial repair and stent in inferior baffle as treatment of baffle stenosis.
 28. The multiplane view is shown. The angles of the cutting planes are seen in the 3D image (right bottom).
 29. The relation between the green plane and red plane is better visualized in the upper images.
 30.

31.
 32. By scrolling through the sagittal plane from posterior to anterior, the inferior baffle is seen
 33. first, with its course almost purely from right to left (Figure 20). At this level, the pulmonary
 34. venous atrium is seen, posterior from this inferior baffle, with the left pulmonary veins draining
 35. from the left lateral side into this compartment. If one scrolls slightly more towards the anterior,
 36. the inferior baffle disappears from this plane and the right pulmonary veins can now be seen
 37. entering the pulmonary venous atrium as well as the connection between the pulmonary
 38. venous atrium and the right atrium (Figure 21).
 39.

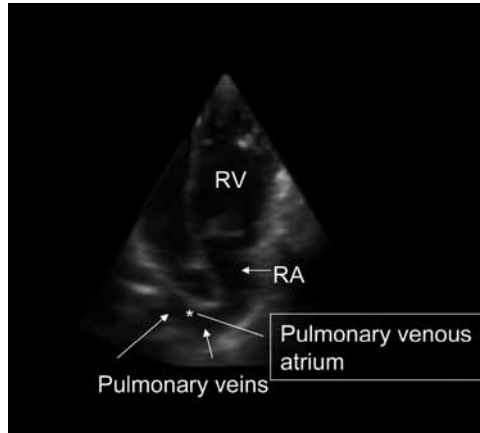


Figure 21 A cross section through the 3D dataset mimicking an apical 4-chamber view in a patient with TGA after Mustard repair. The pulmonary veins are shown along with the connection to the right atrium. Atrial baffles are not seen in this view, because they are in other levels. If one would scroll through the dataset more towards the posterior, the inferior baffle would be seen. Scrolling more anteriorly would show the superior

Most of these 2D cross-sections, now derived from the 3D dataset, can be acquired during the standard 2D echocardiographic workup, implicating that there would be no real added value of RT3DE. However, in our experience, the added value consists of the possibility to establish and appreciate, off-line, the exact level and orientation of these cross-sections in the intracardiac anatomy. Both superior and inferior baffles can be followed over their course, from the caval veins to their entrance in the remnants of the original left atrium. If a baffle stenosis is present, the area and length of a narrowed segment in the baffle can be seen and measured with planimetry. If a patient with TGA after a Mustard or Senning type repair has an endocardial pacemaker, the superior vena cava and the superior baffle are identified easily because they contain a pacemaker wire. If a patient has a stent in the superior or inferior baffle, identification of the anatomic structure that contains the stent is easier (Figure 20).

For patients with a complex transposition and a Rastelli type repair, the intracardiac conduit from the left ventricle towards the anteriorly positioned aortic valve can be visualized and shown in relation to the adjacent structures. It is difficult, just as in 2D echocardiography, to assess the conduit from the right ventricle to the pulmonary artery, because of its anterior-superior position in the chest, just behind the sternum.

CONGENITALLY CORRECTED TRANSPOSITION OF THE GREAT ARTERIES

The now preferred name for this rare anomaly is atrioventricular and ventriculoarterial discordance, but in clinical practice it is still often referred to as congenitally corrected transposition of the great arteries (ccTGA). A more modern term is doubledisco heart.

1.
2.
3.
4.
5.
6.
7.
8.
9.
10.
11.
12.
13.
14.
15.
16.
17.
18.
19.
20.
21.
22.
23.
24.
25.
26.
27.
28.
29.
30.
31.
32.
33.
34.
35.
36.
37.
38.
39.

1. It is a challenge to analyze these patients with 2D echocardiography. A former echocardiographic definition was "if you lose your way in a heart, it is a ccTGA." The most difficult part was the identification of the connections between the ventricles and the great arteries: in one plane it might look that the aorta was connected to the right ventricle (RV) and in another view it looked as if the pulmonary artery was connected to the RV. The advantage of 3D echocardiography is that the entire anatomy is in a full volume 3D dataset and the anatomic relations and connections of the great arteries can be showed unequivocally. In Figures 22, 23, and 24, illustrations are shown that demonstrate the added value of 3D echocardiography in the case of complex anatomy.

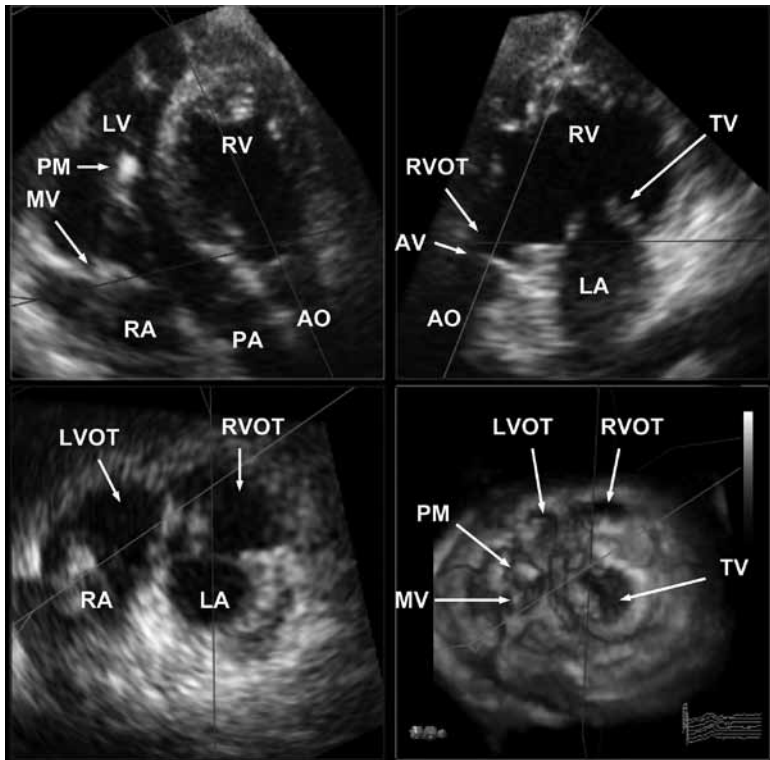


Figure 22 Transthoracic RT3DE dataset with multiplane representation in a 42-year-old woman with ccTGA with the aortic valve (connected to RVOT) left and anterior (bottom right). Individual orientation of the three image planes (red, green, blue) allows for the most comprehensive crosssectional representation of the abnormal anatomic relationships. LV left ventricle, RV right ventricle, RA right atrium, LA left atrium, MV mitral valve, TV tricuspid valve, LVOT left ventricular outflow tract, RVOT right ventricular outflow tract, AO aorta, PA pulmonary artery, PM pacemaker lead.

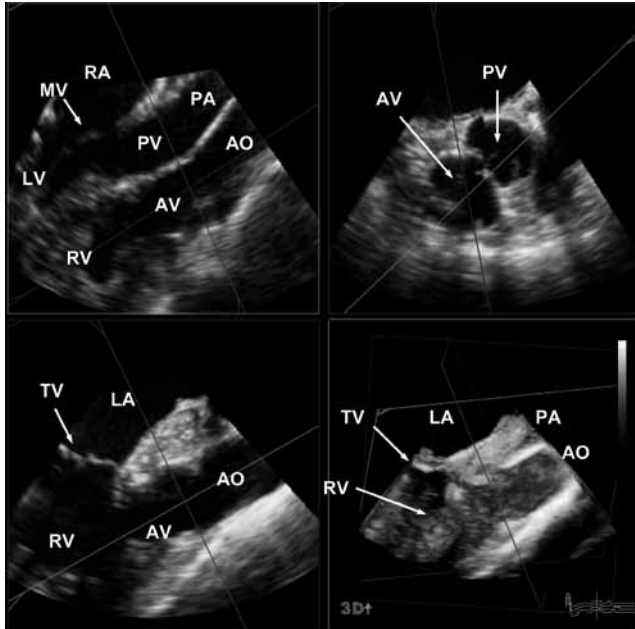


Figure 23 Transesophageal RT3DE dataset with multipane representation in the same patient with congenital corrected TGA shown in Figure 22 with clear demonstration of the abnormal, parallel orientation of the aorta (AO) and aortic valve (AV) to the pulmonary artery (PA) and pulmonary valve (PV) (top left). LV left ventricle, RV right ventricle, RA right atrium, LA left atrium, MV mitral valve, TV tricuspid valve.

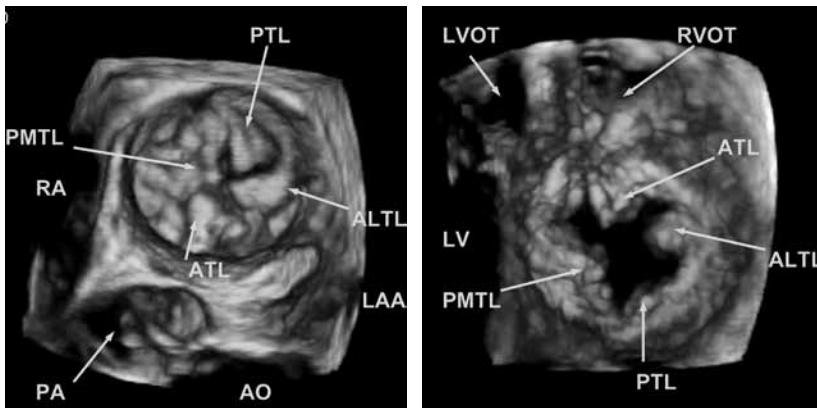


Figure 24 The RT3DE en face view from the left atrium to the tricuspid valve (TV) (left) and from the apex to the TV (right) in the same case shown in Figures 22 and 23. The TV appears to have four leaflets. Note the abnormal left and anterior position of the aorta (AO) in relation to the pulmonary artery (PA). Naming of abnormal anatomic structures, as in this case the abnormal TV, according to its position in the patient's heart (anterior-posterior, superior-inferior and left-right) is the best way to describe these very rare anomalies. Orientation in the heart is made much easier with 3D echocardiography when compared with 2D echocardiography. LAA left atrial appendage, PTL posterior tricuspid leaflet, PMTL posterior-medial tricuspid leaflet, RA right atrium, ALTL antero-lateral tricuspid leaflet, ATL anterior tricuspid leaflet, LVOT left ventricular outflow tract, RVOT right ventricular outflow tract, LV left ventricle.

1.
2.
3.
4.
5.
6.
7.
8.
9.
10.
11.
12.
13.
14.
15.
16.
17.
18.
19.
20.
21.
22.
23.
24.
25.
26.
27.
28.
29.
30.
31.
32.
33.
34.
35.
36.
37.
38.
39.

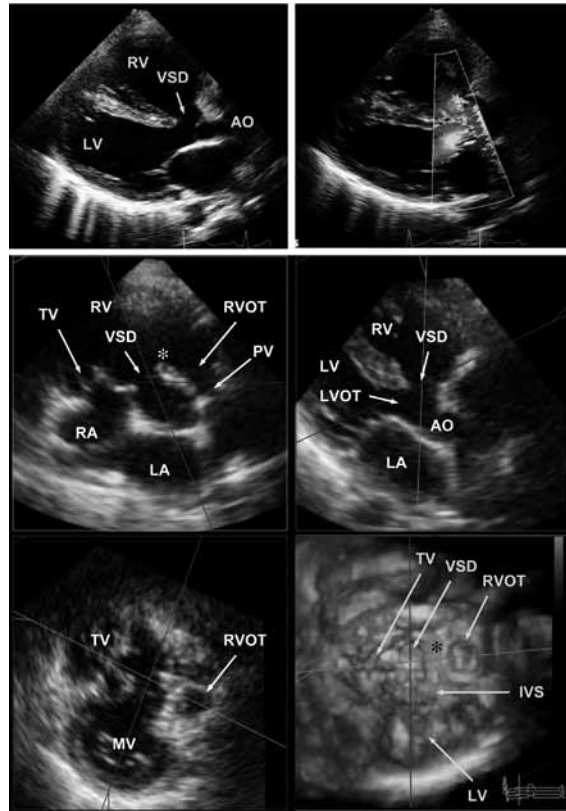


Figure 25 Comparison of 2D and RT3DE representations of a Fallot's tetralogy in a 25-year-old woman presenting with the characteristic combination of overriding aorta, perimembranous (subaortic) ventricular septal defect (VSD), pulmonary valve (PV) stenosis, and right ventricular hypertrophy. The 2D color Doppler image clearly shows direct right ventricular outflow (blue) towards the overriding aorta (AO) (top right). The 3D en face view from the apex to base (bottom right) shows the location of the VSD – connecting the RV to the aorta – located on a (green) line between the tricuspid valve (TV) and right ventricular outflow tract. The right ventricular outflow tract (RVOT) is quite wide for a tetralogy of Fallot. The green plane (middle left) also depicts the relation between the TV, VSD, and RVOT with the typical ventricular infundibulum deviated anteriorly (*) between the LVOT and RVOT, the hallmark of Fallot's tetralogy. LV left ventricle, RV right ventricle, RA right atrium, LA left atrium, MV mitral valve, LVOT left ventricular outflow tract, IVS interventricular septum.

TETRALOGY OF FALLOT

In a complex congenital malformation like tetralogy of Fallot, RT3DE can be of great value for understanding the exact morphology and spatial relationships as demonstrated in Figure 25. However, in adults, the pulmonary valve might be difficult to assess with RT3DE. In normal hearts, LV ejection fraction can be assessed more reliably with RT3DE than with 2D echocardiography. This is also probably true for the LV assessment in tetralogy of Fallot, in which the

shape of the LV is almost always compromised by a substantially dilated RV. Assessment of RV volumes and ejection fraction is extremely relevant in this population, which is addressed separately at the end of this chapter.

RT3DE IN OTHER CONGENITAL CARDIAC MALFORMATIONS

There is very little experience published in the literature about the added value of RT3DE in other malformations than the few described above. Case reports about subaortic stenosis (Figure 26),¹⁹ double orifice mitral valve,²⁰ cleft mitral valve (Figure 16),²¹ double aortic arch,²² right atrial aneurysm,²³ infective endocarditis of a patent foramen ovale,²⁴ and cor triatriatum sinister²⁵ have been reported. These are examples of the growing awareness of the potential for RT3DE in congenital heart disease, but more experience is needed and the exact role of RT3DE in the analysis of these complex congenital cardiac lesions remains to be established.

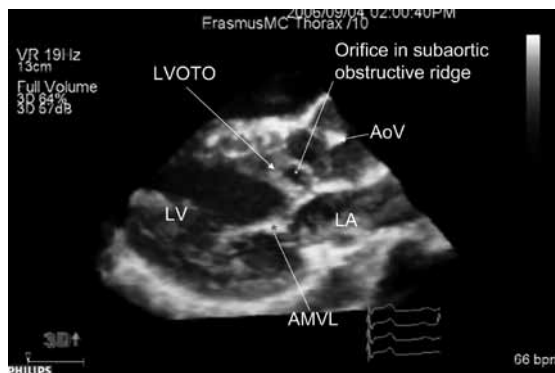


Figure 26 Left lateral view onto the interventricular septum and cutting through the left ventricular outflow tract (LVOT). A complex left ventricular outflow tract obstruction (LVOTO) is indicated (arrow) with only one small orifice. The attachment not only to the ventricular septum but also the mitral valve is nicely shown here. A discrete subaortic stenosis is always a circular structure; in order to visualize this, the en face view of the LVOTO would provide this additional information. AoV aortic valve, LV left ventricle, LA left atrium, AMVL anterior mitral valve leaflet.

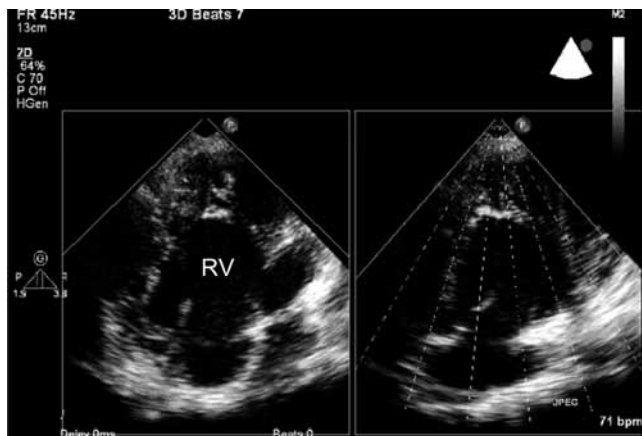
THE ROLE OF RT3DE IN THE ANALYSIS OF RIGHT VENTRICULAR FUNCTION

No geometric assumptions have been proven accurate for the measurement of right ventricular (RV) volumes and function by 2D echocardiography. However, RT3DE is free of geometric assumptions and foreshortened views and would, in principle, be an ideal tool for RV functional analysis. Some studies have shown that RV function using RT3DE is feasible: with cardiac MRI as a reference, this technique proved to be accurate in experimental settings. However, both acquisition and analysis of a 3D dataset are challenging. Some “tips and tricks” are summarized below.

1. Acquisition

2. A 3D dataset containing a RV can be acquired as follows. The patient is positioned in the left
 3. lateral decubitus position. In most cases, the patient needs to be turned slightly back towards
 4. a supine position. The aim is to optimize the quality of the initially displayed 2D image and to
 5. have the RV centrally positioned within the ultrasound sector. Attention needs to be paid to use
 6. the minimum angle mode (large, medium, or small) and depth possible to assure optimal frame
 7. rates. Dilated or hypertrophic RVs, for example after an atrial switch procedure for transposition of
 8. the great arteries, may be difficult to visualize completely in combination with acceptable frame
 9. rates. Frame rates generally vary between 25 and 55 frames per cardiac cycle. Although the 3D
 10. transducer has a footprint that is not larger than a normal 2D transducer, the transducer itself is
 11. somewhat larger. Movement of the transducer in the intercostals spaces may thereby be limited.

12. After optimization of the 2D view, a switch to the real-time display is made where two
 13. orthogonal views are shown (Figure 27). Attention is needed for the inclusion of the RV apex
 14. and lateral wall, while checking the orthogonal view for visualization of the RV outflow tract.
 15. In patients with tetralogy of Fallot, the RV outflow tract may be dilated due to an operatively
 16. placed patch to relieve RV outflow tract obstruction. To visualize this, a more superior angu-
 17. lation of the probe is needed. In most healthy persons, the long axis of the heart is almost
 18. purely superior-inferior (vertical), with the RV positioned just behind the sternum. This position
 19. implies that imaging of the RV outflow tract, anterior, just behind the sternum and superior, can
 20. be quite challenging. In patients with moderately dilated or hypertrophic ventricles, the long
 21. axis of the RV is often more horizontal. The sternum compromises the image quality to a lesser
 22. extent and imaging of the entire RV is more often possible. During one single end-expiratory
 23. breath hold, four or seven wedge-shaped subvolumes gated to the R wave are acquired to form
 24. a dataset containing the whole RV (Figure 28).



38. **Figure 27** Optimally, two orthogonal views should encompass the entire right ventricle (RV). The most
 39. difficult part to include is the right ventricular outflow tract.

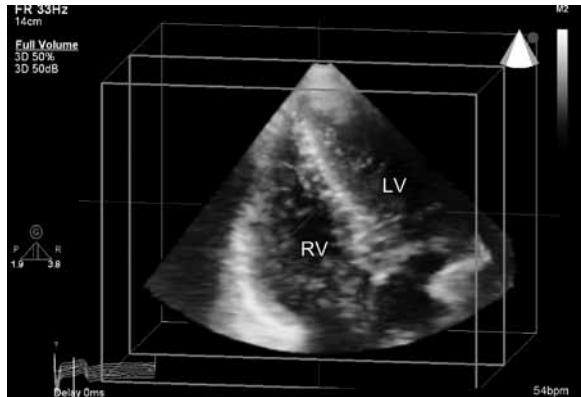


Figure 28 Full volume 3D data set of the right ventricle (RV). LV left ventricle.

With increasing survival of patients with congenital heart disease, rhythm disturbances with consequently an irregular heart rhythm become more frequent, thereby limiting the use of RT3DE, where steering of subvolumes is needed. However, with single heart beat systems this problem will be largely solved.

Analysis

Analysis of the right ventricular datasets is best done with dedicated software (4D RV-Function©, TomTec Imaging Systems, Unterschleissheim, Germany) offering semiautomatic contour detection of the endocardial borders. Hereafter, the program calculates RV volumes and ejection fraction (EF) with the possibility of manual contour revision (Figure 29).

Analysis of patients who have a RV that functions as systemic ventricle, like in congenitally corrected transposition of the great arteries or transposition of the great arteries after a Mustard or Senning repair, is difficult. At present, the role of 3D echocardiography for RV assessment in clinical practice is limited. Extensive validation of 3D echocardiographic measurements is needed before it will be applicable in clinical practice.

In summary, both acquisition and analysis of the right ventricle by RT3DE is feasible in most congenital heart diseases and forms a practical approach, but its value for clinical purposes remains to be established.

CONCLUSIONS

RT3DE is a useful tool for the analysis of adult congenital heart disease; however it still has substantial shortcomings in terms of spatial and temporal resolution and the still rather cumbersome method of obtaining a full volume 3D dataset. It provides additional information that cannot be obtained without a 3D technique. Analysis of ventricular function, which is as important as in “regular” cardiology, is performed better with 3D imaging than with 2D imaging.

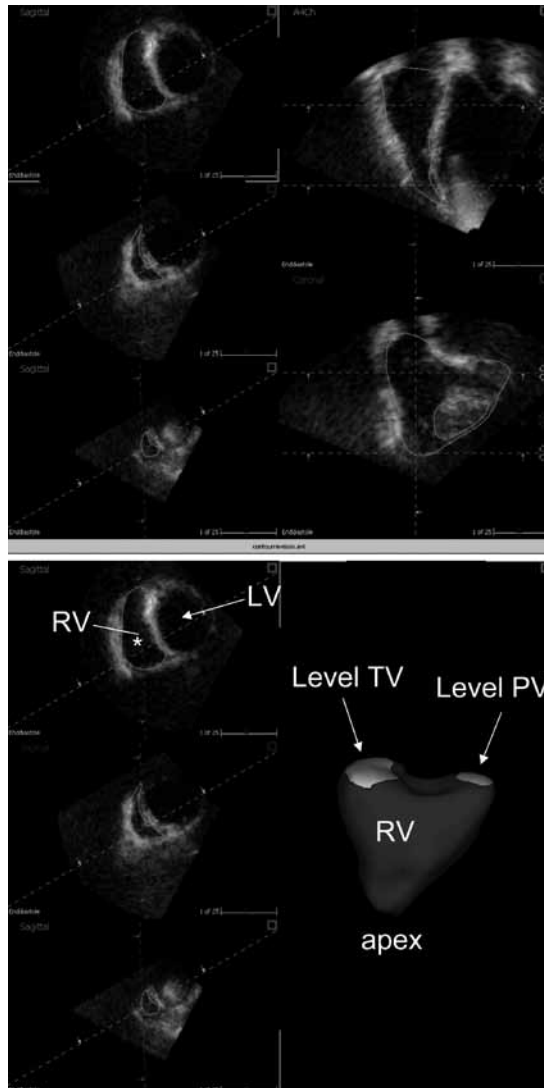


Figure 29 RV volume analysis. Top The endocardial borders are traced manually in three orthogonal planes. Through automated contour detection the endocardial wall is analyzed automatically, based on algorithms. After automatic contour detection, it is possible to go through the entire dataset to see how the lines are drawn. If necessary, the borders can be corrected manually. Bottom Finally, a RV “beutel” is reconstructed, shown (in green). RV right ventricle, PV pulmonary vein, TV tricuspid valve, LV left ventricle.

Understanding of the intracardiac morphology is enhanced by the en face view, a unique feature of 3D echocardiography. Currently, it will not replace the other echocardiographic modalities because of its apparent weaknesses in resolution, but the strengths of RT3DE justify its use in all regular echocardiographic work-ups of patients with congenital heart disease.

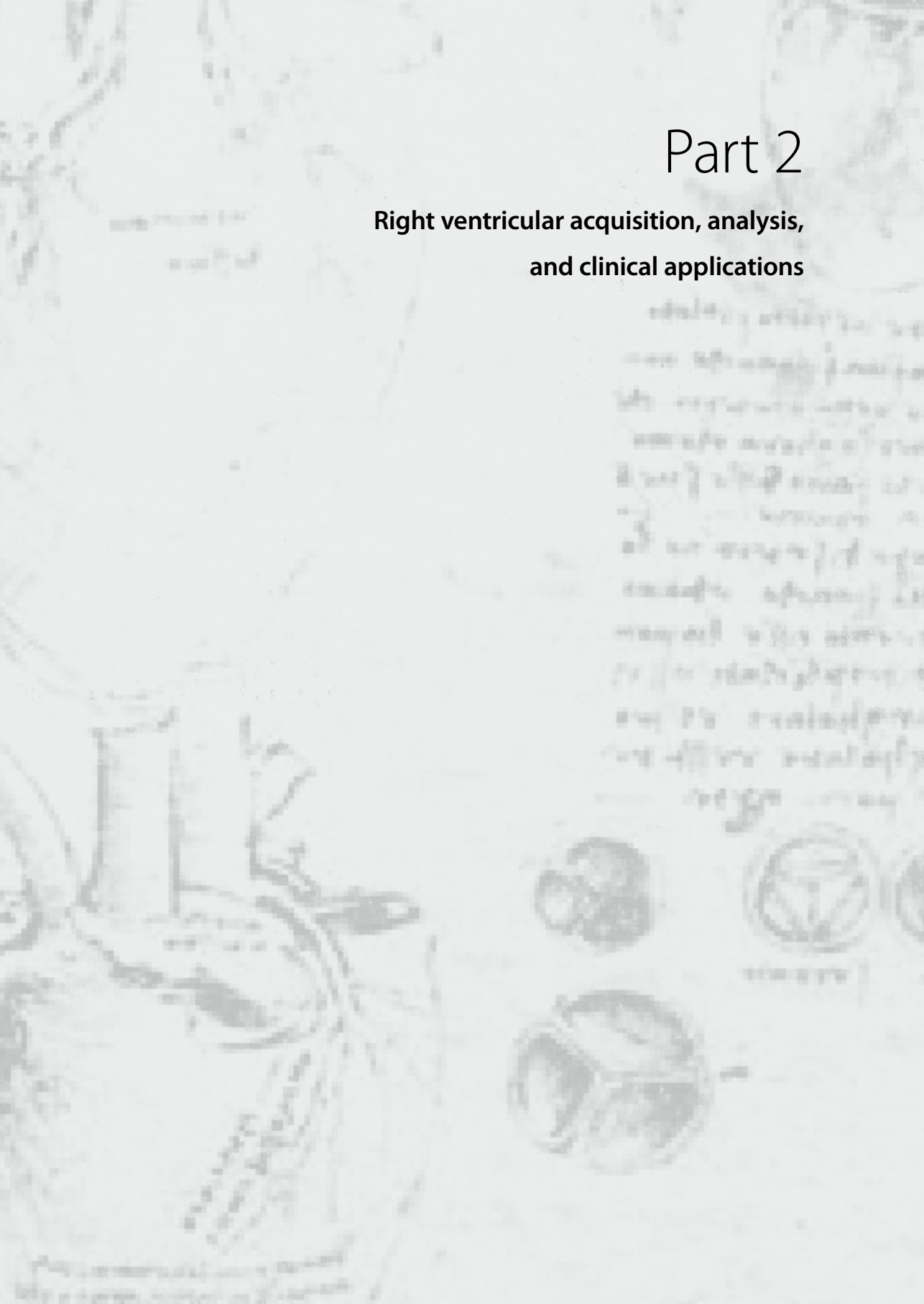
1. Balestrini L, Fleishman C, Lanzoni L, Kisslo J, Resai Bengur A, Sanders SP, et al. Real-time 3-dimensional echocardiography evaluation of congenital heart disease. *J Am Soc Echocardiogr.* 2000;13:171-6. 1.
2. Altmann K, Shen Z, Boxt LM, King DL, Gersony WM, Allan LD, et al. Comparison of three-dimensional echocardiographic assessment of volume, mass, and function in children with functionally single left ventricles with two-dimensional echocardiography and magnetic resonance imaging. *Am J Cardiol.* 1997;80:1060-5. 2.
3. van den Bosch AE, Robbers-Visser D, Krenning BJ, Voormolen MM, McGhie JS, Helbing WA, et al. Real-time transthoracic three-dimensional echocardiographic assessment of left ventricular volume and ejection fraction in congenital heart disease. *J Am Soc Echocardiogr.* 2006;19:1-6. 3.
4. Riehle TJ, Mahle WT, Parks WJ, Sallee D, 3rd, Fyfe DA. Real-time three-dimensional echocardiographic acquisition and quantification of left ventricular indices in children and young adults with congenital heart disease: comparison with magnetic resonance imaging. *J Am Soc Echocardiogr.* 2008;21:78-83. 4.
5. Marx GR, Fulton DR, Pandian NG, Vogel M, Cao QL, Ludomirsky A, et al. Delineation of site, relative size and dynamic geometry of atrial septal defects by real-time three-dimensional echocardiography. *J Am Coll Cardiol.* 1995;25:482-90. 5.
6. van den Bosch AE, Ten Harkel DJ, McGhie JS, Roos-Hesselink JW, Simoons ML, Bogers AJ, et al. Characterization of atrial septal defect assessed by real-time 3-dimensional echocardiography. *J Am Soc Echocardiogr.* 2006;19:815-21. 6.
7. Mathewson JW, Bichell D, Rothman A, Ing FF. Absent posteroinferior and anterosuperior atrial septal defect rims: Factors affecting nonsurgical closure of large secundum defects using the Amplatzer occluder. *J Am Soc Echocardiogr.* 2004;17:62-9. 7.
8. Mehmood F, Vengala S, Nanda NC, Dod HS, Sinha A, Miller AP, et al. Usefulness of live three-dimensional transthoracic echocardiography in the characterization of atrial septal defects in adults. *Echocardiography.* 2004;21:707-13. 8.
9. Franke A, Kuhl HP, Rulands D, Jansen C, Erena C, Grabitz RG, et al. Quantitative analysis of the morphology of secundum-type atrial septal defects and their dynamic change using transesophageal three-dimensional echocardiography. *Circulation.* 1997;96:II-323-7. 9.
10. Chen FL, Hsiung MC, Nanda N, Hsieh KS, Chou MC. Real time three-dimensional echocardiography in assessing ventricular septal defects: an echocardiographic-surgical correlative study. *Echocardiography.* 2006;23:562-8. 10.
11. Mehmood F, Miller AP, Nanda NC, Patel V, Singh A, Duncan K, et al. Usefulness of live/real time three-dimensional transthoracic echocardiography in the characterization of ventricular septal defects in adults. *Echocardiography.* 2006;23:421-7. 11.
12. Hsu JH, Wu JR, Dai ZK, Lee MH. Real-time three-dimensional echocardiography provides novel and useful anatomic insights of perimembranous ventricular septal aneurysm. *Int J Cardiol.* 2007;118:326-31. 12.
13. van den Bosch AE, Ten Harkel DJ, McGhie JS, Roos-Hesselink JW, Simoons ML, Bogers AJ, et al. Feasibility and accuracy of real-time 3-dimensional echocardiographic assessment of ventricular septal defects. *J Am Soc Echocardiogr.* 2006;19:7-13. 13.
14. Seliem MA, Fedec A, Szwast A, Farrell PE, Jr, Ewing S, Gruber PJ, et al. Atrioventricular valve morphology and dynamics in congenital heart disease as imaged with real-time 3-dimensional matrix-array echocardiography: comparison with 2-dimensional imaging and surgical findings. *J Am Soc Echocardiogr.* 2007;20:869-76. 14.
15. van den Bosch AE, Ten Harkel DJ, McGhie JS, Roos-Hesselink JW, Simoons ML, Bogers AJ, et al. Surgical validation of real-time transthoracic 3D echocardiographic assessment of atrioventricular septal defects. *Int J Cardiol.* 2006;112:213-8. 15.
16. Singh A, Romp RL, Nanda NC, Rajdev S, Mehmood F, Baysan O, et al. Usefulness of live/real time three-dimensional transthoracic echocardiography in the assessment of atrioventricular septal defects. *Echocardiography.* 2006;23:598-608. 16.

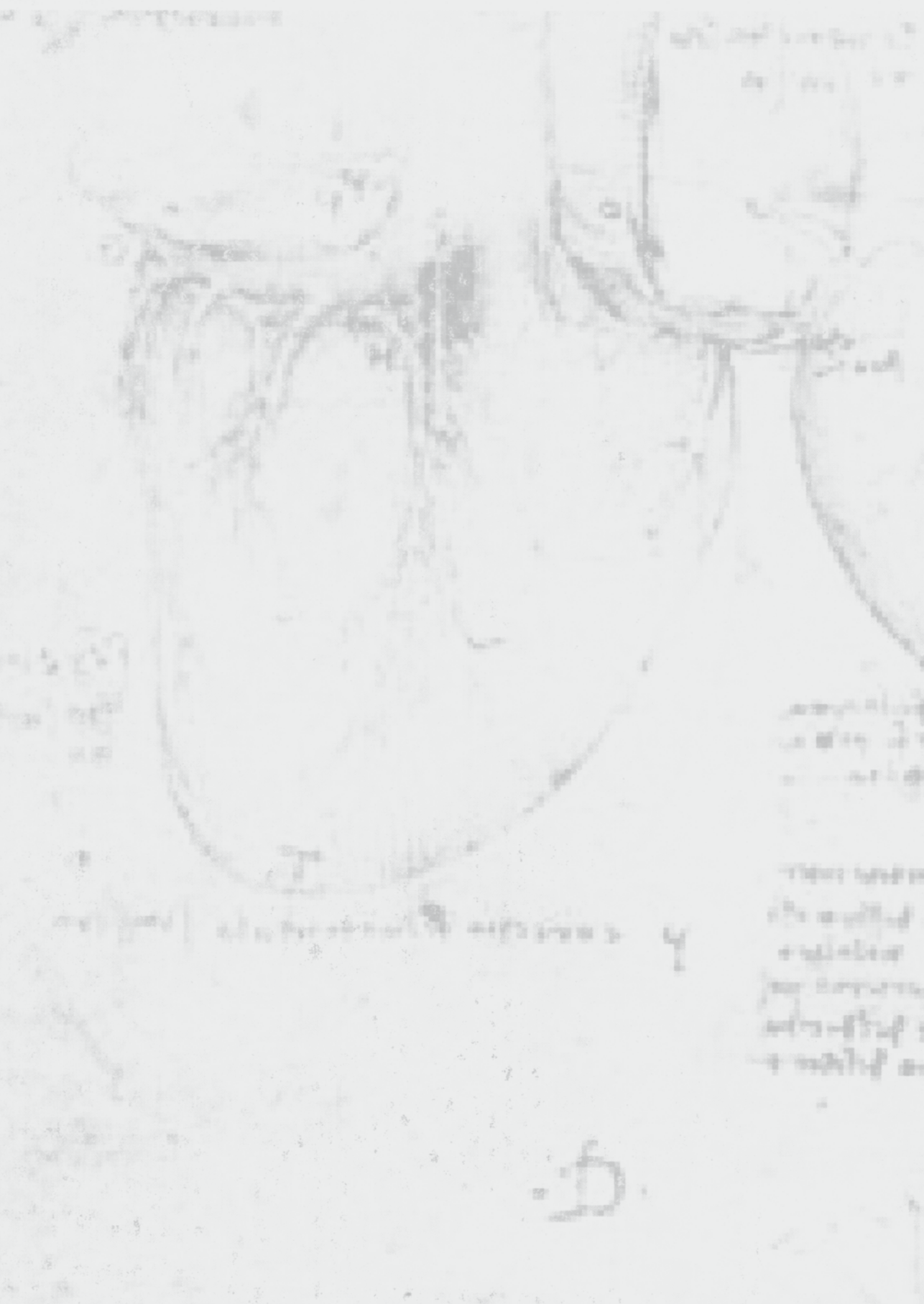
1. 17. Anwar AM, Geleijnse ML, Ten Cate FJ, Meijboom FJ. Assessment of tricuspid valve annulus size, shape and function using real-time three-dimensional echocardiography. *Interact Cardiovasc Thorac Surg*. 2006;5:683-7.
2. 18. Patel V, Nanda NC, Rajdev S, Mehmood F, Velayudhan D, Vengala S, et al. Live/real time three-dimensional transthoracic echocardiographic assessment of Ebstein's anomaly. *Echocardiography*. 2005;22:847-54.
3. 19. Miyamoto K, Nakatani S, Kanzaki H, Tagusari O, Kobayashi J. Detection of discrete subaortic stenosis by 3-dimensional transesophageal echocardiography. *Echocardiography*. 2005;22:783-4.
4. 20. Anwar AM, McGhie JS, Meijboom FJ, Ten Cate FJ. Double orifice mitral valve by real-time three-dimensional echocardiography. *Eur J Echocardiogr*. 2008;9:731-2.
5. 21. Nomoto K, Hollinger I, DiLuozzo G, Fischer GW. Recognition of a cleft mitral valve utilizing real-time three-dimensional transoesophageal echocardiography. *Eur J Echocardiogr*. 2009;10:367-9.
6. 22. Sivaprakasam MC, Vettukattil JJ. 3-D echocardiographic imaging of double aortic arch. *Eur J Echocardiogr*. 2006;7:476-7.
7. 23. Guerra VC, Coles J, Smallhorn JF. Aneurysm of right atrium diagnosed by 3-dimensional real-time echocardiogram. *J Am Soc Echocardiogr*. 2005;18:1221.
8. 24. Acar P, Abadir S, Bassil R. Images in Congenital Heart Disease. Infective endocarditis of the patent oval fossa assessed by three-dimensional echocardiography. *Cardiol Young*. 2007;17:113.
9. 25. Patel V, Nanda NC, Arellano I, Yelamanchili P, Rajdev S, Baysan O. Cor triatriatum sinister: assessment by live/real time three-dimensional transthoracic echocardiography. *Echocardiography*. 2006;23:801-2.
- 10.
- 11.
- 12.
- 13.
- 14.
- 15.
- 16.
- 17.
- 18.
- 19.
- 20.
- 21.
- 22.
- 23.
- 24.
- 25.
- 26.
- 27.
- 28.
- 29.
- 30.
- 31.
- 32.
- 33.
- 34.
- 35.
- 36.
- 37.
- 38.
- 39.



Part 2

Right ventricular acquisition, analysis, and clinical applications





Chapter 4

Right ventricular quantification in clinical practice: two-dimensional versus three-dimensional echocardiography compared with cardiac magnetic resonance imaging

H.B. van der Zwaan
M.L. Geleijnse
J.S. McGhie
E. Boersma
W.A. Helbing
F.J. Meijboom
J.W. Roos-Hesselink

Eur J Echocardiogr. 2011; in press

ABSTRACT

Background. To establish the additional value of three-dimensional echocardiography (3D echo) for assessment of right ventricular (RV) size and function in patients with congenital heart disease (CHD) in everyday clinical practice, the accuracy and reproducibility of 3D echo were compared with conventional two-dimensional echocardiography (2D echo) and cardiac magnetic resonance (CMR) imaging as the reference.

Methods. Patients with CHD and primarily affected right ventricles (RV group, n = 62), patients with CHD and primarily affected left ventricles (LV group, n = 27), and healthy controls (n = 31) were studied. 2D echo-, 3D echo- and CMR datasets were obtained.

Results. Moderate correlations were found between RV dimensions by 2D echo and CMR-derived RV end-diastolic volumes (r 0.32-0.77). The correlations between RV volumes obtained by 3D echo and CMR imaging were better (r 0.71-0.97) than the 2D echo-derived correlations ($P < 0.001$). Only the 2D-echo derived RV inlet diameter correlated better in healthy controls than in the RV group. Receiver operating characteristic curve analysis revealed that 3D echo-derived end-diastolic volume best identified RV dysfunction (sensitivity 95% and specificity 100%). The 3D echo-derived measurements were as reproducible as the 2D echo-derived measurements (n = 37, coefficients of variation ranging from 5 to 19%), with the tricuspid annular plane systolic excursion being the most reproducible measurement (coefficient of variation 6%).

Conclusions. 3D echo improved quantitative RV size and function assessment compared with 2D echo in patients as well as in healthy controls. Everyday clinical use of 3D echo for RV assessment can be reality with the currently available software and provides incremental benefit in assessment of the right ventricle.

1.
2.
3.
4.
5.
6.
7.
8.
9.
10.
11.
12.
13.
14.
15.
16.
17.
18.
19.
20.
21.
22.
23.
24.
25.
26.
27.
28.
29.
30.
31.
32.
33.
34.
35.
36.
37.
38.
39.

1. INTRODUCTION

2.

3. Right ventricular (RV) size and function assessment based on two-dimensional echocardiogra-
 4. phy (2D echo) or cardiac magnetic resonance (CMR) imaging is used as a decision-making tool
 5. in patients with congenital heart disease (CHD).¹ Accurate quantification of RV volumes and
 6. ejection fraction (EF) is therefore essential. Guidelines on the assessment of RV size and func-
 7. tion by M-mode and 2D echo include various imaging planes to measure dimensions, areas,
 8. and the tricuspid annular plane systolic excursion (TAPSE).² The accuracy of these 2D echo
 9. and M-mode-derived measurements has been investigated compared with CMR imaging,³⁻⁵
 10. and resulted in a moderate to poor agreement. It has been suggested that 2D echo-derived
 11. measurements were less accurate in patients with CHD and enlarged right ventricles than in
 12. healthy controls.⁶ Volumetric calculations based on 2D echo were unreliable because of the
 13. need of geometric assumptions that were impossible to fit onto the complex, non-symmetric
 14. morphology of the right ventricle.⁷

15. In several studies the accuracy of real-time three-dimensional echocardiography (3D echo)
 16. has been investigated compared with CMR imaging and resulted in good agreement.⁸⁻¹⁰
 17. Currently, software that enables a fast reconstruction of RV volumes and EF is commercially
 18. available. An advantage of 3D echo is that it is not reliant on correct image orientation at acqui-
 19. sition and the associated geometric assumptions.¹¹ Consequently, 3D echo has the potential of
 20. improved accuracy, even though past findings have been varying.¹² Improved reproducibility
 21. of 3D echo compared with the area-length method, the modified two-dimensional subtraction
 22. method, and Simpson's method of disc summation has been reported.¹³ None of the cited
 23. studies clearly investigated the additional value of combined 2D echo and 3D echo measure-
 24. ments for RV size or function assessment.

25. Therefore, we investigated the accuracy and reproducibility of 3D echo compared with 2D
 26. echo measurements for the assessment of RV size and function. Moreover, we compared the
 27. ability of 3D echo versus 2D echo to identify RV dysfunction. For the purpose of this study,
 28. we assessed 2D echo, 3D echo, and CMR images of the right ventricle in patients with various
 29. CHD. Moreover, a group of healthy controls was studied to assess possible differences between
 30. patients and healthy controls.

31.

32.

33. METHODS

34.

35. Study population

36.

37. *Congenital heart disease patients*

38. We prospectively recruited 89 patients in sinus rhythm with complex and/or surgically repaired
 39. CHD referred for quantitative analysis of their cardiac function by CMR imaging. The patients

underwent 2D echo, full-volume 3D echo, and CMR examinations. The 3D echo examination was made by the same sonographer who had performed the 2D echo study.

Healthy controls

Thirty-one healthy controls underwent 2D echo, full-volume 3D echo, and CMR examinations (Figure 1). Controls were eligible for inclusion in the study if they had no medical history or current symptoms suggestive of cardiovascular disease, including hypertension or a systemic illness with a potential cardiovascular component such as diabetes or thyroid disease. Participants taking any cardiovascular medications were excluded from the study. In all included healthy controls, heart rate and blood pressure were measured (in a supine position) and they underwent physical examinations and a complete routine 2D echocardiogram to exclude cardiac abnormalities.

The medical ethics committee approved the study and written informed consent was obtained from all healthy controls, patients and/or their parents (if required).

Two-dimensional echocardiography

Echocardiographic studies were performed with a commercially available ultrasound system (Philips Medical Systems, Best, the Netherlands) equipped with a broadband S5-1 transducer (frequency transmitted 1.7 MHz, received 3.4 MHz) with the patient in the left lateral decubitus position. Using a standard clinical protocol, RV outflow tract dimensions were measured on parasternal short-axis views at aortic valve level, RV measurements as specified in the ASE recommendations² were measured on modified apical four-chamber views. The mean frame rate was 58 ± 9 frames per cardiac cycle (range 39 – 82).

The datasets were digitally exported to a TomTec server (TomTec Imaging Systems, Unterschleissheim, Germany) connected to a terminal workstation for further analyses. Two-dimensional echo-derived RV parameters were analyzed using TomTec Image Arena version 4.1. All RV diameters were measured at end-diastole. The diameters were measured I) perpendicular to the aortic valve and II) abreast the pulmonary annulus level. On the modified apical four-chamber view, the RV inflow diameter was measured just above the level of the tricuspid valve annulus and the long-axis diameter was measured from the apex to the tricuspid valve annulus. The areas in end-diastole and end-systole were measured in a dynamic mode and the RV fractional area change (end-diastolic area minus end-systolic area, divided by the end-diastolic area, expressed as a percentage) was calculated. The TAPSE was measured at the lateral tricuspid annulus using M-mode.

Acquisition and analysis by real-time three-dimensional echocardiography

Real-time 3D echo harmonic imaging was performed using the iE33 ultrasound system (Philips Medical Systems, Best, the Netherlands) equipped with an X3-1 matrix array transducer with the patient in the left lateral decubitus position. A full-volume scan from seven R-wave gated

1.
2.
3.
4.
5.
6.
7.
8.
9.
10.
11.
12.
13.
14.
15.
16.
17.
18.
19.
20.
21.
22.
23.
24.
25.
26.
27.
28.
29.
30.
31.
32.
33.
34.
35.
36.
37.
38.
39.

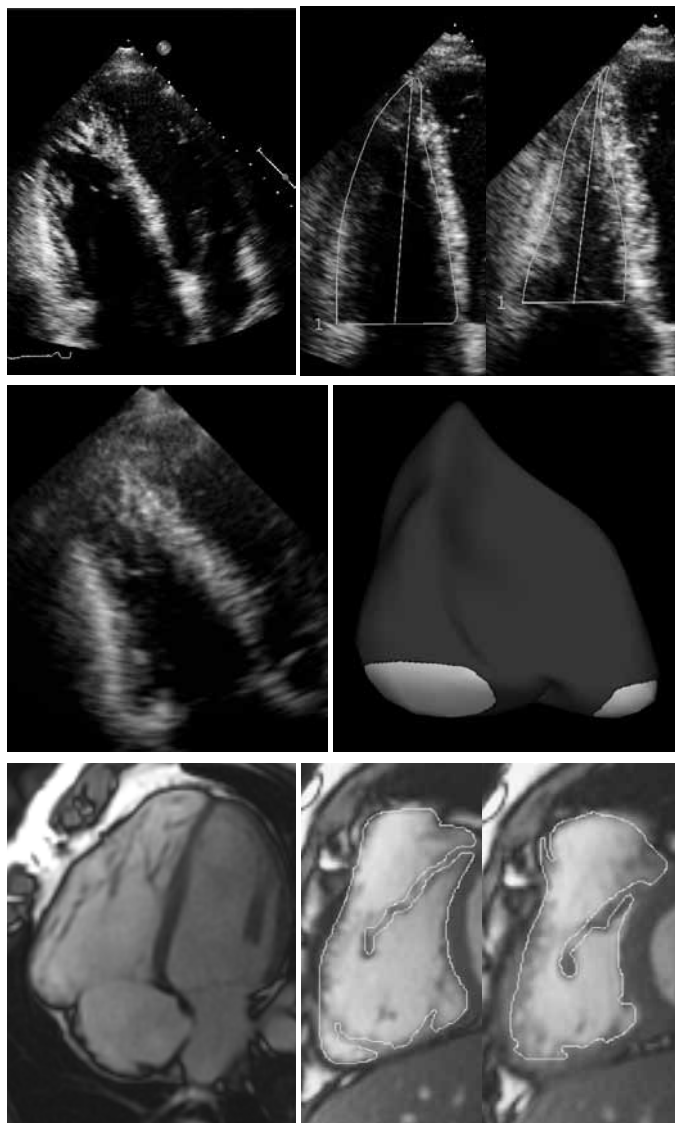


Figure 1 Example of radial long-axis images of the right ventricle obtained at end-diastole from a patient with pulmonary valve stenosis displayed by 2-dimensional echocardiography (top), 3-dimensional echocardiography (center) and cardiac magnetic resonance imaging (bottom) with their respective measurements.

subvolumes during a single end-expiratory breath-hold was acquired from a modified apical four-chamber position. The depth and angle of the ultrasound sector were adjusted to a minimal level still encompassing the RV. Each image was optimized for endocardial border visualization by modifying time gain and compression and then the overall gain was slightly increased before the acquisition. The mean volume rate was 26 ± 5 frames per cardiac cycle (range 14 – 39).

The digital RV 3D echo datasets were analyzed offline using the TomTec four-dimensional RV Function program version 1.2. With this software, three-dimensional semiautomated border detection of RV volumes over one cardiac cycle are done. It uses a physics-based modelling algorithm that makes no assumptions regarding RV geometry. The working of the RV Function program is reported in detail elsewhere.¹⁰ In short, the end-diastolic and end-systolic phases have to be identified. Endocardial border contours are drawn onto still frames of the apical four-chamber view, short-axis view, and coronal view in both phases. Once these contours have been traced, the software automatically delineates the RV endocardial border from the end-diastolic and end-systolic phases and, by sequential analysis, creates a RV mathematic dynamic three-dimensional endocardial surface that represents the changes in the RV cavity over the cardiac cycle. From this three-dimensional endocardial surface, global RV volumes and EF are calculated.

Acquisition and analysis by cardiac magnetic resonance imaging

CMR images were acquired using a Signa 1.5 Tesla scanner (GE Medical Systems, Milwaukee, Wisconsin). Subjects were positioned in the supine position with dedicated phased-array cardiac surface coils placed over the thorax. The CMR imaging protocol included cine steady state free precession sequences in short-axis planes to assess RV volumes. Electrocardiogram gating and repeated breath holds were applied to minimize the influence of cardiac and respiratory motion. RV volumes were measured from a multi-section image set of 8 to 12 contiguous slices parallel to the plane of the atrioventricular valves covering the full length of the right ventricle. Imaging parameters were as follows: slice thickness 7 to 10 mm, inter-slice gap 0 mm, field of view 280 to 370 mm, phase field of view 0.75, matrix 160 x 128 mm, repetition time 3.5 ms, echo time 1.5 ms, 12 views/segment, flip angle 45°, mean in-plane resolution 2 mm², range of temporal resolution 22 to 37 ms.

The short-axis dataset was analyzed quantitatively on a commercially available Advanced Windows workstation (GE Medical Systems) using Advanced Windows version 5.1 of the MR Analytical Software System (Medis Medical Imaging Systems, Leiden, the Netherlands). The RV end-diastolic volume (EDV), end-systolic volume (ESV) and EF were calculated using manual detection of endocardial borders in end-diastole and end-systole with exclusion of trabeculae as described by Robbers-Visser et al.¹⁴

Statistical analysis

Statistical analysis was performed using SPSS version 15.0 (SPSS, Inc, Chicago, Illinois). Categorical variables are summarized as numbers and percentages. Continuous variables are presented as mean \pm SD. Patients were divided into two groups: primarily affected RV CHD (RV group), and primarily affected left ventricular (LV) CHD (LV group). Differences between the two patient groups and controls were analyzed using ANOVA between groups. Both 3D echo and

1. CMR-derived volumes were indexed to the body surface area, which was calculated according
2. to the formula by Dubois: $BSA (m^2) = \text{weight (kg)}^{0.425} * \text{height (cm)}^{0.725} * 71.84 * 10^{-4}$.

3. Regression analysis with Pearson's correlation coefficient was used to evaluate the relation
4. between 2D echo, 3D echo, and CMR imaging. The Z-statistic was used to evaluate differences
5. between two correlation coefficients. The agreement between 3D echo and CMR measure-
6. ments was evaluated using Bland-Altman analysis by calculating the bias (mean difference) and
7. the 95% limits of agreement (two SDs around the mean difference).¹⁵ Paired *t* tests were used
8. to analyze the significance of the biases in volumes and EF between 3D echo and CMR imaging.

9. Receiver operating characteristic (ROC) curves were created to obtain the sensitivity, speci-
10. ficity, positive, and negative predictive values of 2D echo and 3D echo to identify RV dysfunction
11. in patients with CHD. RV dysfunction was defined as indexed EDV >129 ml, indexed ESV >58 ml,
12. and/or RV EF <48% obtained by CMR imaging.¹⁶ We report the area under the ROC curve (or
13. c-index) as well as the 'optimal' cut-off value for each parameter to detect RV dysfunction, which
14. is defined as the value of the parameter that corresponds with the highest sum of specificity
15. and sensitivity. The method of DeLong was used to study differences in areas under the curve
16. between two correlated ROC curves.¹⁷

17. The reproducibility of the 2D- and 3D echo measurements was evaluated in 37 randomly
18. selected persons (22 patients and 15 healthy controls). We expressed the intra-observer and
19. inter-observer variability by the coefficient of variation, which is defined as the standard
20. deviation of the difference between the two readings (or readers) divided by their mean value,
21. times 100. All statistical tests were two-sided, and P-value <0.05 was considered statistically
22. significant.

23.

24.

25. **RESULTS**

26.

27. The baseline characteristics of the RV group (n = 62, mainly patients with tetralogy of Fallot,
28. pulmonary stenosis ± ventricular septal defect and transposition of the great arteries after an
29. atrial switch), of the LV group (n = 27, mainly aortic valve pathology and transposition of the
30. great arteries after an arterial switch) and of the healthy controls (n = 31) are listed in Table 1.
31. The patients with CHD had increased heart rates (P <0.001) and shorter statures (P <0.001),
32. compared with the healthy controls.

33. Table 2 displays the 2D echo, 3D echo and CMR-derived measurements of RV size and func-
34. tion. All RV diameters by 2D echo were larger in the RV group compared with the other two
35. groups. TAPSE was lower in the RV group (P <0.001) while these patients had higher indexed
36. EDV and ESV and lower EF by 3D echo and CMR imaging (all: P ≤0.001).

37.

38.

39.

Table 1. Baseline characteristics

Variable	RV group	LV group	Healthy controls	P-value*
Number	62	27	31	
Men (%)	45	29	52	0.25
Age (years)	29 ± 11	25 ± 8	31 ± 7	0.082
Heart rate (beats/min)	71 ± 11	64 ± 11	59 ± 8	<0.001
Systolic blood pressure (mmHg)	125 ± 17	131 ± 17	122 ± 14	0.54
Diastolic blood pressure (mmHg)	73 ± 10	71 ± 9	73 ± 9	0.13
Height (cm)	171 ± 13	177 ± 11	177 ± 8	< 0.001
Weight (kg)	67 ± 16	71 ± 13	72 ± 11	0.21
Body mass index (kg/m ²)	23 ± 4	23 ± 3	23 ± 3	0.97
Body surface area (m ²)	1.8 ± 0.3	1.9 ± 0.2	1.9 ± 0.2	0.25

*P-value derived from ANOVA between groups. RV denotes right ventricle, LV left ventricle.

Table 2. Right ventricular measurements by echocardiography and cardiac magnetic resonance imaging

		All	RV group	LV group	Healthy controls	P-value*
2-Dimensional echocardiography	PSAX RVOT 1 (mm/m ²)	19 ± 6	20 ± 7	15 ± 5	18 ± 2	0.001
	PSAX RVOT 2 (mm/m ²)	11 ± 4	11 ± 4	9 ± 4	11 ± 2	0.044
	AP4C inlet (mm/m ²)	24 ± 5	27 ± 6	22 ± 4	21 ± 3	<0.001
	AP4C long-axis (mm/m ²)	47 ± 6	49 ± 7	46 ± 6	43 ± 3	<0.001
	Area ED (cm ² /m ²)	17 ± 5	20 ± 5	15 ± 3	12 ± 2	<0.001
	Area ES (cm ² /m ²)	11 ± 4	13 ± 4	9 ± 2	7 ± 2	<0.001
	FAC (%)	37 ± 8	36 ± 9	38 ± 6	40 ± 8	0.032
M-mode	TAPSE (mm)	23 ± 7	20 ± 5	-	29 ± 5	<0.001
Real-time 3-dimensional echocardiography	EDV (ml/m ²)	93 ± 32	107 ± 36	78 ± 19	75 ± 12	<0.001
	ESV (ml/m ²)	46 ± 22	55 ± 25	38 ± 12	33 ± 7	<0.001
	EF (%)	52 ± 8	50 ± 9	52 ± 7	57 ± 4	0.001
Cardiac magnetic resonance imaging	EDV (ml/m ²)	102 ± 36	119 ± 41	84 ± 23	82 ± 13	<0.001
	ESV (ml/m ²)	48 ± 26	60 ± 29	36 ± 12	32 ± 8	<0.001
	EF (%)	55 ± 9	51 ± 9	58 ± 6	61 ± 6	<0.001

*P-value derived from ANOVA between groups. PSAX denotes parasternal short axis, RVOT right ventricular outflow tract, AP4C apical four-chamber, ED(V) end-diastole (volume), ES(V) end-systole (volume), FAC fractional area change, TAPSE tricuspid annular plane systolic excursion, EF ejection fraction.

Accuracy of 2-dimensional versus 3-dimensional echocardiography

As shown in Table 3, the correlations for the 2D echo measurements ranged from 0.32 (RV outflow tract at pulmonary valve level) to 0.74 (end-diastolic area) compared with the CMR-derived EDV. The end-systolic area correlated with a coefficient of 0.77 with the ESV by CMR imaging. Fractional area change and TAPSE correlated with CMR-derived EF with correlation coefficients of 0.37 and 0.40, respectively. The correlations for 3D echo-derived volumes and EF ranged from 0.71-0.97 (Figure 2). The 3D echo-derived measurements correlated better with CMR imaging than the 2D-echo derived ones (All P <0.001). The strength of the correlations varied slightly between the RV group- and healthy control group, but only the RV inlet correlated significantly better in healthy controls than in the RV group (P = 0.042). The mean differences

Table 3. Correlation of echocardiographic measurements and cardiac magnetic resonance imaging

CMR	Echo	All	RV Group	LV Group	Healthy controls	Mean difference	95% LOA	P-value*
End-diastolic volume	PSAX RVOT 1	0.47	0.46	0.27	0.35 [#]			0.56
	PSAX RVOT 2	0.32	0.47	0.20	0.11 [#]			0.092
	AP4C inlet	0.46	0.33	0.47	0.67			0.042
	AP4C long-axis	0.65	0.71	0.55	0.76			0.64
	Area ED	0.74	0.69	0.71	0.73			0.73
EDV		0.97	0.97	0.96	0.93	-17	(-19;53)	0.065
	End-systolic volume	Area ES	0.77	0.73	0.65	0.58		0.25
ESV		0.96	0.96	0.94	0.91	-3	(-25;32)	0.076
	FAC	0.37	0.35	0.35 [#]	0.08 [#]			0.21
Ejection fraction	TAPSE	0.40	0.29 [^]	-	0.21			0.73
	EF	0.71	0.71	0.52	0.63	-3	(-9;16)	0.54

Data are displayed as correlation coefficients. All correlation coefficients had a P-value <0.01 unless otherwise indicated. [^] P-value <0.05, but larger than 0.01. * P-value indicates the difference between the correlation coefficients of the RV group versus healthy controls. [#] Did not reach statistical significance. Abbreviations and units of the measurements, see Table 2.

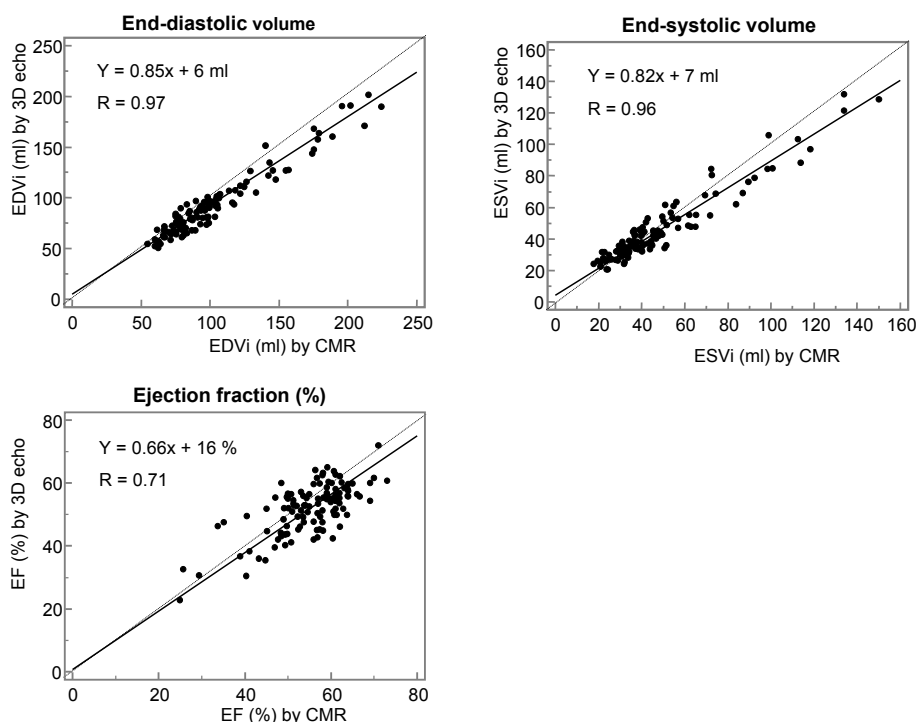


Figure 2 Linear regression analysis for right ventricular measurements by 3-dimensional echocardiography versus cardiac magnetic resonance imaging. The indexed end-diastolic volume (top), end-systolic volume (center), and ejection fraction (bottom).

between 3D echo and CMR imaging were -17 ml for EDV, -3 ml for ESV, -3% for EF, with 95% limits of agreement of ± 36 ml for EDV, ± 29 ml for ESV, and $\pm 13\%$ for EF (Figure 3).

The indexed EDV and ESV by 3D echo were the most sensitive and specific parameters to identify RV dysfunction (AUC 0.99 (0.95-1.0); 0.96 (0.90-0.99)), while the best 2D echo-derived parameters were the areas in end-diastole and end-systole (AUC 0.87 (0.78-0.93); 0.85 (0.75-0.91)) (Table 4). The 3D echo-derived volumes were better than any of the 2D echo-derived RV measurements in identifying RV dysfunction ($P = 0.008$). In addition, 3D echo-derived EF was superior to TAPSE ($P = 0.001$) for identification of diminished RV EF (Figure 4).

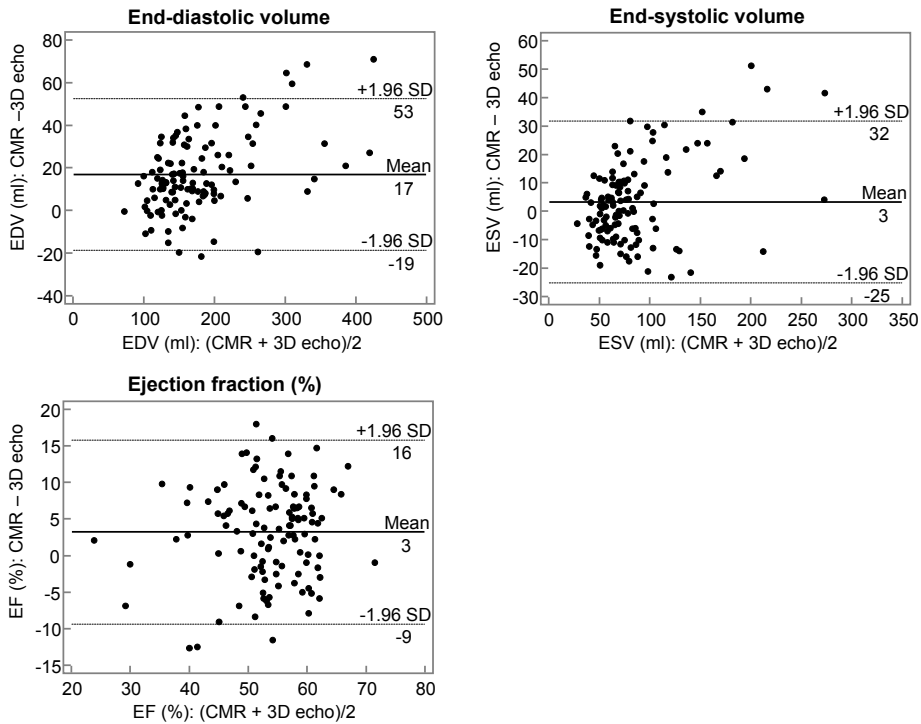


Figure 3 Bland-Altman analysis for right ventricular measurements by 3-dimensional echocardiography versus cardiac magnetic resonance imaging. The indexed end-diastolic volume (top), end-systolic volume (center), and ejection fraction (bottom).

Reproducibility of 2-dimensional versus 3-dimensional echocardiography

For 2D echo-derived RV measurements, the inter-observer variability ranged from 8% up to 19%, while the intra-observer variability ranged from 3% up to 15%. The inter-observer value for TAPSE was 6% and the intra-observer value 5%. For RV EDV, ESV, and EF by 3D echo, the inter-observer variability was 10%, 13% and 12%. The intra-observer variability was 6% for EDV, 11% for ESV, and 6% for EF (Table 5).

Table 4. ROC characteristics and optimal cut-off values of echocardiographic parameters to identify right ventricular dysfunction

		AUC (95% CI)	P-value	Cut-off value	Sensitivity	Specificity
2-Dimensional echocardiography	PSAX RVOT 1	0.74 (0.63-0.84)	0.001	22	63	83
	PSAX RVOT 2	0.69 (0.57-0.80)	0.013	13	56	83
	AP4C inlet	0.73 (0.63-0.82)	<0.001	27	60	81
	AP4C long-axis	0.71 (0.60-0.80)	0.001	50	65	68
	Area ED	0.87 (0.78-0.93)	<0.001	16	100	57
	Area ES	0.85 (0.75-0.91)	<0.001	12	91	72
	FAC	0.76 (0.66-0.85)	<0.001	34	80	73
M-mode	TAPSE	0.72 (0.61-0.81)	0.004	22	90	57
Real-time	EDV	0.99 (0.95-1.0)	<0.001	116	95	100
3-dimensional echocardiography	ESV	0.96 (0.90-0.99)	<0.001	47	100	81
	EF	0.86 (0.78-0.93)	<0.001	50	87	69

Data are expressed as mean (95% confidence interval). All right ventricular diameters, areas and volumes are indexed. ROC denotes receiver operating characteristic, other abbreviations and units of measurements, see Table 2.

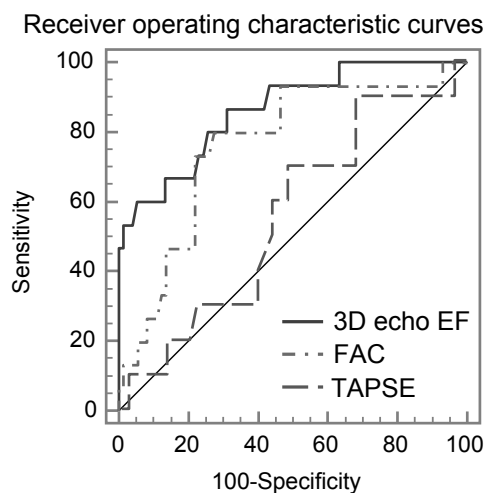
**Figure 4** Receiver operating characteristic curves displaying the ability of 3-dimensional echocardiography derived ejection fraction, 2-dimensional echocardiography derived fractional area change and tricuspid annular plane systolic excursion to identify diminished right ventricular ejection fraction.

Table 5. Reproducibility of the echocardiographic measurements

		Inter-observer		Intra-observer	
		Mean difference	Coefficient of variation	Mean difference	Coefficient of variation
2-Dimensional echocardiography	PSAX RVOT 1	2.9 ± 3.0	8	2.1 ± 2.9	8
	PSAX RVOT 2	3.0 ± 2.7	13	2.9 ± 3.1	15
	AP4C inlet	3.8 ± 5.1	12	2.2 ± 2.0	5
	AP4C long-axis	5.7 ± 7.4	9	3.3 ± 2.9	3
	Area ED	2.8 ± 3.1	11	2.6 ± 1.4	5
	Area ES	2.2 ± 1.9	11	2.2 ± 1.9	11
	FAC	8.2 ± 7.1	19	6.3 ± 5.0	13
M-mode	TAPSE	1.6 ± 1.5	6	1.5 ± 1.3	5
Real-time 3-dimensional echocardiography	EDV	26 ± 18	10	14 ± 11	6
	ESV	15 ± 12	13	11 ± 10	11
	EF	5 ± 6	12	5 ± 3	6

Coefficients of variation are calculated as the standard deviation of the difference between the 2 readings (or readers) divided by their mean value times 100. Abbreviations and units of measurements, see Table 2.

DISCUSSION

In the current study we directly compared 3D echo-derived RV volumes and EF versus multiple 2D echo-derived measurements for RV assessment. A better agreement between 3D echo versus 2D echo compared with CMR imaging was found. Furthermore, 3D echo established higher specificity to exclude RV dysfunction in patients with CHD, in line with published studies that focussed on the left ventricle.^{18,19} To investigate whether the superior accuracy would be at cost of the reproducibility of the RV measurements, we studied the reproducibility of 3D echo versus 2D echo. The 3D echo measurements turned out to be at least as reproducible as the 2D echo-derived RV dimensions and areas, with TAPSE being the most reproducible RV measurement.

Comparison with other studies

The agreement between 2D echo, 3D echo, and CMR imaging has been studied before by Kjaergaard et al¹² who found only moderate correlations between 3D echo and CMR imaging. They concluded that, for routine clinical purposes, TAPSE is the preferred method for RV EF estimation. They did not report on reproducibility. Their results differ at two points from ours: first, we found that 3D echo agreed better with CMR imaging than measurements by M-mode or 2D echo and second, in our study TAPSE correlated only moderately with CMR imaging. This discrepancy could be explained by the older 3D echo platform Kjaergaard et al¹² used in which analysis of the RV dataset was based on the disc summation method. Moreover, they included patients post myocardial infarction or with a history of pulmonary embolism while we studied patients with CHD. In both groups regional RV function abnormalities were observed. Especially in patients with tetralogy of Fallot, such regional RV function abnormalities are present. During the initial operation in the latter patients, a large transannular patch was placed, resulting in

1. abnormal function of their RV outflow tract. Morcos et al²⁰ found that TAPSE was of limited
 2. value in patients with tetralogy of Fallot, because assessing only the longitudinal RV shortening
 3. at the inlet (TAPSE) does not represent global RV function if extensive regional abnormalities
 4. are present.

5. Jenkins et al¹³ compared 2D echo and 3D echo-derived volumes with CMR imaging in
 6. patients after acute myocardial infarctions. They found 3D echo to be more reproducible com-
 7. pared with the 2D echo-based area-length method, the modified 2D subtraction method, and
 8. Simpson's disc summation method. Furthermore, studies on the accuracy of 2D echo compared
 9. with CMR imaging reported various strengths of correlations^{4, 6, 21} depending on the meth-
 10. odology used and the patient population studied. The agreement between 3D echo and CMR
 11. imaging has been investigated in several studies and resulted in better agreement compared
 12. with 2D echo versus CMR imaging.^{8, 22}

13. An issue addressed by Lai et al⁶ was whether 2D echo-derived measurements agreed better
 14. with CMR imaging in healthy controls than in patients with CHD. They found that the differences
 15. between 2D echo and CMR-derived measurements were more pronounced in patients with
 16. RV volume overload and concluded that 2D echo appears to be less accurate in patients with
 17. CHD and a dilated right ventricle. We could not confirm these findings, as we found agreement
 18. between the two techniques being comparable in the RV group and in the healthy controls.
 19. Only the 2D-echo derived RV inlet diameter correlated better in healthy controls than in the
 20. RV group. Thus, even in dilated right ventricles, 2D echo and 3D echo can be applied and are as
 21. accurate as in healthy controls.

22.

23. Clinical implications

24. When assessing RV function in clinical practice, all echo modalities - M-mode, 2D echo, and 3D
 25. echo - have their pitfalls. M-mode measurement of TAPSE is sensitive and reproducible for the
 26. follow-up of longitudinal RV function, but it is angle-dependent and when the cursor is not
 27. placed in the direction of the myocardial motion, underestimation of the annular excursion
 28. will occur. This can be prevented using a modified, more lateral four-chamber view focused
 29. on the right ventricle. As illustrated before, TAPSE cannot always be extrapolated to global RV
 30. function.²⁰ The accuracy of 2D echo measurements is influenced by the image quality. When
 31. imaging from an apical four-chamber view, the right ventricle appears in the poor lateral reso-
 32. lution of the transducer. To improve the resolution, the transducer can be moved more laterally
 33. so that the right ventricle appears more in the center of the image sector. The RV myocardial
 34. performance index (Tei index) has also been used as a measurement for RV function,²³ but we
 35. decided not to use this measurement as only in systemic right ventricles a good correlation
 36. with CMR imaging has been described.²⁴ Moreover, the validity of this index for RV function
 37. assessment is much debated, since it includes isovolumic contraction and relaxation which,
 38. on pressure-volume analysis of the normal subpulmonary right ventricle, are not present.^{25, 26}
 39. Consequently, the relevance of the index is controversial.

To use 3D echo for RV imaging in clinical practice, the following conditions should be kept in mind. Firstly, one has to invest in an ultrasound system with 3D echo capabilities and in the training of a dedicated sonographer. In our practice, we found that an average of 40 datasets was needed to learn how to accurately apply 3D echo for RV imaging. Secondly, even though the analysis of 3D datasets takes little time – approximately 2 to 5 minutes – it should be noted that the endocardial border identification may be challenging as echo dropouts frequently occur, especially of the anterior wall and the RV outflow tract. Thirdly, endocardial border identification can be difficult, because the fibrous trabecular network is highly echogenic and appears as a solid muscular layer, giving little differentiation between RV myocardium and trabeculae. As a consequence, the RV cavity borders can be misleading. This is the main source of the difference between 3D echo and CMR imaging in the assessment of RV volumes and the reason why the RV cavity is underestimated using 3D echo. The development of more powerful echocardiographic systems will improve the contrast resolution, thereby improving the accuracy of the analyses.

Currently there is no single echo modality or measurement that will provide “the” measure for RV function. Therefore, we would advice a combination of 2D echo-derived areas, TAPSE, and 3D echo-derived volumes and EF to judge RV size and function for serial follow-up. Areas by 2D echo and TAPSE can be used because of their simplicity and good reproducibility, respectively. As the accuracy of each of these measurements is limited, multiple 2D parameters must be used. Using 3D echo will result in more accurate, good reproducible measurements provided the technique has been mastered during an appropriate learning period for acquisition and analysis. If doubts arise or significant changes in measurements are found over time, CMR imaging is indicated to confirm the echocardiographic data.

Limitations

In some patients the echocardiogram was not made at the same day as the CMR examination. Since measurements of RV volumes and EF are load-dependent this may have caused differences in volumes that are not technique related, but that are caused by hemodynamic changes over time. Moreover, we choose not to calculate volumes based on 2D echo images, since these measurements are not advised by the guidelines² and their accuracy has proven to be limited because of the complicated RV geometry. Recently however, a relatively simple model based on the 2D echo-derived end-diastolic area has been developed to quantify RV end-diastolic volumes.²⁷

CONCLUSIONS

3D echo improved the quantitative RV size and function assessment compared with 2D echo in patients with CHD as well as in healthy controls. No single echocardiography modality will

1. provide “the” measure for RV function. Therefore, we would advice a combination of 2D echo-
2. derived areas, TAPSE, and 3D echo-derived volumes and EF to judge RV size and function for
3. serial follow-up. Everyday clinical use of 3D echo for RV assessment can be reality with the cur-
4. rently available software and provides incremental benefit in assessment of the right ventricle.

5.

6.

7.

8.

9.

10.

11.

12.

13.

14.

15.

16.

17.

18.

19.

20.

21.

22.

23.

24.

25.

26.

27.

28.

29.

30.

31.

32.

33.

34.

35.

36.

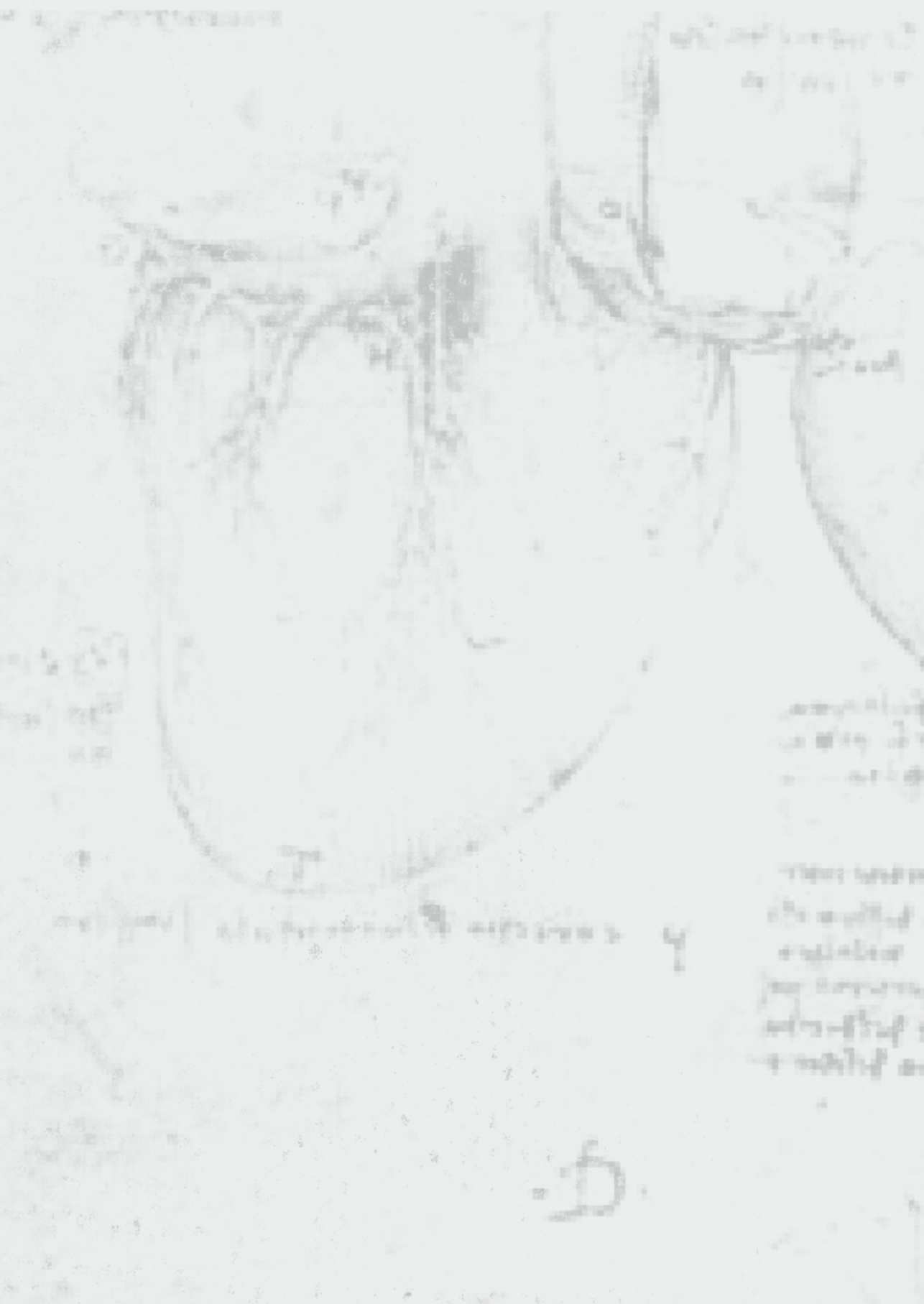
37.

38.

39.

1. Friedberg MK, Rosenthal DN. New developments in echocardiographic methods to assess right ventricular function in congenital heart disease. *Curr Opin Cardiol*. 2005;20:84-8. 1.
2. Rudski LG, Lai WW, Afilalo J, Hua L, Handschumacher MD, Chandrasekaran K, et al. Guidelines for the echocardiographic assessment of the right heart in adults: a report from the American Society of Echocardiography endorsed by the European Association of Echocardiography, a registered branch of the European Society of Cardiology, and the Canadian Society of Echocardiography. *J Am Soc Echocardiogr*. 2010;23:685-713; quiz 86-8. 2.
3.
4.
5.
3. Puchalski MD, Williams RV, Askovich B, Minich LL, Mart C, Tani LY. Assessment of right ventricular size and function: echo versus magnetic resonance imaging. *Congenit Heart Dis*. 2007;2:27-31. 6.
4. Hui W, Abd El Rahman MY, Dsebissowa F, Gutberlet M, Alexi-Meskishvili V, Hetzer R, et al. Comparison of modified short axis view and apical four chamber view in evaluating right ventricular function after repair of tetralogy of Fallot. *Int J Cardiol*. 2005;105:256-61. 7.
8.
5. Koestenberger M, Nagel B, Ravekes W, Everett AD, Stueger HP, Heinzl B, et al. Systolic right ventricular function in pediatric and adolescent patients with tetralogy of Fallot: echocardiography versus magnetic resonance imaging. *J Am Soc Echocardiogr*. 2011;24:45-52. 9.
10.
6. Lai WW, Gauvreau K, Rivera ES, Saleeb S, Powell AJ, Geva T. Accuracy of guideline recommendations for two-dimensional quantification of the right ventricle by echocardiography. *Int J Cardiovasc Imaging*. 2008;24:691-8. 11.
12.
7. Jiang L, Levine RA, Weyman AE. Echocardiographic Assessment of Right Ventricular Volume and Function. *Echocardiography*. 1997;14:189-206. 13.
14.
8. Grewal J, Majdalary D, Syed I, Pellikka P, Warnes CA. Three-dimensional echocardiographic assessment of right ventricular volume and function in adult patients with congenital heart disease: comparison with magnetic resonance imaging. *J Am Soc Echocardiogr*. 2010;23:127-33. 15.
16.
9. Khoo NS, Young A, Occlshaw C, Cowan B, Zeng IS, Gentles TL. Assessments of right ventricular volume and function using three-dimensional echocardiography in older children and adults with congenital heart disease: comparison with cardiac magnetic resonance imaging. *J Am Soc Echocardiogr*. 2009;22:1279-88. 17.
18.
10. van der Zwaan HB, Helbing WA, McGhie JS, Geleijnse ML, Luijnenburg SE, Roos-Hesselink JW, et al. Clinical Value of Real-Time Three-Dimensional Echocardiography for Right Ventricular Quantification in Congenital Heart Disease: Validation With Cardiac Magnetic Resonance Imaging. *J Am Soc Echocardiogr*. 2010;23:134-40. 19.
20.
21.
11. Sugeng L, Mor-Avi V, Weinert L, Niel J, Ebner C, Steringer-Mascherbauer R, et al. Multimodality Comparison of Quantitative Volumetric Analysis of the Right Ventricle. *JACC Cardiovasc Imaging*. 2010;3:10-8. 22.
23.
12. Kjaergaard J, Petersen CL, Kjaer A, Schaadt BK, Oh JK, Hassager C. Evaluation of right ventricular volume and function by 2D and 3D echocardiography compared to MRI. *Eur J Echocardiogr*. 2006;7:430-8. 24.
25.
13. Jenkins C, Chan J, Bricknell K, Strudwick M, Marwick TH. Reproducibility of right ventricular volumes and ejection fraction using real-time three-dimensional echocardiography: comparison with cardiac MRI. *Chest*. 2007;131:1844-51. 26.
27.
14. Robbers-Visser D, Boersma E, Helbing WA. Normal biventricular function, volumes, and mass in children aged 8 to 17 years. *J Magn Reson Imaging*. 2009;29:552-9. 28.
29.
15. Bland JM, Altman DG. Statistical methods for assessing agreement between two methods of clinical measurement. *Lancet*. 1986;1:307-10. 30.
31.
16. van der Zwaan HB, Helbing WA, Boersma E, Geleijnse ML, McGhie JS, Soliman OI, et al. Usefulness of real-time three-dimensional echocardiography to identify right ventricular dysfunction in patients with congenital heart disease. *Am J Cardiol*. 2010;106:843-50. 32.
33.
17. DeLong ER, DeLong DM, Clarke-Pearson DL. Comparing the areas under two or more correlated receiver operating characteristic curves: a nonparametric approach. *Biometrics*. 1988;44:837-45. 34.
35.
36.
37.
38.
39.

18. Soliman OI, Kirschbaum SW, van Dalen BM, van der Zwaan HB, Mahdavian Delavary B, Vletter WB, et al. Accuracy and reproducibility of quantitation of left ventricular function by real-time three-dimensional echocardiography versus cardiac magnetic resonance. *Am J Cardiol.* 2008;102:778-83.
19. Jacobs LD, Salgo IS, Goonewardena S, Weinert L, Coon P, Bardo D, et al. Rapid online quantification of left ventricular volume from real-time three-dimensional echocardiographic data. *Eur Heart J.* 2006;27:460-8.
20. Morcos P, Vick GW, 3rd, Sahn DJ, Jerosch-Herold M, Shurman A, Sheehan FH. Correlation of right ventricular ejection fraction and tricuspid annular plane systolic excursion in tetralogy of Fallot by magnetic resonance imaging. *Int J Cardiovasc Imaging.* 2008.
21. Lissin LW, Li W, Murphy DJ, Jr., Hornung T, Swan L, Mullen M, et al. Comparison of transthoracic echocardiography versus cardiovascular magnetic resonance imaging for the assessment of ventricular function in adults after atrial switch procedures for complete transposition of the great arteries. *Am J Cardiol.* 2004;93:654-7.
22. Iriart X, Montaudon M, Lafitte S, Chabaneix J, Reant P, Balbach T, et al. Right ventricle three-dimensional echography in corrected tetralogy of fallot: accuracy and variability. *Eur J Echocardiogr.* 2009.
23. Schwerzmann M, Samman AM, Salehian O, Holm J, Provost Y, Webb GD, et al. Comparison of echocardiographic and cardiac magnetic resonance imaging for assessing right ventricular function in adults with repaired tetralogy of fallot. *Am J Cardiol.* 2007;99:1593-7.
24. Salehian O, Schwerzmann M, Merchant N, Webb GD, Siu SC, Therrien J. Assessment of systemic right ventricular function in patients with transposition of the great arteries using the myocardial performance index: comparison with cardiac magnetic resonance imaging. *Circulation.* 2004;110:3229-33.
25. Redington AN, Rigby ML, Shinebourne EA, Oldershaw PJ. Changes in the pressure-volume relation of the right ventricle when its loading conditions are modified. *Br Heart J.* 1990;63:45-9.
26. Yoshifuku S, Otsuji Y, Takasaki K, Yuge K, Kisanuki A, Toyonaga K, et al. Pseudonormalized Doppler total ejection isovolume (Tei) index in patients with right ventricular acute myocardial infarction. *Am J Cardiol.* 2003;91:527-31.
27. Greutmann M, Tobler D, Biaggi P, Mah ML, Crean A, Oechslin EN, et al. Echocardiography for assessment of right ventricular volumes revisited: a cardiac magnetic resonance comparison study in adults with repaired tetralogy of Fallot. *J Am Soc Echocardiogr.* 2010;23:905-11.



Chapter 5

Test-retest variability of volumetric right ventricular measurements using real-time three-dimensional echocardiography

H.B. van der Zwaan

M.L. Geleijnse

O.I.I. Soliman

J.S. McGhie

E.J.A. Wiegiers-Groeneweg

W.A. Helbing

J.W. Roos-Hesselink

F.J. Meijboom

J Am Soc Echocardiogr. 2011; in press

ABSTRACT

Background. Substantial variability in sequential echocardiographic right ventricular (RV) quantification may exist. Inter- and intra-observer values are well known, but acquisition (test-retest) variability has been rarely assessed. The objective of this study was to determine the test-retest variability of sequential RV volume and ejection fraction (EF) measurements by real-time three-dimensional echocardiography in patients with congenital heart disease and healthy controls.

Methods. Twenty-eight participants (21 patients with congenital heart disease, seven healthy controls; mean age, 30 ± 14 years; 43% men) underwent a series of three echocardiographic studies. To obtain inter-observer and intra-observer test-retest variability, two sonographers acquired sequential RV datasets in each participant during one outpatient visit. RV volumetric quantification was done using semiautomated three-dimensional border detection. The variability data were analyzed using correlation coefficients, Bland-Altman analysis, and coefficients of variation.

Results. Absolute mean differences for sequential intra-observer acquisitions were 12 ± 12 ml for end-diastolic volume, 7 ± 6 ml for end-systolic volume, and $4 \pm 3\%$ for EF. Inter-observer and intra-observer test-retest variability, respectively, were 7% and 7% for RV end-diastolic volume, 14% and 7% for end-systolic volume, and 8% and 6% for EF.

Conclusions. Good test-retest variability, besides the practical nature of real-time three-dimensional echocardiography for RV volume and EF assessment, makes it a valuable technique for serial follow-up. Although it may be challenging to diminish all factors that can influence echocardiographic examination for serial follow-up, standardization of RV size and function measurements should be a goal to produce more interchangeable data.

1.
2.
3.
4.
5.
6.
7.
8.
9.
10.
11.
12.
13.
14.
15.
16.
17.
18.
19.
20.
21.
22.
23.
24.
25.
26.
27.
28.
29.
30.
31.
32.
33.
34.
35.
36.
37.
38.
39.

1. INTRODUCTION

2.

3. Right ventricular (RV) volumes and ejection fraction (EF) are important factors for the initiation
4. of therapy and assessment of response to treatment in patients with congenital heart disease
5. (CHD).¹⁻⁴ Therefore, RV volumes and EF are tested sequentially in everyday clinical practice.⁵
6. Subjective visual evaluation of RV function may be appropriate for single assessment, but it
7. is insufficiently reliable for sequential use.⁶ Longitudinal RV function can more accurately be
8. determined by measuring the tricuspid annular plane systolic excursion or the myocardial
9. performance index.⁷ Quantification of RV dimensions and function can be done by two-
10. dimensional echocardiography,⁷ although the value of the estimations of RV volumes and
11. EF is limited due to the need of geometric assumptions that are especially not true for the
12. abnormal hearts that are of interest. Consequently, cardiac magnetic resonance (CMR) imaging
13. has become the indicated technique for RV volume and EF assessment,⁵ even though the cost
14. and availability of CMR imaging may hamper its use in routine clinical practice.⁸⁻⁹

15. Real-time three-dimensional (3D) echocardiography (RT3DE) is an alternative imaging
16. modality for quantification of RV volumes and EF.¹⁰ In various studies, improved accuracy and
17. inter-observer and intra-observer values of RT3DE compared with two-dimensional echocar-
18. diography in patients with CHD have been shown.¹¹⁻¹³ However, these inter-observer and intra-
19. observer values reflect only the variability caused by variations in analysis of the same dataset.
20. Another source of variability is the difference in the acquisition of the datasets, the test-retest
21. variability between datasets that are acquired and subsequently analyzed. To what extent this
22. affects patients with CHD with abnormally shaped right ventricles is unknown. Therefore, the
23. objective of this study was to determine the test-retest variability of RT3DE for RV volumes and
24. EF.

25.

26.

27. METHODS

28.

29. Study design

30. We prospectively recruited 33 participants (21 patients with complex and/or surgically repaired
31. CHD and 12 healthy controls) in sinus rhythm, who all underwent a RT3DE examination. The
32. patients were referred to the echocardiography laboratory for routine measurements of their
33. cardiac function and had sufficient acoustic windows. The healthy controls were employees
34. of the university or the hospital who had no medical histories or current symptoms sugges-
35. tive of cardiovascular disease, including hypertension and/or a systemic illness with potential
36. cardiovascular components, such as diabetes or thyroid disease. The medical ethics committee
37. approved the study, and informed consent was obtained from all patients and healthy controls.

38. To assess inter-observer and intra-observer test-retest variability in a way that closely reflects
39. everyday clinical practice, the following schedule was applied (Figure 1). Sonographer 1 (J.S.M)

acquired a RV real-time 3D echocardiographic dataset, after which sonographer 2 (E.J.A.W.-G.) independently acquired a dataset using the same machine. Thereafter, sonographer 1 acquired a second dataset. In this manner, RV datasets were obtained independently by two sonographers with various levels of experience regarding 3D echocardiographic assessment of the right ventricle (4 and 2 years, respectively), who were blinded to each other's results. After the acquisitions, they analyzed their own datasets in a blinded fashion, resulting in inter-observer and intra-observer test-retest variability. Furthermore, inter-observer variability was determined by having all datasets that were acquired by sonographer 2 also analyzed by sonographer 1.

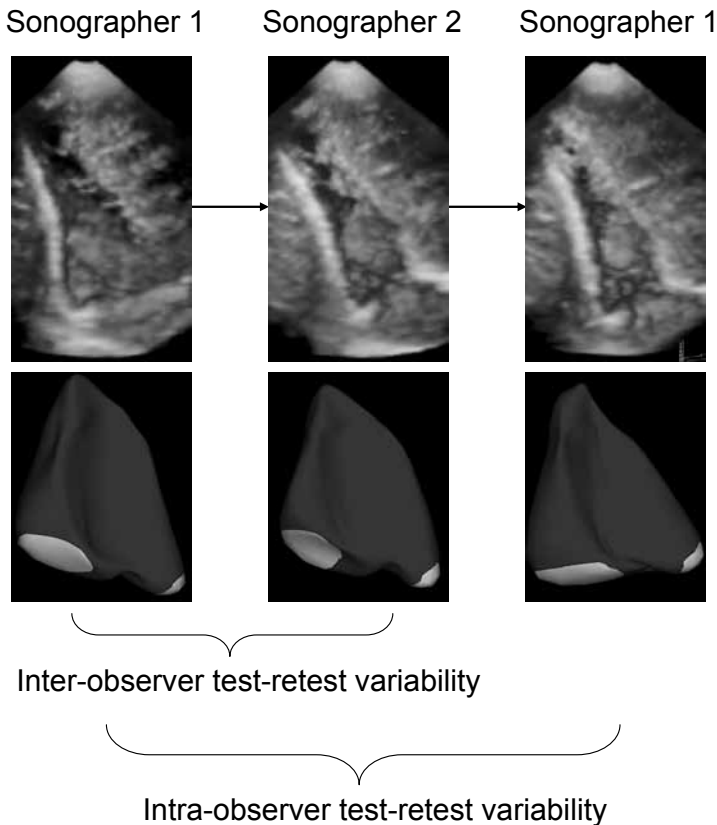
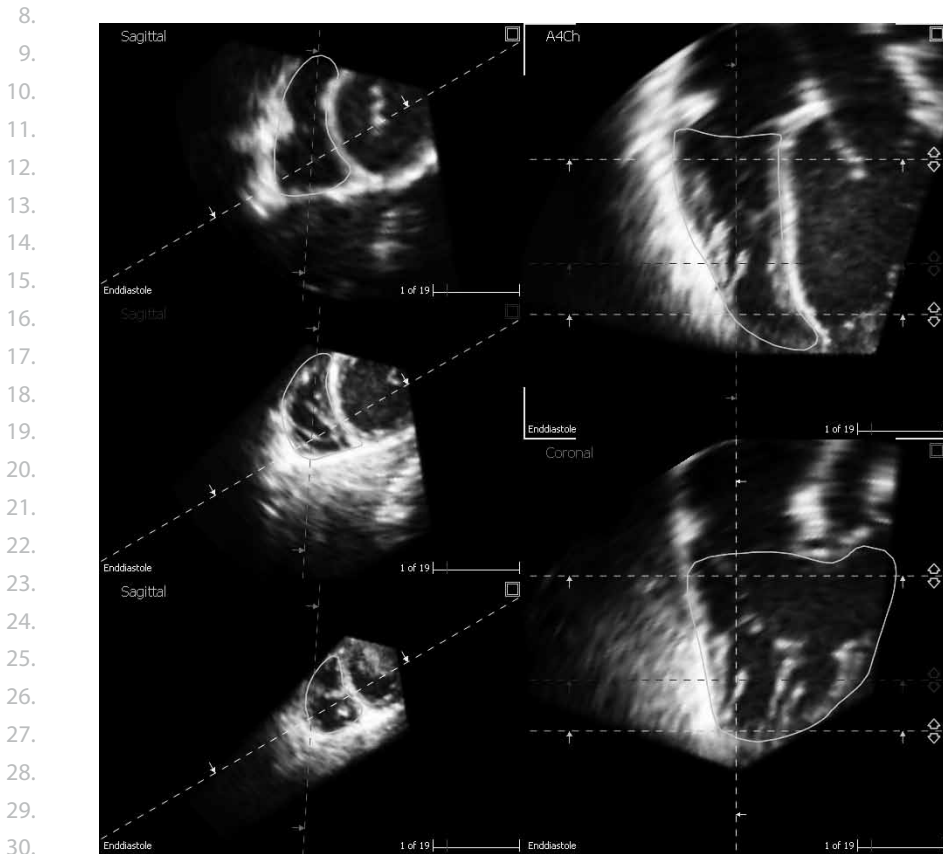


Figure 1 Flowchart displaying the study design to obtain data on test-retest variability for right ventricular assessment by real-time 3-dimensional echocardiography.

Acquisition and analysis by real-time three-dimensional echocardiography

Real-time 3D echocardiographic harmonic imaging was performed using the iE33 ultrasound system (Philips Medical Systems, Best, the Netherlands) equipped with an X3-1 matrix array transducer with the patient in the left lateral decubitus position. A full-volume scan was acquired from a modified apical transducer position in harmonic mode from seven

1. R-wave-gated subvolumes during a single end-expiratory breath-hold. The depth and angle of
2. the ultrasound sector were adjusted to a minimal level still encompassing the right ventricle.
3. Before each acquisition, images were optimized for endocardial border visualization by modify-
4. ing time gain and compression and increasing the overall gain. The mean volume rate was 29
5. frames/ cardiac cycle (range, 20 – 45 frames/ cardiac cycle). The datasets were digitally exported
6. to a TomTec server (TomTec Imaging Systems, Unterschleissheim, Germany) connected to a
7. terminal workstation for further analyses.



31. **Figure 2** Display from the 4D RV-Function TomTec analysis program in a representative patient who
 32. can be found in everyday clinical practice, showing the final stage of contour detection in which manual
 33. correction of the contours can be applied in any cross-section or phase of the cardiac cycle.

34.
 35. The digital real-time 3D echocardiographic RV datasets were analyzed offline using Tom-
 36. Tec's four-dimensional RV Function version 1.2. The datasets were judged for image quality:
 37. they should include an analyzable RV apex, lateral wall, and tricuspid valve area. The software
 38. performs 3D semiautomated border detection of RV volumes over one cardiac cycle. It uses a
 39. physics-based modelling algorithm that makes no assumptions regarding RV geometry. The

function of the TomTec analysis program is reported in detail elsewhere.¹² In short, the end-diastolic (largest RV volume) and end-systolic (smallest RV volume) phases need to be identified. Endocardial border contours are drawn onto still frames of the apical four-chamber view, short-axis view, and coronal view in both end-diastole and end-systole (Figure 2). After the steps followed for contour tracing the software automatically delineates the RV endocardial border from the end-diastolic and end-systolic phases. By sequential analysis, the software creates an RV mathematic dynamic 3D endocardial surface that represents changes in the RV cavity over the cardiac cycle. From this 3D endocardial surface, global RV volumes and EF are calculated.

Statistical analysis

Statistical analysis was performed using SPSS version 15.0 (SPSS, Inc, Chicago, Illinois). Categorical data are summarized as numbers and percentages, and continuous data are presented as mean \pm SD. Agreement between the sequential acquisitions was evaluated by linear regression analysis with Pearson's correlation coefficient. The Z-statistic was used to evaluate differences between two correlation coefficients. Furthermore, the agreement was evaluated using Bland-Altman analysis by calculating the bias (mean difference) and the 95% limits of agreement (2 standard deviations around the mean difference).¹⁴ Paired *t* tests were used to analyze the significance of the biases in volumes and EF between sequential acquisitions. Moreover, the coefficients of variation were defined as the standard deviation of the difference between the two readings (or readers) divided by their mean value times 100. All statistical tests were two-sided, and P-values <0.05 were considered statistically significant.

RESULTS

Of the original 33 participants, five were excluded from analysis for echocardiographic images of insufficient quality (four because of poor acoustic windows and one because of the inability to include the RV lateral wall and apex). The baseline characteristics of 28 participants (mean age, 30 ± 14 years; 43% men) are listed in Table 1. The patients who were included had the following types of CHD: atrial septal defect ($n = 5$), tetralogy of Fallot ($n = 3$), aortic valve pathology ($n = 5$), pulmonary stenosis with or without ventricular septal defect ($n = 2$), double-outlet right ventricle ($n = 1$), ventricular septal defect ($n = 1$), arterial switch for transposition of the great arteries ($n = 1$), coarctation of the aorta ($n = 1$), mitral valve insufficiency ($n = 1$), and patent arterial duct ($n = 1$). The heart rates did not change significantly over the various examinations.

The RV volumes and EF obtained by the two sonographers are displayed in Table 2. Measurements on the sequential datasets by one sonographer were not different, while the end-diastolic volume measurements by the second sonographer differed from those obtained by the first sonographer ($P = 0.017$).

Table 1. Baseline characteristics (n = 28)

Variable	Value
Men (%)	43
Age (years)	30 ± 14
Heart rate (beats/min)	60 ± 10
Height (cm)	172 ± 10
Weight (kg)	67 ± 8
Body surface area (m ²)	1.8 ± 0.1
Specific characteristics of patients	
Age at initial repair (years), (n = 16)	10 ± 19
Right-sided congenital heart disease (number)	11
Left-sided congenital heart disease (number)	10

Data are presented as mean ± SD or number.

Table 2. Right ventricular volumes and ejection fraction by real-time three-dimensional echocardiography

	Sonographer 1			Sonographer 2	
	Acquisition 1	Acquisition 2	P-value*	Acquisition 1	P-value#
End-diastolic volume (ml)	183 ± 43	180 ± 37	0.36	173 ± 39	0.017
End-systolic volume (ml)	88 ± 30	86 ± 23	0.79	83 ± 28	0.076
Stroke volume (ml)	95 ± 22	94 ± 19	0.41	91 ± 19	0.14
Ejection fraction (%)	53 ± 7	53 ± 6	0.70	53 ± 7	0.68

Data are expressed as mean ± SD.

*Paired t test for sequential measurements recorded by one sonographer.

Paired t test for sequential measurements between two sonographers.

Inter-observer test-retest variability

The Z-statistic revealed no differences in the strength of the correlations found by sequential acquisitions and the corresponding measurements between sonographers versus correlations found by sequential acquisitions and measurements by one sonographer. The results of linear regression and Bland-Altman analysis for the assessment of the inter-observer test-retest variability are displayed in Figure 3. For RV end-diastolic volume, end-systolic volume, and EF, the inter-observer test-retest variability was 7%, 14%, and 8%, respectively (Table 3).

Table 3. Sequential (test-retest) and inter-observer variability measurements by real-time three-dimensional echocardiography

	Sequential acquisitions between sonographers		Sequential acquisitions by one sonographer		Inter-observer reproducibility	
	Absolute mean difference	Coefficient of variation	Absolute mean difference	Coefficient of variation	Absolute mean difference	Coefficient of variation
End-diastolic volume	15 ± 13	7%	12 ± 12	7%	13 ± 9	5%
End-systolic volume	12 ± 12	14%	7 ± 6	7%	11 ± 8	9%
Stroke volume	13 ± 10	11%	12 ± 10	11%	11 ± 10	10%
Ejection fraction	5 ± 4	8%	4 ± 3	6%	5 ± 4	8%

Coefficients of variation represent the standard deviation of the difference between two sonographers, two measurements, or two observers divided by the mean of the measurements, expressed as a percentage.

Sequential acquisitions between sonographers

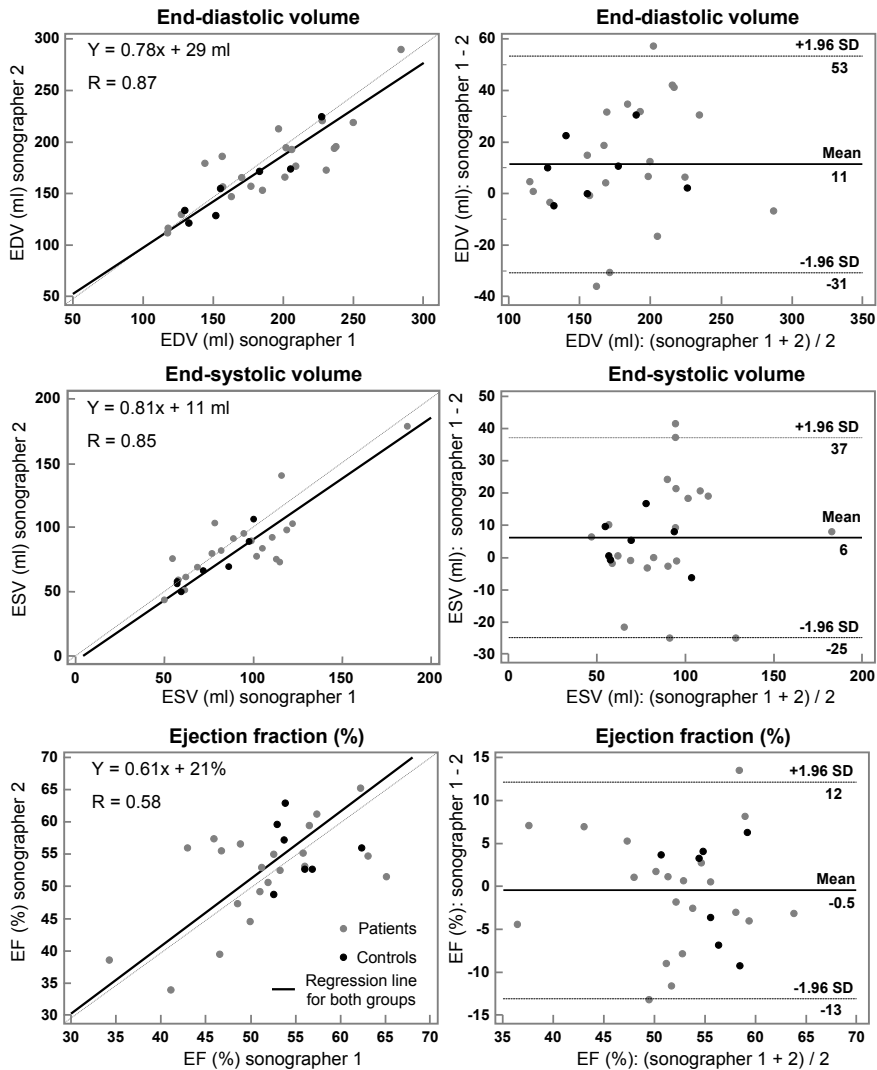


Figure 3 Linear regression (left) and Bland-Altman analysis (right) for sequential right ventricular acquisitions between two sonographers by three-dimensional echocardiography. End-diastolic volume (EDV; top), end-systolic volume (ESV; center), and ejection fraction (bottom) are shown. Patients are displayed in grey (n = 21) and healthy controls are displayed in black (n = 7). The regression line represents both groups.

Intra-observer test-retest variability

The results of linear regression and Bland-Altman analysis for the assessment of the intra-observer test-retest variability are displayed in Figure 4. The variations coefficients indicating intra-observer test-retest variability were 7% for end-diastolic volume, 7% for end-systolic volume, and 6% for EF (Table 3).

Sequential acquisitions by one sonographer

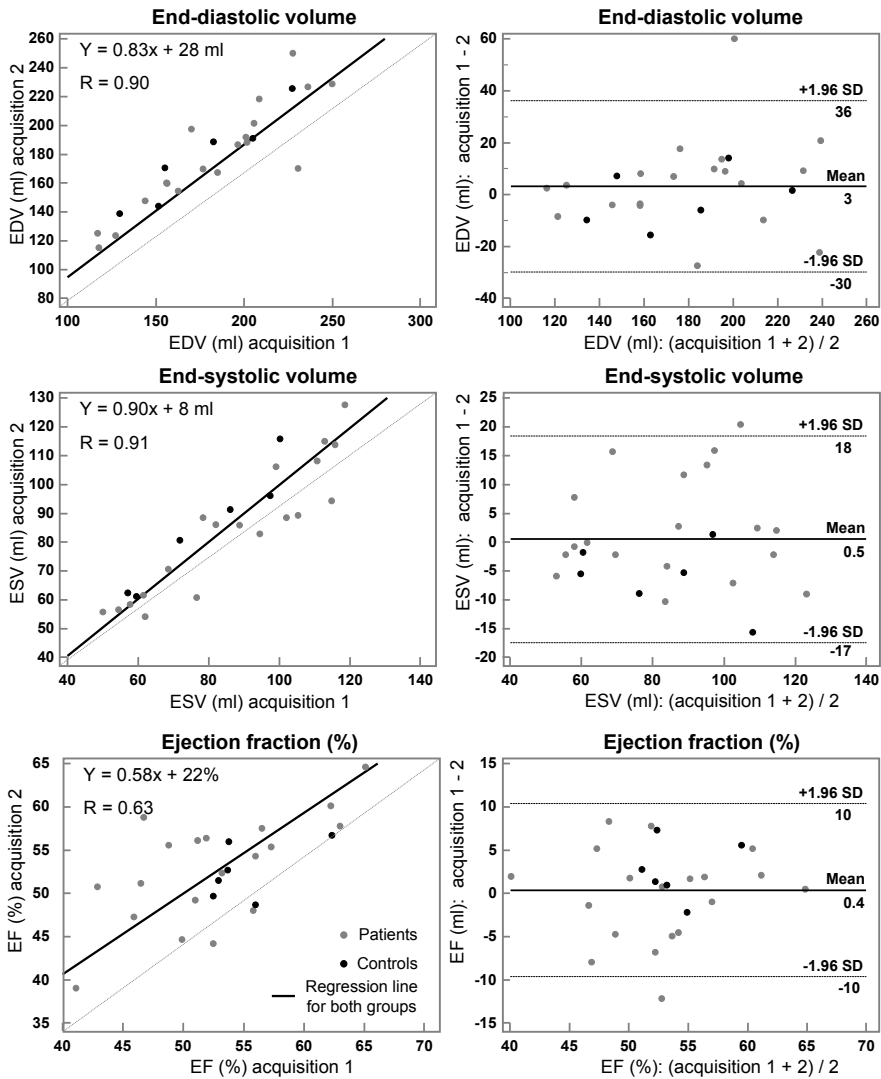


Figure 4 Linear regression (a) and Bland-Altman analysis (b) for sequential right ventricular acquisitions by one sonographer by three-dimensional echocardiography. End-diastolic volume (EDV; top), end-systolic volume (ESV; center), and ejection fraction (bottom) are shown. Patients are displayed in grey (n = 21) and healthy controls are displayed in black (n = 7). The regression line represents both groups.

Inter-observer variability

Figure 5 shows the linear regression and Bland-Altman analysis for the inter-observer reproducibility. Absolute mean differences and coefficients of variation that were found for inter-observer variability are displayed in Table 3. The variation coefficients for inter-observer variability were 5% for end-diastolic volume, 9% for end-systolic volume, and 8% for EF.

Inter-observer reproducibility

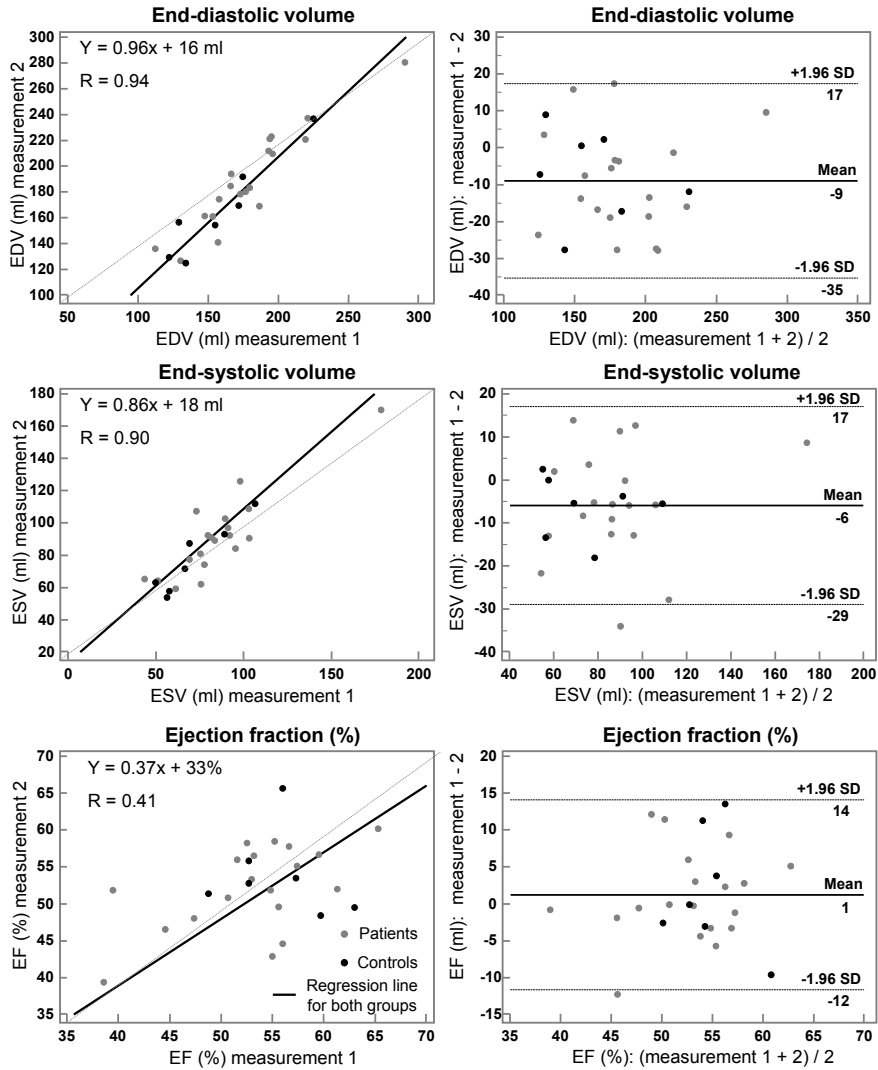


Figure 5 Linear regression (a) and Bland-Altman analysis (b) for sequential right ventricular measurements by two observers by three-dimensional echocardiography. End-diastolic volume (EDV; top), end-systolic volume (ESV; center), and ejection fraction (bottom) are shown. Patients are displayed in grey ($n = 21$) and healthy controls are displayed in black ($n = 7$). The regression line represents both groups.

1.
2.
3.
4.
5.
6.
7.
8.
9.
10.
11.
12.
13.
14.
15.
16.
17.
18.
19.
20.
21.
22.
23.
24.
25.
26.
27.
28.
29.
30.
31.
32.
33.
34.
35.
36.
37.
38.
39.

1. DISCUSSION

2.

3. In this study we investigated the test-retest variability of RT3DE for RV volumes and EF assess-
 4. ment. In order to include a heterogeneous population with wider ranges of observed measure-
 5. ments, we included not only healthy controls but patients with various types of CHD as well.
 6. The smallest coefficients of variation were found for end-diastolic volume and EF. The larger
 7. variability found in the end-systolic volumes can be attributed to the more difficult endocardial
 8. border identification in end-systole due to more densely packed trabeculations and papil-
 9. lary muscles. The inter-observer test-retest variability of RV EF was 8%, which is comparable
 10. with results reported for CMR imaging.¹⁵ Khoo et al¹⁶ demonstrated no significant difference
 11. between RT3DE and CMR imaging on conventional reproducibility testing, suggesting that
 12. RT3DE was comparable with CMR imaging. Furthermore, the found test-retest variability
 13. was comparable with the conventional inter-observer reproducibility found in this study and
 14. reported by others for RT3DE-derived RV assessment.¹²⁻¹³

15. The reproducibility of RT3DE for RV assessment has been studied extensively.^{11-13, 17} Only in
 16. a few studies has intra-observer test-retest variability been reported, while the inter-observer
 17. variability (i.e., the variability caused by acquisitions and analysis by different sonographers)
 18. has not been described as yet.^{11, 17-18} In one study, test-retest variability of RV volumes in 50
 19. patients with left ventricular wall motion abnormalities was reported. RT3DE was found to have
 20. lower intra-observer test-retest variability for RV volumes and EF than any two-dimensional
 21. echocardiographic measurement.¹⁸ Small absolute mean differences were found (0 ± 5 ml for
 22. the end-diastolic volume, 0 ± 3 ml for the end-systolic volume, and $0 \pm 4\%$ for EF). In our study,
 23. the differences were slightly larger, but this may be explained by the fact that we also included
 24. patients with CHD with enlarged right ventricles. The relative RV volume differences will there-
 25. fore be less substantial. Grewal et al¹¹ evaluated test-retest variability in 15 patients with severe
 26. pulmonary regurgitation and found variability of 10.6% for the end-diastolic volume. This value
 27. is somewhat larger than the value we found (6%). Tamborini et al¹⁷ found coefficients of varia-
 28. tion of 1.9% for end-diastolic volume, 6.1% for end-systolic volume, 3.0% in stroke volume, and
 29. 2.2% for EF in 20 healthy controls.

30. The test-retest variability can be partitioned into patient-related (body mass index, blood
 31. pressure, or heart frequency), acquisition-related (laboratory and sonographer), and reader-
 32. related variability. Because RV volumes and EF are strongly influenced by differences in load-
 33. ing conditions over time, we sought to minimize these by repeating the study over a short
 34. time frame, so that the main source of variation was related to imaging considerations. The
 35. differences between repeated studies might be expected to influence acquisition variability
 36. adversely.¹⁹ Although it may be hard to diminish these influences, guidelines containing pre-
 37. cise instructions for RV size and function measurements⁷ should be developed to create more
 38. standardized, robust, and interchangeable measurements.

39.

Clinical implications

Sequential assessment of RV size and function is important in the everyday management of adults with CHD, because RV function yields prognostic information.^{1-2, 20-21} Although some other imaging modalities are thought to have superior spatial resolution, such as CMR imaging or computed tomography, the use of repeated echocardiography is attractive since no ionizing radiation is needed and patient discomfort is minimal. In clinical practice, sequential patient studies may be performed by different sonographers and may be interpreted by different readers, possibly readers with different approaches or without standardization of reading styles. However, the different readers necessarily use a similar, modified apical four-chamber approach for real-time 3D echocardiographic dataset acquisition and the same RV analysis software with well-known and standardized steps for RV reconstruction.

Accurate and reproducible measurements are essential to permit meaningful comparison between echocardiographic studies. Changes in these measurements may reflect improvement or worsening of disease, but changes should always be seen in the light of test-retest variability. Leibundgut et al²² presented limits of agreement of about $\pm 10\%$ for the intra-observer and inter-observer variability of RV EF. They pointed out that these limits of agreement are not yet sufficient to detect subtle changes in RV contractility during follow-up examinations. We can underline these findings with the results on limits of agreement for RV EF estimation of the current study. Therefore, the magnitude of RV EF changes that one can expect to find using RT3DE that yields clinical clues should be $>10\%$ to overcome the variability in measurements caused by the technique itself. For example, if RV function in a patient with tetralogy of Fallot with a significant pulmonary valve insufficiency is examined twice a year, a decrease in RV EF larger of $>10\%$ can provide the physician with a clue to start considering a pulmonary valve replacement. Any decreases in RV EF of $<10\%$ may be caused erroneously by the technique itself. It is important to realize that these measurement errors are not an exclusive characteristic of echocardiography, but these errors are found with all imaging techniques used in clinical practice, including CMR imaging and computed tomography.

Limitations

Our study was not designed to apply multivariate regression analysis that could have identified the predictors of variability, because the study population was not large enough. However, consistent with earlier studies,¹⁹ we expect that a relatively poor dataset quality adversely affects the test-retest variability for the RV measurements. Therefore, only datasets of sufficient quality should be analyzed.¹²

1. CONCLUSIONS

2.

3. The good test-retest variability of RT3DE for RV volume and EF assessment makes it a valu-
4. able technique for serial follow-up. Furthermore, sequential use of this technique is attractive
5. becausee no ionizing radiation is needed and patient discomfort is minimal. In clinical practice,
6. different approaches to echocardiographic examination for repeated studies influence the
7. acquisition variability adversely. Even though it may be challenging to diminish these influ-
8. ences, standardization of RV size and function measurements should be a goal to produce
9. more interchangeable measurements.

10.

11.

12.

13.

14.

15.

16.

17.

18.

19.

20.

21.

22.

23.

24.

25.

26.

27.

28.

29.

30.

31.

32.

33.

34.

35.

36.

37.

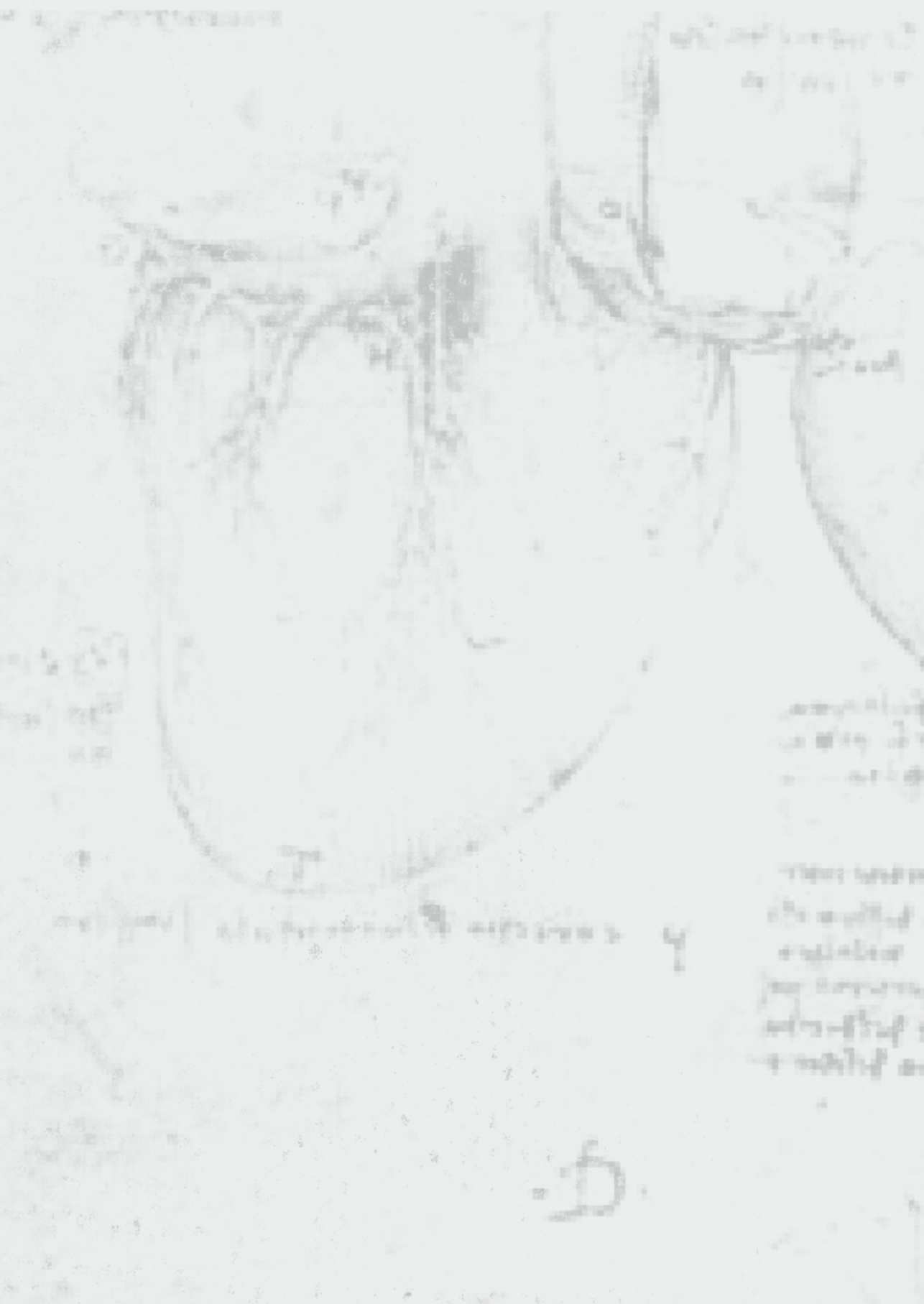
38.

39.

1. Knauth AL, Gauvreau K, Powell AJ, Landzberg MJ, Walsh EP, Lock JE, et al. Ventricular size and function assessed by cardiac MRI predict major adverse clinical outcomes late after tetralogy of Fallot repair. *Heart*. 2008;94:211-6. 1.
2. Murphy JG, Gersh BJ, Mair DD, Fuster V, McGoon MD, Ilstrup DM, et al. Long-term outcome in patients undergoing surgical repair of tetralogy of Fallot. *N Engl J Med*. 1993;329:593-9. 2.
3. Haddad F, Doyle R, Murphy DJ, Hunt SA. Right ventricular function in cardiovascular disease, part II: pathophysiology, clinical importance, and management of right ventricular failure. *Circulation*. 2008;117:1717-31. 3.
4. Tobler D, Williams WG, Jegatheeswaran A, Van Arsdell GS, McCrindle BW, Greutmann M, et al. Cardiac outcomes in young adult survivors of the arterial switch operation for transposition of the great arteries. *J Am Coll Cardiol*. 2010;56:58-64. 4.
5. Endorsed by the Association for European Paediatric C, Authors/Task Force M, Baumgartner H, Bonhoeffer P, De Groot NM, de Haan F, et al. ESC Guidelines for the management of grown-up congenital heart disease (new version 2010): The Task Force on the Management of Grown-up Congenital Heart Disease of the European Society of Cardiology (ESC). *Eur Heart J*. 2010. 5.
6. Puchalski MD, Williams RV, Askovich B, Minich LL, Mart C, Tani LY. Assessment of right ventricular size and function: echo versus magnetic resonance imaging. *Congenit Heart Dis*. 2007;2:27-31. 6.
7. Rudski LG, Lai WW, Afilalo J, Hua L, Handschumacher MD, Chandrasekaran K, et al. Guidelines for the echocardiographic assessment of the right heart in adults: a report from the American Society of Echocardiography endorsed by the European Association of Echocardiography, a registered branch of the European Society of Cardiology, and the Canadian Society of Echocardiography. *J Am Soc Echocardiogr*. 2010;23:685-713; quiz 86-8. 7.
8. Babu-Narayan SV, Gatzoulis MA, Kilner PJ. Non-invasive imaging in adult congenital heart disease using cardiovascular magnetic resonance. *J Cardiovasc Med (Hagerstown)*. 2007;8:23-9. 8.
9. Bleeker GB, Steendijk P, Holman ER, Yu CM, Breithardt OA, Kaandorp TA, et al. Assessing right ventricular function: the role of echocardiography and complementary technologies. *Heart*. 2006;92 Suppl 1:i19-26. 9.
10. Mangion JR. Right ventricular imaging by two-dimensional and three-dimensional echocardiography. *Curr Opin Cardiol*. 2010;22:423-9. 10.
11. Grewal J, Majdalany D, Syed I, Pellikka P, Warnes CA. Three-dimensional echocardiographic assessment of right ventricular volume and function in adult patients with congenital heart disease: comparison with magnetic resonance imaging. *J Am Soc Echocardiogr*. 2010;23:127-33. 11.
12. van der Zwaan HB, Helbing WA, McGhie JS, Geleijnse ML, Luijnenburg SE, Roos-Hesselink JW, et al. Clinical Value of Real-Time Three-Dimensional Echocardiography for Right Ventricular Quantification in Congenital Heart Disease: Validation With Cardiac Magnetic Resonance Imaging. *J Am Soc Echocardiogr*. 2010;23:134-40. 12.
13. Iriart X, Montaudon M, Lafitte S, Chabaneix J, Reant P, Balbach T, et al. Right ventricle three-dimensional echography in corrected tetralogy of fallot: accuracy and variability. *Eur J Echocardiogr*. 2009;10:784-92. 13.
14. Bland JM, Altman DG. Statistical methods for assessing agreement between two methods of clinical measurement. *Lancet*. 1986;1:307-10. 14.
15. Luijnenburg SE, Robbers-Visser D, Moelker A, Vliegen HW, Mulder BJ, Helbing WA. Intra-observer and interobserver variability of biventricular function, volumes and mass in patients with congenital heart disease measured by CMR imaging. *Int J Cardiovasc Imaging*. 2010;26:57-64. 15.
16. Khoo NS, Young A, Occlshaw C, Cowan B, Zeng IS, Gentles TL. Assessments of right ventricular volume and function using three-dimensional echocardiography in older children and adults with congenital heart disease: comparison with cardiac magnetic resonance imaging. *J Am Soc Echocardiogr*. 2009;22:1279-88. 16.

1.
2.
3.
4.
5.
6.
7.
8.
9.
10.
11.
12.
13.
14.
15.
16.
17.
18.
19.
20.
21.
22.
23.
24.
25.
26.
27.
28.
29.
30.
31.
32.
33.
34.
35.
36.
37.
38.
39.

1. 17. Tamborini G, Marsan NA, Gripari P, Maffessanti F, Brusoni D, Muratori M, et al. Reference values for right ventricular volumes and ejection fraction with real-time three-dimensional echocardiography: evaluation in a large series of normal subjects. *J Am Soc Echocardiogr.* 2010;23:109-15.
2. 18. Jenkins C, Chan J, Bricknell K, Strudwick M, Marwick TH. Reproducibility of right ventricular volumes and ejection fraction using real-time three-dimensional echocardiography: comparison with cardiac MRI. *Chest.* 2007;131:1844-51.
3. 19. Gottdiener JS, Panza JA, St John Sutton M, Bannon P, Kushner H, Weissman NJ. Testing the test: the reliability of echocardiography in the sequential assessment of valvular regurgitation. *Am Heart J.* 2002;144:115-21.
4. 20. Geva T, Sandweiss BM, Gauvreau K, Lock JE, Powell AJ. Factors associated with impaired clinical status in long-term survivors of tetralogy of Fallot repair evaluated by magnetic resonance imaging. *J Am Coll Cardiol.* 2004;43:1068-74.
5. 21. Piran S, Veldtman G, Siu S, Webb GD, Liu PP. Heart failure and ventricular dysfunction in patients with single or systemic right ventricles. *Circulation.* 2002;105:1189-94.
6. 22. Leibundgut G, Rohner A, Grize L, Bernheim A, Kessel-Schaefer A, Bremerich J, et al. Dynamic assessment of right ventricular volumes and function by real-time three-dimensional echocardiography: a comparison study with magnetic resonance imaging in 100 adult patients. *J Am Soc Echocardiogr.* 2010;23:116-26.
7. 15.
8. 16.
9. 17.
10. 18.
11. 19.
12. 20.
13. 21.
14. 22.
15. 23.
16. 24.
17. 25.
18. 26.
19. 27.
20. 28.
21. 29.
22. 30.
23. 31.
24. 32.
25. 33.
26. 34.
27. 35.
28. 36.
29. 37.
30. 38.
31. 39.



Chapter 6

Clinical value of real-time three-dimensional echocardiography for right ventricular quantification in congenital heart disease: validation with cardiac magnetic resonance imaging

H.B. van der Zwaan
W.A. Helbing
J.S. McGhie
M.L. Geleijnse
S. Luijnenburg
J.W. Roos-Hesselink
F.J. Meijboom

J Am Soc Echocardiogr. 2010 Feb;23(2):134-40

ABSTRACT

Background. The objective of this study was to test the feasibility, accuracy, and reproducibility of the assessment of right ventricular (RV) volumes and ejection fraction (EF) by real-time three-dimensional echocardiography (RT3DE) in patients with congenital heart disease (CHD), using cardiac magnetic resonance imaging (CMR) as a reference.

Methods. RT3DE datasets and short-axis cine CMR were obtained in 62 consecutive patients (mean age 27 ± 10 years, 68% men) with various CHDs. RV volumetric quantification was done using semiautomated 3-dimensional border detection for RT3DE images and manual tracing of contours in multiple slices for CMR images.

Results. Adequate RV RT3DE datasets could be analysed in 50 of 62 patients (81%). The time needed for RV acquisition and analysis was less for RT3DE than for CMR ($P < 0.001$). Compared with CMR, RT3DE underestimated RV end-diastolic and end-systolic volumes and EF by 34 ± 65 ml, 11 ± 55 ml and $4 \pm 13\%$ ($P < 0.05$) with 95% limits of agreement of ± 131 ml, ± 109 ml, and $\pm 27\%$, as shown by Bland-Altman analyses, with highly significant correlations ($r = 0.93$, $r = 0.91$, and $r = 0.74$, respectively, $p < 0.001$). Inter-observer variability was $1 \pm 15\%$, $6 \pm 17\%$, and $8 \pm 13\%$ for end-diastolic and end-systolic volumes and EF, respectively.

Conclusions. In the majority of unselected patients with complex CHD, RT3DE provides a fast and reproducible assessment of RV volumes and EF with fair to good accuracy compared with CMR reference data when using current commercially available hardware and software. Further studies are warranted to confirm our data in similar and other patient populations to establish its use in clinical practice.

1.
2.
3.
4.
5.
6.
7.
8.
9.
10.
11.
12.
13.
14.
15.
16.
17.
18.
19.
20.
21.
22.
23.
24.
25.
26.
27.
28.
29.
30.
31.
32.
33.
34.
35.
36.
37.
38.
39.

1. INTRODUCTION

2.

3. Because of improved surgical techniques and medical care, a growing number of patients with
4. congenital heart disease (CHD) survive into adulthood. Right ventricular (RV) dysfunction is
5. a common problem in these patients, associated with significant morbidity and mortality.¹⁻⁴
6. Therefore, regular assessments of RV function in these patients are essential for clinical man-
7. agement. Accurate and accessible tools are needed to monitor RV function, which will lead to
8. better timing of surgical re-intervention and medical therapy, ultimately with better survival.

9. Currently, cardiac magnetic resonance (CMR) imaging is the standard for the quantification
10. of RV volumes and ejection fraction (EF). However, CMR imaging is not widely available and is
11. expensive,^{5,6} acquisition and offline analysis are time-consuming, and a substantial number of
12. patients with CHD have pacemakers or implantable cardioverterdefibrillators and thus (rela-
13. tive) contraindications for CMR.⁷

14. In routine clinical practice, two-dimensional (2D) echocardiography is most commonly used
15. for the noninvasive evaluation of cardiac function. However, it is well known that because of
16. the complex cardiac geometry, 2D echocardiography has important limitations in the assess-
17. ment of left⁸⁻¹⁰ and in particular RV volumes and EF.¹¹ To overcome the problem of geometric
18. assumptions and apical foreshortening, real-time three-dimensional echocardiography (RT3DE)
19. was developed, which allows the fast acquisition of a pyramidal dataset that contains the entire
20. right ventricle. In experimental settings, this imaging modality was successfully applied for RV
21. volume and EF calculation in both healthy volunteers^{12, 13} and pediatric patients with CHD.^{14,}
22. ¹⁵ These studies were limited by selected, nonconsecutive subjects or the use of older or not
23. commercially available data analysis methods. In vitro validation has been done to investigate
24. variables influencing the accuracy of RV RT3DE, in which optimal gain settings and long-axis
25. tracings were found to significantly affect RV volumes.¹⁶

26. The purpose of our study was to determine whether current commercially available hard-
27. ware and software for the assessment of RV volumes and EF with RT3DE can be applied in
28. routine clinical CHD practice.

29.

30.

31. METHODS

32.

33. Study population

34. RT3DE full-volume acquisition of the right ventricle was performed on 62 consecutive patients
35. with complex and/or surgically repaired CHD. They were in sinus rhythm and represented a
36. wide range of RV EFs. The patients were referred for CMR for quantitative analysis of cardiac
37. function for clinical reasons and underwent RT3DE examinations within 2 hours of CMR to
38. pursue comparable loading conditions. The medical ethical committee approved this study,
39. and written informed consent was obtained from all patients and/or their parents (if required).

Real-time three-dimensional echocardiography protocol and data analysis 1.

Data acquisition 2.
3.

RT3DE harmonic imaging was performed using the iE33 ultrasound system (Philips Medical Systems, Best, The Netherlands) equipped with an X3-1 matrix array transducer, with the patient in the left lateral decubitus position. To encompass the entire right ventricle into the RT3DE dataset, a full-volume scan was acquired from a modified apical transducer position in harmonic mode from seven R wave-gated subvolumes during a single end-expiratory breath hold. The output therefore was not truly real-time but reconstructed from seven subvolumes. The depth and angle of the ultrasound sector were adjusted to a minimal level still encompassing the entire right ventricle. Before each acquisition, images were optimized for endocardial border visualization by modifying the time gain and compression and increasing the overall gain. An average of three datasets was acquired per patient, to ensure optimal datasets without motion artifacts that may have occurred during the acquisition. The mean volume rate was 25 frames per cardiac cycle (range 14 – 36). The datasets were digitally exported to a TomTec server (TomTec Imaging Systems, Unterschleissheim, Germany) connected to a terminal workstation for further analyses. 4.
5.
6.
7.
8.
9.
10.
11.
12.
13.
14.
15.
16.
17.

Data analysis 18.
19.

The digital RT3DE RV datasets were analyzed offline using four-dimensional RV- Function version 1.2 (TomTec Imaging Systems) by an investigator blinded to the results of the CMR measurements (H.B.Z). This software performs 3D semiautomated border detection of RV volumes over one cardiac cycle. It uses a physics-based modelling algorithm that makes no assumptions regarding RV geometry. Analysis of a RT3DE dataset was judged possible when both the apex and the lateral wall were visible in the four-chamber view, allowing adequate tracing of the endocardial border. Analysis of the dataset was considered good when the RV anterior wall or the outflow tract was visible. 20.
21.
22.
23.
24.
25.
26.
27.

Once the TomTec analysis program starts, the screen displays a short-axis view (top), an apical four- chamber view (left), and a coronal view (right) (Figure 1). RV quantification starts by definition of the correct apical four-chamber view, with avoidance of RV foreshortening. Then it is made sure that the displayed vertical lines are in the middle of the tricuspid valve and apex in both the apical four -chamber and the coronal views. Subsequently, the horizontal line displayed on the apical four -chamber view is moved to the level of the atrioventricular valves, resulting in a view of both valve orifices at the short-axis view. The next step is to place landmarks in both the tricuspid and mitral valve orifices. Then the horizontal line is moved up to the left ventricular apex, resulting in a short-axis view of the apex at the top. A third landmark is placed at the apex. Afterward, the end-diastolic (largest RV volume) and end-systolic (smallest RV volume) phases are identified. Then the endocardial border contours are drawn onto the apical four -chamber view in both the end-diastolic and end-systolic frames. At the side of 28.
29.
30.
31.
32.
33.
34.
35.
36.
37.
38.
39.

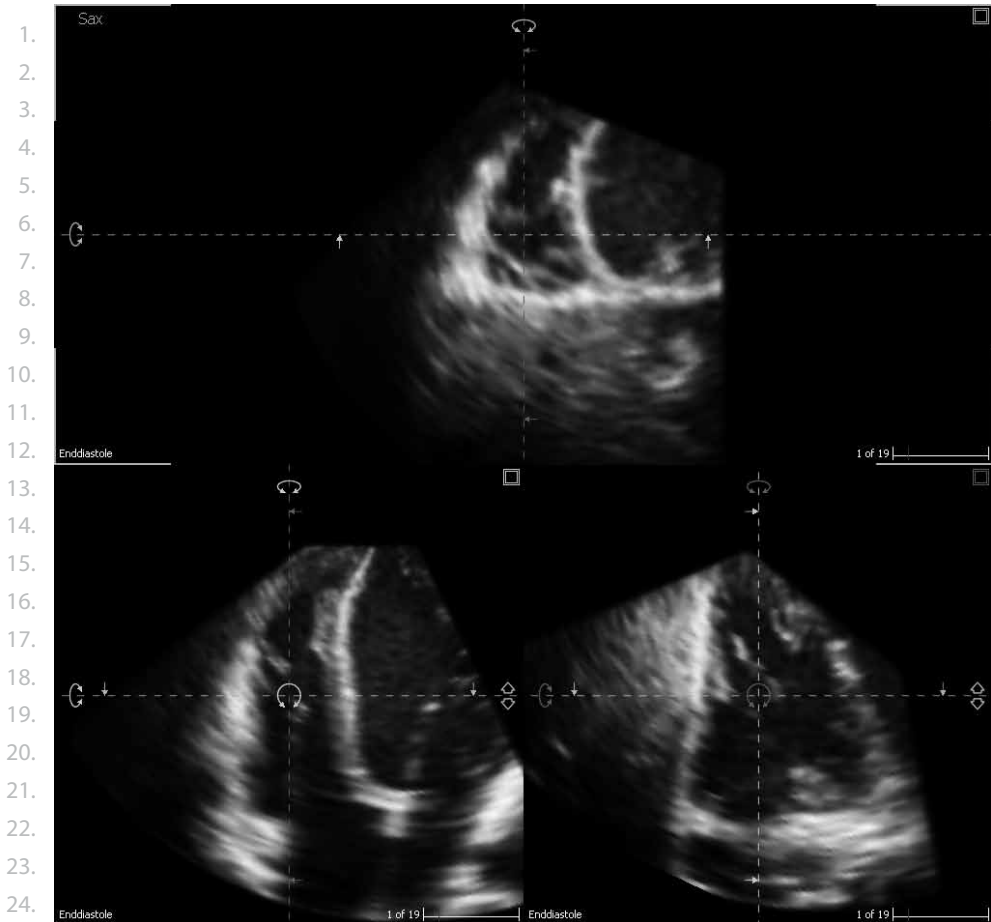


Figure 1. Display from the 4D RV function TomTec analysis program showing the initial stage of contour detection in which anatomical landmarks have to be placed at the tricuspid and mitral valve orifices and at the apex.

these frames, a movie of the current view is displayed to facilitate detection of the endocardial contours that are drawn in the still-frames. The contours are adjusted as close as possible to the endocardial border. Trabeculae are mostly excluded from the volume, due to poor differentiation of trabeculae and myocardium (Figure 2). On the basis of these contours traced from the apical four-chamber view, two reference markers are extrapolated onto the sagittal view. Onto this sagittal view, endocardial border contours are traced, with care to include the two extrapolated reference markers in the end-diastolic and end-systolic frames. Hereafter, contours are drawn in the coronal view, again with attention to include the three reference markers that were extrapolated from the 4-chamber and sagittal views. Hereafter the software automatically delineates the RV endocardial border from the end-diastolic and end-systolic phases, and by sequential analysis the software creates an RV mathematic dynamic three-dimensional

endocardial surface that represents changes in the RV cavity over the cardiac cycle. From this three-dimensional endocardial surface, RV end-diastolic volume (EDV), end-systolic volume (ESV) and EF (defined as $[\text{EDV}-\text{ESV}]/\text{EDV} * 100$) are derived. The background computation of the RV volumetric data is described in detail by Iriart *et al.*¹⁷ Hereafter, manual correction of the contours can be done in any cross-section or phase of the cardiac cycle (Figure 3, Movie 1).

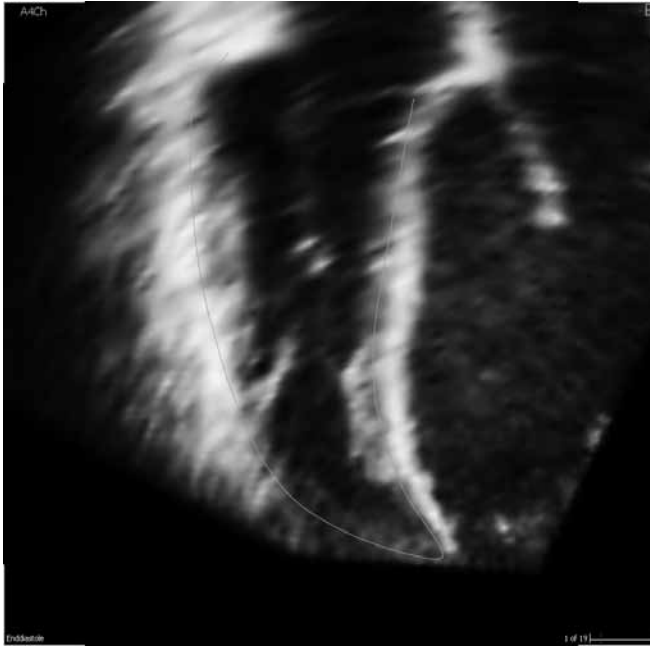


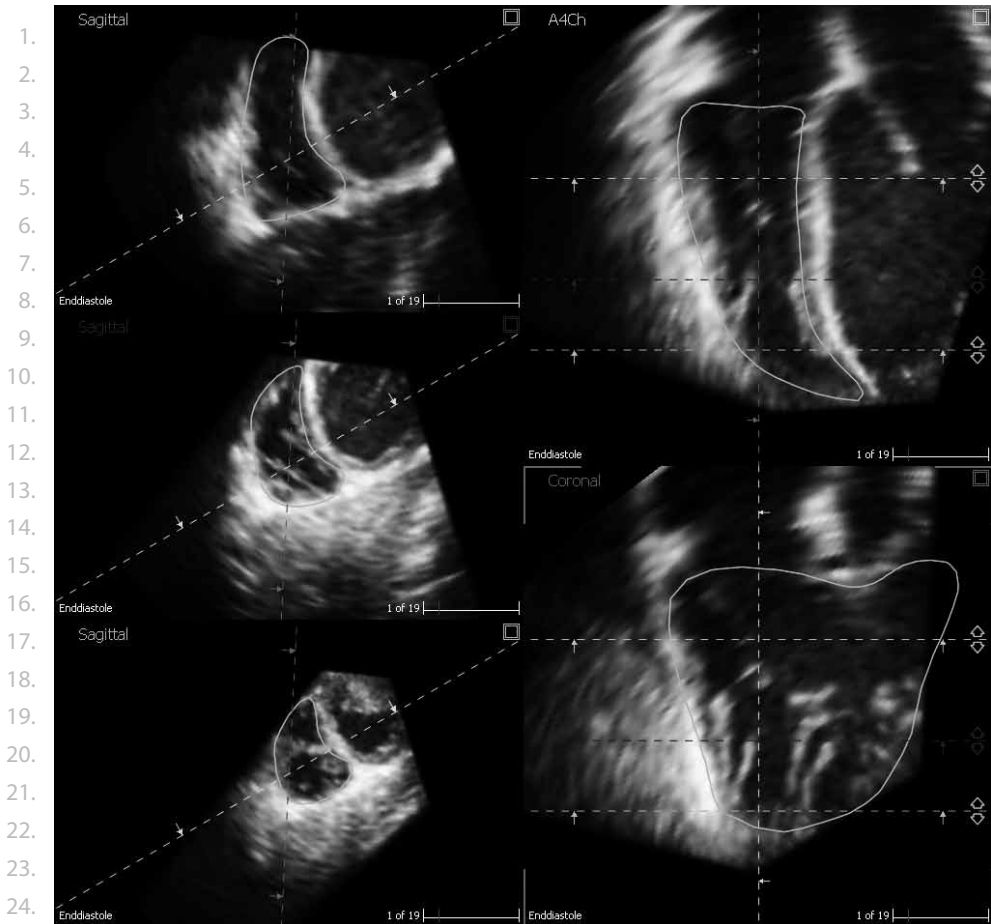
Figure 2. Display from the 4D RV function TomTec analysis program showing the endocardial border contour in the right ventricle at the apical four-chamber view.

Real-time three-dimensional echocardiography reproducibility analysis

RT3DE measurements were repeated in 25 randomly selected patients by the same observer after ≥ 1 month from the original measurements to obtain intra-observer values blinded to CMR results. A second observer (J.S.M.) repeated the measurements in 25 randomly selected patients for inter-observer comparison.

Cardiac magnetic resonance imaging

CMR images were acquired using a Signa 1.5-T scanner (GE Medical Systems, Milwaukee, Wisconsin). Patients were positioned in the supine position with dedicated phased-array cardiac surface coils placed over the thorax. The CMR protocol included cine steady-state free precession sequences in short-axis planes to assess the ventricular volumes. Electrocardiogram gating and repeated breath holds were applied to minimize the influence of cardiac and respiratory motion.



25. **Figure 3.** Display from the 4D RV function TomTec analysis program showing the final stage of contour
 26. detection in which manual correction of the contours can be applied in any cross-section or phase of the
 27. cardiac cycle.

29. Ventricular volumes were measured from a multisection image set of 8 to 12 contiguous
 30. slices parallel to the plane of the atrioventricular valves covering the full length of both ven-
 31. tricles. Imaging parameters were as follows: slice thickness, 7 to 10 mm; slice gap, 0 mm; field
 32. of view, 280 to 370 mm; phase field of view, 0.75; matrix size, 160 x 128 mm; repetition time, 3.5
 33. ms; echo time 1.5 ms; and flip angle, 45°.

34. Three months after analysis of the RT3DE datasets, one physician (H.B.Z) analyzed the CMR
 35. ventricular volumetric dataset quantitatively on a commercially available Advanced Windows
 36. workstation (GE Medical Systems) using Advanced Windows version 5.1 of the MR Analytical
 37. Software System (Medis Medical Imaging Systems, Leiden, The Netherlands). All CMR datasets
 38. were analyzed in a blinded way to prevent influence of the analyzer by the results of RT3DE.
 39. Using manual detection of endocardial borders in end-diastole and end-systole, the RV EDV,

ESV and EF were calculated with exclusion of trabeculae, as described by Alfakih et al.¹⁸ In a random subgroup of 15 patients, we determined the volume of the trabeculae on the CMR images by subtraction of the volume with inclusion of trabeculae and the volume with exclusion of trabeculae.

Statistical analysis

Statistical analysis was performed using SPSS version 15.0 (SPSS, Inc, Chicago, Illinois). Categorical variables are summarized as numbers and percentages. Continuous variables are presented as mean \pm standard deviation (SD), and differences were analyzed using Student's *t* tests. Linear regression analysis with Pearson's correlation coefficient was used to evaluate the relation between RT3DE and CMR. The agreement between RT3DE and CMR measurements was evaluated using Bland-Altman analysis¹⁹ by calculating the bias (mean difference) and the 95% limits of agreement (2 SDs around the mean difference). Paired *t* tests were used to analyze the significance of biases in volumes and EF between RT3DE and CMR. The reproducibility of RT3DE was evaluated by calculating the intra- and inter-observer variability by a variation coefficient, which was defined as the absolute difference expressed as a percentage of the mean of both values. All statistical tests were two sided, and a *P* value <0.05 was considered statistically significant.

RESULTS

Population characteristics

Of the 62 consecutively enrolled patients (mean age 27 ± 10 years, 68% men), 12 (19%) had to be excluded because of insufficient image quality. Age, sex, weight, and type of CHD in these patients were not different from these variables in patients with sufficient image quality. The final cohort comprised 50 patients with a wide range of RV morphology and loading conditions. These included normal right ventricles in left-sided heart disease such as aortic valve pathology, subpulmonary right ventricles facing pressure overload as in pulmonary valve stenosis, volume overload as in atrial septal defects, and right ventricles with severely dilated RV outflow tracts as in tetralogy of Fallot. The patient characteristics are presented in Table 1.

Volume analysis

Table 2 shows the mean RV EDV, ESV, and EF for RT3DE and CMR. Linear regression analysis (Table 2, Figure 4) showed acceptable correlations between RT3DE and CMR for EDV ($r = 0.93$, $y = 0.76x + 19$ ml, $P < 0.001$), ESV ($r = 0.91$, $y = 0.71x + 22$ ml, $P < 0.001$), and EF ($r = 0.74$, $y = 0.60x + 16$ %, $P < 0.001$). Bland-Altman analysis showed mean differences of 34 ml for EDV, 11 ml for ESV, 4% for EF and 95% limits of agreement of ± 65 ml for EDV, ± 55 ml for ESV, ± 13 % for EF (all *P* values <0.05 ; Figure 5). The mean value of the trabeculae on CMR images was 19 ± 13 ml in systole and diastole.

Table 1. Patient characteristics (n = 50)

Variable	Value
Clinical Data	
Age (years)	27 ± 11
Men	68%
Heart rate (beats/min)	72 ± 13
Body mass index (kg/m ²)	23 ± 4
Body surface area (m ²)	1.8 ± 0.3
Pathology	
Tetralogy of Fallot	21
Pulmonary stenosis +/- ventricular septal defect	5
Pulmonary atresia +/- ventricular septal defect	3
Transposition of the great arteries, atrial switch	4
Anomalous pulmonary venous drainage	1
Tricuspid insufficiency	1
Atrial septal defect	1
Aortic valve pathology	10
Transposition of the great arteries, arterial switch	3
Cardiomyopathy	1

Data are expressed as mean ± SD, percentage, or number.

Table 2. Accuracy and reproducibility of right ventricular volumes and function by real-time three-dimensional echocardiography

Variable	RT3DE	CMR	Bland Altman comparison			Reproducibility* of RT3DE	
			Linear regression(r)	Mean difference	95% limits of agreement	Interobserver	Intraobserver
RV EDV (ml)	185 ± 71	219 ± 86	93	34	-32 to 99	1 ± 15	1 ± 12
RV ESV (ml)	103 ± 48	114 ± 62	91	11	-43 to 66	6 ± 17	7 ± 14
RV EF (%)	46 ± 8	49 ± 10	74	4	-10 to 17	8 ± 13	6 ± 9

Data are expressed as mean ± SD.

* Interobserver and intraobserver variability are expressed as percentage s of the absolute mean difference divided by the average of the two readings.

Time needed for acquisition and analysis

The average time for RV acquisition was 5.7 ± 3.0 minutes for RT3DE versus 20.5 ± 4.6 minutes for CMR ($P < 0.001$). Analysis time for RT3DE by an experienced analyzer was 2.1 ± 0.5 (range, 1.5-3.5 minutes), compared with 20.1 ± 3.3 minutes for CMR ($P < 0.001$). With a less experienced analyzer, analysis time for RT3DE was 6.3 ± 3.7 (range, 3-20 minutes).

Reproducibility of real-time three-dimensional echocardiography

For RV EDV, ESV, and EF inter-observer variability was 1 ± 15%, 6 ± 17%, and 8 ± 13%. Intra-observer variability was 1 ± 12% for EDV, 7 ± 14% for ESV, and 6 ± 9% for EF (Table 2).

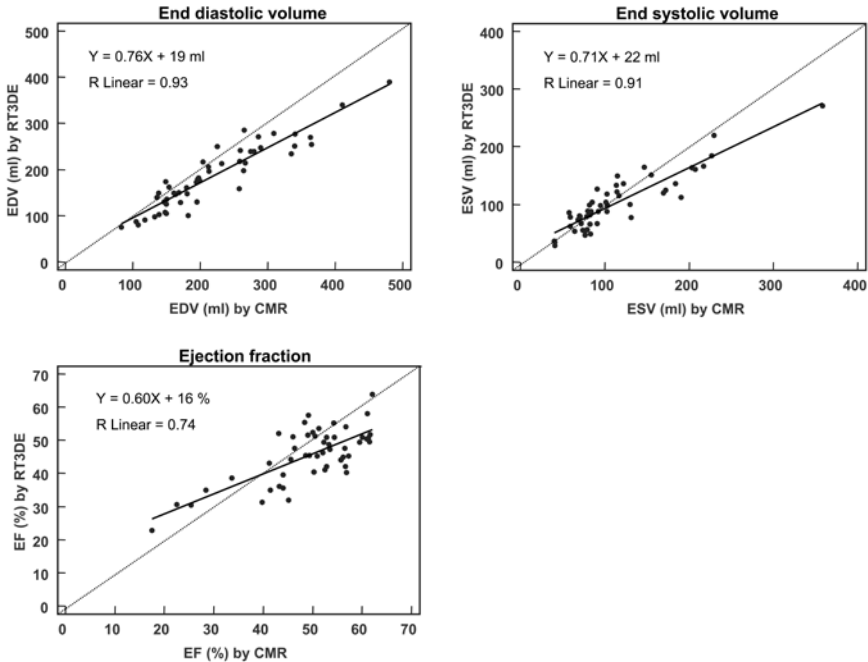


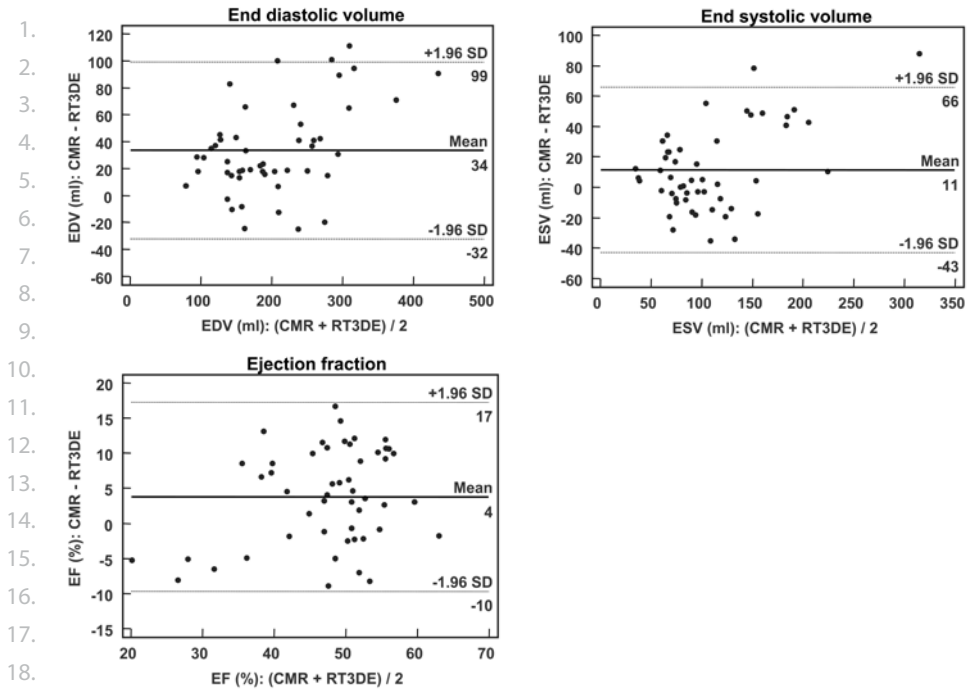
Figure 4. Results of linear regression analysis for real-time 3-dimensional echocardiography right ventricular measurements versus cardiac magnetic resonance values for end-diastolic volume (a), end-systolic volume (b) and ejection fraction (c).

DISCUSSION

The major finding of this study is that in consecutive, unselected patients with complex and/or surgically repaired CHD, RT3DE of the right ventricle was feasible in >80%, and analysis took only a few minutes. RT3DE volume estimates and EF were in agreement with the CMR reference, although systematically significant lower volumes on RT3DE were found. There was substantial variation in EF measures between different techniques because of the inherent difficulty of measuring the right ventricle with any type of imaging technology.

The importance of the assessment of RV EF for clinical decision making was outlined by Piran et al⁴ in patients with single or systemic right ventricles; they found that patients with low systemic ventricular EFs (<35%) as assessed by 2D echocardiography were particularly likely to develop symptomatic heart failure ($P < 0.01$). Rutledge et al¹ found poor RV function to be a predictor of mortality in patients with a congenitally corrected transposition of the great arteries, thereby justifying the regular assessment of RV EF for individual risk stratification.

In clinical practice CMR is considered the standard for RV volumes and EF. The feasibility, accuracy (compared with human RV cadaveric cardiac casts), and reproducibility of CMR have been demonstrated in both healthy subjects and in various disease states.²⁰⁻²³ Nevertheless,



19. **Figure 5.** Results of Bland-Altman analysis for real-time 3-dimensional echocardiography right
 20. ventricular measurements versus cardiac magnetic resonance values for end-diastolic volume (a), end-
 21. systolic volume (b) and ejection fraction (c).

22.
 23. CMR has important limitations such as the relatively low temporal resolution, resulting in inac-
 24. curate definitions of the true end-diastolic and end-systolic times and consequently volumes.
 25. Furthermore, the tricuspid and pulmonary valves are not well visible in the short-axis scanning
 26. method, causing disagreement on the definition of the basal slice. The axial orientation method,
 27. in which slices are made parallel to the tricuspid valve, has been suggested to be more accurate
 28. for RV quantification than the short-axis method.²⁴ However, the latter is most often applied
 29. in routine clinical practice, because it is preferred for left ventricular acquisition and analysis.
 30. More important, CMR is expensive^{5,6} and time-consuming, and the presence of a pacemaker or
 31. implantable cardioverter-defibrillator constitutes a (relative) contraindication.⁷

32. Compared with CMR, benefits of RT3DE are the relative ease of acquisition and analysis, low
 33. cost, and its potential for wide availability and bedside approach.^{5,6} Importantly, we found
 34. that both RT3DE RV acquisition and analysis took little time. This finding is a major step forward
 35. compared with earlier studies using rotational 3D echocardiography, in which acquisition and
 36. analysis were very time-consuming.^{25,26,27} However, echocardiographic imaging of the right
 37. ventricle remains challenging because of several factors. The right ventricle is thin walled and
 38. retrosternally positioned, making visualization of the RV anterior wall and the outflow tract
 39. difficult, because ultrasound cannot penetrate bone structures. From the apical 4-chamber

view, most of the right ventricle is located in the lateral beam of the transducer, where the resolution is suboptimal. By moving the transducer more laterally towards the axilla, so that the right ventricle appears more in the axial resolution, image quality can be improved. In children, the subcostal view can be a realistic alternative for RV imaging, but for adults, this view is mostly insufficient because of abdominal fat. Heavy trabeculations in the right ventricle cause some difficulties in proper endocardial contour placement, needed for volumetric analysis.

Our findings on RV volumes and EF are consistent with earlier studies in healthy subjects and selected patients with CHD.^{12, 14, 28} In a recent study, Iriart et al,¹⁷ focusing on patients with tetralogy of Fallot with dilated right ventricles using a 3D prototype platform, came to comparable conclusions: systematic underestimations of both EDV and ESV on RT3DE compared with CMR. Discrepancies in volumetric RV analysis between RT3DE and CMR may be explained by intrinsic characteristics of RT3DE and CMR and by differences in analysis methods. Mor-avi et al²⁹ studied the potential sources of volume underestimation by RT3DE as compared with CMR for the left ventricle. They found two important sources of volume underestimation: 1) minimal changes in endocardial surface position resulted in significant differences in measured volumes and 2) the exclusion of trabeculae and the mitral valve plane from the CMR reference eliminated the intermodality bias.

There are potential sources of RV volume underestimation by RT3DE compared with CMR. First there are the above-discussed intrinsic inaccuracies of both techniques. Second, there are some essential differences in acquisition and analysis. The RT3DE dataset is a true 3D volumetric pyramid in which the entire right ventricle is included, whereas the CMR dataset is built up through the summation of multiple 2D slices. Analysis of RT3DE datasets is based on a semiautomated contour detection algorithm using the surface geometry reconstructed in the dataset as a guide while searching for true 3D endocardial border along defined rays placed orthogonal to the vertices of the surface geometry. Contours are drawn in several imaging planes. Identifying the proper place for the endocardial contours is far more difficult than in the egg-shaped phantom as described by Mor-avi et al²⁹, so even more pronounced differences in volumes are expected. Even so, in a substantial number of patients, the RV anterior wall and the outflow tract are suboptimally visualized, and extrapolation of the endocardial contours is applied by the semi-automatic TomTec software. Absence of these segments contributes to the bias of RT3DE as compared with CMR, and importantly, these dropouts are poorly controlled. Echocardiographic contrast may improve endocardial border definition, but this remains to be established. Moreover, Soliman et al³⁰ showed that different semiautomated analysis algorithms had a significant impact on left ventricular volumetric calculation of the same RT3DE dataset. The analysis of CMR datasets is done by manual, endocardial contour detection in multiple short-axis slices. Accuracy of this analysis can be improved by the use of a long-axis correction method, as can be used for the left ventricle. For the RV there is no such long-axis correction method feasible, causing a partial volume defect.

1.
2.
3.
4.
5.
6.
7.
8.
9.
10.
11.
12.
13.
14.
15.
16.
17.
18.
19.
20.
21.
22.
23.
24.
25.
26.
27.
28.
29.
30.
31.
32.
33.
34.
35.
36.
37.
38.
39.

1. Third, a final important methodological difference between RT3DE and CMR is the in- or
2. exclusion of trabeculae in the volumes, as suggested earlier by Nesser et al.³¹ In the analysis of
3. RT3DE and CMR short axis datasets, it is common to exclude trabeculae from the RV EDV and
4. ESV. However, the identification (and consequently exclusion) of trabeculae and tracing of true
5. endocardial borders is more challenging in RT3DE, with a lower spatial resolution than in CMR
6. or computed tomography. The mean trabecular volume as determined by CMR in our study
7. was 19 ± 13 ml; if this is only partially identified by RT3DE, it explains most of the difference
8. between the two modalities.

9. Despite the bias in RV volumes and EF that could be explained by methodological differ-
10. ences, RT3DE had good correlations with the reference CMR for RV volumes and a fair correla-
11. tion for RV EF. Moreover, RT3DE offers fast and reproducible assessments for RV volumes and
12. EF. Therefore, RT3DE provides a practical method for serial RV assessment, a crucial element in
13. management of patients with CHD.

14.

15. Study limitations

16. As we pointed out in the “Methods” section, the use of the name “real-time” 3D echocar-
17. diography may be misleading. The maximum angle of the real-time scan mode of the echo
18. equipment we used for our study is limited, and stitching of multiple (4 or 7) subvolumes is
19. needed to create a full-volume dataset. Since this technique has been systematically referred
20. to in literature as RT3DE, we have used that term in our paper to avoid confusion and to stay in
21. line with previous publications.

22. Because full-volume acquisition requires 7 R wave-gated subvolumes, patients with irregular
23. heart rhythms, such as atrial fibrillation, were excluded. Irregular R-R intervals cause stitching
24. artifacts at the interfaces of subvolumes in the full-volume dataset. Newer systems with full-
25. volume from a single heartbeat might overcome this problem, but only partially. With irregular
26. heart rate and consequent irregular filling of the ventricles, it will remain difficult to choose
27. which volume to trace and which EF to report.

28. The feasibility we report in the current study is based on the acquisitions made by one very
29. experienced sonographer. These data cannot be extrapolated to a situation in which multiple
30. sonographers not yet familiar with or experts in 3D echocardiographic acquisition, use RT3DE
31. for RV volumes.

32. Because of our research question, whether RT3DE would be applicable in clinical practice,
33. we used a commercially available echocardiographic software package that did not allow
34. analysis of the CMR datasets with the same software. Niemann et al¹⁴ used prototype software
35. enabling both RV RT3DE and CMR images analyses and found excellent correlations, whereas
36. comparable results to ours were seen when RT3DE was compared with the conventional CMR
37. disc summation method.

38.

39.

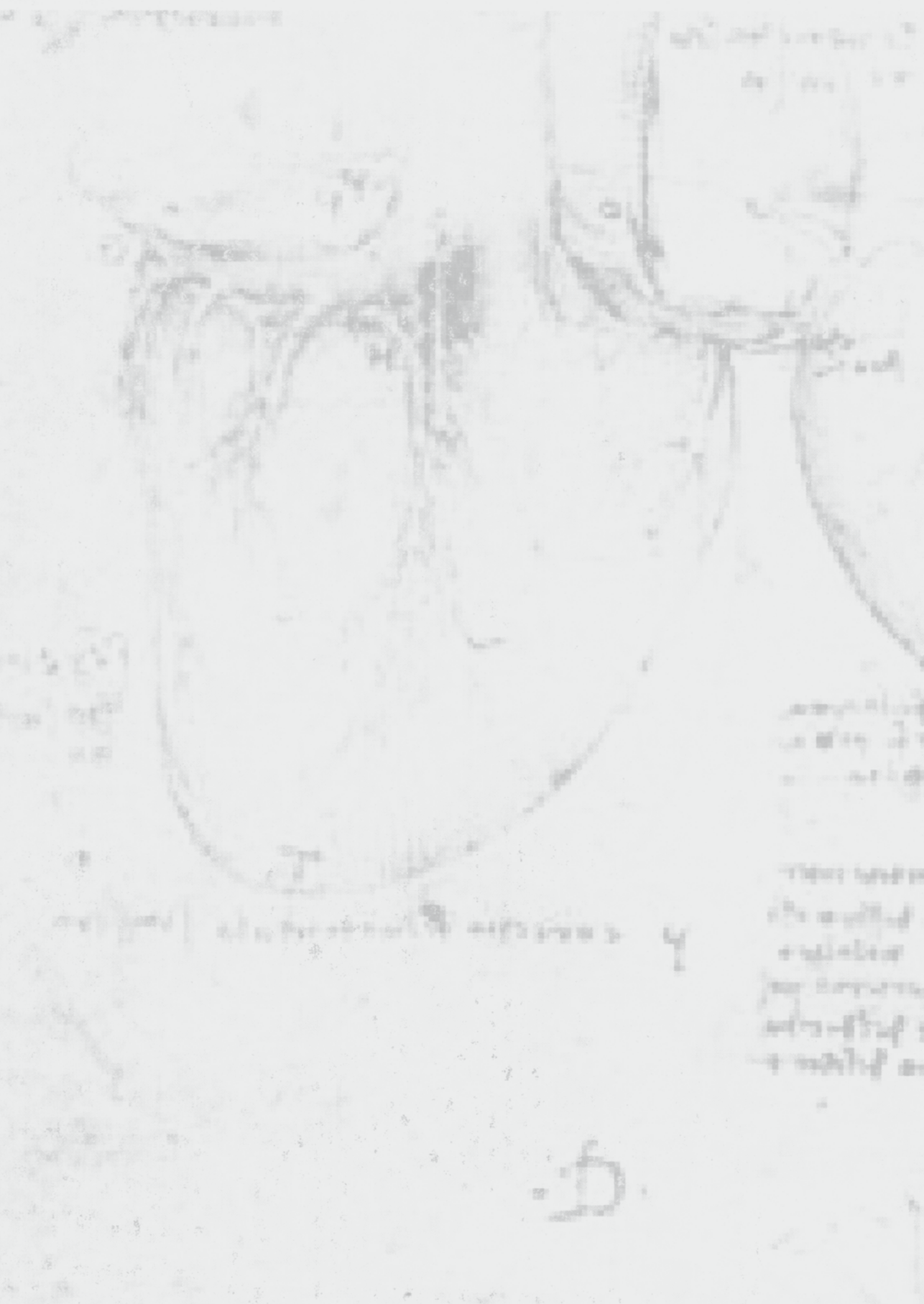
CONCLUSIONS

In the majority of unselected patients with complex CHD, RT3DE provides fast and reproducible assessments of RV volumes and EF, with a fair to good accuracy compared with CMR reference data when using current commercially available hardware and software. Therefore, RT3DE provides a practical method for serial RV assessment, a crucial element in the management of patients with CHD. Further studies are warranted to confirm our data in similar and other patient populations. We expect that RT3DE will be applied in clinical practice as soon as some more technological developments have taken place.

1.
2.
3.
4.
5.
6.
7.
8.
9.
10.
11.
12.
13.
14.
15.
16.
17.
18.
19.
20.
21.
22.
23.
24.
25.
26.
27.
28.
29.
30.
31.
32.
33.
34.
35.
36.
37.
38.
39.

1. Rutledge JM, Nihill MR, Fraser CD, Smith OE, McMahon CJ, Bezold LI. Outcome of 121 patients with congenitally corrected transposition of the great arteries. *Pediatr Cardiol.* 2002;23:137-45.
2. Murphy JG, Gersh BJ, Mair DD, Fuster V, McGoon MD, Ilstrup DM, et al. Long-term outcome in patients undergoing surgical repair of tetralogy of Fallot. *N Engl J Med.* 1993;329:593-9.
3. Davlouros PA, Niwa K, Webb G, Gatzoulis MA. The right ventricle in congenital heart disease. *Heart.* 2006;92 Suppl 1:i27-38.
4. Piran S, Veldtman G, Siu S, Webb GD, Liu PP. Heart failure and ventricular dysfunction in patients with single or systemic right ventricles. *Circulation.* 2002;105:1189-94.
5. Bleeker GB, Steendijk P, Holman ER, Yu CM, Breithardt OA, Kaandorp TA, et al. Assessing right ventricular function: the role of echocardiography and complementary technologies. *Heart.* 2006;92 Suppl 1:i19-26.
6. Babu-Narayan SV, Gatzoulis MA, Kilner PJ. Non-invasive imaging in adult congenital heart disease using cardiovascular magnetic resonance. *J Cardiovasc Med (Hagerstown).* 2007;8:23-9.
7. Pulver AF, Puchalski MD, Bradley DJ, Minich LL, Su JT, Saarel EV, et al. Safety and imaging quality of MRI in pediatric and adult congenital heart disease patients with pacemakers. *Pacing Clin Electrophysiol.* 2009;32:450-6.
8. Sugeng L, Mor-Avi V, Weinert L, Niel J, Ebner C, Steringer-Mascherbauer R, et al. Quantitative assessment of left ventricular size and function: side-by-side comparison of real-time three-dimensional echocardiography and computed tomography with magnetic resonance reference. *Circulation.* 2006;114:654-61.
9. Soliman OI, Kirschbaum SW, van Dalen BM, van der Zwaan HB, Delavary BM, Vletter WB, et al. Accuracy and reproducibility of quantitation of left ventricular function by real-time three-dimensional echocardiography versus cardiac magnetic resonance. *Am J Cardiol.* 2008;102:778-83.
10. van den Bosch AE, Robbers-Visser D, Krenning BJ, Voormolen MM, McGhie JS, Helbing WA, et al. Real-time transthoracic three-dimensional echocardiographic assessment of left ventricular volume and ejection fraction in congenital heart disease. *J Am Soc Echocardiogr.* 2006;19:1-6.
11. Helbing WA, Bosch HG, Maliepaard C, Rebergen SA, van der Geest RJ, Hansen B, et al. Comparison of echocardiographic methods with magnetic resonance imaging for assessment of right ventricular function in children. *Am J Cardiol.* 1995;76:589-94.
12. Gopal AS, Chukwu EO, Iwuchukwu CJ, Katz AS, Toole RS, Schapiro W, et al. Normal values of right ventricular size and function by real-time 3-dimensional echocardiography: comparison with cardiac magnetic resonance imaging. *J Am Soc Echocardiogr.* 2007;20:445-55.
13. Kjaergaard J, Sogaard P, Hassager C. Quantitative echocardiographic analysis of the right ventricle in healthy individuals. *J Am Soc Echocardiogr.* 2006;19:1365-72.
14. Niemann PS, Pinho L, Balbach T, Galuschky C, Blankenhagen M, Silberbach M, et al. Anatomically oriented right ventricular volume measurements with dynamic three-dimensional echocardiography validated by 3-Tesla magnetic resonance imaging. *J Am Coll Cardiol.* 2007;50:1668-76.
15. Lu X, Nadvoretzkiy V, Bu L, Stolpen A, Ayres N, Pignatelli RH, et al. Accuracy and reproducibility of real-time three-dimensional echocardiography for assessment of right ventricular volumes and ejection fraction in children. *J Am Soc Echocardiogr.* 2008;21:84-9.
16. Hoch M, Vasilyev NV, Soriano B, Gauvreau K, Marx GR. Variables influencing the accuracy of right ventricular volume assessment by real-time 3-dimensional echocardiography: an in vitro validation study. *J Am Soc Echocardiogr.* 2007;20:456-61.
17. Iriart X, Montaudon M, Lafitte S, Chabaneix J, Reant P, Balbach T, et al. Right ventricle three-dimensional echography in corrected tetralogy of fallot: accuracy and variability. *Eur J Echocardiogr.* 2009.
18. Alfakih K, Plein S, Thiele H, Jones T, Ridgway JP, Sivananthan MU. Normal human left and right ventricular dimensions for MRI as assessed by turbo gradient echo and steady-state free precession imaging sequences. *J Magn Reson Imaging.* 2003;17:323-9.
19. Bland JM, Altman DG. Statistical methods for assessing agreement between two methods of clinical measurement. *Lancet.* 1986;1:307-10.

20. Grothues F, Moon JC, Bellenger NG, Smith GS, Klein HU, Pennell DJ. Interstudy reproducibility of right ventricular volumes, function, and mass with cardiovascular magnetic resonance. *Am Heart J*. 2004;147:218-23. 1.
21. Keenan NG, Pennell DJ. CMR of ventricular function. *Echocardiography*. 2007;24:185-93. 2.
22. Sarwar A, Shapiro MD, Abbara S, Cury RC. Cardiac magnetic resonance imaging for the evaluation of ventricular function. *Semin Roentgenol*. 2008;43:183-92. 3.
23. Catalano O, Antonaci S, Opasich C, Moro G, Mussida M, Perotti M, et al. Intra-observer and interobserver reproducibility of right ventricle volumes, function and mass by cardiac magnetic resonance. *J Cardiovasc Med (Hagerstown)*. 2007;8:807-14. 4.
24. Alfakih K, Plein S, Bloomer T, Jones T, Ridgway J, Sivananthan M. Comparison of right ventricular volume measurements between axial and short axis orientation using steady-state free precession magnetic resonance imaging. *J Magn Reson Imaging*. 2003;18:25-32. 5.
25. Fujimoto S, Mizuno R, Nakagawa Y, Dohi K, Nakano H. Estimation of the right ventricular volume and ejection fraction by transthoracic three-dimensional echocardiography. A validation study using magnetic resonance imaging. *Int J Card Imaging*. 1998;14:385-90. 6.
26. Papavassiliou DP, Parks WJ, Hopkins KL, Fyfe DA. Three-dimensional echocardiographic measurement of right ventricular volume in children with congenital heart disease validated by magnetic resonance imaging. *J Am Soc Echocardiogr*. 1998;11:770-7. 7.
27. Vogel M, Gutberlet M, Dittrich S, Hosten N, Lange PE. Comparison of transthoracic three dimensional echocardiography with magnetic resonance imaging in the assessment of right ventricular volume and mass. *Heart*. 1997;78:127-30. 8.
28. Soriano BD, Hoch M, Ithualde A, Geva T, Powell AJ, Kussman BD, et al. Matrix-array 3-dimensional echocardiographic assessment of volumes, mass, and ejection fraction in young pediatric patients with a functional single ventricle: a comparison study with cardiac magnetic resonance. *Circulation*. 2008;117:1842-8. 9.
29. Mor-Avi V, Jenkins C, Kuhl HP, Nesser HJ, Marwick T, Franke A, et al. Real-time 3-dimensional echocardiographic quantification of left ventricular volumes: multicenter study for validation with magnetic resonance imaging and investigation of sources of error. *JACC Cardiovasc Imaging*. 2008;1:413-23. 10.
30. Soliman OI, Krenning BJ, Geleijnse ML, Nemes A, Bosch JG, van Geuns RJ, et al. Quantification of left ventricular volumes and function in patients with cardiomyopathies by real-time three-dimensional echocardiography: a head-to-head comparison between two different semiautomated endocardial border detection algorithms. *J Am Soc Echocardiogr*. 2007;20:1042-9. 11.
31. Nesser HJ, Tkalec W, Patel AR, Masani ND, Niel J, Markt B, et al. Quantitation of right ventricular volumes and ejection fraction by three-dimensional echocardiography in patients: comparison with magnetic resonance imaging and radionuclide ventriculography. *Echocardiography*. 2006;23:666-80. 12.



Chapter 7

Usefulness of real-time three-dimensional echocardiography to identify right ventricular dysfunction in patients with congenital heart disease

H.B. van der Zwaan
W.A. Helbing
E. Boersma
M.L. Geleijnse
J.S. McGhie
O.I.I. Soliman
J.W. Roos-Hesselink
F.J. Meijboom

Am J Cardiol. 2010 Sep 15;106(6):843-50

ABSTRACT

Background. Because right ventricular (RV) dysfunction predicts a poor outcome in patients with congenital heart disease (CHD), regular monitoring of RV function is indicated. To date, cardiac magnetic resonance (CMR) imaging has been the reference method. A more practical, more accessible, and accurate tool would be preferred.

Methods. We defined normality regarding RV systolic function using healthy controls and tested the ability of real-time three-dimensional echocardiography (RT3DE) to identify patients with CHD with RV dysfunction. The cut-off values for the RV volumes and ejection fraction (EF) were derived from CMR imaging from 41 healthy controls (mean age 27 ± 8 years, 56% men). In 100 patients with varying CHDs (mean age 27 ± 11 years, 65% men), both RT3DE datasets (IE33) and short axis CMR (1.5T) images were obtained within two hours. The RT3DE and CMR RV volumes and EF were calculated using commercially available software. Receiver operating characteristic curves were created to obtain the sensitivity and the specificity of RT3DE to identify RV dysfunction.

Results. Applying the cut-off values derived from the healthy controls using the CMR data of patients with CHD, we identified 23 patients with an enlarged indexed end-diastolic volume, 29 patients with an enlarged indexed end-systolic volume, and 21 patients with an impaired RV EF. The best cut-off values predicting RV dysfunction using RT3DE were identified (indexed end-diastolic volume >105 ml/m², indexed end-systolic volume >54 ml/m², and EF $<43\%$). The RT3DE findings revealed 23 patients with impaired RV EF, with 95% sensitivity, 89% specificity, and a negative predictive value of 99%.

Conclusions. RT3DE is a very sensitive tool to identify RV dysfunction in patients with CHD and could be applied clinically to rule out RV dysfunction or to indicate additional quantitative analysis of RV function.

1.
2.
3.
4.
5.
6.
7.
8.
9.
10.
11.
12.
13.
14.
15.
16.
17.
18.
19.
20.
21.
22.
23.
24.
25.
26.
27.
28.
29.
30.
31.
32.
33.
34.
35.
36.
37.
38.
39.

1. INTRODUCTION

2.

3. The ideal index to assess right ventricular (RV) contractility - independent of the pre- and after-
4. load, independent of heart size and mass, easy and safe to apply, and proven useful in the
5. clinical setting – does not yet exist.¹ Thus, determination of the ejection fraction (EF) is still the
6. most commonly used method to assess systolic RV performance. Cardiac magnetic resonance
7. (CMR) imaging has become the reference method for the assessment of RV EF but has a num-
8. ber of drawbacks, including limited availability, high cost, and time-consuming acquisition and
9. analysis.^{2, 3} Owing to the complex RV geometry and the presence of myocardial trabeculae,
10. two-dimensional echocardiography is considered inaccurate and a three-dimensional image
11. technology, such as real-time three-dimensional echocardiography (RT3DE), is mandatory.⁴
12. Earlier studies have shown that RT3DE can assess RV volumes and EF in various patient
13. groups.⁵⁻⁷ If proven to be a robust and reliable technique, RT3DE might replace CMR for RV
14. systolic functional assessment in a substantial proportion of patients. To be usable in clinical
15. practice, a prerequisite is the reliability of RT3DE to detect RV dysfunction. This has not been
16. previously studied. The purposes of the present study were to define normality regarding
17. systolic RV function using CMR values derived from healthy controls and to test the ability of
18. RT3DE to accurately identify RV dysfunction in patients with congenital heart disease (CHD),
19. according to the reference method CMR imaging. For the purposes of the present study, the
20. cut-off values for the RV volumes and EF were identified and applied to differentiate between
21. normal and impaired RV function - to define RV dysfunction.

22.

23.

24. METHODS

25.

26. A total of 41 healthy controls underwent full-volume RT3DE and CMR imaging to establish the
27. reference RV volumes and EF values. The controls were employees of the university or the hos-
28. pital or their relatives who were willing to undergo a CMR scan. They were eligible for inclusion
29. in the study if they had no medical history or current symptoms suggestive of cardiovascular
30. disease, including hypertension or a systemic illness with a potential cardiovascular compo-
31. nent such as diabetes or thyroid disease. Participants taking any cardiovascular medications
32. were excluded from the present study.

33. In all included healthy controls heart rate and blood pressure were measured (with the
34. subject supine), and they underwent routine two-dimensional echocardiography to exclude
35. cardiac abnormalities.

36. A total of 100 consecutive patients, in sinus rhythm, with complex and/or surgically repaired
37. CHD underwent full-volume RT3DE and CMR acquisition of the right ventricle. They were
38. referred for CMR imaging for a quantitative analysis of their cardiac function for clinical reasons

39.

and underwent a RT3DE examination within two hours of CMR imaging to pursue comparable loading conditions. 1. 2.

The medical ethical committee approved the study, and all healthy controls, patients and/or their parents (if required) provided written informed consent. 3. 4.

CMR images were acquired using a Signa 1.5 Tesla scanner (GE Medical Systems, Milwaukee, Wisconsin). The subjects were positioned supine with dedicated phased-array cardiac surface coils placed over the thorax. The CMR protocol included cine steady-state free precession sequences in the short-axis planes to assess the RV volumes. Electrocardiogram gating and repeated breath holds were applied to minimize the influence of cardiac and respiratory motion. 5. 6. 7. 8. 9. 10.

The RV volumes were measured from a multisection image set of 8 to 12 contiguous slices parallel to the plane of the atrioventricular valves and covering the full-length of both ventricles. The imaging parameters were as follows: slice thickness 7 to 10 mm, interslice gap 0 mm, field of view 280 to 370 mm, phase field of view 0.75, matrix 160 x 128 mm, repetition time 3.5 ms, echo time 1.5 ms, flip angle 45°. 11. 12. 13. 14. 15.

One physician (HBZ) analyzed the CMR RV volumetric dataset quantitatively on a commercially available Advanced Windows workstation (GE Medical Systems) using Advanced Windows, version 5.1, of the MR Analytical Software System (Medis Medical Imaging Systems, Leiden, The Netherlands). The RV end-diastolic volume, end-systolic volume, and EF were calculated using manual detection of the endocardial borders in end-systole and end-diastole with exclusion of trabeculae, as described by Robbers-Visser et al.⁸ 16. 17. 18. 19. 20. 21.

RT3DE harmonic imaging was performed using the iE33 ultrasound system (Philips Medical Systems, Best, The Netherlands) equipped with an X3-1 matrix array transducer with the patient in the left lateral decubitus position. To encompass the entire right ventricle into the RT3DE dataset, a full-volume scan was acquired from a modified apical transducer position in harmonic mode from seven R wave-gated subvolumes during a single end-expiratory breath-hold. The output therefore was not truly real-time but was reconstructed from seven subvolumes. The depth and angle of the ultrasound sector were adjusted to a minimal level, still encompassing the entire right ventricle. Before each acquisition, the images were optimized for endocardial border visualization by modifying the time gain and compression and increasing the overall gain. An average of three datasets was acquired per patient, to ensure optimal datasets without motion artifacts that might have occurred during the acquisition. The mean volume rate was 25 frames (range 14 to 38) per cardiac cycle. The datasets were digitally exported to a TomTec server (TomTec Imaging Systems, Unterschleissheim, Germany) connected to a terminal workstation for additional analyses. 22. 23. 24. 25. 26. 27. 28. 29. 30. 31. 32. 33. 34. 35.

The digital RT3DE RV datasets were analyzed offline using the TomTec four-dimensional RV Function Program, version 1.2, by an investigator (HBZ) unaware of the results of the CMR measurements. This software performs three-dimensional semiautomated border detection of RV volumes over one cardiac cycle. It uses a physics-based modelling algorithm that makes 36. 37. 38. 39.

1. no assumptions regarding RV geometry. The analysis of a RT3DE dataset was judged accurate,
2. when both the apex and the lateral wall were both visible in the four-chamber view, allowing
3. adequate tracing of the endocardial border.
4. The functioning of the TomTec analysis program (Figure 1) has been previously reported in
5. detail.⁶ In brief, the program starts with a screen displaying a short-axis view (top), an apical
6. four-chamber view (left), and a coronal view (right). The right ventricle must be outlined in
7. the middle of the dataset. Next, by movement of a horizontal axis, landmarks can be placed
8. in the tricuspid and mitral valve orifices and apex. Subsequently the end-diastolic (largest RV
9. volume) and end-systolic (smallest RV volume) phases are identified. The endocardial border
10. contours are drawn onto the apical four-chamber still frames in both end-diastole and end-
11. systole. Using these contours, two reference markers are extrapolated onto the sagittal view
12. in which the endocardial border contours are traced with care to include the two extrapolated
13. reference markers. Next, the contours are drawn in the coronal view, again with attention to
14. include the three reference markers that were extrapolated from the four-chamber and sagittal
15. views. After these steps the software automatically delineates the RV endocardial border from
16. the end-diastolic and end-systolic phases, and by sequential analysis the software creates an
17. RV mathematic dynamic three-dimensional endocardial surface that represents changes in the
18. RV cavity over the cardiac cycle. From this three-dimensional endocardial surface, RV volumes
19. and EF are calculated.

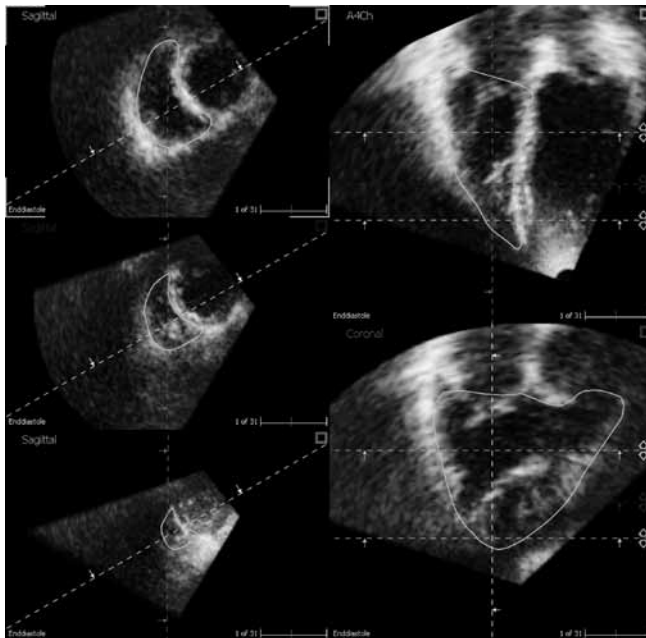


Figure 1 Display from the 4D RV function TomTec analysis program showing the final stage of contour detection in which manual correction of the contours can be applied in any cross-section or phase of the cardiac cycle.

Statistical analysis was done using the Statistical Package for Social Sciences, version 15.0 (SPSS, Chicago, Illinois). The categorical data are summarized as numbers and percentages and the continuous data are presented as the mean \pm SD. Differences between patients and controls were analyzed using chi-square tests or Student's *t* tests as appropriate.

Both RT3DE and CMR volumes were indexed to body surface area. The body surface area was calculated according to the formula by Dubois: $BSA (m^2) = \text{weight (kg)}^{0.425} \times \text{height (cm)}^{0.725} \times 71.84 \times 10^{-4}$.

All statistical tests were 2-sided, and $P < 0.05$ was considered statistically significant.

Because no standard on definition of RV dysfunction is available⁹, we defined RV dysfunction as follows. Using the CMR volumetric data from the healthy controls, we identified a range of normal RV function by the mean \pm 2 SDs. Next, we defined the indexes of RV dysfunction either as a diminished RV EF (less than the mean minus 2 SDs in healthy controls), an enlarged indexed end-diastolic volume or an enlarged indexed end-systolic volume (both greater than the mean plus 2 SDs in healthy controls).

Using these cut-off values, we dichotomized the CMR data derived from our CHD group. Receiver operating characteristic curves were created to predict RV dysfunction using the RT3DE data. From the receiver operating characteristic curves, the sensitivity and specificity of the RT3DE findings were derived, as well as the area under the curves. Next, two by two tables were created to calculate the positive and negative predictive values of the RT3DE findings to identify RV dysfunction using the CMR data. The cut-off RT3DE values to obtain the maximum sum of the sensitivity and specificity, the greatest sensitivity and specificity, were calculated.

RESULTS

The baseline characteristics of the healthy controls (mean age 27 ± 8 years, 56% men) and the patients with CHD (mean age 27 ± 10 years, 65% men) are listed in Table 1. The patients with CHD had a greater heart rate ($P < 0.001$) and shorter stature ($P = 0.04$) than the healthy controls. Table 2 lists the types of CHD the patients had.

Table 3 lists the absolute and indexed RV volumes and EF obtained using CMR imaging. The patients with CHD had a greater indexed end-diastolic volume and end-systolic volume and lower EF (all $P < 0.001$). Similar outcomes were measured using RT3DE. The end-diastolic volume and end-systolic volume were greater in the patients with CHD ($P < 0.001$) and their EF was lower ($P < 0.001$; Table 4).

The cumulative percentage and median values of the indexed end-diastolic volume, end-systolic volume, and EF in the healthy controls and patients with CHD are depicted in Figure 2. The mean values and 95% confidence intervals of the end-diastolic volume, end-systolic volume, and EF as measured using RT3DE and CMR imaging in patients with CHD are shown

Table 1. Baseline characteristics

Variable	Healthy controls			Patients with CHD			P-value*
	All	Men	Women	All	Men	Women	
Number	41	23	18	100	65	35	0.33
Age (years)	27 ± 8	26 ± 9	28 ± 7	27 ± 10	26 ± 10	28 ± 11	0.89
Age at initial repair (years), (n = 94)	-	-	-	5 ± 10	6 ± 10	6 ± 12	-
Age at reoperation (years), (n = 51)	-	-	-	11 ± 10	11 ± 10	10 ± 10	-
Heart rate (beats/min)	64 ± 13	64 ± 14	63 ± 14	72 ± 12	70 ± 13	75 ± 11	< 0.001
Systolic blood pressure (mmHg)	121 ± 14	128 ± 13	114 ± 12	125 ± 18	126 ± 17	123 ± 20	0.29
Diastolic blood pressure (mmHg)	73 ± 8	74 ± 7	71 ± 9	72 ± 10	71 ± 10	73 ± 11	0.58
Height (cm)	177 ± 8	181 ± 6	171 ± 5	172 ± 13	176 ± 13	165 ± 7	0.04
Weight (kg)	70 ± 11	73 ± 10	66 ± 11	68 ± 15	70 ± 17	63 ± 12	0.36
Body mass index (kg/m ²)	22 ± 3	22 ± 3	23 ± 3	22 ± 4	22 ± 5	23 ± 4	0.80
Body surface area (m ²)	1.9 ± 0.2	1.9 ± 0.1	1.8 ± 0.1	1.8 ± 0.3	1.8 ± 0.4	1.7 ± 0.2	0.04

Data are expressed as mean ± SD.

*Difference between healthy controls and patients with CHD.

Table 2. Congenital heart diseases (CHDs) studied

Pathology	Patients (n)
Tetralogy of Fallot	38
Aortic valve pathology	17
Pulmonary stenosis +/- ventricular septal defect	12
Pulmonary atresia +/- ventricular septal defect	4
Transposition of the great arteries, atrial switch	10
Transposition of the great arteries, arterial switch	9
Coarctation of the aorta	2
Ebstein's anomaly	2
Double outlet right ventricle	1
Double inlet left ventricle	1
Ventricular septal defect	1
Anomalous pulmonary venous connection	1
Perinatal tricuspid insufficiency	1
Congenital hypertrophic cardiomyopathy	1

in Figure 3. In patients with CHD and the healthy controls, significantly smaller volumes were measured using RT3DE than using CMR imaging.

We derived cut-off values from the CMR data from healthy controls as indicators of RV dysfunction (indexed end-diastolic volume >129 ml/m², indexed end-systolic volume >58 ml/m² and a RV EF <48 %). Using these cut-off values for CMR data from the patients with CHD, we identified 23 patients (23%) with an enlarged indexed end-diastolic volume, 29 patients (29%) with an enlarged indexed end-systolic volume and 21 patients (21%) with an impaired RV EF. Of the 21 patients with impaired RV function according to the RV EF, half had tetralogy of Fallot and a quarter had undergone a Mustard or Senning operation for transposition of the great arteries.

Table 3. Cardiac magnetic resonance imaging: right ventricular volumes and ejection fraction

Variable	Healthy controls			Patients with CHD			P-value*
	All	Men	Women	All	Men	Women	
Absolute values							
End-diastolic volume (ml)	158 ± 32	172 ± 29	139 ± 27	193 ± 72	195 ± 72	190 ± 75	< 0.001
End-systolic volume (ml)	65 ± 18	70 ± 17	58 ± 17	94 ± 47	96 ± 49	91 ± 46	< 0.001
Stroke volume (ml)	93 ± 19	107 ± 18	82 ± 15	100 ± 34	101 ± 34	99 ± 36	0.15
Ejection fraction (%)	60 ± 6	60 ± 6	59 ± 6	53 ± 9	52 ± 10	53 ± 8	< 0.001
Normalized to body surface area							
End-diastolic volume (ml/m ²)	86 ± 21	90 ± 15	79 ± 13	109 ± 37	108 ± 36	112 ± 39	< 0.001
End-systolic volume (ml/m ²)	35 ± 11	37 ± 9	33 ± 9	54 ± 25	53 ± 26	54 ± 24	< 0.001
Stroke volume (ml/m ²)	51 ± 12	53 ± 9	46 ± 6	56 ± 18	55 ± 17	59 ± 20	0.04

Data are expressed as mean ± SD.

* Difference between healthy controls and patients with CHD.

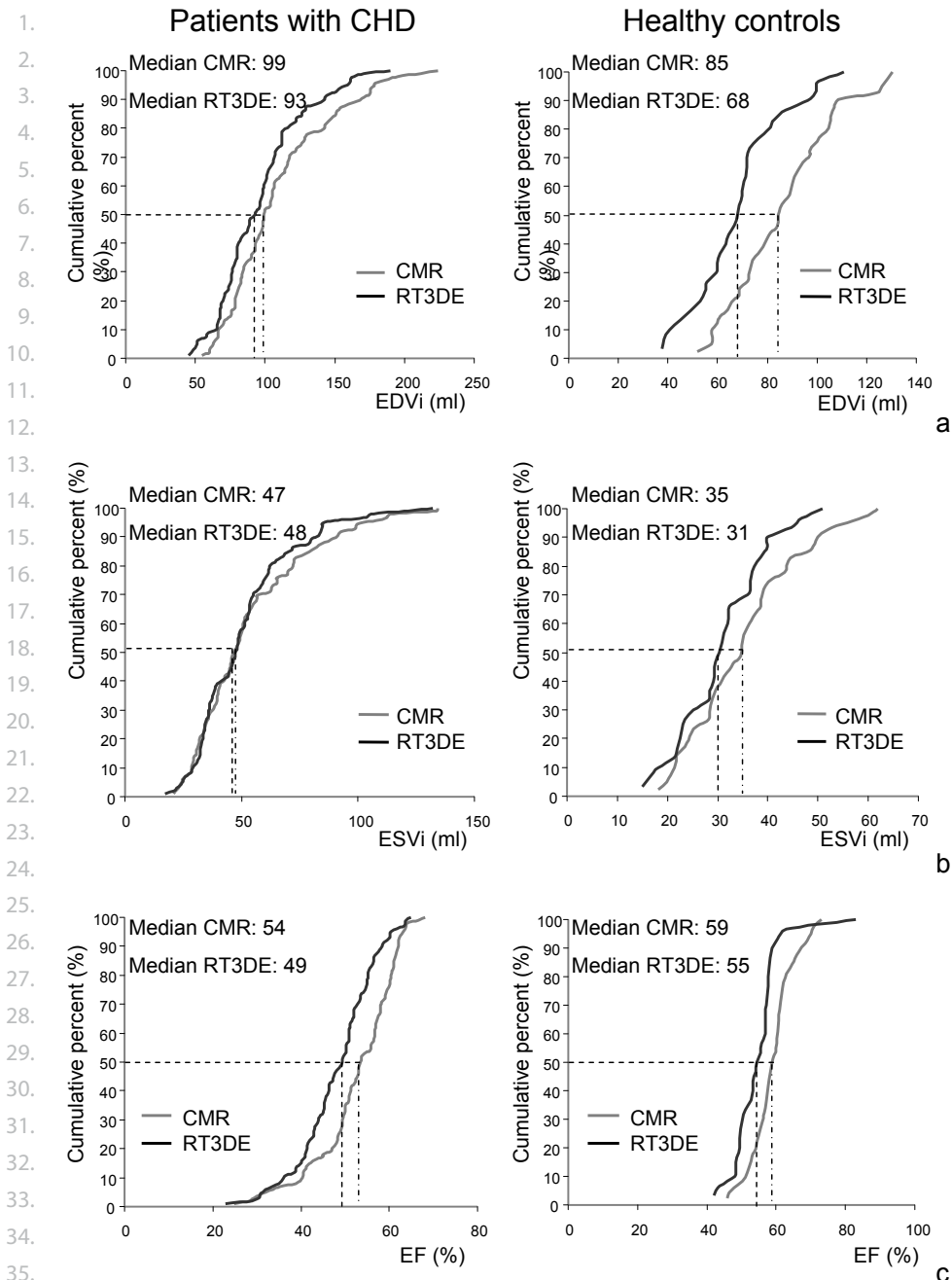
Table 4. Real-time three-dimensional echocardiography: right ventricular volumes and ejection fraction

Variable	Healthy controls			CHD patients			P-value*
	All	Men	Women	All	Men	Women	
Absolute values							
End-diastolic volume (ml)	127 ± 32	144 ± 31	108 ± 22	170 ± 61	175 ± 60	160 ± 61	< 0.001
End-systolic volume (ml)	58 ± 16	66 ± 14	48 ± 10	96 ± 44	98 ± 44	79 ± 35	< 0.001
Stroke volume (ml)	69 ± 19	78 ± 20	60 ± 14	80 ± 26	80 ± 24	80 ± 30	0.001
Ejection fraction (%)	55 ± 5	54 ± 5	56 ± 5	48 ± 9	46 ± 9	52 ± 7	< 0.001
Normalized to body surface area							
End-diastolic volume (ml/m ²)	68 ± 18	73 ± 14	66 ± 10	96 ± 31	97 ± 30	94 ± 32	< 0.001
End-systolic volume (ml/m ²)	31 ± 9	34 ± 6	27 ± 5	51 ± 22	53 ± 23	46 ± 19	< 0.001
Stroke volume (ml/m ²)	37 ± 11	39 ± 9	33 ± 6	45 ± 14	44 ± 12	47 ± 16	0.005

Data are expressed as mean ± SD.

* Difference between healthy controls and patients with CHD.

Receiver operating characteristic curves were created to obtain the sensitivity, specificity, and positive and negative predictive values of RT3DE to identify systolic RV dysfunction (Table 5 and Figures 3 and 4). Scatter plots of the indexed end-diastolic volume, end-systolic volume, and EF measured using CMR imaging in healthy controls are shown in Figure 3, together with the best cut-off values predicting RV dysfunction in patients with CHD using the RT3DE data (indexed end-diastolic volume >105 ml/m², indexed end-systolic volume >54 ml/m², and EF <43%). In Table 5, 3 alternative scenarios are listed. RT3DE could either be a test with a maximum sum of the sensitivity and specificity, a test with an optimal sensitivity or a test with an optimal specificity.



36. **Figure 2** Cumulative percentages with their median values for real-time 3-dimensional
 37. echocardiography and cardiac magnetic resonance imaging of the indexed RV end-diastolic volumes (a),
 38. indexed end-systolic volumes (b), and ejection fractions (c). CHD denotes congenital heart disease, RT3DE
 39. real-time 3-dimensional echocardiography, CMR cardiac magnetic resonance, EDVi indexed end diastolic
 volume, ESVi indexed end systolic volume, EF ejection fraction.

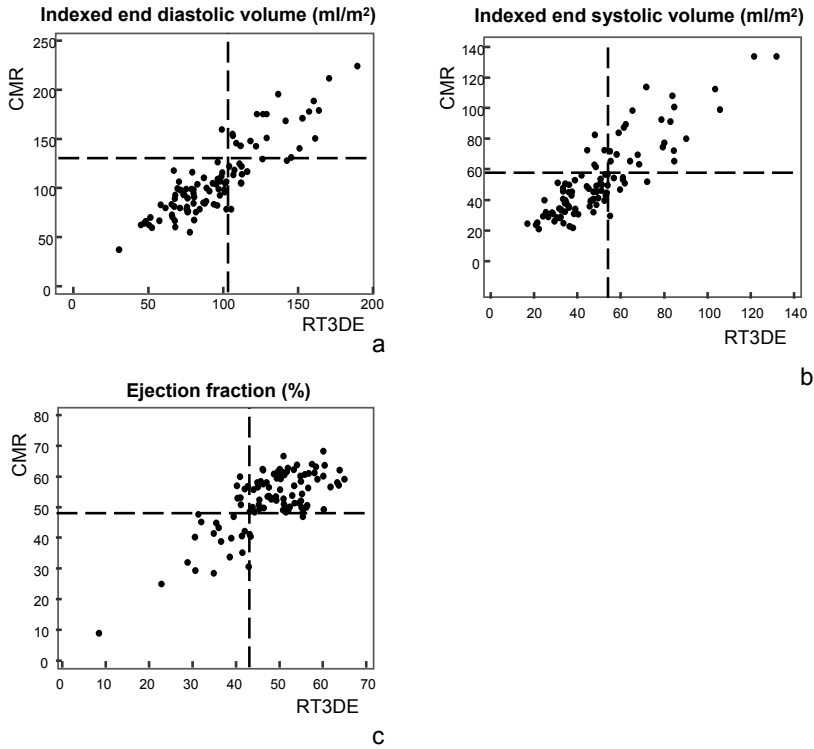


Figure 3 Correlations between real-time 3-dimensional echocardiography derived and cardiac magnetic resonance imaging derived volumes (a, b) and ejection fraction (c). Dotted lines represent the best cut-off values predicting right ventricular dysfunction.

DISCUSSION

The backbone of the present study was the data on RV volumes and EF we measured using CMR imaging in a group of 41 healthy controls. These data, consistent with previous studies,¹⁰⁻¹⁴ have provided normal reference data for the definition of RV function. Combined with predetermined cut-off values for normality derived using the CMR data, RT3DE data proved to be highly sensitive to identify RV systolic dysfunction in patients with various CHDs. RV systolic dysfunction, defined as a RV EF <43%, could be identified from the RT3DE findings in 23 patients (23%), with a sensitivity of 95%, specificity of 89%, and negative predictive value of 99%. The high sensitivity and negative predictive value imply that the RT3DE findings can be used as a screening tool to exclude RV systolic dysfunction in patients with CHD.

It is important to accurately measure RV volumes and EF because impaired RV function is known to be a predictor of adverse outcome and poor remodelling after pulmonary valve replacement. The relation between the RV volumes and/or EF with the long-term outcome in patients with CHD has been studied in both the subpulmonary and the systemic right

Table 5. Test characteristics of real-time three-dimensional echocardiography to identify right ventricular dysfunction

	RV indexed EDV	RV indexed ESV	RV EF
Maximum sum sensitivity + specificity			
Cut-off value	105	54	43
Area under the curve (95% CI)	0.97 (0.92-1.0)	0.96 (0.90-0.99)	0.93 (0.86-0.97)
Sensitivity	96 (78-99)	83 (64-94)	95 (75-99)
Specificity	88 (78-94)	90 (80-96)	89 (80-95)
Positive predictive value	69 %	75 %	61 %
Negative predictive value	99 %	93 %	99 %
Maximum sensitivity			
Cut-off value	99	44	55
Sensitivity	100 (85-100)	100 (88-100)	100 (83-100)
Specificity	77 (65-86)	60 (47-72)	23 (14-33)
Positive predictive value	58 %	51 %	26 %
Negative predictive value	100 %	100 %	100 %
Maximum specificity			
Cut-off value	143	72	31
Sensitivity	39 (20-61)	45 (27-64)	20 (6-44)
Specificity	100 (95-100)	100 (95-100)	100 (95-100)
Positive predictive value	100 %	100 %	100 %
Negative predictive value	85 %	83 %	83 %

Data are presented as mean (95% confidence intervals).

Cut-off values, sensitivity and specificity were calculated using receiver operating characteristic curves.

EDV = end-diastolic volume; ESV = end-systolic volume; EF = ejection fraction.

ventricle.¹⁵⁻¹⁷ Knauth et al¹⁵ published an interesting study in which they identified the cut-off values for indexed end-diastolic volume, end-systolic volume, and EF measured using CMR imaging as predictors of major adverse cardiac events in patients late after tetralogy of Fallot repair. In patients with systemic right ventricles, Piran et al¹⁶ found that a RV EF <35% was a strong prognostic risk factor for the development of heart failure. In general, experts have agreed that a systemic RV EF >50% should be considered normal.¹⁸ When we compared these data with our own data, we found that only 10% of the patients we studied had a systemic right ventricle. RV dysfunction was present in half of them according to their CMR data.

Discussion remains on the relevance of defining absolute cut-off values for impaired systolic RV function in patients with CHD. Earlier studies based their judgment of RV performance on visualization of the two-dimensional echocardiographic images and defined poor RV function subjectively as moderately or severely reduced function.^{16, 17, 19, 20} CMR imaging and RT3DE data made accurate, quantitative assessment of systolic RV function possible. We should define normality for these techniques and, consequently, the cut-off points for abnormality. Therrien et al²¹, for example, suggested thresholds for end-diastolic volume and end-systolic volume, measured using CMR imaging, for adequate reverse remodelling after pulmonary valve replacement late after tetralogy of Fallot repair.^{21, 22}

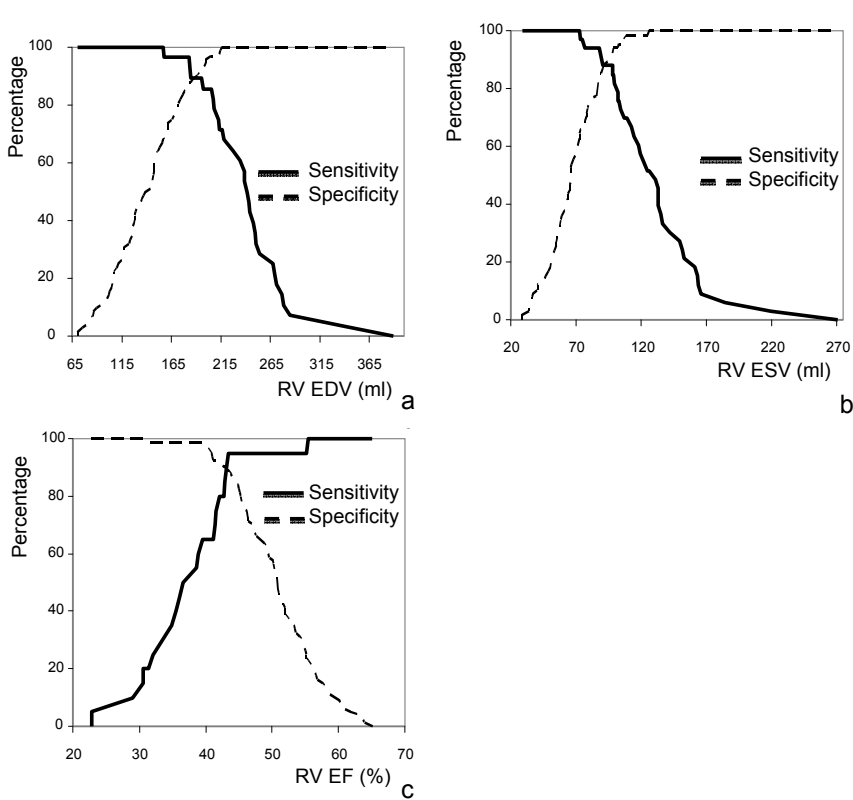


Figure 4 Plots of the sensitivity versus the specificity for the indexed end diastolic (a) and end systolic volumes (b) and ejection fraction (c).

The EF is an easy to apply measurement to assess RV contractility, but it is quite variable and dependent on both the pre- and afterload. Thus, in the interpretation of EF the underlying absolute volumes should also be taken into account. These volumes provide information on the loading conditions of the heart: a larger volume is related to greater wall stress and impaired contractile reserve during exercise.²³ In addition to the volumes and/or EF as indicators of systolic RV function, several techniques, such as tissue Doppler imaging or speckle tracking echocardiography, focus on regional RV function. Thus, RV regional longitudinal or circumferential contractility or deformation can be assessed. Especially in cases where the EF is unreliable for information of RV myocardial function, such as in tricuspid valve insufficiency, these regionally orientated techniques could provide more accurate information on, for example, RV longitudinal function. In contrast, regional techniques are only valuable when their results can be extrapolated to the global RV function. For example, tricuspid annular systolic plane excursion is a useful measurement for RV function in various patient groups. In operated patients however, the RV longitudinal function will be reduced but the EF will remain constant; thus, this measurement will not give accurate information on RV performance.²⁴

1. With the introduction of RT3DE, an alternative technique became available to assess global
2. RV function. RT3DE offers the possibility to provide easy, inexpensive, fast, bedside information.
3. We evaluated the ability of the RT3DE findings to identify systolic RV dysfunction; however, the
4. prognostic relation of RT3DE-derived RV volumes and EF needs to be established.

5. The main limitation of RT3DE is related to the spatial and temporal resolution. Moreover,
6. echocardiographic imaging of the right ventricle is challenged by the retrosternal position of
7. the right ventricle. Seven subvolumes that are acquired over seven heartbeats are needed to
8. gather a full-volume dataset. Irregularity of the heart rate causes stitching artifacts and unus-
9. able datasets. However, we expect that these technical features will improve within the near
10. future.

11. In contrast, the CMR estimation of RV volumes and EF uses two-dimensional images com-
12. bined with a fixed slice height and, therefore, is not a three-dimensionally based technique. Also,
13. the temporal resolution of CMR is restricted. Identification of the upper slice containing part of
14. the right ventricle is challenging, and both the acquisition and analysis are time-consuming.

15. The present study did not provide any prognostic information on RV dysfunction or informa-
16. tion for the various CHDs separately. Moreover, certain CHDs, such as an atrial septal defect or
17. tetralogy of Fallot, primarily affect the right ventricle, and these ventricles are morphologically
18. abnormal. Monitoring the global RV function in such ventricles is needed from early childhood
19. onward. In the present study, we did not investigate such young children.

20.
21.
22.
23.
24.
25.
26.
27.
28.
29.
30.
31.
32.
33.
34.
35.
36.
37.
38.
39.

1. Carabello BA. Evolution of the study of left ventricular function: everything old is new again. *Circulation*. 2002;105:2701-3. 1.
2. Babu-Narayan SV, Gatzoulis MA, Kilner PJ. Non-invasive imaging in adult congenital heart disease using cardiovascular magnetic resonance. *J Cardiovasc Med (Hagerstown)*. 2007;8:23-9. 2.
3. Bleeker GB, Steendijk P, Holman ER, Yu CM, Breithardt OA, Kaandorp TA, et al. Assessing right ventricular function: the role of echocardiography and complementary technologies. *Heart*. 2006;92 Suppl 1:i19-26. 3.
4. Lai WW, Gauvreau K, Rivera ES, Saleeb S, Powell AJ, Geva T. Accuracy of guideline recommendations for two-dimensional quantification of the right ventricle by echocardiography. *Int J Cardiovasc Imaging*. 2008;24:691-8. 4.
5. Sugeng L, Mor-Avi V, Weinert L, Niel J, Ebner C, Steringer-Mascherbauer R, et al. Multimodality Comparison of Quantitative Volumetric Analysis of the Right Ventricle. *JACC Cardiovasc Imaging*. 2010;3:10-8. 5.
6. van der Zwaan HB, Helbing WA, McGhie JS, Geleijnse ML, Luijnenburg SE, Roos-Hesselink JW, et al. Clinical Value of Real-Time Three-Dimensional Echocardiography for Right Ventricular Quantification in Congenital Heart Disease: Validation With Cardiac Magnetic Resonance Imaging. *J Am Soc Echocardiogr*. 2010;23:134-40. 6.
7. Tamborini G, Marsan NA, Gripari P, Maffessanti F, Brusoni D, Muratori M, et al. Reference values for right ventricular volumes and ejection fraction with real-time three-dimensional echocardiography: evaluation in a large series of normal subjects. *J Am Soc Echocardiogr*. 2010;23:109-15. 7.
8. Robbers-Visser D, Boersma E, Helbing WA. Normal biventricular function, volumes, and mass in children aged 8 to 17 years. *J Magn Reson Imaging*. 2009;29:552-9. 8.
9. Puchalski MD, Williams RV, Askovich B, Minich LL, Mart C, Tani LY. Assessment of right ventricular size and function: echo versus magnetic resonance imaging. *Congenit Heart Dis*. 2007;2:27-31. 9.
10. Alfakih K, Plein S, Thiele H, Jones T, Ridgway JP, Sivananthan MU. Normal human left and right ventricular dimensions for MRI as assessed by turbo gradient echo and steady-state free precession imaging sequences. *J Magn Reson Imaging*. 2003;17:323-9. 10.
11. Teo KS, Carbone A, Piantadosi C, Chew DP, Hammett CJ, Brown MA, et al. Cardiac MRI assessment of left and right ventricular parameters in healthy Australian normal volunteers. *Heart Lung Circ*. 2008;17:313-7. 11.
12. Maceira AM, Prasad SK, Khan M, Pennell DJ. Reference right ventricular systolic and diastolic function normalized to age, gender and body surface area from steady-state free precession cardiovascular magnetic resonance. *Eur Heart J*. 2006;27:2879-88. 12.
13. Hudsmith LE, Petersen SE, Francis JM, Robson MD, Neubauer S. Normal human left and right ventricular and left atrial dimensions using steady state free precession magnetic resonance imaging. *J Cardiovasc Magn Reson*. 2005;7:775-82. 13.
14. Lorenz CH, Walker ES, Morgan VL, Klein SS, Graham TP, Jr. Normal human right and left ventricular mass, systolic function, and gender differences by cine magnetic resonance imaging. *J Cardiovasc Magn Reson*. 1999;1:7-21. 14.
15. Knauth AL, Gauvreau K, Powell AJ, Landzberg MJ, Walsh EP, Lock JE, et al. Ventricular size and function assessed by cardiac MRI predict major adverse clinical outcomes late after tetralogy of Fallot repair. *Heart*. 2008;94:211-6. 15.
16. Piran S, Veldtman G, Siu S, Webb GD, Liu PP. Heart failure and ventricular dysfunction in patients with single or systemic right ventricles. *Circulation*. 2002;105:1189-94. 16.
17. Rutledge JM, Nihill MR, Fraser CD, Smith OE, McMahon CJ, Bezold LI. Outcome of 121 patients with congenitally corrected transposition of the great arteries. *Pediatr Cardiol*. 2002;23:137-45. 17.
18. Davlouros PA, Niwa K, Webb G, Gatzoulis MA. The right ventricle in congenital heart disease. *Heart*. 2006;92 Suppl 1:i27-38. 18.

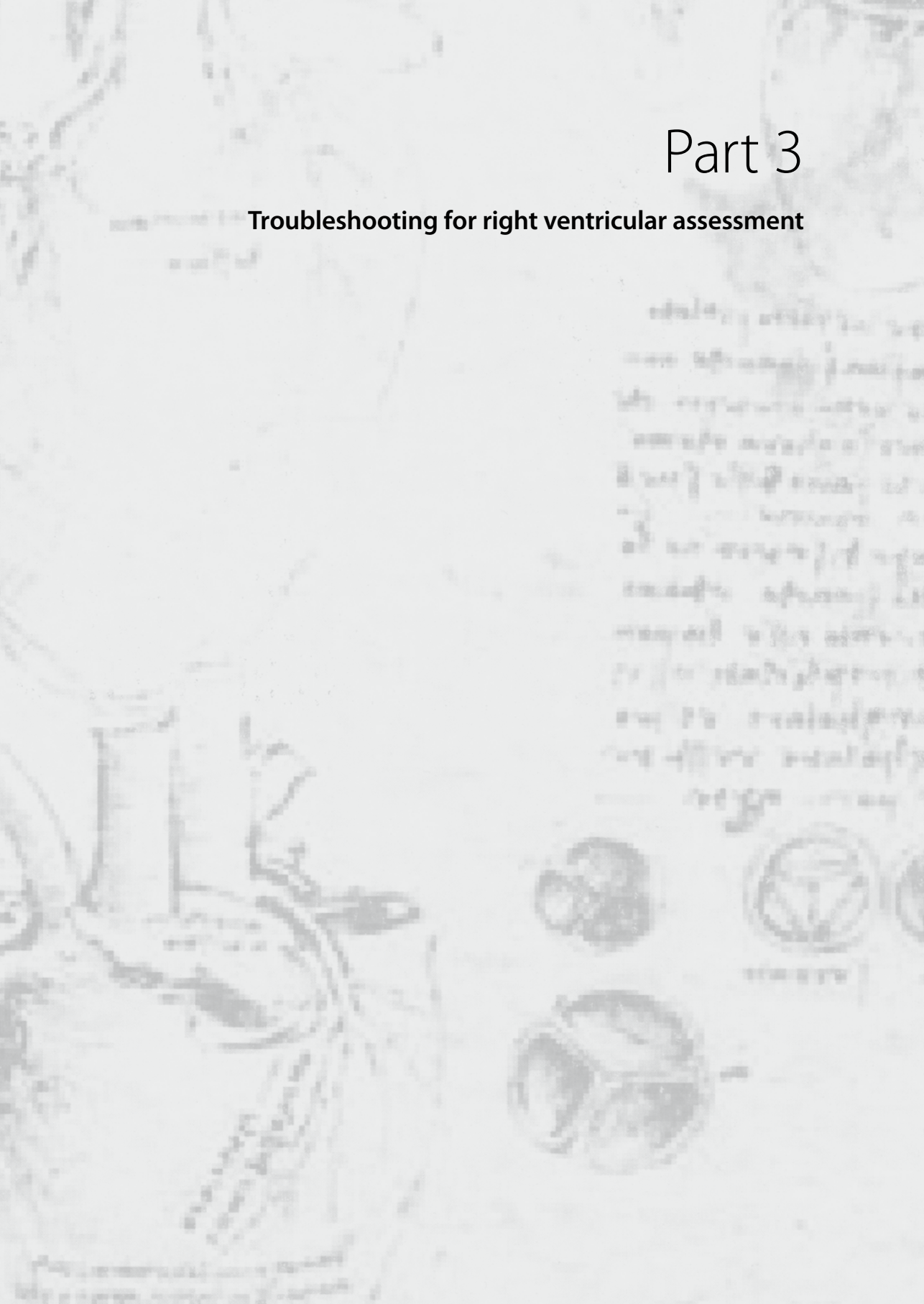
1.
2.
3.
4.
5.
6.
7.
8.
9.
10.
11.
12.
13.
14.
15.
16.
17.
18.
19.
20.
21.
22.
23.
24.
25.
26.
27.
28.
29.
30.
31.
32.
33.
34.
35.
36.
37.
38.
39.

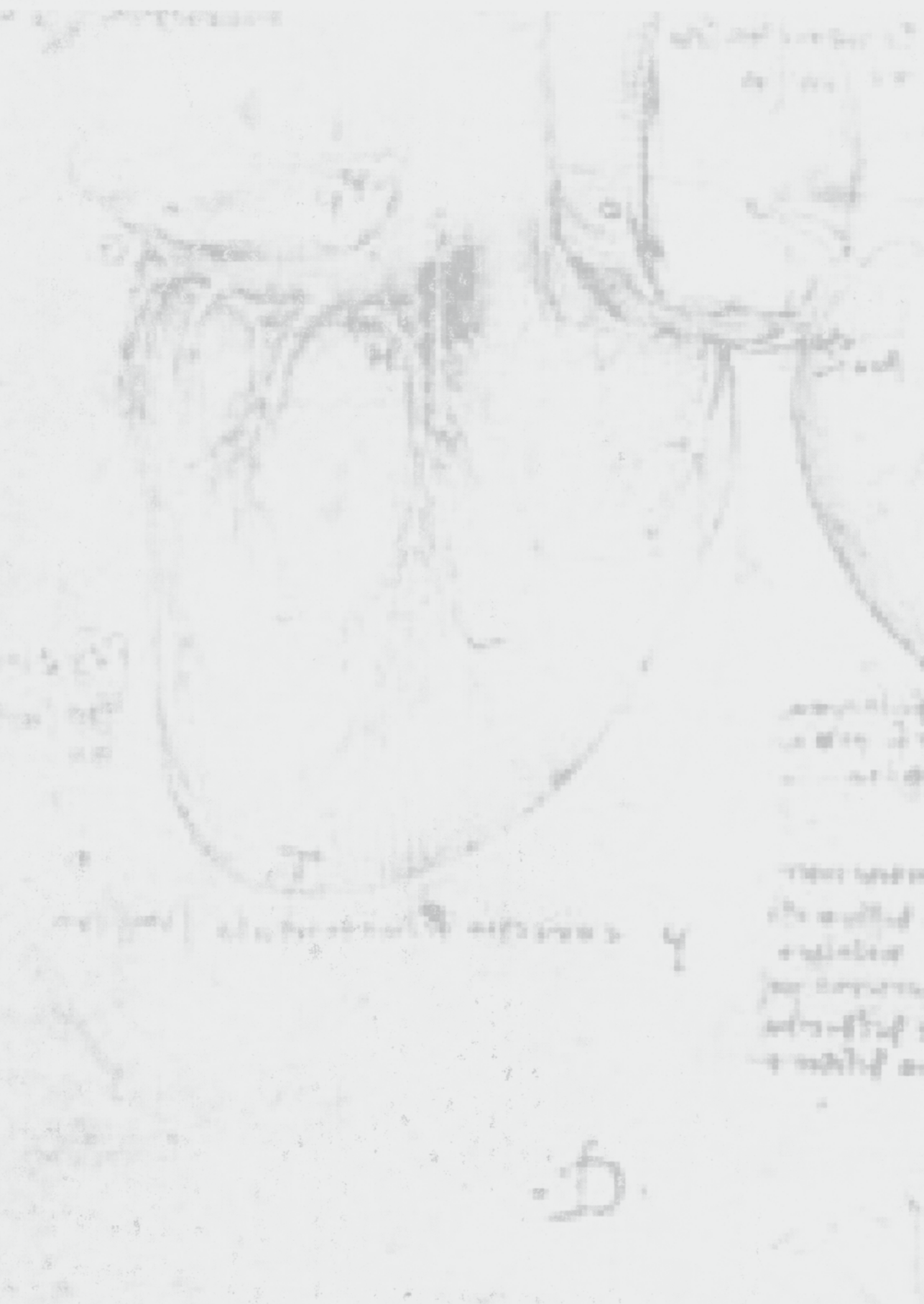
1. 19. Meijboom F, Szatmari A, Deckers JW, Utens EM, Roelandt JR, Bos E, et al. Long-term follow-up (10 to 17 years) after Mustard repair for transposition of the great arteries. *J Thorac Cardiovasc Surg.* 1996;111:1158-68.
- 2.
3. 20. Roos-Hesselink JW, Meijboom FJ, Spitaels SE, van Domburg R, van Rijen EH, Utens EM, et al. Decline in ventricular function and clinical condition after Mustard repair for transposition of the great arteries (a prospective study of 22-29 years). *Eur Heart J.* 2004;25:1264-70.
- 4.
5. 21. Therrien J, Provost Y, Merchant N, Williams W, Colman J, Webb G. Optimal timing for pulmonary valve replacement in adults after tetralogy of Fallot repair. *Am J Cardiol.* 2005;95:779-82.
- 6.
7. 22. Buechel ER, Dave HH, Kellenberger CJ, Dodge-Khatami A, Pretre R, Berger F, et al. Remodelling of the right ventricle after early pulmonary valve replacement in children with repaired tetralogy of Fallot: assessment by cardiovascular magnetic resonance. *Eur Heart J.* 2005;26:2721-7.
- 8.
9. 23. Apitz C, Sieverding L, Latus H, Uebing A, Schoof S, Hofbeck M. Right ventricular dysfunction and B-type natriuretic peptide in asymptomatic patients after repair for tetralogy of Fallot. *Pediatr Cardiol.* 2009;30:898-904.
- 10.
11. 24. Tamborini G, Muratori M, Brusoni D, Celeste F, Maffessanti F, Caiani EG, et al. Is right ventricular systolic function reduced after cardiac surgery? A two- and three-dimensional echocardiographic study. *Eur J Echocardiogr.* 2009;10:630-4.
- 12.
- 13.
- 14.
- 15.
- 16.
- 17.
- 18.
- 19.
- 20.
- 21.
- 22.
- 23.
- 24.
- 25.
- 26.
- 27.
- 28.
- 29.
- 30.
- 31.
- 32.
- 33.
- 34.
- 35.
- 36.
- 37.
- 38.
- 39.



Part 3

Troubleshooting for right ventricular assessment





Chapter 8

Sources of differences in volumetric right ventricular estimation: real-time three-dimensional echocardiography and cardiac magnetic resonance imaging in patients with tetralogy of Fallot

H.B. van der Zwaan
W.A. Helbing
O.I.I. Soliman
G. van Burken
J.G. Bosch
J.S. McGhie
J.W. Roos-Hesselink
F.J. Meijboom
M. L. Geleijnse
K.Y.E. Leung

Submitted for publication

ABSTRACT

Background. It has not been investigated in detail why right ventricular (RV) volumes assessed by real-time three-dimensional echocardiography (RT3DE) differ from those obtained using cardiac magnetic resonance (CMR) imaging. We sought to study systematically the potential sources of RV volume differences in patients with tetralogy of Fallot.

Methods. Customized software was used that displays images obtained by RT3DE and CMR imaging in exactly the same anatomical plane to facilitate side-by-side comparison. The endocardial contours, derived from semiautomated three-dimensional border detection for RT3DE and manual tracing of contours in multiple slices for CMR imaging, were superimposed onto the images. A 9-segment model was used to estimate segmental RV volume differences.

Results. A total of 26 patients with tetralogy of Fallot (mean age 26 ± 9 years, 62% men) were included. Global RV volumes calculated using RT3DE were on average 23 ± 26 ml smaller than CMR imaging-derived volumes in end-diastole, and 10 ± 16 ml in end-systole. However, no statistically significant bias was found in RV ejection fraction ($1.9 \pm 6.3\%$). Volume differences were mainly caused by poorer visualization of the RV anterior wall using RT3DE, corroborated by regional quantitative analysis (46% volume difference in the anterior segments). The use of disc summation by CMR imaging resulted in differences in the apical and pulmonary valve area. Trabeculae were more distinguishable from RV myocardium by CMR imaging than RT3DE; the wall appeared to be thicker using RT3DE.

Conclusions. The main sources of volume differences between RT3DE and CMR imaging in this patient population are caused by suboptimal visualization of the RV anterior wall by RT3DE, the use of disc summation by CMR imaging, and the visualization and management of trabeculae. The understanding of this intermodality discordance will help to implement RT3DE into clinical practice.

1. INTRODUCTION

2.

3. The prognosis of patients with tetralogy of Fallot has increased over the last decades, because
4. of improved surgical techniques and pediatric care. Now that operative mortality of the early
5. repair has fallen to low levels, attention has turned to improvement of longer-term outcomes
6. and preservation of cardiac function. A substantial proportion of adults with tetralogy of Fallot
7. develop right ventricular (RV) dysfunction and clinical symptoms of heart failure,¹⁻³ because
8. their right ventricles are often volume overloaded. Therefore, it is important to monitor RV
9. function with accurate imaging techniques.

10. The assessment of RV volumes and ejection fraction (EF) by two-dimensional echocar-
11. diography has been cumbersome.⁴ Complicated geometric models have been used, but have
12. been found inaccurate.⁵ Three-dimensional echocardiography avoids the need for geometric
13. assumptions, because the right ventricle can be included into one dataset. Real-time three-
14. dimensional echocardiography (RT3DE), allows a fast volumetric analysis of RV volumes and
15. EF based on semiautomated endocardial surface detection.⁶ Despite reasonably good correla-
16. tions, several studies have reported that, within the same patient, systematic differences existed
17. in RV volumes derived of RT3DE and cardiac magnetic resonance (CMR) imaging.⁶⁻⁹ There is no
18. consensus regarding the factors contributing to this intermodality discordance. The potential
19. factors are the suboptimal visibility of certain parts of the right ventricle by RT3DE, differences
20. in the spatial resolution between RT3DE and CMR imaging, variation in the contrast resolution
21. that affects the identification of the endocardial boundaries, and to what extent trabeculae are
22. included in the imaged RV volumes.¹⁰ Also, the intermodality discordance may be increased by
23. analysis-related variations, such as different views used to identify the endocardial boundary as
24. well as different algorithms used to calculate volumes in the software packages.¹¹

25. Accordingly, this study was designed to identify and quantify the potential sources of RV
26. volume differences by RT3DE and CMR imaging. We hypothesized that the main reasons for
27. the intermodality discordance are: 1) the inability of RT3DE to include the RV outflow tract
28. in the sector and 2) differences in the identification of the endocardial surface details such as
29. trabeculae. To test this hypothesis, we used software that enabled a systematic and side-by-
30. side comparison of the RV segments by RT3DE and CMR imaging.

31.

32.

33. METHODS

34.

35. Study population

36. A total of 26 patients with tetralogy of Fallot were included in the study. The patients were
37. referred for CMR imaging for a quantitative analysis of their cardiac function. All patients under-
38. went a RT3DE examination within two hours from CMR imaging, to pursue comparable loading

39.

conditions. The medical ethical committee approved the study and written informed consent was obtained from all patients and/or their parents if required.

Image acquisition and analysis by cardiac magnetic resonance imaging

CMR images were acquired using a Signa 1.5 Tesla scanner (GE Medical Systems, Milwaukee, Wisconsin). Subjects were positioned in the supine position with dedicated phased-array cardiac surface coils placed over the thorax. The CMR protocol included cine steady state free precession sequences in short-axis planes to assess RV volumes. Electrocardiogram gating and repeated breath holds were applied to minimize the influence of cardiac and respiratory motion.

RV volumes were measured from a multi-section image set of 8 to 12 contiguous slices parallel to the plane of the atrioventricular valves covering the full length of both ventricles. Imaging parameters were as follows: slice thickness 7 to 10 mm, inter-slice gap 0 mm, field of view 280 to 370 mm, phase field of view 0.75, matrix 160 x 128 mm, repetition time 3.5 ms, echo time 1.5 ms, 12 views/segment, flip angle 45°, mean in-plane resolution 2 mm², range of temporal resolution 22–37 ms.

The short-axis dataset was analyzed quantitatively on a commercially available Advanced Windows workstation (GE Medical Systems) using Advanced Windows version 5.1 of the MR Analytical Software System (Medis Medical Imaging Systems, Leiden, the Netherlands). The RV endocardial borders in end-diastole and end-systole were manually delineated in the short-axis slices with exclusion of trabeculae as described by Robbers-Visser et al.¹²

Image acquisition and analysis by real-time three-dimensional echocardiography

RT3DE harmonic imaging was performed using the iE33 ultrasound system (Philips Medical Systems, Best, the Netherlands) equipped with an X3-1 matrix array transducer with the patient in the left lateral decubitus position. A full-volume scan was acquired from a modified apical transducer position in harmonic mode from seven R-wave gated subvolumes during a single end-expiratory breath-hold. The depth and angle of the ultrasound sector were adjusted to a minimal level still encompassing the right ventricle. Before each acquisition, images were optimized for endocardial border visualization by modifying time gain and compression and increasing the overall gain. The volume rate was 24 ± 4 frames per cardiac cycle. The datasets were digitally exported to a server (TomTec Imaging Systems, Unterschleissheim, Germany) connected to a terminal workstation for further analyses.

The digital RT3DE RV datasets were analyzed offline using the four-dimensional RV Function program version 1.2. This software performs three-dimensional semiautomated border detection of RV volumes over the cardiac cycle. It uses a physics-based modelling algorithm that makes no assumptions regarding RV geometry. The details of the RV Function program are reported elsewhere.⁶ In short, the end-diastolic (largest RV volume) and end-systolic (smallest RV volume) phases need to be identified. Endocardial border contours are drawn onto still frames of the apical four-chamber view, short-axis view, and coronal view in both end-diastole

1. and end-systole. After the contour tracing steps, the software automatically delineates the RV
 2. endocardial border from the end-diastolic and end-systolic phases and by sequential analysis
 3. the software creates an RV mathematic dynamic three-dimensional endocardial surface that
 4. represents changes in the RV cavity over the cardiac cycle.

5.

6. Software for side-by-side analysis

7. The RT3DE and CMR images and the endocardial contours derived from the software packages
 8. described above, were analyzed using software developed in-house (3DStressView, Erasmus
 9. MC, Rotterdam, the Netherlands).¹³ With this software, the RT3DE and CMR images and the
 10. endocardial contours can be aligned systematically using a standardized protocol, thereby
 11. generating the corresponding anatomical views. These views can then be analyzed synchro-
 12. nized and displayed side-by-side, to distinguish the differences in image appearance and in
 13. border delineation.

14. To get the anatomically corresponding views, the RT3DE and CMR images were manipulated
 15. as follows. Optimal anatomical views were obtained by manually annotating the RV apex and
 16. the tricuspid valve hinge points, initially in an apical four-chamber view in end-diastole. An
 17. orthogonal view through the RV long-axis was then generated. The annotation process was
 18. repeated in this orthogonal long-axis view and if necessary multiple times in both views, to
 19. quickly and accurately approximate the RV long-axis as described previously.¹⁴ The coronal
 20. view was then obtained by selecting the correct angle. The correspondence between RT3DE
 21. and CMR views is expressed as a spatial transformation (translation and rotation), which is then
 22. used to align the RT3DE and CMR endocardial contours. This allows us to superimpose the
 23. RT3DE based contours onto the CMR image and vice versa.

24. The anatomically corresponding views and contours can then be played in a cineloop,
 25. synchronized on the electrocardiographic R-peak. Zooming and navigation can be performed
 26. for all views simultaneously, so that the view correspondence is preserved. The software can
 27. display long-axis views and short-axis views in the apical, mid, and basal planes. Figure 1 shows
 28. an example of the aligned RT3DE and CMR images and their contours.

29.

30. Image appearance, volume quantification, and statistical analysis

31. We visually inspected the RT3DE images and judged the quality of the following RV walls: the
 32. anterior, lateral, and inferior walls at the basal, mid, and apical level. The segments were scored
 33. as: 4 = excellent quality without possibility to improve, 3 = good quality without artifacts, 2 =
 34. sufficient quality without artifacts or good quality with artifacts, 1 = poor or moderate quality
 35. with artifacts and 0 = nonvisualized.¹³

36. Differences in endocardial border delineation were assessed quantitatively by calculating
 37. global and segmental RV volumes and EF. The calculation of the global RV volumes is described
 38. above. For segmental analysis, the right ventricle was divided into three longitudinal and three
 39. vertical regions resulting in a total of nine segments, as described by Klein et al¹⁵ (Figure 2).

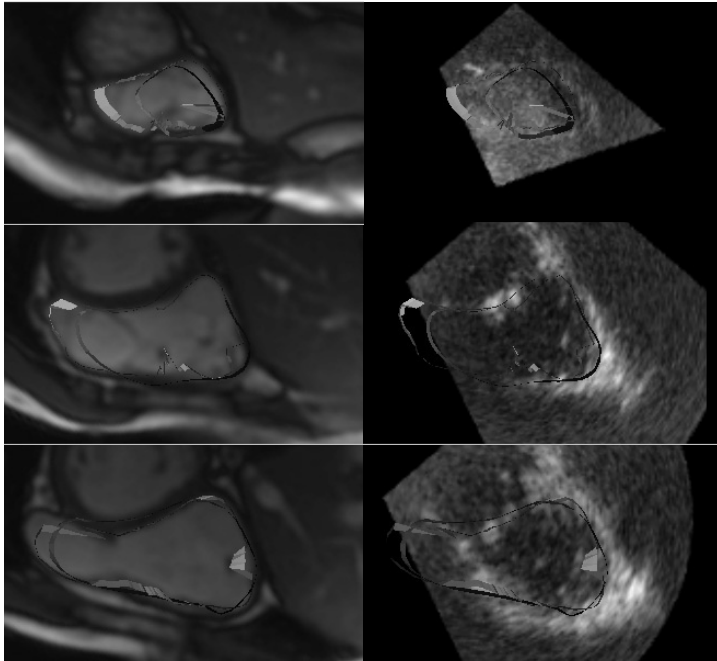


Figure 1 Display of the right ventricle in short-axis views, at the basal, mid and apical level, displayed by cardiac magnetic resonance imaging (left) and real-time 3-dimensional echocardiography (right), with the magnetic resonance contours in green and the real-time 3-dimensional echo contours in different colors.

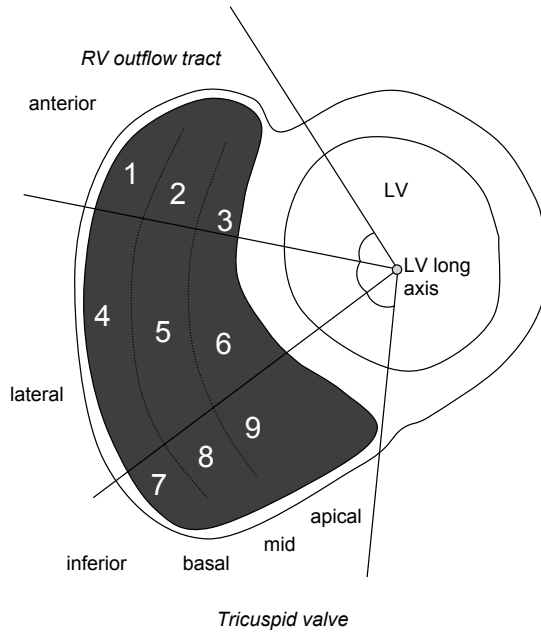


Figure 2 The 9-segment model used to divide the right ventricle into various regions.

1.
2.
3.
4.
5.
6.
7.
8.
9.
10.
11.
12.
13.
14.
15.
16.
17.
18.
19.
20.
21.
22.
23.
24.
25.
26.
27.
28.
29.
30.
31.
32.
33.
34.
35.
36.
37.
38.
39.

1. Statistical testing was performed using Student's paired *t* tests. All statistical tests were two-
2. sided, and a P-value <0.05 was considered statistically significant.

3.

4.

5. RESULTS

6.

7. The baseline characteristics of the study population are summarized in Table 1. The mean age at
8. initial repair was 2 ± 2 years; 14 patients underwent re-operations at 15 ± 12 years.

9.

10. **Table 1.** Baseline characteristics

11. Age (years)	26 ± 9
12. Men (%)	62
13. Age at initial repair (years)	2 ± 2
14. Age at reoperation (years), (n = 14)	15 ± 12
15. Heart rate (beats/min)	74 ± 11
16. Systolic blood pressure (mmHg)	123 ± 18
17. Diastolic blood pressure (mmHg)	72 ± 11
18. Height (cm)	170 ± 14
19. Weight (kg)	64 ± 16
20. Body mass index (kg/m ²)	22 ± 4
21. Body surface area (m ²)	1.7 ± 0.3

21. Image appearance

22. The anterior wall was often suboptimally visualized in the RT3DE images, especially in the mid
23. and basal regions. In contrast, the inferior wall was well imaged. Trabeculae were displayed
24. more prominently and the wall appeared to be thicker when viewed by RT3DE (Table 2).

25.

26. **Table 2.** Visual evaluation of the real-time three-dimensional echocardiographic image quality

27. Segment	Apical	Mid	Basal	Total
28. Anterior	1.1 ± 0.8	0.4 ± 0.6	0.4 ± 0.6	0.6 ± 0.5
29. Lateral	1.3 ± 0.9	1.5 ± 1.1	2.3 ± 1.1	1.7 ± 0.8
30. Inferior	1.8 ± 1.2	3.3 ± 0.8	3.1 ± 0.8	2.8 ± 0.7
31. Total	1.4 ± 0.6	1.8 ± 0.6	2.8 ± 0.7	1.7 ± 0.5

31. Values are indicated in percentages of the absolute volume difference as mean ± standard deviation.
32. Scoring as follows: The segments were scored as: 4 = excellent quality without possibility to improve, 3
33. = good quality without artifacts, 2 = sufficient quality without artifacts or good quality with artifacts, 1 =
34. poor or moderate quality with artifacts and 0 = nonvisualized.

35.

35. Border delineation

36. When comparing the delineated contours of the RT3DE and CMR images, we found the largest
37. difference in the anterior region (RV outflow tract) when we visually judged these contours.

38. Delineation in the anterior segments based on RT3DE images was complicated by poor visual-
39. ization of the anterior wall, resulting in varying degrees of RV volume underestimation (Figure

3). On the other hand, because the delineation by CMR imaging was confined to short-axis 1.
 planes, differences in identifying the height of the apex, tricuspid valve, and pulmonary valve 2.
 were noticeable (Figure 4). Endocardial borders were traced more toward the ventricular cavity 3.
 on RT3DE images, especially when many trabeculae were present (Figure 5). 4.
 5.
 6.
 7.
 8.
 9.
 10.
 11.
 12.
 13.
 14.
 15.
 16.
 17.
 18.
 19.

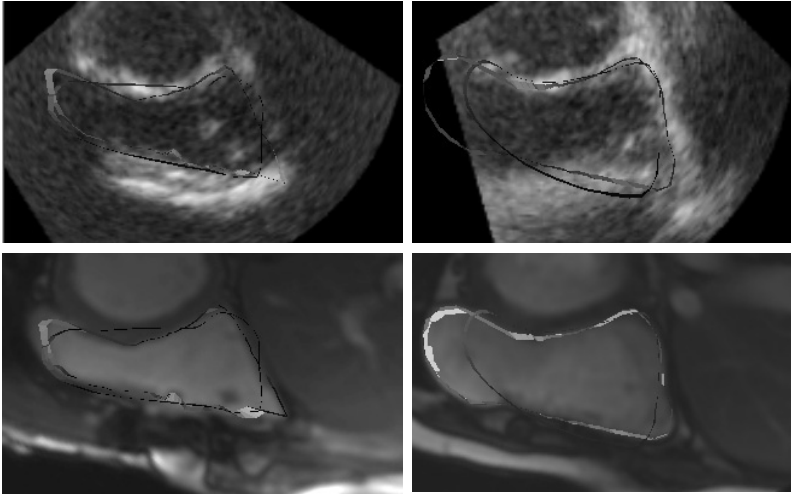


Figure 3 Two examples of contour delineation in mid short-axis views, showing different degrees of 20.
 underestimation by real-time 3-dimensional echocardiography. 21.
 22.

Quantitative analysis 23.

Global differences in RV volumes and EF were assessed by subtracting the RT3DE values 24.
 from the CMR values (Table 3). The average global RV volume difference was 23 ± 26 ml 25.
 in end-diastole, and 10 ± 16 ml in end-systole. In both cases, there was a statistically significant 26.
 underestimation ($P < 0.001$). In contrast, RV EF was not different between the two techniques 27.
 with a bias of only $2 \pm 6\%$. 28.
 29.

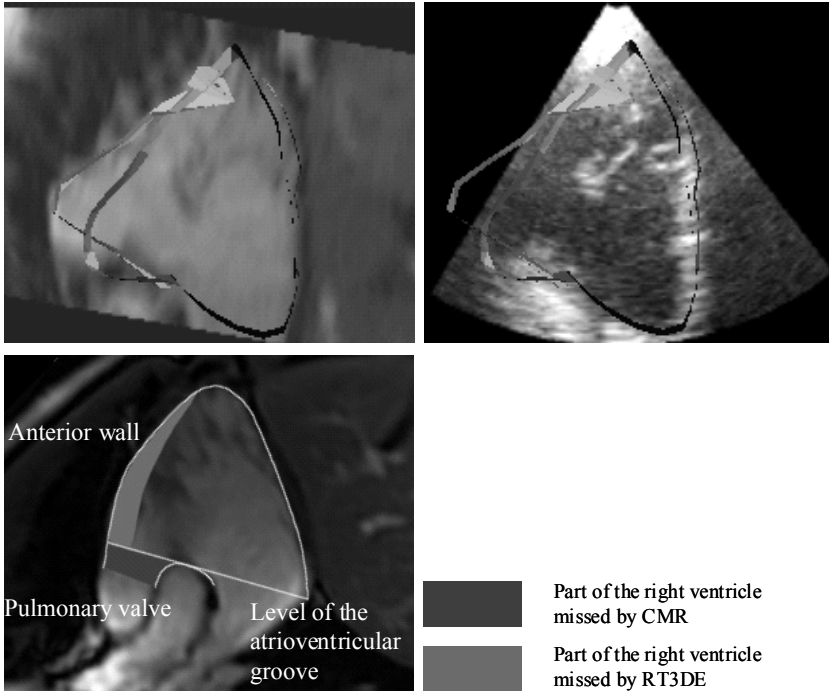
Table 3. Global right ventricular volumes and ejection fraction 30.

	CMR	RT3DE	CMR – RT3DE
End-diastolic volume (ml)	234 ± 88	211 ± 84	$23.0 \pm 25.5^*$
End-systolic volume (ml)	123 ± 62	113 ± 55	$9.8 \pm 16.0^*$
Stroke volume (ml)	111 ± 35	98 ± 37	$13.2 \pm 21.9^*$
Ejection fraction (%)	49.3 ± 9.1	47.4 ± 8.4	1.9 ± 6.3

CMR = cardiac magnetic resonance imaging, RT3DE = real-time 3-dimensional echocardiography. Values 35.
 are indicated as mean \pm standard deviation.

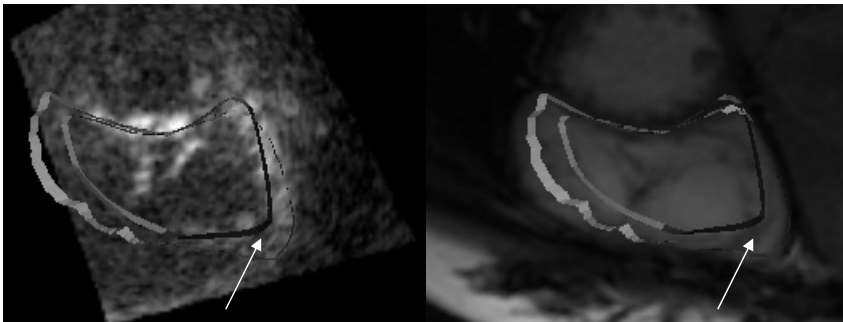
*Denotes statistically significant ($p < 0.05$) underestimation by real-time 3-dimensional echocardiography. 36.
 37.
 38.
 39.

1.
2.
3.
4.
5.
6.
7.
8.
9.
10.
11.
12.
13.
14.
15.
16.
17.
18.



19. **Figure 4** Differences in contour delineation in the anterior segments, caused by difficulties in
20. visualization by real-time 3-dimensional echocardiography, and the use of short-axis planes in cardiac
21. magnetic resonance imaging.

22.
23.
24.
25.
26.
27.
28.
29.
30.



31. **Figure 5** Delineation difficulties when many trabeculae is present.

32.
33.
34.
35.
36.
37.
38.
39.

By dividing the right ventricle into nine segments, we quantified the difference between RT3DE and CMR derived volumes for each RV segment (Table 4). The smaller RV volumes found by RT3DE were contributed mostly by the anterior segments in both end-diastole and end-systole. To evaluate which regions contribute most to regional volume differences, regardless of over or underestimation, we calculated the absolute regional volume differences as a percentage of the absolute volume differences. In accordance with the signed regional volume differences, the largest volume difference (46%) was located in the anterior segments (Table 5).

Table 4. Signed right ventricular volume differences (ml) per segment

Segment	Apical	Mid	Basal	Total
End-diastole				
Anterior	11.3 ± 10.0*	5.9 ± 12.3	-2.6 ± 10.6	14.6 ± 19.9
Lateral	-1.2 ± 4.4	4.1 ± 6.6*	3.4 ± 12.8	6.3 ± 14.8
Inferior	6.0 ± 5.5*	-3.7 ± 4.9*	-0.3 ± 8.8	2.0 ± 12.3
Total	16.3 ± 13.7	6.4 ± 18.5	0.6 ± 23.6	23.0 ± 25.5
End-systole				
Anterior	3.9 ± 10.4*	8.8 ± 8.7*	0.4 ± 6.9	13.0 ± 11.7
Lateral	-1.2 ± 2.3	0.5 ± 5.1	3.9 ± 10.4	3.2 ± 13.2
Inferior	0.3 ± 3.8	-5.7 ± 5.6*	-1.1 ± 6.7	-6.4 ± 12.0
Total	3.0 ± 8.1	3.5 ± 11.2	3.3 ± 16.5	9.8 ± 16.0

Mean ± standard deviation of signed regional volume differences (CMR – RT3DE).

* Denotes statistically significant under- or overestimation of regional volume (P < 0.05).

Table 5. Absolute right ventricular volume differences (%) per segment

Segment	Apical	Mid	Basal	Total
End-diastole				
Anterior	17.4 ± 10.4	14.1 ± 10.0	14.1 ± 12.4	45.6 ± 15.5
Lateral	5.5 ± 3.6	9.0 ± 5.5	12.0 ± 11.0	26.4 ± 12.4
Inferior	10.4 ± 9.2	7.4 ± 6.1	10.2 ± 6.8	27.9 ± 13.2
Total	33.2 ± 13.4	30.5 ± 13.8	36.3 ± 15.1	100
End-systole				
Anterior	10.0 ± 6.6	21.3 ± 10.3	12.9 ± 8.6	44.1 ± 12.8
Lateral	4.7 ± 3.0	7.1 ± 5.4	13.9 ± 9.2	25.7 ± 11.1
Inferior	6.1 ± 5.3	12.6 ± 7.7	11.6 ± 7.4	30.2 ± 8.5
Total	20.7 ± 8.6	40.9 ± 9.6	38.3 ± 10.2	100

Mean ± standard deviation of signed regional volume differences (CMR – RT3DE).

* Denotes statistically significant under- or overestimation of regional volume (P < 0.05).

DISCUSSION

In the current study we investigated the global and segmental RV volume differences between RT3DE and CMR imaging in patients with tetralogy of Fallot using software that facilitates side-by-side comparison. The differences found for RV volumes by RT3DE and CMR imaging were caused by several sources related to either the anatomical characteristics of the right ventricle or technological limitations of the used techniques. Firstly, the RV anterior segments were poorly visualized by RT3DE in most patients (Table 2). This is due to the retrosternal position of the RV anterior wall that is difficult to image from a modified apical four-chamber view. The anterior wall, including the RV outflow tract, could possibly be better visualized from a parasternal short-axis view, but including the apex in the dataset from that view is impossible in most instances. In children the subcostal view can be used to image the right ventricle, but in adults this is complicated because of abdominal subcutaneous tissue. The poor visualization of the RV anterior segments causes an important part of the intermodality discordance, namely

1. 46%. Lack of visualization of the anterior segments resulted generally in underestimation of
2. regional volumes by RT3DE. However, this underestimation was consistent in both phases, so
3. that no statistically significant bias was found in EF.

4. Secondly, definition of the correct short-axis plane containing the apex and pulmonary valve
5. using CMR imaging is difficult. The long-axis resolution in the short-axis datasets is inferior (7
6. to 10 mm) compared with the in-plane resolution (average 2 mm²). Moreover, the short-axis
7. datasets are planned from the atrioventricular groove down to the apex, while the pulmonary
8. valve often is in a plane more superior to the atrioventricular groove. Consequently, the true
9. length of the RV outflow tract may not be optimally imaged. To overcome the analysis related
10. problems by CMR imaging, the use of three-dimensional reconstruction software packages
11. for CMR images were tested. Sugeng et al⁹ compared RV volumes obtained by CMR imaging,
12. RT3DE, and computed tomography with true volumes from a RV phantom. They found that
13. using the method of disc summation resulted in an overestimation of 20% of the true RV vol-
14. umes, while the RV Function program adapted to CMR images, which is a three-dimensional
15. approach, resulted in the most accurate estimation of the true volume. The incorporation of
16. information from the long-axis view, in addition to the short-axis views used by the disc sum-
17. mation method, has been suggested to improve the delineation of the complex RV anatomy.¹⁶

18. Thirdly, there exist differences between RT3DE and CMR imaging in the visualization of tra-
19. beculae. In RT3DE, it is difficult to distinguish between the RV myocardium and the trabeculae,
20. because the inner border of the trabeculae responds more strongly to the ultrasound. As a
21. consequence, the endocardial contours are traced more inwards the RV cavity thereby exclud-
22. ing the trabeculae. CMR imaging provides images with clearer differentiation between the
23. myocardium and trabeculae, because it has a favourable signal-to-noise ratio. This results in a
24. sharply depicted endocardial contour where only the large trabeculae are visible and can be
25. excluded from the RV cavity. This discrepancy between exclusion of all trabeculae and part of
26. the RV cavity by RT3DE and exclusion of only a part of the trabeculae by CMR imaging contrib-
27. utes to the RV volume difference between the two imaging modalities in all segments.

28. In various studies, variables influencing the accuracy of left ventricular and RV volumes by
29. RT3DE have been investigated.¹⁷⁻¹⁹ In a phantom, Mor-Avi et al¹⁹ found minimal changes in
30. the position of the endocardial contours (1 mm) to result in significant differences in measured
31. left ventricular volumes (11%) and consequently, imply larger inter-observer variability. RT3DE-
32. derived RV volume calculations based on disc summation of latex models derived from excised
33. lamb hearts, were used to test the hypothesis that variables in RT3DE acquisition and off-line
34. analysis would alter RV volume measurements.¹⁸ Gain settings, size, and orientation of the cut
35. planes (either short-axis or long-axis) were found to affect the calculated RV volumes. Khoo et
36. al⁷ discussed the main culprits for the volume underestimation by RT3DE imaging compared
37. with CMR imaging in patients with congenital heart disease. They hypothesized the poor
38. endocardial border definition, limited size of the RT3DE imaging volume, and gain settings dur-
39. ing offline analysis to influence the calculated RV volumes. In the current study, we found the

visualization of the anterior segment being the main cause in regional RV volume differences, 1.
mostly due to difficulties in imaging the anterior segments from the modified apical transducer 2.
position. 3.

In addition, the software platforms that were used to calculate the RV volumes could pro- 4.
duce different volumes due to different tracing algorithms and available background models 5.
used to produce RV casts. The planes used to trace contours at the endocardial border for 6.
RT3DE images are an apical four-chamber view, a short-axis view and a coronal view, while for 7.
CMR images, only the short-axis orientation is used to trace contours. The analysis software 8.
used for RT3DE images is based on a semiautomated contour detection algorithm. This algo- 9.
rithm reconstructs a surface geometry from the dataset as a guide while searching for the true 10.
3-dimensional endocardial border along defined rays placed orthogonal to the vertices of the 11.
surface geometry. In CMR imaging volumes are reconstructed from 2-dimensional images. A 12.
uniform method for analysis, and more importantly, clear agreement on how to handle RT3DE 13.
drop-outs and trabeculae, is needed to reduce the intertechnique discordance. 14.

In summary, echocardiography has practical advantages above CMR imaging in everyday 15.
clinical practice. It is crucial to pay attention to correct visualization of the anterior wall for reli- 16.
able RV volume assessment. Also, it would be of great importance to establish guidelines on 17.
how to handle trabeculae, because their visualization on RT3DE and CMR images varies from 18.
patient to patient. Such guidelines would ensure more uniform methodology and result in less 19.
disparity between measurements performed by different operators in different hospitals. 20.

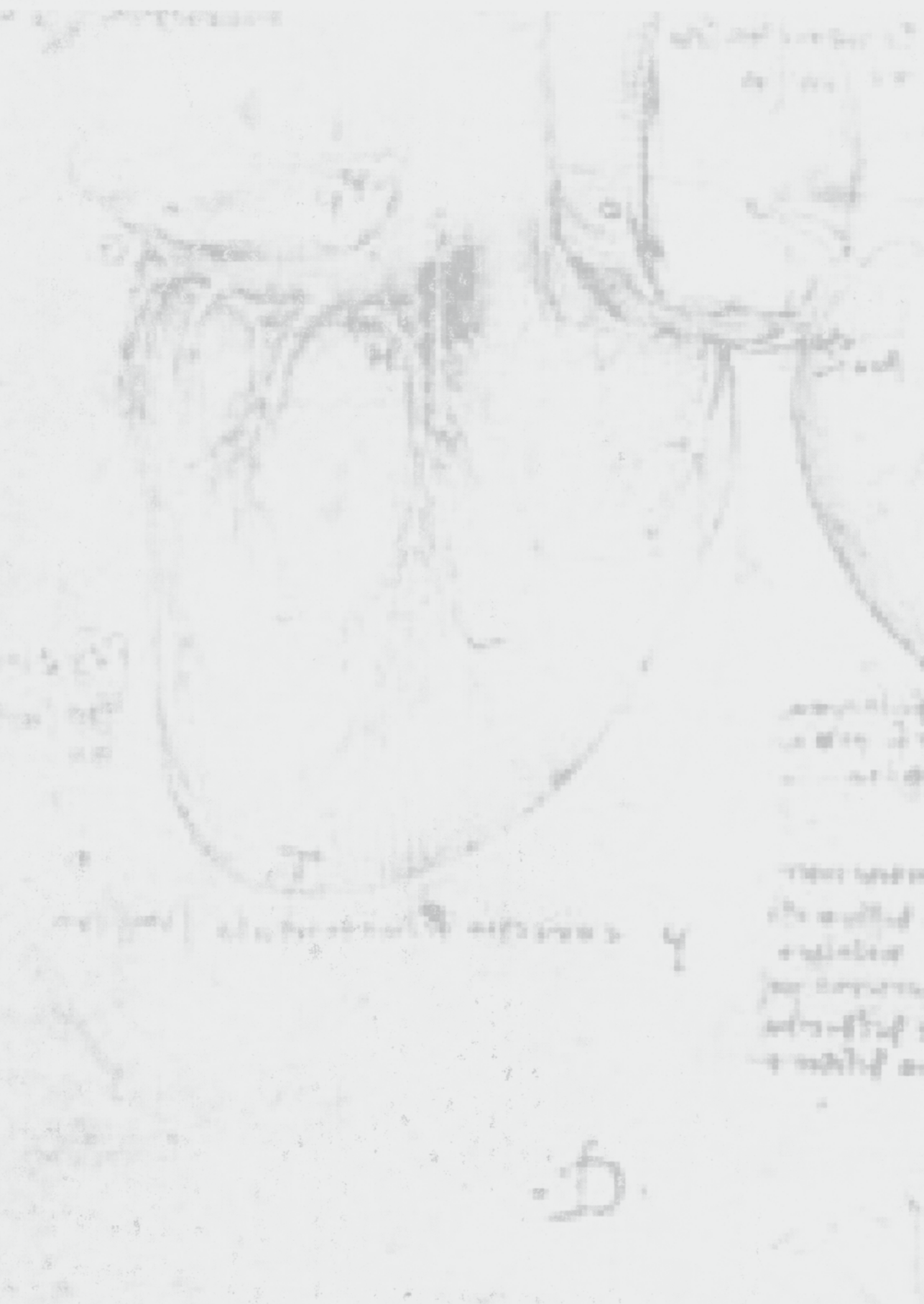
CONCLUSIONS 23.

The main sources of RV volume differences between RT3DE and CMR in patients with tetralogy 25.
of Fallot are the RV anterior region which is poorly visualized by RT3DE, the use of disc summa- 26.
tion by CMR imaging, and the visualization and management of trabeculae. The understanding 27.
of this intermodality discordance will help to implement RT3DE into clinical practice, assuming 28.
that consensus will be reached regarding a uniform methodology for contour delineation. 29.

30.
31.
32.
33.
34.
35.
36.
37.
38.
39.

1. Kantor PF, Redington AN. Pathophysiology and management of heart failure in repaired congenital heart disease. *Heart Fail Clin.* 2010;6:497-506, ix.
2. Knauth AL, Gauvreau K, Powell AJ, Landzberg MJ, Walsh EP, Lock JE, et al. Ventricular size and function assessed by cardiac MRI predict major adverse clinical outcomes late after tetralogy of Fallot repair. *Heart.* 2008;94:211-6.
3. Murphy JG, Gersh BJ, Mair DD, Fuster V, McGoon MD, Ilstrup DM, et al. Long-term outcome in patients undergoing surgical repair of tetralogy of Fallot. *N Engl J Med.* 1993;329:593-9.
4. Lai WW, Gauvreau K, Rivera ES, Saleeb S, Powell AJ, Geva T. Accuracy of guideline recommendations for two-dimensional quantification of the right ventricle by echocardiography. *Int J Cardiovasc Imaging.* 2008;24:691-8.
5. Jiang L, Levine RA, Weyman AE. Echocardiographic Assessment of Right Ventricular Volume and Function. *Echocardiography.* 1997;14:189-206.
6. van der Zwaan HB, Helbing WA, McGhie JS, Geleijnse ML, Luijnenburg SE, Roos-Hesselink JW, et al. Clinical Value of Real-Time Three-Dimensional Echocardiography for Right Ventricular Quantification in Congenital Heart Disease: Validation With Cardiac Magnetic Resonance Imaging. *J Am Soc Echocardiogr.* 2010;23:134-40.
7. Khoo NS, Young A, Occlshaw C, Cowan B, Zeng IS, Gentles TL. Assessments of right ventricular volume and function using three-dimensional echocardiography in older children and adults with congenital heart disease: comparison with cardiac magnetic resonance imaging. *J Am Soc Echocardiogr.* 2009;22:1279-88.
8. Leibundgut G, Rohner A, Grize L, Bernheim A, Kessel-Schaefer A, Bremerich J, et al. Dynamic assessment of right ventricular volumes and function by real-time three-dimensional echocardiography: a comparison study with magnetic resonance imaging in 100 adult patients. *J Am Soc Echocardiogr.* 2010;23:116-26.
9. Sugeng L, Mor-Avi V, Weinert L, Niel J, Ebner C, Steringer-Mascherbauer R, et al. Multimodality Comparison of Quantitative Volumetric Analysis of the Right Ventricle. *JACC Cardiovasc Imaging.* 2010;3:10-8.
10. Nesser HJ, Tkalec W, Patel AR, Masani ND, Niel J, Markt B, et al. Quantitation of right ventricular volumes and ejection fraction by three-dimensional echocardiography in patients: comparison with magnetic resonance imaging and radionuclide ventriculography. *Echocardiography.* 2006;23:666-80.
11. Soliman OI, Krenning BJ, Geleijnse ML, Nemes A, van Geuns RJ, Baks T, et al. A comparison between QLAB and TomTec full volume reconstruction for real time three-dimensional echocardiographic quantification of left ventricular volumes. *Echocardiography.* 2007;24:967-74.
12. Robbers-Visser D, Boersma E, Helbing WA. Normal biventricular function, volumes, and mass in children aged 8 to 17 years. *J Magn Reson Imaging.* 2009;29:552-9.
13. Nemes A, Leung KY, van Burken G, van Stralen M, Bosch JG, Soliman OI, et al. Side-by-side viewing of anatomically aligned left ventricular segments in three-dimensional stress echocardiography. *Echocardiography.* 2009;26:189-95.
14. Leung KYE, Van Stralen M, Nemes A, Voormolen MM, Van Burken G, Geleijnse ML, et al. Sparse Registration for Three-Dimensional Stress Echocardiography. *IEEE Trans Med Imag.* 2008;27:1568-79.
15. Klein SS, Graham TP, Jr., Lorenz CH. Noninvasive delineation of normal right ventricular contractile motion with magnetic resonance imaging myocardial tagging. *Ann Biomed Eng.* 1998;26:756-63.
16. Moroseos T, Mitsumori L, Kerwin WS, Sahn DJ, Helbing WA, Kilner PJ, et al. Comparison of Simpson's method and three-dimensional reconstruction for measurement of right ventricular volume in patients with complete or corrected transposition of the great arteries. *Am J Cardiol.* 2010;105:1603-9.
17. Chukwu EO, Barasch E, Mihalatos DG, Katz A, Lachmann J, Han J, et al. Relative importance of errors in left ventricular quantitation by two-dimensional echocardiography: insights from three-dimensional echocardiography and cardiac magnetic resonance imaging. *J Am Soc Echocardiogr.* 2008;21:990-7.

18. Hoch M, Vasilyev NV, Soriano B, Gauvreau K, Marx GR. Variables influencing the accuracy of right ventricular volume assessment by real-time 3-dimensional echocardiography: an in vitro validation study. *J Am Soc Echocardiogr.* 2007;20:456-61. 1.
19. Mor-Avi V, Jenkins C, Kuhl HP, Nesser HJ, Marwick T, Franke A, et al. Real-time 3-dimensional echocardiographic quantification of left ventricular volumes: multicenter study for validation with magnetic resonance imaging and investigation of sources of error. *JACC Cardiovasc Imaging.* 2008;1:413-23. 2.
- 3.
- 4.
- 5.
- 6.
- 7.
- 8.
- 9.
- 10.
- 11.
- 12.
- 13.
- 14.
- 15.
- 16.
- 17.
- 18.
- 19.
- 20.
- 21.
- 22.
- 23.
- 24.
- 25.
- 26.
- 27.
- 28.
- 29.
- 30.
- 31.
- 32.
- 33.
- 34.
- 35.
- 36.
- 37.
- 38.
- 39.



Chapter 9

Right ventricular visualization and quantification using contrast-enhanced real-time three-dimensional echocardiography

H.B. van der Zwaan
F. Gommans
M.L. Geleijnse
J.S. McGhie
F.J. Meijboom
A.P. van Dijk
J.W. Roos-Hesselink

Submitted for publication

ABSTRACT

Background. Real-time three-dimensional echocardiography (RT3DE) can be used for right ventricular (RV) assessment. Proper endocardial border definition is a prerequisite for reliable assessment. We investigated the potential incremental value of using contrast on RV visualization and RV volume measurements by RT3DE.

Methods. A total of 45 healthy participants (28 ± 8 years; 96% men) underwent non contrast-enhanced and contrast-enhanced RT3DE to evaluate global RV systolic function. A 17-segment RV model was used to grade the endocardial border definition as follows: 0, not visible; 1, barely visible; 2, visible; and 3, optimal. Three image-quality groups (good, fair, and uninterpretable) were identified. RV volumes and ejection fraction were obtained using semiautomated three-dimensional border detection software.

Results. The number of RV segments with optimal visualization of the endocardial border increased from 36% to 44% ($P < 0.001$) during contrast-enhanced RT3DE, compared with non contrast-enhanced RT3DE. The number of participants with a good-quality echocardiogram increased from 18% to 42% ($P = 0.009$). Non contrast-enhanced RT3DE provided significantly higher values of RV end-diastolic- and end-systolic volumes as compared with contrast-enhanced RT3DE (86 ± 13 ml versus 79 ± 11 ml and 41 ± 7 ml versus 36 ± 5 ml, $P < 0.001$). Using contrast did not significantly improve the intra-observer variability.

Conclusions. Even though contrast-enhanced RT3DE improved the RV endocardial contour definition of the RV anterior and lateral walls as compared with non contrast-enhanced RT3DE, the definition of the inferior wall and RV outflow tract appeared worse. Furthermore, smaller RV volumes were found using contrast-enhanced RT3DE. To make clinical application of contrast-enhanced RT3DE for RV assessment possible, the image quality of contrast-enhanced images needs to improve.

1.
2.
3.
4.
5.
6.
7.
8.
9.
10.
11.
12.
13.
14.
15.
16.
17.
18.
19.
20.
21.
22.
23.
24.
25.
26.
27.
28.
29.
30.
31.
32.
33.
34.
35.
36.
37.
38.
39.

1. INTRODUCTION

2.

3. Right ventricular (RV) function assessment is important in a variety of disease states such as
4. left sided heart failure, pulmonary hypertension and several congenital heart lesions.¹ Cardiac
5. magnetic resonance imaging is the reference technique for the assessment of RV volumes and
6. ejection fraction (EF).² In clinical practice, two-dimensional echocardiography is widely used
7. to obtain measurements on RV size and function, but it is operator dependent as it requires
8. multiple, successive acquisitions.³ Moreover, RV volumes and EF cannot easily be obtained
9. by two-dimensional echocardiography, since geometric assumptions are needed and often
10. inadequate.⁴ With the introduction of real-time three-dimensional echocardiography (RT3DE)
11. volumetric RV measurements can be acquired, since there is no longer a need of geometric
12. modeling. Furthermore, using RT3DE improved the accuracy and reproducibility of RV assess-
13. ment^{5, 6} and identified RV dysfunction accurately.⁷ Despite significant improvements in
14. ultrasound technology, endocardial border definition during echocardiography is still limited
15. in about 20% of routine echocardiographic examinations.^{8, 9} The right ventricle contains abun-
16. dant trabeculae and the definition of the endocardial border is most problematic in end-systole
17. as the trabeculae are densely packed in this phase of the cardiac cycle.

18. Left ventricular quantification by RT3DE using echo contrast resulted in a more accurate
19. assessment of left ventricular function as well as lower inter- and intra-observer variability
20. compared with non contrast-enhanced RT3DE.⁹⁻¹¹ Using echo contrast combined with RT3DE
21. to improve the endocardial border visualization of the RV has not been investigated so far. Our
22. aim was to study the potential incremental value of using echo contrast on RV endocardial
23. border visualization, RV volume measurements, and variability using RT3DE.

24.

25.

26. METHODS

27.

28. Study population

29. A total of 45 healthy participants in sinus rhythm were included, who were employees of the
30. university or the hospital in Nijmegen (n = 40) or Rotterdam (n = 5). All participants underwent
31. non contrast-enhanced, and afterwards, contrast-enhanced full-volume RT3DE examinations.
32. Participants were enrolled consecutively and not selected based on image quality. Participants
33. were eligible for inclusion in the study if they had no medical history or current symptoms
34. suggestive of cardiovascular disease, including hypertension or a systemic illness with a
35. potential cardiovascular component such as diabetes or thyroid disease. Participants taking
36. any cardiovascular medications were excluded from the study. In all included participants heart
37. rate was measured and they underwent physical examinations and a routine two-dimensional
38. echocardiogram to exclude cardiac abnormalities.

39.

The medical ethical committee approved the study and written informed consent was obtained from all participants.

Echocardiographic acquisition

RT3DE harmonic imaging was performed using the iE33 ultrasound system (Philips Medical Systems, Best, the Netherlands) equipped with an X3-1 matrix array transducer with the patient in the left lateral decubitus position. A full-volume scan from four to seven R-wave gated sub-volumes during a single end-expiratory breath-hold was acquired from a (modified) apical four-chamber position. The depth and angle of the ultrasound sector were adjusted to a minimal level still encompassing the right ventricle. Each image was optimized for endocardial border visualization by modifying time gain and compression and then the overall gain was slightly increased before the acquisition. After non contrast-enhanced image acquisition, imaging was repeated with intravenous infusion of SonoVue contrast agent (Bracco, Milan, Italy). SonoVue was prepared according to the manufacturers' recommendation by mixing with 5 ml saline. A bolus injection of 0.8 ml was slowly injected in a peripheral vein and flushed with saline. Imaging was performed using the machines' integrated contrast preset function in harmonic mode at a low mechanical index (0.24), and care was taken to record the images at a phase when the contrast agent flow was relatively stable with absent or minimal attenuation close to the septum.

The mean volume rate was 15 ± 5 frames per cardiac cycle (range 10 – 33) for non contrast-enhanced images and 12 ± 3 frames per cardiac cycle (range 9 - 20) for contrast-enhanced images. The datasets were digitally exported to a QLAB server (Philips Medical Systems, Best, The Netherlands) and a TomTec server (TomTec Imaging Systems, Unterschleissheim, Germany) connected to a terminal workstation for further analyses.

Echocardiographic analysis

Analyses of the digital RV RT3DE data sets were performed on a QLAB workstation using the multi-plane reconstruction viewer (3DQ-Advanced version 8.0; Philips Medical Systems) and the four-dimensional RV Function program version 1.2.

Endocardial border definition

Qualitative assessment of the endocardial border was performed in both non contrast-enhanced and contrast-enhanced images. A 17-segment model was used¹² (Figure 1). The endocardial border was judged by displaying three RV short-axis views (at basal, medial and apical level), a modified four-chamber view and a coronal view derived from the RT3DE datasets. Two experienced observers (H.B.Z. and J.S.M.) analyzed the endocardial border definition of the aforementioned image planes in a dynamic format and on an ordinal scale: 0, not visible; 1, barely visible (myocardial boundaries undefined); 2, visible (endocardial boundaries defined) and 3, optimal (excellent delineation of the endocardial border).¹² A global endocardial visualization score was calculated as the sum of each RV segment's score.

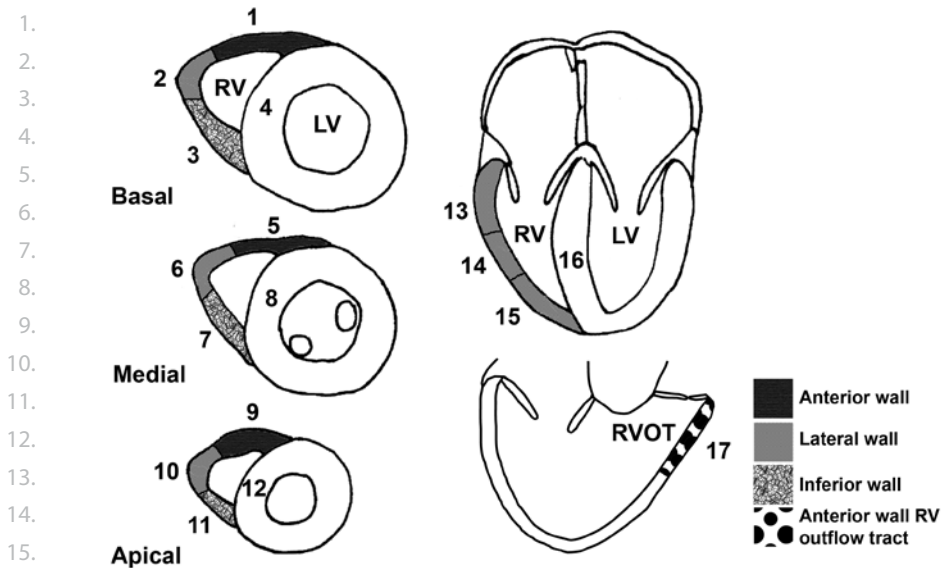


Figure 1 A 17-segment model of the right ventricle showing the parasternal short-axis images recorded at 3 equivalent levels (basal, medial, apical), the apical four-chamber view and the coronal view. Right ventricular segments, short-axis view: 1, anterobasal; 2, laterobasal; 3, inferobasal; 5, anteromedial; 6, lateromedial; 7, inferomedial; 9, anteroapical; 10, lateroapical; 11, inferoapical. Four-chamber view: 13, four-chamber laterobasal; 14, lateromedial; 15, lateroapical. Coronal view: 17, right ventricular outflow tract. Interventricular septum: 4, basal septum; 8, medial septum; 12, apical septum and 16, four-chamber septum.

On the basis of the global score, 3 image quality groups were defined: good (37-51), fair (22-37) and uninterpretable (≤ 21). Uninterpretable echocardiograms were considered non-diagnostic, and further analysis of RV volumes and EF was deemed not feasible.

Right ventricular volumes and ejection fraction analysis

With the RV Function program, three-dimensional semiautomated border detection of RV volumes was performed. The program uses a physics-based modeling algorithm without assumptions regarding RV geometry. The working of the RV Function program is reported in detail elsewhere.⁶ In short, the end-diastolic and end-systolic phases are identified. Endocardial border contours are drawn onto still frames of the apical four-chamber view, short-axis view, and coronal view in both phases (Figure 2). Once these contours have been traced, the software automatically delineates the RV endocardial border from the end-diastolic and end-systolic phases and by sequential analysis creates a RV mathematic dynamic three-dimensional endocardial surface that represents the changes in the RV cavity over the cardiac cycle. From this three-dimensional endocardial surface, global RV volumes and EF are calculated. The non contrast-enhanced images were analyzed blindly and at least one month apart from the contrast-enhanced images to prevent influencing of the consecutive measurements.

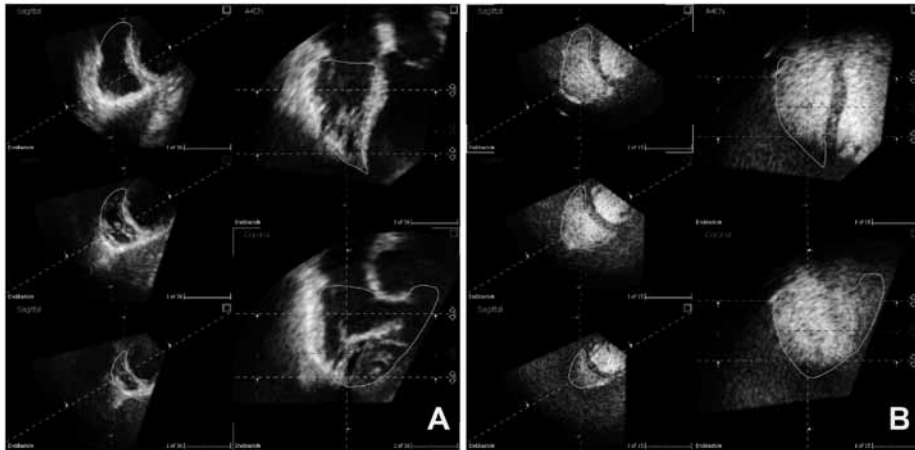


Figure 2 Example of a fair-quality echocardiogram by non contrast-enhanced RT3DE (A), and contrast-enhanced RT3DE (B) in a 38 years-old female. Display from the four-dimensional RV function analysis program showing the final stage of contour detection in which manual correction of the contours can be applied in any cross-section or phase of the cardiac cycle.

Statistical analysis

Statistical analysis was performed using SPSS version 15.0 (SPSS, Inc, Chicago, Illinois). Categorical data are summarized as numbers and percentages. Continuous data are presented as mean \pm SD.

The agreement between non-contrast enhanced- and contrast-enhanced RT3DE measurements was evaluated using Bland-Altman analysis by calculating the bias (mean difference) and the 95% limits of agreement (two SDs around the mean difference).¹³ The paired Student's *t* test was used to analyze the significance of the differences in RV volumes and EF and the variability of the measurements between non contrast-enhanced data versus contrast-enhanced data.

The reproducibility of the non contrast-enhanced and contrast-enhanced measurements was evaluated in 16 randomly selected participants. We expressed the intra-observer variability by the coefficient of variation, which is defined as the standard deviation of the difference between the two readings divided by their mean value, times 100. All statistical tests were two-sided, and a *P*-value <0.05 was considered statistically significant.

RESULTS

All 45 participants completed the imaging protocol without any adverse events occurring during contrast infusion. Because of insufficient image quality of the non contrast-enhanced and/or contrast enhanced RT3DE (endocardial contour definition score ≤ 21), 13 participants were excluded from RV volumes and EF analysis. The mean age of the participants was 28 ± 8 years;

1. 96% was male. The mean heart rate was 65 ± 13 beats per minute. The mean body surface area
2. was 2.0 ± 0.2 m². The total infusion dose of contrast was on average 0.8 ml.
- 3.
4. Right ventricular endocardial border definition
5. During non contrast-enhanced RT3DE, from the total number of 765 RV segments, the endo-
6. cardial border was invisible in 201 (26%) and barely visible in 140 (18%). In 279 (36%) the endo-
7. cardial border was visualized optimally (Table 1). The mean global endocardial visualization
8. score was 28 ± 11 . A total of 8 (18%) patients had a good quality echocardiogram, whereas 24
9. (53%) and 13 (29%) had a fair quality or uninterpretable echocardiogram, respectively.

Table 1. Right ventricular endocardial border definition: non contrast-enhanced versus contrast-enhanced real-time three-dimensional echocardiography

	Non contrast-enhanced images	Contrast-enhanced images	P-value
Overall segments (n = 765)			<0.001
Invisible	201 (26%)	166 (22%)	
Barely visible	140 (18%)	120 (16%)	
Visible	145 (19%)	143 (19%)	
Optimal	279 (36%)	336 (44%)	
Anterior segments (n = 135)			<0.001
Invisible	102 (76%)	63 (47%)	
Barely visible	18 (13%)	23 (17%)	
Visible	11 (8%)	24 (18%)	
Optimal	4 (3%)	25 (19%)	
Outflow tract (n = 45)			0.013
Invisible	33 (73%)	44 (98%)	
Barely visible	9 (20%)	1 (2%)	
Visible	3 (7%)	0 (0%)	
Optimal	0 (0%)	0 (0%)	
Lateral segments (n = 270)			<0.001
Invisible	57 (21%)	44 (16%)	
Barely visible	64 (24%)	49 (18%)	
Visible	77 (29%)	51 (19%)	
Optimal	72 (27%)	126 (47%)	
Inferior segments (n = 135)			0.004
Invisible	5 (4%)	11 (8%)	
Barely visible	27 (20%)	28 (21%)	
Visible	18 (13%)	31 (23%)	
Optimal	85 (63%)	65 (48%)	
Septal segments (n = 180)			0.37
Invisible	4 (2%)	4 (2%)	
Barely visible	22 (12%)	19 (11%)	
Visible	36 (20%)	37 (21%)	
Optimal	118 (66%)	120 (67%)	

37. The quality of the endocardial border visibility of the real-time three-dimensional echo datasets
38. judged in a dynamic format: 0, not visible; 1, barely visible (myocardial boundaries undefined); 2, visible
39. (endocardial boundaries defined) and 3, optimal (excellent delineation of the endocardial border).

During contrast-enhanced RT3DE, optimal visualization of the border was possible in 336 (44%) segments ($P < 0.001$ versus non contrast-enhanced RT3DE) (Table 1). The RV endocardial border definition significantly improved in the anterior and lateral wall segments. As compared with non contrast-enhanced RT3DE, the mean global endocardial visualization score improved to 31 ± 13 ($P 0.009$). A total of 19 (42%) patients had a good quality echocardiogram, whereas 15 (33%) had a fair quality and 11 (24%) an uninterpretable echocardiogram. An example of non contrast-enhanced RT3DE and contrast-enhanced RT3DE in the same participant is depicted in Figure 2.

Right ventricular volumes and ejection fraction

Non contrast-enhanced RT3DE provided significantly higher RV end-diastolic volumes compared with contrast-enhanced RT3DE (86 ± 13 ml versus 79 ± 11 ml, $P < 0.001$) (Table 2, Figure 3). The RV end-systolic volumes by non contrast-enhanced RT3DE were also higher (41 ± 7 ml versus 36 ± 5 ml, $P < 0.001$). Accordingly, the values of RV EF were not different between the two techniques ($53 \pm 4\%$ versus $54 \pm 4\%$, $P = 0.091$).

Table 2. Right ventricular volumetric measurements: non contrast-enhanced versus contrast-enhanced real-time three-dimensional echocardiography

	Non contrast-enhanced	Contrast-enhanced	P-value*
End-diastolic volume (ml)	168 ± 30	154 ± 24	<0.001
End-systolic volume (ml)	79 ± 17	71 ± 12	<0.001
Stroke volume (ml)	88 ± 15	84 ± 15	0.072
Ejection fraction (%)	53 ± 4	54 ± 4	0.091
Normalized to body surface area			
End-diastolic volume (ml / m ²)	86 ± 13	79 ± 11	<0.001
End-systolic volume (ml / m ²)	41 ± 7	36 ± 5	<0.001
Stroke volume (ml / m ²)	45 ± 7	43 ± 7	0.083

Data are expressed as mean \pm SD. *P-value derived from a paired Student's *t* test.

Bland-Altman analysis for non contrast-enhanced versus contrast-enhanced RV volumes and EF by RT3DE are displayed in Figure 4. Bland-Altman analysis showed mean differences of 19 ml for end-diastolic volume, 11 ml for end-systolic volume, and -1% for EF with 95% limits of agreement of ± 23 ml for end-diastolic volume, ± 12 ml for end-systolic volume, and $\pm 4\%$ for EF (Figure 4).

Variability measurements

The intra-observer variability measurements of the non contrast versus contrast-enhanced RT3DE measurements are displayed in Table 3. The use of contrast resulted in lower variability measurements for end-diastolic volume measurements (19 ± 13 versus 11 ± 10 , $P 0.039$). Using contrast showed no effect on the variability of the other measurements.

1.
2.
3.
4.
5.
6.
7.
8.
9.
10.
11.
12.
13.
14.
15.
16.
17.
18.
19.
20.
21.
22.
23.
24.
25.
26.
27.
28.
29.
30.
31.
32.
33.
34.
35.
36.
37.
38.
39.

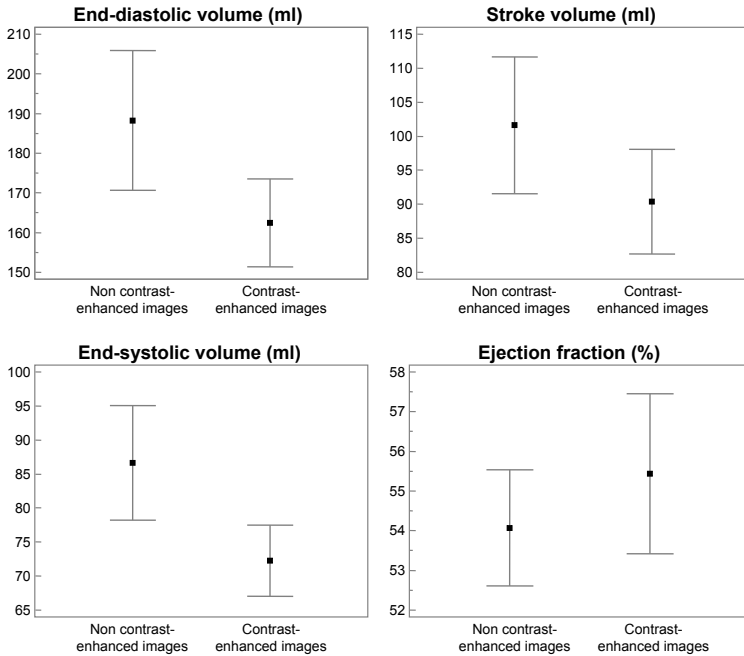


Figure 3 RV end-diastolic volume (top left), end-systolic volume (bottom left), stroke volume (top right), and ejection fraction (bottom right) by non contrast-enhanced versus contrast-enhanced real-time 3-dimensional echocardiography.

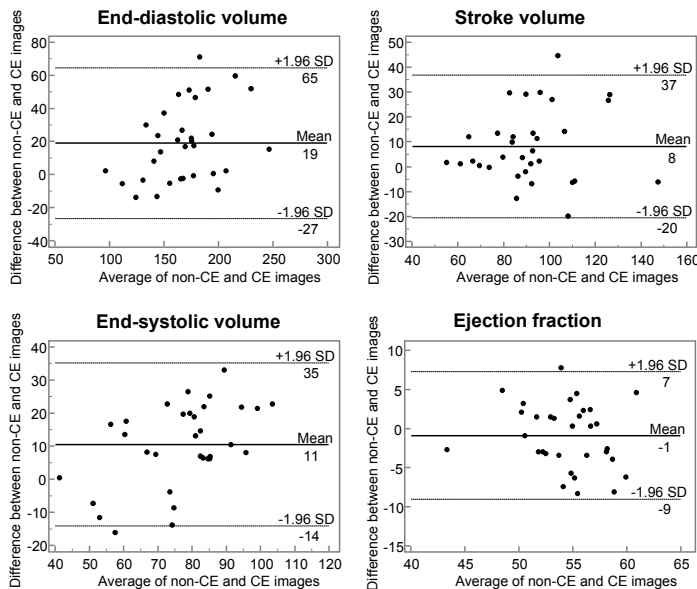


Figure 4 Bland-Altman analysis of non contrast-enhanced (non-CE) versus contrast-enhanced (CE) RV end-diastolic volume (top left), end-systolic volume (bottom left), stroke volume (top right), and ejection fraction (bottom right) by real-time 3-dimensional echocardiography.

Table 3. Intra-observer variability measurements: non contrast-enhanced versus contrast-enhanced real-time three-dimensional echocardiography

	Non contrast- enhanced		Contrast- enhanced	
	Absolute mean difference	Coefficient of variation	Absolute mean difference	Coefficient of variation
End-diastolic volume (ml)	19 ± 13	7	11 ± 10	6
End-systolic volume (ml)	9 ± 6	7	5 ± 4	5
Stroke volume (ml)	12 ± 9	10	11 ± 8	10
Ejection fraction (%)	3 ± 3	5	4 ± 2	4

Coefficients of variation represent the SD of the difference between two measurements divided by the mean of the measurements, expressed as a percentage.

DISCUSSION

The current study shows that, among unselected healthy participants, contrast-enhanced RT3DE improved the endocardial contour definition of the right ventricle, especially of the RV anterior and lateral walls, compared with non contrast-enhanced RT3DE. On the other hand, the RV outflow tract and inferior wall appeared worse compared with non contrast-enhanced RT3DE. Furthermore, smaller RV volumes were found when using contrast-enhanced RT3DE compared with non contrast-enhanced RT3DE. The intra-observer variability improved for end-diastolic volume measurements based on contrast-enhanced RT3DE compared with non contrast-enhanced RT3DE, but the variability was not different for the other variability measurements.

Proper endocardial contour delineation is essential for accurate and reproducible RV measurements. A good signal-to-noise ratio adds in delineating endocardial border contours. One of the big advantages of cardiac magnetic resonance imaging, the reference technique for RV volumes and EF assessment, is the favorable signal-to-noise ratio. Using contrast to enhance RV cavity opacification, will add to the signal-to-noise ratio in echocardiographic images. In the harmonic setting of an ultrasound machine, the machine “filters” out all returning fundamental frequencies from the tissue and by that the microbubble harmonic signal is enhanced. Therefore, second harmonic detection systems improve the signal-to-noise ratio of contrast images and contrast intensity. In addition, harmonic imaging helps to reduce artifacts and shadowing effects and enhances detection of contrast in areas of low microbubble concentration.⁹

The anterior wall and the RV outflow tract are the most challenging parts of the right ventricle to image using echocardiography. The retrosternal position of these RV walls is responsible for the suboptimal visualization by echocardiography besides their location in the far field of the ultrasound transducer when imaging from a modified or RV focused four-chamber view. As a consequence, the delineation of the endocardial contours is difficult in the anterior wall and RV outflow tract. In the current study we found a clear improvement in the endocardial contour definition of the anterior wall, but the definition of the RV outflow tract was poorer. These

1. regional differences in endocardial border visualization may be attributed to their anatomical
2. position, fiber orientation, and beam interception.

3. The RV volumes by contrast-enhanced RT3DE were found to be smaller than the RV vol-
4. umes by non contrast-enhanced RT3DE. This will result in a larger bias compared with cardiac
5. magnetic resonance imaging-derived RV volumes, since the reported RV volumes found by
6. cardiac magnetic resonance imaging were larger than for RT3DE.^{6, 14} Initially, this may look
7. paradoxical, because it would be expected that using contrast would lead to opacification of
8. the intertrabecular spaces, resulting in larger RV volumes. The following factors made their
9. contribution to our findings and should be considered when using contrast-enhanced RT3DE.

10. Firstly, the definition of the tricuspid annular plane is difficult in contrast-enhanced images,
11. because not only the RV lumen is opacified with contrast, but also the lumen of the right atrium.
12. Therefore, it is not as straightforward as in non contrast-enhanced images to define the level
13. of the tricuspid valve and this may lead to uncertainty during RV analysis. Secondly, specific,
14. integrated imaging functions are used to improve the detection of ultrasound contrast agents
15. such as power modulation, which is integrated in preset functions on the ultrasound machine.
16. In power modulation, a multipulse technique is used whereby the acoustic amplitude of the
17. transmitted pulses is changed. Although this method improves contrast imaging quality, this
18. function nearly halves the frame rate.^{10, 15} Because the RT3DE volume rates are already lower as
19. compared with conventional two-dimensional echocardiography, this is an undesirable effect.
20. The datasets we included only had 12 ± 3 frames per cardiac cycle and this has affected the cal-
21. culated RV volumes. Thirdly, in most datasets, the RV outflow tract was obliterated by a shadow.
22. Most probably this was caused by attenuation from contrast within the left ventricular cavity.
23. Using agitated saline could possibly improve this issue, because this contrast agent does not
24. pass the pulmonary circulation because of the large sized microbubbles that live shortly and
25. rapidly diffuse. Furthermore, no distinction of the RV inflow portion, the left ventricular outflow
26. portion, and the right ventricular outflow portion could be made, while this is a key landmark
27. in the analysis of the RT3DE datasets. Additionally, by leaving the integrated contrast preset
28. functions and by adjusting resolution and penetration, a better definition of the RV outflow
29. tract may be achieved.

30. The feasibility that we reported in this study, 71%, is lower than what we published before
31. in patients with a variety of congenital heart defects.⁶ This may be caused by the following
32. factors. Most likely the poorer feasibility in healthy controls can be attributed to the fact that
33. echocardiography of a normal right ventricle is limited by the retrosternal position of this heart
34. chamber. The normal-sized right ventricle lies mainly directly behind the sternum. In contrast,
35. in the diseased right ventricle, which in most cases is dilated, only a small area of the right
36. ventricle is behind the sternum, i.e. the RV anterior wall. In addition, most of the healthy partici-
37. pants were included in a hospital different from the patients with congenital heart defects of
38. our previous study. Various levels of experience of the sonographers may have influenced the
39. image quality of the RT3DE datasets.

Regarding the clinical applications of contrast ultrasound imaging for RV assessment, the American Society of Echocardiography stated that commercially available contrast agents have been used successfully and safely to show various abnormalities of RV morphology.¹⁶ Furthermore, they pointed out that contrast agents can be helpful in the endocardial border definition of geometrically unusual chambers, such as repaired tetralogy of Fallot or systemic right ventricles, thereby aiding in function assessment. An example of the latter application is provided by Van den Bosch et al¹² who investigated 10 patients with tetralogy of Fallot and 10 patients with systemic right ventricles by two-dimensional echocardiography. They concluded contrast-enhanced echocardiography to be superior to conventional two-dimensional echocardiography for RV endocardial border definition and the potential for a more accurate assessment of RV dimensions and function.

Clinical perspectives

RV imaging using echo contrast agents requires a slow injection of the contrast media in order to avoid attenuation artifacts, and also requires optimizing the transducer position for visualizing the RV.¹⁷ Furthermore, specific preset functions on the ultrasound machine should be applied and even modified to improve the endocardial border definition in all RV segments. At this moment, the image quality of contrast-enhanced RT3DE datasets prevents this technique to be applied in clinical practice. With advances in the RT3DE ultrasound system, it may be expected that contrast-enhanced RT3DE can be used to visualize cardiac morphology and to enhance RV volume and EF assessment. Another future development may be the fusion of various datasets to improve image resolution. Because non contrast-enhanced and contrast enhanced datasets appear to be complementary to each other, fusion of these datasets may result in the best possible definition of RV images by RT3DE.¹⁸

Study limitations

The study participants did not undergo cardiac magnetic resonance imaging, the reference technique for RV volume and EF assessment.¹⁹ Therefore, data on the accuracy of contrast-enhanced RT3DE could not be provided. However, various studies have been published on the agreement of RV volumes and EF by RT3DE versus cardiac magnetic resonance imaging.^{6, 14, 20-22} RV volumes obtained by RT3DE were found to be smaller compared with the reference technique. In the current study, our aim was not to study accuracy, but to establish the additional value on RV border delineation and to find possible differences in RV volumes using contrast-enhanced versus non contract-enhanced RT3DE.

1. CONCLUSIONS

2.

3. Even though contrast-enhanced RT3DE improved the RV endocardial contour definition of the
4. RV anterior and lateral walls as compared with non contrast-enhanced RT3DE, the definition
5. of the inferior wall and RV outflow tract appeared worse. Furthermore, smaller RV volumes
6. were found using contrast-enhanced RT3DE. To make clinical application of contrast-enhanced
7. RT3DE for RV assessment possible, the image quality of contrast-enhanced images needs to
8. improve.

9.

10.

11.

12.

13.

14.

15.

16.

17.

18.

19.

20.

21.

22.

23.

24.

25.

26.

27.

28.

29.

30.

31.

32.

33.

34.

35.

36.

37.

38.

39.

1. Haddad F, Doyle R, Murphy DJ, Hunt SA. Right ventricular function in cardiovascular disease, part II: pathophysiology, clinical importance, and management of right ventricular failure. *Circulation*. 2008;117:1717-31. 1.
2. Kilner PJ, Geva T, Kaemmerer H, Trindade PT, Schwitter J, Webb GD. Recommendations for cardiovascular magnetic resonance in adults with congenital heart disease from the respective working groups of the European Society of Cardiology. *Eur Heart J*. 2010;31:794-805. 2.
3. Rudski LG, Lai WW, Afilalo J, Hua L, Handschumacher MD, Chandrasekaran K, et al. Guidelines for the echocardiographic assessment of the right heart in adults: a report from the American Society of Echocardiography endorsed by the European Association of Echocardiography, a registered branch of the European Society of Cardiology, and the Canadian Society of Echocardiography. *J Am Soc Echocardiogr*. 2010;23:685-713; quiz 86-8. 3.
4. Jiang L, Levine RA, Weyman AE. Echocardiographic Assessment of Right Ventricular Volume and Function. *Echocardiography*. 1997;14:189-206. 4.
5. Jenkins C, Chan J, Bricknell K, Strudwick M, Marwick TH. Reproducibility of right ventricular volumes and ejection fraction using real-time three-dimensional echocardiography: comparison with cardiac MRI. *Chest*. 2007;131:1844-51. 5.
6. van der Zwaan HB, Helbing WA, McGhie JS, Geleijnse ML, Luijnenburg SE, Roos-Hesselink JW, et al. Clinical Value of Real-Time Three-Dimensional Echocardiography for Right Ventricular Quantification in Congenital Heart Disease: Validation With Cardiac Magnetic Resonance Imaging. *J Am Soc Echocardiogr*. 2010;23:134-40. 6.
7. van der Zwaan HB, Helbing WA, Boersma E, Geleijnse ML, McGhie JS, Soliman OI, et al. Usefulness of real-time three-dimensional echocardiography to identify right ventricular dysfunction in patients with congenital heart disease. *Am J Cardiol*. 2010;106:843-50. 7.
8. Mor-Avi V, Sugeng L, Lindner JR. Imaging the forgotten chamber: is the devil in the boundary? *J Am Soc Echocardiogr*. 2010;23:141-3. 8.
9. Soliman OI, De Jong N, Van Der Zwaan HB, Galema TW, Vletter WB, Van Dalen BM, et al. Contrast echocardiography: mechanism of action, safety and clinical applications. *Minerva Cardioangiol*. 2010;58:343-55. 9.
10. Krenning BJ, Kirschbaum SW, Soliman OI, Nemes A, van Geuns RJ, Vletter WB, et al. Comparison of contrast agent-enhanced versus non-contrast agent-enhanced real-time three-dimensional echocardiography for analysis of left ventricular systolic function. *Am J Cardiol*. 2007;100:1485-9. 10.
11. Nemes A, Geleijnse ML, Krenning BJ, Soliman OI, Anwar AM, Vletter WB, et al. Usefulness of ultrasound contrast agent to improve image quality during real-time three-dimensional stress echocardiography. *Am J Cardiol*. 2007;99:275-8. 11.
12. van den Bosch AE, Meijboom FJ, McGhie JS, Roos-Hesselink JW, Ten Cate FJ, Roelandt JR. Enhanced visualisation of the right ventricle by contrast echocardiography in congenital heart disease. *Eur J Echocardiogr*. 2004;5:104-10. 12.
13. Bland JM, Altman DG. Statistical methods for assessing agreement between two methods of clinical measurement. *Lancet*. 1986;1:307-10. 13.
14. Shimada YJ, Shiota M, Siegel RJ, Shiota T. Accuracy of right ventricular volumes and function determined by three-dimensional echocardiography in comparison with magnetic resonance imaging: a meta-analysis study. *J Am Soc Echocardiogr*. 2010;23:943-53. 14.
15. Krenning BJ, Vletter WB, Nemes A, Geleijnse ML, Roelandt JR. Real-time 3-dimensional contrast stress echocardiography: a bridge too far? *J Am Soc Echocardiogr*. 2007;20:1224-5. 15.
16. Mulvagh SL, Rakowski H, Vannan MA, Abdelmoneim SS, Becher H, Bierig SM, et al. American Society of Echocardiography Consensus Statement on the Clinical Applications of Ultrasonic Contrast Agents in Echocardiography. *J Am Soc Echocardiogr*. 2008;21:1179-201; quiz 281. 16.
17. Mangion JR. Right ventricular imaging by two-dimensional and three-dimensional echocardiography. *Curr Opin Cardiol*. 2010;22:423-9. 17.

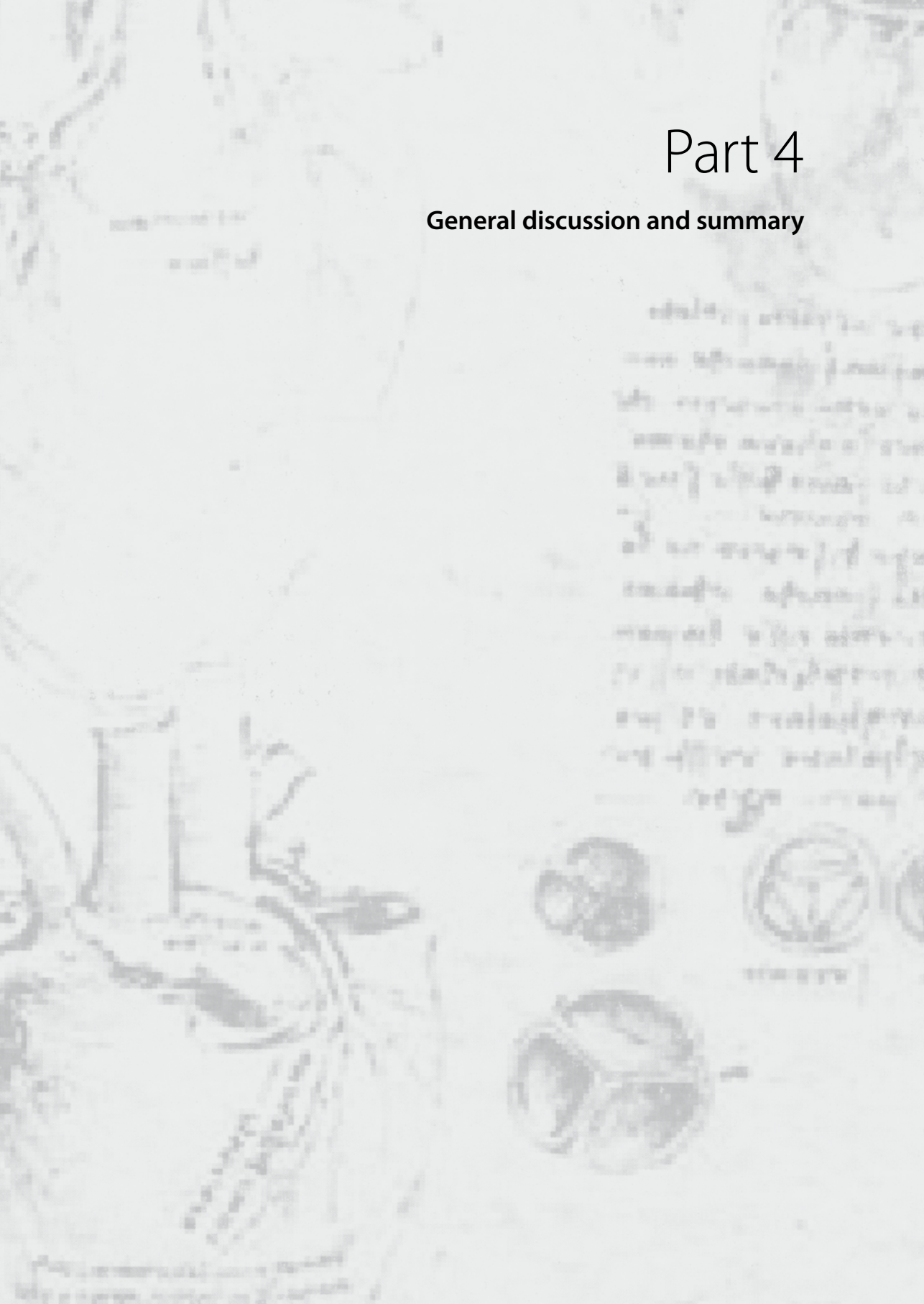
1.
2.
3.
4.
5.
6.
7.
8.
9.
10.
11.
12.
13.
14.
15.
16.
17.
18.
19.
20.
21.
22.
23.
24.
25.
26.
27.
28.
29.
30.
31.
32.
33.
34.
35.
36.
37.
38.
39.

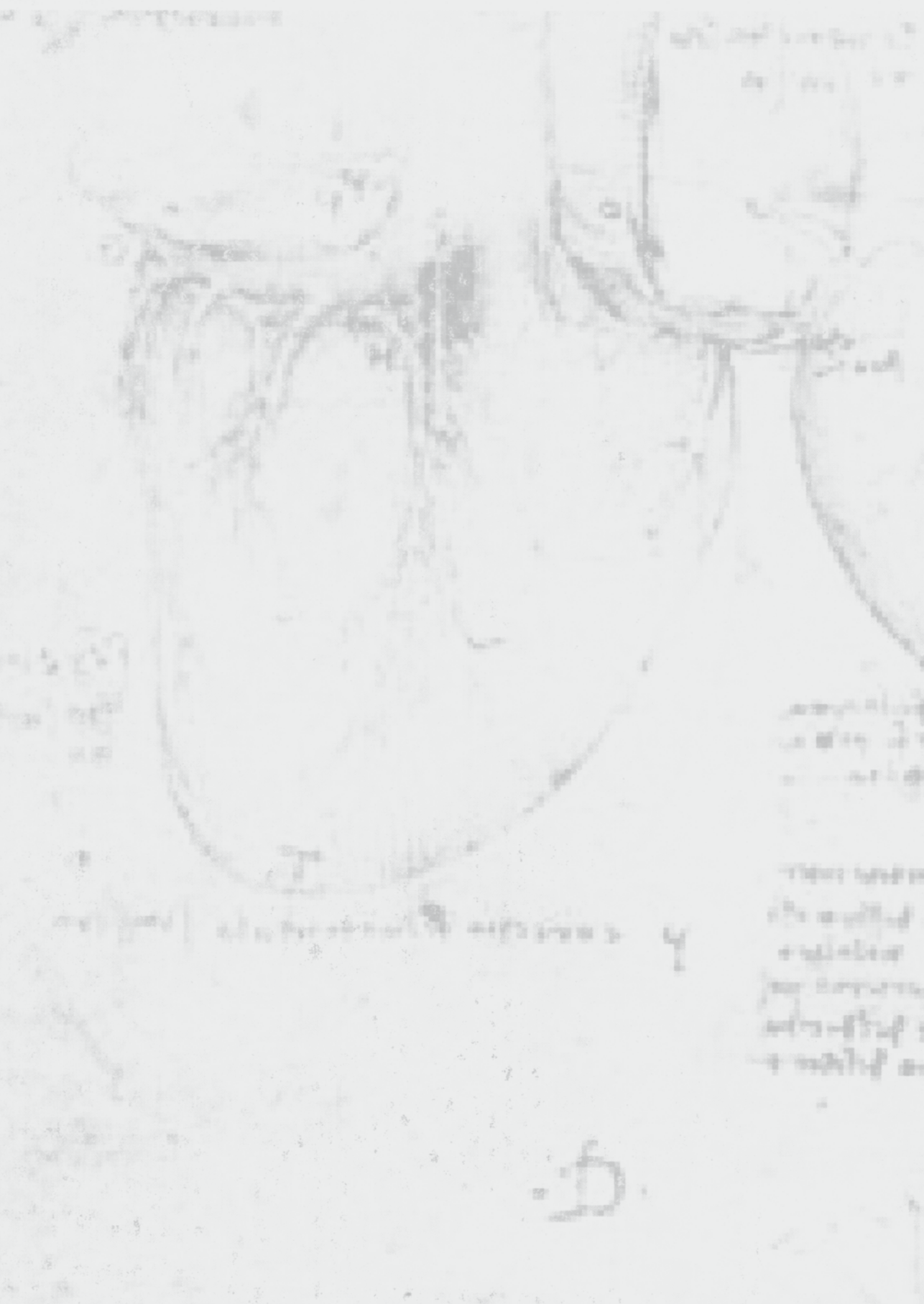
1. 18. Szmigielski C, Rajpoot K, Grau V, Myerson SG, Holloway C, Noble JA, et al. Real-time 3D fusion echocardiography. *JACC Cardiovasc Imaging*. 2010;3:682-90.
2. 19. Endorsed by the Association for European Paediatric C, Authors/Task Force M, Baumgartner H, Bonhoeffer P, De Groot NM, de Haan F, et al. ESC Guidelines for the management of grown-up congenital heart disease (new version 2010): The Task Force on the Management of Grown-up Congenital Heart Disease of the European Society of Cardiology (ESC). *Eur Heart J*. 2010.
- 3.
- 4.
5. 20. Grewal J, Majdalany D, Syed I, Pellikka P, Warnes CA. Three-dimensional echocardiographic assessment of right ventricular volume and function in adult patients with congenital heart disease: comparison with magnetic resonance imaging. *J Am Soc Echocardiogr*. 2010;23:127-33.
- 6.
7. 21. Iriart X, Montaudon M, Lafitte S, Chabaneix J, Reant P, Balbach T, et al. Right ventricle three-dimensional echography in corrected tetralogy of fallot: accuracy and variability. *Eur J Echocardiogr*. 2009;10:784-92.
- 8.
- 9.
10. 22. Khoo NS, Young A, Occlshaw C, Cowan B, Zeng IS, Gentles TL. Assessments of right ventricular volume and function using three-dimensional echocardiography in older children and adults with congenital heart disease: comparison with cardiac magnetic resonance imaging. *J Am Soc Echocardiogr*. 2009;22:1279-88.
- 11.
- 12.
- 13.
- 14.
- 15.
- 16.
- 17.
- 18.
- 19.
- 20.
- 21.
- 22.
- 23.
- 24.
- 25.
- 26.
- 27.
- 28.
- 29.
- 30.
- 31.
- 32.
- 33.
- 34.
- 35.
- 36.
- 37.
- 38.
- 39.



Part 4

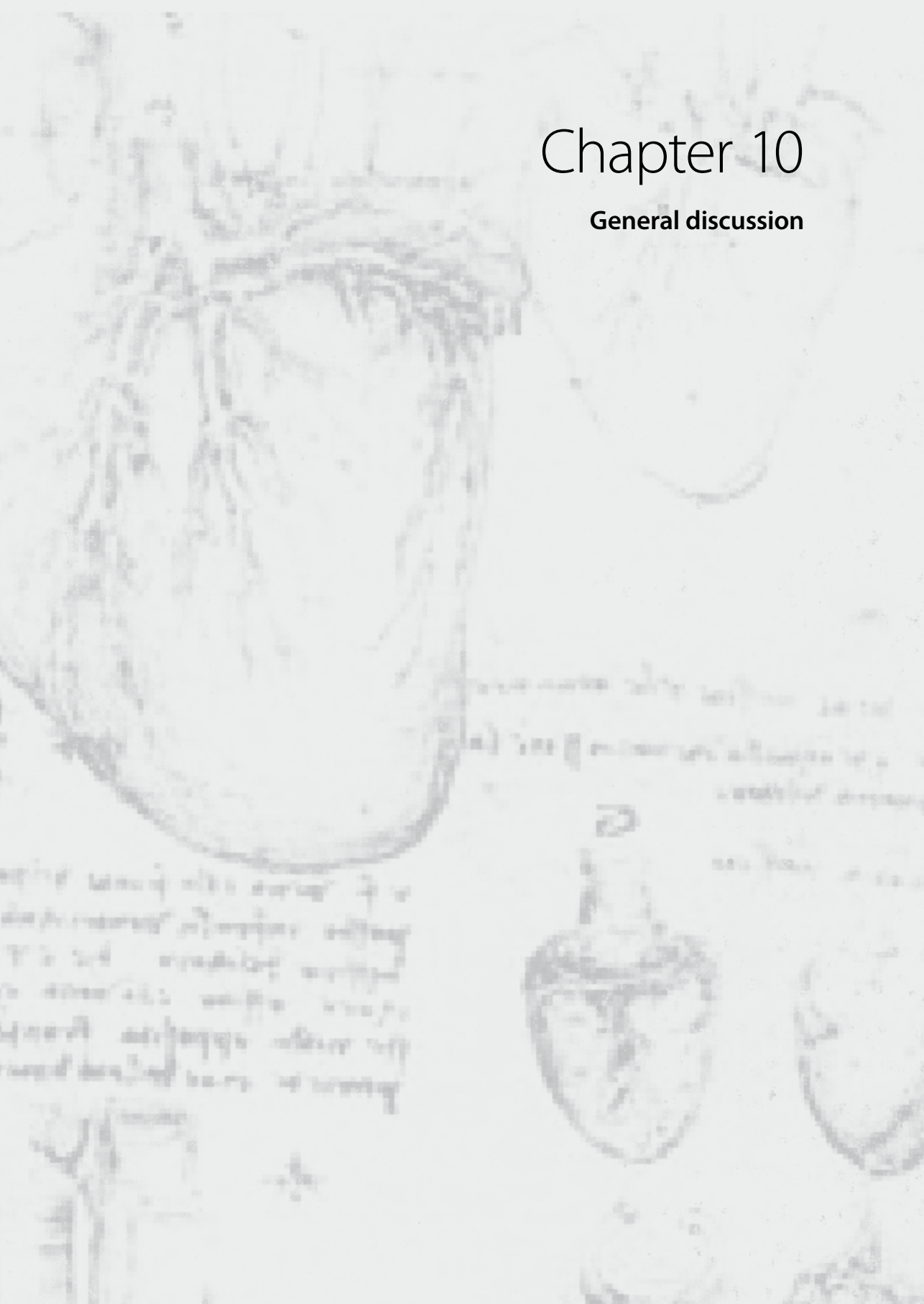
General discussion and summary





Chapter 10

General discussion



1. One of the opinion leaders in the field of right ventricular (RV) function, Andrew Redington,
2. once defined easily applicable, real-time, three-dimensional assessment of RV volumes as the
3. “holy grail” in RV imaging.¹ The quest for this grail has by no means ended, but with the studies
4. summarized in this thesis we hope that some steps in the right direction are made. A number
5. of important requirements in RV assessment are fulfilled using the currently available real-time
6. three-dimensional (3D) echocardiography (echo) system. In this last chapter, we will sum-
7. marize our data on RV assessment using real-time 3D echo, discuss the outcomes against the
8. background of the published literature, and comment on its present strengths and limitations.
9. Insights on regional RV function provided by echocardiographic techniques and stress testing
10. will be highlighted. Thereafter, new developments in RV quantification using cardiac magnetic
11. resonance (CMR) imaging will be discussed as well as the place of computed tomography for
12. this purpose. The prognostic implications of imaging findings will be mentioned and expected
13. future directions for RV imaging will be discussed.

14.

15.

16. **RIGHT VENTRICULAR IMAGING**

17.

18. Most patients with congenital heart defects currently survive into adulthood. The operations
19. performed for the more complex congenital heart lesions are rarely entirely curative.² Residual
20. lesions or sequelae are the rule. The severity and hemodynamic impact may change over time,
21. which implies that lifelong follow-up is generally required to optimize the quality and span of
22. life.^{3,4} Heart failure in patients with congenital heart disease is often predominantly a problem
23. of the right ventricle. Especially in patients with systemic right ventricles and tetralogy of Fallot,
24. RV dysfunction can develop.^{5,6} Four imaging modalities are at present available for RV imaging:
25. echocardiography, CMR imaging, radionuclide angiography, and computed tomography. For
26. understanding of the next paragraphs, it is necessary to know that CMR imaging is considered
27. the clinical standard to evaluate RV function, because it reliably quantifies RV volumes and ejec-
28. tion fraction (EF) when used in a standardized way. The calculation of RV volumes and EF using
29. CMR imaging is based on the disc summation method. A stack of short-axis slices are created
30. from the tricuspid valve down to the apex. Manual tracing of the contours in each end-diastolic
31. and end-systolic slice results in end-diastolic and end-systolic volumes from which EF can be
32. derived.

33.

34. **Echocardiography**

35. Echocardiography remains the first line cardiovascular imaging modality in patients with con-
36. genital heart disease, although suboptimal acoustic access can be problematic after previous
37. cardiovascular surgery.⁷ Numerous echocardiographic indices can be used to quantitatively
38. assess RV systolic function,⁸ for example the tricuspid annular plane systolic excursion (TAPSE),
39. fractional area change, myocardial performance index, tissue velocity, strain, and strain rate.

A systematic review of the clinical value of these modalities in patients with congenital heart disease is presented in Chapter 2 of this thesis.

Right ventricular volumes and ejection fraction

Using two-dimensional echocardiography to estimate RV volumes and EF has not led to clinical applications.⁹ The proposed geometric models were either very complex and/or were not valid in abnormally shaped right ventricles. Therefore, a true 3D approach was needed. The history of 3D echo extends approximately 15 years. Previous 3D echo methods were offline and based on sequential rotational or fanlike scanning and acquisition of multiple cross-sectional images.¹⁰ RV volume quantification was derived from adding multiple slice volumes.¹¹ These methods were hampered by long acquisition and analysis times and poor image quality. The introduction of real-time 3D echo allowed visualization of the right ventricle in a realistic fashion with instantaneous online volume-rendered reconstruction. Fullvolume data acquisition and subsequent offline analysis of RV volumes and EF with the TomTec's four-dimensional RV Function program, now allows fast (mean time needed for analysis 3 minutes), and practical RV quantification.

Real-time 3D echo has some obvious strengths being its ease of use, patient comfort, portability, speed, and relative inexpensiveness compared with CMR imaging or computed tomography. The three-dimensional approach results in actual three-dimensional acquisitions and measurements. This does distinguish real-time 3D echo from CMR imaging. Real-time 3D echo does not rely on geometric assumptions about RV shape and this is an advantage, especially in abnormally shaped right ventricles or ventricles with wall motion abnormalities. On the other hand, real-time 3D echo has some limitations for RV assessment, being its operator dependency, need for adequate acoustic windows, limited temporal resolution compared with two-dimensional echocardiography, and the retrosternal position of the right ventricle resulting in suboptimal visualization of the RV anterior wall and RV outflow tract. In case of poor acoustic windows, endocardial blurring may affect the semi-automated tracking algorithm used in the 4D RV Function program. Furthermore, dedicated training for acquisition and analysis is needed, although a short learning period is needed in those already familiar with echocardiography.

A prerequisite for implementation of a new imaging technique in everyday clinical practice, is that the technique can be applied in the majority of the target population. Therefore, we tested the feasibility of real-time 3D echo by including consecutive, unselected patients with complex and/or surgically repaired congenital heart disease. Real-time 3D echo of the right ventricle turned out to be feasible in ~80% of patients (Chapter 4 of this thesis).¹² This is in accordance with other studies using real-time 3D echo in patients with congenital heart disease, showing feasibility between 52% and 100%.¹³⁻¹⁶ In healthy controls a somewhat lower feasibility of ~70% was found (Chapter 10 of this thesis). Most likely this poorer feasibility can be attributed to the fact that echocardiography of a normal right ventricle is limited by the

1. retrosternal position of this heart chamber. The normal-sized right ventricle lies mainly directly
2. behind the sternum. In contrast, in the diseased right ventricle, which in most cases is dilated,
3. only a small area of the right ventricle is behind the sternum, i.e. the RV anterior wall.

4. Because CMR imaging is the reference technique for RV assessment, the accuracy of echo-
5. cardiography has been studied, with CMR imaging as the reference. Significant biases between
6. real-time 3D echo and CMR imaging were found for RV volumes and EF measurements (Chap-
7. ters 4 and 5 of this thesis). These biases were confirmed in a meta-analysis including 807 par-
8. ticipants.¹⁷ Larger RV volumes were associated with increased underestimation of RV volumes,
9. explained mainly by blurring of the endocardium. Blurring would prompt observers to exclude
10. that area from the RV volume, considering this portion as part of the RV endocardium, and thus
11. trace inside the endocardial border, resulting in an increase of the volume underestimation. To
12. understand the connection of the RV volumes obtained by real-time 3D echo, CMR imaging,
13. and computed tomography, and true RV volumes, Sugeng et al¹⁸ analyzed RV volumes and EF
14. on images obtained in RV shaped phantoms. RV volumes that were measured in vitro, were
15. compared with the true volumes. These in vitro measurements showed that volumetric analysis
16. of CMR images yielded the most accurate measurements. This volumetric analysis comprised
17. analysis of the CMR images using a modified version of the TomTec's four-dimensional RV Func-
18. tion program. In contrast, using the aforementioned disc summation method resulted in RV
19. volumes that were consistently overestimated by ~20% compared with the true volumes. In
20. patients, computed tomography measurements showed a slight overestimation and real-time
21. 3D echo images a small underestimation, but with wider margins of error. Eliminating analysis-
22. related intermodality differences by using the four-dimensional RV Function program for all
23. images, allowed fair comparisons and highlighted the limitations of each imaging modality.

24. To gain further insight into the bias between real-time 3D echo and CMR imaging, we
25. studied 26 patients with tetralogy of Fallot (Chapter 8 of this thesis). We used software that dis-
26. played images obtained by real-time 3D echo and CMR imaging in exactly the same anatomical
27. plane to facilitate side-by-side comparison. Volume differences were mainly caused by inferior
28. visualization of the RV anterior wall on real-time 3D echocardiographic images, corroborated
29. by regional quantitative analysis (46% difference in the anterior segments). Furthermore, using
30. disc summation by CMR imaging resulted in biases in the apical and pulmonary valve areas.
31. Trabeculae were more distinguishable from RV myocardium in CMR imaging than in real-time
32. 3D echo; the RV wall appeared to be thicker on real-time 3D echocardiographic images. In addi-
33. tion, Hoch et al¹⁹ found variables in real-time 3D echo acquisition and analysis, including gain
34. settings, thickness, and orientation of discs, to alter RV volume measurements. Latex phantoms
35. derived from excised lamb hearts were used for comparison. Different gain settings and long-
36. axis tracings significantly affected RV volumes. Mor-avi et al²⁰ studied the potential sources of
37. left ventricular volume underestimation by real-time 3D echo in a multicenter study including
38. phantom imaging, intermodality analysis-related differences, and differences in left ventricular
39. boundary identification. Minimal changes in endocardial surface position (1 mm) resulted

in significant differences in the measured volumes (11%). Exclusion of trabeculae and mitral valve plane from the CMR reference eliminated the intermodality bias. They advised tracing the endocardium including trabeculae in the left ventricular cavity.

One of the challenges, for both real-time 3D echo and CMR imaging, when analyzing the right ventricle, is proper endocardial border delineation. Using contrast-enhanced two-dimensional echocardiography in patients with tetralogy of Fallot or a systemic right ventricle has resulted in improved endocardial border definition.²¹ We evaluated the potential incremental value of using contrast-enhanced real-time echo on RV endocardial border visualization, RV volume measurements and inter-observer and intra-observer variability (Chapter 9 of this thesis). The number of RV segments with optimal visualization of the endocardial border increased using contrast-enhanced real-time 3D echo, compared with non contrast-enhanced real-time 3D echo. However, significantly lower RV volumes were found, which would make the difference with CMR-derived volumes even bigger. With differences in measurements between contrast-enhanced real-time 3D echo and CMR-derived RV volumes exceeding 20%, it is questioned whether this should be used in clinical practice. Another indication for using contrast for ventricular function assessment is the reduction of inter- and intra-observer variability. This has been shown for contrast use in three-dimensional echocardiographic assessment of the left ventricle.²² We found no improvement of inter-observer and intra-observer variability using contrast-enhanced real-time 3D echo-derived images for RV assessment. Based on these findings, we concluded that using contrast is not recommended in real-time 3D echo-derived assessment of the right ventricle so far.

Because echocardiography is accessible, fast, and relatively inexpensive, it would be an ideal technique to use for screening patients who are at risk of RV dysfunction. We therefore tested the sensitivity and specificity of real-time 3D echo to identify congenital heart disease patients with RV dysfunction²³ (Chapter 7 of this thesis). Before identifying RV dysfunction, one should first agree on normal values. Normal values obtained by CMR imaging have been reported by various research groups (Table 1).²³⁻³⁰ In addition, five groups defined normal values using real-time 3D echo. Tamborini et al³¹ provided reference values for RV volumes and EF in 245 healthy controls using the 4D RV Function program. The mean RV end-diastolic volume was 49 ± 10 ml/m², the mean end-systolic volume was 16 ± 6 ml/m², and the mean RV EF was $67 \pm 8\%$ (Table 1). Aune and coworkers³² obtained reference ranges for RV volumes in 166 participants using real-time 3D echo combined with analysis software that was developed for left ventricular volume calculation. Normal reference values were 40 ± 11 ml/m² for end-diastolic volume, 16 ± 6 ml/m² for end-systolic volume, and $61 \pm 10\%$ for RV EF. Gopal et al²⁹ studied 71 healthy controls using real-time 3D echo with the disk summation method for analysis. The mean indexed normal end-diastolic volume was 70 ± 14 ml/m², end-systolic volume 33 ± 10 ml/m² and for RV EF $53 \pm 10\%$. Kjaergaard et al³³ studied 54 healthy controls and found a mean indexed RV end-diastolic volume of 60 ± 12 ml/m², end-systolic volume of 28 ± 7 ml/m², and RV EF of $53 \pm 6\%$ using three-dimensional echocardiography based on the disk summation method. The

1. real-time 3D echo-derived RV volumetric values are again significantly smaller than found in
2. studies on healthy controls using CMR imaging. The reported EF of $67 \pm 8\%$ ³¹ is in our opinion
3. an overestimation of the true RV function. Somewhat smaller RV volumes may be expected
4. using real-time 3D echo compared with CMR imaging, but a mean normal RV EF is around 55%
5. for both techniques.
6. Because of the discrepancies in literature regarding normal values, we decided to establish
7. our own normal values. We found a mean RV EF by real-time 3D echo of $55 \pm 5\%$ versus $60 \pm$
8. 6% using CMR imaging (Chapter 7 of this thesis). After defining normal values, we determined
- 9.

10. **Table 1.** Reported normal right ventricular volumes and ejection fraction

11. Real-time 3D echo	Number	End-diastolic volume (ml/m ²)	End-systolic volume (ml/m ²)	Ejection fraction (%)
12. Aune (2009)	166	40 ± 11	16 ± 6	61 ± 10
13. Gopal (2007)	71	70 ± 14	33 ± 10	53 ± 10
14. Kjaergaard (2006)	54	60 ± 12	28 ± 7	53 ± 6
15. Tamborini (2010)	245	49 ± 10	16 ± 6	67 ± 8
16. Van der Zwaan (2010)	41	68 ± 18	31 ± 9	55 ± 5
17. CMR				
17. Alfakih (2003)	60	81 ± 14	35 ± 10	57 ± 5
18. Gopal (2007)	71	71 ± 13	34 ± 10	53 ± 9
19. Hudsmith (2005)	108	91 ± 16	36 ± 10	61 ± 6
20. Lorenz (1999)	75	75 ± 13	30 ± 10	61 ± 7
21. Maceira (2006)	120	88 ± 11	34 ± 7	61 ± 6
21. Robbers-Visser (2009)	60	82 ± 15	30 ± 8	65 ± 5
22. Teo (2008)	60	81 ± 23	45 ± 17	46 ± 12
23. Van der Zwaan (2010)	41	86 ± 21	35 ± 11	60 ± 6

- 24.
25. cut-off values indicating RV dysfunction. We found real-time 3D echo to be a very sensitive tool
26. to identify RV dysfunction in patients with congenital heart disease. Real-time 3D echo can
27. clinically be applied to rule out RV dysfunction or to indicate further quantitative analysis of RV
28. function, for example using CMR imaging.
29. The reproducibility of real-time 3D echo-derived measurements is important to consider
30. when using this technique for serial measurements or as a screening tool in clinical practice.
31. To be suitable for clinical use, the coefficients of variation (i.e., the standard deviation of the
32. difference between two measurements, divided by the mean of the measurements) should
33. be within the clinically acceptable 15% range.¹⁸ We therefore tested the inter-observer, intra-
34. observer, and test-retest variability of real-time 3D echo-derived RV volumes and EF (Chapters
35. 4, 5, and 6 of this thesis). The coefficients of variation found, ranged from 5 to 13% and were
36. thus all within the 15% range. For inter-observer variability of end-diastolic volumes, consis-
37. tently lower coefficients of variation were found than for end-systolic volumes, in accordance
38. with CMR imaging findings. The variability of CMR-derived measurements has been found
39. to range from 3% to 8% in patients with congenital heart disease.³⁴ Interestingly, in a study

that assessed the variability of real-time 3D echo and CMR measurements, the variability of real-time 3D echo was found to be lower than that of CMR imaging.¹⁸ In addition, test-retest variability represents not only the difference in the analysis of datasets, but also the variation in the acquisition of datasets. We found a good test-retest variability that was comparable with our measurements on conventional reproducibility. These findings indicate that real-time 3D echo is a valuable technique for serial follow-up. We agree with Mor-Avi et al³⁵ who state in an editorial that RV assessment by real-time 3D echo will become a milestone in the management of diseases involving the right ventricle. Guidelines should be developed to ensure a uniform methodology of acquisition and analysis of RV volumes and EF measurements, and will result in more interchangeable data between different operators in different laboratories.

Right ventricular systolic function

Contractility is the fundamental ability of the heart muscle to do its job. Therefore, a lot of focus on the measurement of contractility has been generated. The ideal measure of contractility should be independent of pre- and afterload, independent of the cardiac shape or mass, easy and safe to apply, and proven to be useful in clinical practice.³⁶ Despite many investigations, this ideal measure was never found. EF was then chosen by the cardiology community and remains the index used to assess cardiac function. EF represents the hearts global pump performance and is not only dependent on contractility, but also upon preload and afterload. Interestingly, in various acquired and congenital heart diseases, EF is preserved whereas techniques focusing on regional RV systolic function reveal a diminished RV performance. Over time, RV EF may deteriorate as well, symptoms may develop which will affect outcome. Techniques focussing on regional RV function may therefore be sensitive to detect early RV deterioration. Because we think this is an interesting approach, in the following section we will highlight some echocardiographic measurements on regional, i.e. myocardial RV function in patients with congenital heart disease, i.e. tetralogy of Fallot or systemic right ventricle.

Tetralogy of Fallot

Greutmann et al³⁷ studied patients with repaired tetralogy of Fallot and identified, as expected, an impaired RV outflow tract function. Patients with a normal CMR-derived RV EF were found to compensate the loss of this RV outflow tract function with increased contractions of the RV body, measured as fractional area change on short-axis and on four-chamber views. In contrast, patients with repaired tetralogy of Fallot and abnormal global RV EF showed significantly lower systolic function of the RV-body compared with normal controls. They found a simple regression model, incorporating fractional shortening of the RV outflow tract and fractional area change on four-chamber view to allow accurate echocardiographic estimation of CMR-derived RV EF. Scherp tong et al³⁸ evaluated adult patients with corrected tetralogy of Fallot twice with a time-interval of 4 years using two-dimensional speckle-derived strain to evaluate global and regional RV performance and compared this to CMR-derived EF. Strain imaging measures

1. the degree of myocardial shortening or lengthening (in the longitudinal and circumferential
2. directions), or thickening or thinning (in the radial direction), whereas strain rate is the defor-
3. mation over time.⁸ RV EF was found to remain unchanged during these 4 years, whereas RV
4. longitudinal peak systolic strain of the RV free wall decreased, suggesting that strain may be a
5. sensitive marker to detect early deterioration in RV performance.³⁸ Two-dimensional speckle
6. tracking-derived strain was used to establish the relation between RV performance and RV time
7. delay. RV outlet deformation has been found to be delayed and related to impaired RV perfor-
8. mance.³⁹ In contrast to the reduced strain found in the RV free wall, strain in the interventricular
9. septum turned out to be normal. Solarz et al⁴⁰ speculated that the septal function is preserved
10. as a compensatory mechanism for impaired RV free wall function. Tissue Doppler-derived
11. myocardial velocities were found to be decreased in pediatric patients with tetralogy of Fallot
12. and were related to the severity of pulmonary regurgitation.⁴¹ Salehian et al⁴² also found lower
13. myocardial velocities and found RV peak systolic velocity to be an independent predictor of
14. maximal oxygen consumption during exercise. In summary, both the longitudinal RV function
15. as well as the function of the outlet portion has been judged to be reduced in patients with
16. tetralogy of Fallot.

17.

18. *Systemic right ventricle*

19. Patients that underwent an atrial switch procedure for transposition of the great arteries, had
20. reduced RV myocardial velocities and deformation. The reduced deformation parameters cor-
21. related well with global RV EF assessed by CMR imaging. More specifically, the global RV long-
22. axis RV function was found to be diminished.^{43, 44} Reduced systemic RV myocardial velocities
23. and deformation have also been found in patients with a congenitally corrected transposition
24. of the great arteries, even when patients were asymptomatic.⁴⁵ Besides tissue Doppler-derived
25. indices of deformation, two-dimensional speckle tracking has been used to assess systemic
26. RV function, and provided comparable data. Global longitudinal strain and strain rate were
27. found to be reduced.⁴⁶ Using deformation imaging has provided information on the adaptive
28. response of the right ventricle in order to sustain systemic pressures. In a very interesting study
29. by Pettersen et al⁴⁷, it was stated that reduced longitudinal systemic RV function has been inter-
30. preted as ventricular dysfunction. But longitudinal shortening is only one aspect of myocardial
31. deformation. Therefore, they assessed not only the longitudinal, but also the circumferential
32. deformation. They found a predominant circumferential over longitudinal free wall shortening
33. in the systemic right ventricle, comparable with a normal left ventricle. Of note, the systemic
34. right ventricle did not display torsion as is found in the normal left ventricle. Thus, deformation
35. imaging does not only reveal information on regional RV performance, but does also provide
36. us with information on adaptive mechanisms in various pathologic states

37.

38.

39.

The right ventricle during exercise

A reduction in exercise tolerance may be the first sign of deterioration of cardiac function in patients with congenital heart disease.⁴⁸ Changes in cardiac function that are not apparent at rest may become evident during exercise testing. In addition, parameters of submaximal exercise testing may provide important information on risk assessment and long-term prognosis. Therefore, we briefly describe some outcomes of RV function assessment during exercise.

Stress echocardiography and stress CMR imaging have been found feasible and safe, and can either be done using physical exercise or pharmacological stress. In the detection of viability or in the early diagnosis of RV dysfunction in patients with congenital heart disease, dobutamine stress functional CMR imaging can be useful.^{49,48} In 26 patients with transposition of the great arteries after atrial switch repair, RV longitudinal two-dimensional strain was found to be homogeneously reduced compared with healthy controls. RV transverse two-dimensional strain on the other hand, was greater than longitudinal strain, opposite from findings in the normal RV free wall. Furthermore, transverse two-dimensional strain best predicted exercise capacity.⁵⁰ Harada et al⁵¹ assessed RV functional reserve during exercise using tissue Doppler imaging in patients with repaired tetralogy of Fallot. The magnitude of increase in tissue velocities was less in patients than in healthy controls. Patients with a systemic RV who were unable to increase RV EF during stress CMR imaging, were found to have an increased risk of adverse outcomes such as hospitalization for heart failure, cardiac surgery, aborted cardiac arrest, or death.⁵²

The right ventricle is the most affected ventricle during exercise. Ominous ventricular tachyarrhythmias of RV origin – associated with mild reduction in systolic function – have been reported in highly trained cyclists. In athletes presenting with ventricular tachycardia, RV abnormalities were detected in 89%, whereas left ventricular abnormalities were evident in only 3%. A lack of evidence of inherited disease would imply that extreme exercise may be the cause of RV dysfunction and arrhythmias.⁵³ Whether transient RV dysfunction results in chronic remodelling and/ or clinical events is an important issue. It is the RV that should be the focus of attention when assessing the clinical impact of endurance training.⁵³

Cardiac magnetic resonance imaging

CMR imaging has some advantages and disadvantages compared with echocardiography. The strengths of CMR imaging are the unrestricted access to cardiovascular anatomy and function, non-invasiveness, favourable signal to noise ratio, and comprehensiveness. With a single study, assessment of RV performance can be linked to cardiac and pericardial morphology and myocardial tissue characteristics, flow patterns and great vessel anatomy. This approach provides the clinician a complete view, not only of the right ventricle as such, but also of the right ventricle being an essential part of the cardiopulmonary system.^{7, 49}

On the other hand, limited availability, high cost, time-consuming RV analysis and acquisition, claustrophobia, and poor patient compliance restrict the use of CMR imaging. Patients are required to lie still in a tubular bore of magnet, which may not be tolerated by a percentage

1. of patients (~ 5%). Limited ability to comply with breath-hold instructions can be an added
2. problem in patients with Down syndrome or other cognitive or behavioural issues, although
3. this is less often a problem in the adult than the paediatric population.⁷ A substantial number
4. of patients with congenital heart disease have pacemakers or implantable cardioverter defibril-
5. lators and thus (relative) contraindications for CMR imaging.⁵⁴ To realize its full potential and
6. to avoid pitfalls, CMR imaging of congenital heart disease requires training and experience.⁷

7. So far, CMR imaging for longitudinal follow-up of patients is hampered by continuous
8. updates and changes of the hardware, software, and scanning techniques over the years. CMR-
9. derived RV images are analyzed by manually tracing the endocardial contours; the observer has
10. to define the most basal and apical images that contain part of the right ventricle. This results in
11. substantial inter-observer and intra-observer variability, especially when studies are acquired
12. and analyzed by different laboratories and over many years. Reproducibility data in research
13. settings have been reported.^{24, 26, 28, 34} Grothues et al⁵⁵ described inter-observer variability in
14. 60 patients, being 6% for end-diastolic volume, 14% for end-systolic volume, and 8% for EF.
15. Using slices oriented in the axial direction rather than the conventional short-axis direction, has
16. resulted in reproducible RV measurements in patients with corrected tetralogy of Fallot.^{49, 56}

17. Some developments in the analysis of CMR-derived images have taken place. As mentioned
18. before, CMR-derived RV volumes were found to be most accurate compared with true volumes
19. using the 4D RV Function program.¹⁸ Moroseos et al⁵⁷ compared RV volumes measured using
20. the conventional method of disc summation versus three-dimensional reconstruction by the
21. piecewise smooth subdivision surface method, in patients with complete or corrected trans-
22. position of the great arteries. The piecewise smooth subdivision surface method uses images
23. acquired from combinations of views to reconstruct the three-dimensional shape of the right
24. ventricle. The authors suggested incorporating information from additional images to obtain
25. accurate analysis of the short-axis views for RV volume measurements.

26. So far, using real-time 3D echo does not give information on the function or size of various
27. RV regions, whilst the function of various regions may differ significantly in various congenital
28. heart defects. Bodhey et al⁵⁸ used CMR imaging in patients with tetralogy of Fallot and found
29. the apical trabecular region to take up the greatest part of the volume overload caused by
30. pulmonary valve regurgitation; the ejecting force of the outlet was decreased. In another study,
31. three-dimensional RV endocardial surface models were reconstructed to obtain regional EFs
32. in patients late after tetralogy of Fallot repair. The RV outflow tract did dysfunction most, and
33. contributed to global RV dysfunction independent of RV size, degree of pulmonary regurgita-
34. tion, and other confounding factors. Measures of regional dysfunction were associated with
35. decreased exercise capacity, sustained ventricular tachycardia, and symptoms of heart failure.⁵⁹

36. Computed tomography

37. Thoracic computed tomography (CT) is widely used to evaluate thoracic disorders, some of
38. which can potentially affect the right ventricle. CT is not the first line technique for RV function

assessment, because it requires radiation exposure and needs iodinated contrast medium injections. CT offers a good spatial resolution, relatively unrestricted access, and shorter acquisition times than CMR imaging. In patients with a pacemaker or implantable cardioverterdefibrillator, CT provides an alternative to CMR imaging. Initially, CT had a limited temporal resolution, but by using the 64-slice multidetector row CT, the resolution improved. Drawbacks compared with CMR imaging include less versatile tissue characterization, inferior ability to evaluate cardiovascular physiology, and reliance on a radio-opaque contrast agent.⁷

With the introduction of the electrocardiogram (ECG)-gated cardiac CT, scans can be obtained through retrospective or prospective techniques.⁶⁰ Prospective ECG-gated acquisition allows imaging at lower radiation doses than retrospectively ECG-gated CT, but it requires both a latest generation multidetector row CT with large volume coverage and adequate heart rate control. Beta-blockers are commonly used for patients with high heart rates (> 75 beats/min). When conditions for prospective ECG-gated acquisition are not met, a retrospective technique is used, enabling reconstruction of the RV end-diastolic and the end-systolic images from the same MDCT data for the purposes of the functional analysis.⁶¹ Even non-ECG-gated contrast-enhanced MDCT of the thorax can provide information about the right ventricle, mainly about its structure, because RV volumes and septal bowing can be assessed without gating.⁶⁰

RV function assessment can be optimized using bi- or multiphasic contrast injection or by mixing saline with a contrast medium, to allow a more accurate distinction between myocardium and endocardium.⁶² RV function assessment using multidetector row CT led to overestimation of the end-diastolic and end-systolic volumes.¹⁸ The limited temporal resolution of CT compared with CMR imaging is considered the main reason for this phenomenon.⁶² Inter-observer variability of multidetector row CT was not significantly different from that of CMR imaging. Accurate assessment of RV volumes by 16-detector CT is feasible but still rather time-consuming.⁶³ Gao et al⁶¹ compared RV volumes and EF using 64-row CT and CMR imaging in patients with chronic obstructive pulmonary disease or cor pulmonale. Semi-manual analysis was compared with automated analysis for volumetric RV assessment using multidetector CT.⁶⁴ RV volumes were significantly larger when using the automated method. Not surprisingly, the automated analysis method was perfectly reproducible, since no user input was required.

RV function assessment using CT is usually done as part of a more extensive screening in patients with coronary artery disease, pulmonary embolism, pulmonary hypertension, or after myocardial infarction.⁶² In young adults for whom successive examinations are necessary, one is especially concerned about the radiation exposure and its associated stochastic effects. This risk is dose-, age-, and gender-dependent and makes repeat CT examinations or studies in young patients unattractive.⁷ In addition, if the patient is young, the ALARA (as low as reasonably achievable) principle has to be followed, reducing the dose exposure, but without losing diagnostic information by applying specific protocols.^{65, 66}

1. **PROGNOSTIC IMPORTANCE OF RIGHT VENTRICULAR IMAGING PARAMETERS**

2.

3. Besides exploring the accuracy and reproducibility of an imaging technique, its prognostic
4. value needs to be established to enhance clinical validation.

5.

6. Congenital heart disease

7. In this thesis, patients with congenital heart defects were studied; most of them of young

8. adult age. Various research groups established the prognostic value of RV dysfunction using

9. various imaging parameters. Knauth et al^{66, 67} assessed 88 patients with tetralogy of Fallot by

10. CMR imaging, ~20 years post initial repair. Severe RV dilatation and either left ventricular or

11. RV dysfunction were found to be predictive of major adverse clinical outcomes, i.e. death,

12. sustained ventricular tachycardia, increase in New York Heart Association class to grade III or

13. IV. In another study, clinical records of 121 patients with congenitally corrected transposition

14. of the great arteries were retrospectively reviewed.⁶⁸ Using multivariate analysis, poor RV

15. function assessed by eyeballing turned out to be a risk factor of death. Eyeballing-derived

16. RV dysfunction was identified as risk factor for death in 123 patients with an atrial corrected

17. transposition of the great arteries.⁶⁹ Piran et al⁷⁰ studied a cohort of 188 patients with single

18. or systemic right ventricles. They found patients who had a low systemic EF (<35%) measured

19. by two-dimensional echocardiography, or falling systemic ventricular EF during exercise by

20. radionuclide ventriculography, were particularly likely to develop symptomatic heart failure.

21. Prediction of clinical outcome in patients with systemic right ventricles was done using regres-

22. sion analysis to identify prognostic echocardiographic variables.⁷¹ The qualitative systemic RV

23. and the subpulmonary left ventricular function as well as TAPSE were found to determine New

24. York Heart Association class, maximal exercise capacity, and NT-pro-BNP levels. In summary,

25. RV dysfunction assessed by various imaging modalities, is found to be predictive of death and

26. poor clinical conditions in patients with congenital heart diseases.

27.

28. Pulmonary hypertension

29. Not only in congenital heart disease the importance of RV assessment has been recognized,
30. but also in patients with pulmonary hypertension, heart failure, or post myocardial infarction.

31. Forfia et al⁷² used the TAPSE to risk stratify patients with pulmonary hypertension. Survival

32. estimates at 1 and 2 years were 94% and 88%, respectively, in those with a TAPSE of ≥ 18 mm,

33. versus 60% and 50%, respectively, in patients with a TAPSE less than 18 mm. Progressive RV dila-

34. tation measured by CMR imaging in patients with idiopathic pulmonary arterial hypertension,

35. independently predicted 1-year mortality beside a decrease in stroke volume and a decrease

36. in left ventricular end-diastolic volume.⁷³ Nath et al⁷⁴ evaluated the correlation between RV

37. indices and clinical improvement in epoprostenol treated pulmonary hypertension. Changes in

38. New York Heart Association class did not correlate with changes in the myocardial performance

39. index. They concluded that the myocardial performance index was insensitive to the clinical

response to epoprostenol therapy. In patients with chronic thromboembolic pulmonary hypertension, RV function was judged by echocardiography before and after pulmonary endarterectomy. RV fractional area change, TAPSE, and mid-apical and basal strain, and strain rate based on color-coded tissue Doppler imaging were used. RV function was found to improve after pulmonary endarterectomy, but this was not reflected by TAPSE because of postoperative changes in overall heart motion. Motion independent deformation parameters, strain and strain rate, appeared superior in the accurate description of regional RV function or the contractile status of the RV free wall.⁷⁵ In conclusion, TAPSE was found to be predictive of survival in patients with pulmonary hypertension, but not in those after operations. The myocardial performance index did not correlate with changes in patient's clinical condition.

Coronary heart disease and heart failure

In 377 patients with heart failure, the prognostic value of thermodilution-derived RV EF has been investigated. During a median follow-up period of 17 ± 9 months, 105 patients died and 35 underwent heart transplantation. Besides pulmonary artery pressure, RV EF turned out to be an independent prognostic predictor.⁷⁶ In addition, radionuclide angiography-derived RV EF was found to be an independent predictor of survival in 205 patients with moderate heart failure.⁷⁷ RV fractional area change was a predictor of mortality, cardiovascular mortality, and heart failure in 416 patients with left ventricular dysfunction.⁷⁸ Antoni et al⁷⁹ studied the prognostic value of the RV fractional area change, TAPSE, and two-dimensional speckle tracking-derived strain in 621 patients treated with primary percutaneous intervention for acute myocardial infarction. After multivariate analysis, RV fractional area change and strain turned out to independently predict the composite endpoint of mortality, reinfarction, and hospitalization for heart failure at 24 months of follow-up. After multivariate analysis TAPSE no longer predicted the composite endpoint.

FUTURE DIRECTIONS OF RIGHT VENTRICULAR IMAGING

Even though it may sound paradoxical, we hope that all that has been investigated in this thesis will be outdated soon, since this would imply that the development of real-time 3D echo has continued rapidly. In the following section we will outline some of these future developments.

Technical improvements

The currently used ultrasound systems have various imaging options for using 3D echocardiography. To obtain information on ventricular function, full-volume real-time 3D echo is needed. Up to a few months ago, it was required to stitch multiple (4 to 7) subvolumes that were collected over several cardiac cycles together, to create a volume large enough to encompass a complete right or left ventricle. At this moment, ultrasound systems are available that can

1. acquire a full-volume dataset in a single or in two heartbeats.^{80, 81} The advantages are that
2. the acquisition is less influenced by patient movement, for example in small infants, and the
3. technique may even be applied in patients with irregular heart rhythms. So far, irregular heart
4. rhythms such as atrial fibrillation resulted in stitching artifacts and therefore real-time 3D echo,
5. as well as CMR imaging, could not be used in these patients. With the acquisition in a single
6. heartbeat, stitching is no longer required. On the other hand, ventricular filling varies a lot dur-
7. ing irregular heart rhythms and therefore we would recommend acquiring multiple datasets
8. and taking the mean volumes and EF that are calculated from these datasets for an adequate
9. estimation of cardiac function.

10. Because RV volume and EF assessment is critically dependent on echocardiographic image
11. quality, optimization of image quality is essential. Even though the temporal resolution of real-
12. time 3D echo is comparable with CMR imaging, it is worse compared with two-dimensional
13. echocardiography. The newer ultrasound probes provide images with higher temporal
14. resolution and will result in more accurate estimations of RV end-systolic volumes. The spa-
15. tial resolution of echocardiography is higher compared with CMR imaging, and the newer
16. echocardiographic probes obtain higher spatial resolutions. The details seen at for example
17. the endocardial border, such as trabeculae, will appear even more prominent. This may further
18. influence the difference in RV volumes by echocardiography and CMR imaging, and neces-
19. sitates a clear consensus statement on how to handle these endocardial structures during RV
20. volume calculations.

21. The introduction of semi-automated border detection software dedicated to RV function
22. analysis (4D RV Function program) meant a big step forward to clinical RV assessment based on
23. real-time 3D echo. As described in this thesis, analyses only take few minutes for a moderately
24. experienced observer. RV analysis is still more complex however, compared with left ventricular
25. volume analysis. For the latter analysis, only three points need to be marked: the lateral and
26. medial mitral valve annulus, and the left ventricular apex.⁸² Thereafter, the software calculates
27. left ventricular volumes and EF. For RV analysis, manual endocardial contour delineation is
28. needed in three different views, where after the software calculates RV volumes and EF. The
29. more automated the analysis will become, the better reproducible the measurements will be.
30. We expect new analysis software to be developed that will more closely resemble the analysis
31. of the left ventricle. Furthermore, images obtained by different imaging techniques may be
32. analyzed by one software package, such as investigated by Sugeng et al¹⁸ By this means, analy-
33. sis related differences that influence RV measurements by various techniques will be reduced.
34. The results of a study in which real-time 3D echo and CMR-derived RV volumes and EF were
35. analyzed within one software package, are promising.¹⁶

36.

37. Prognostic importance

38. Besides a thorough validation of the basic characteristics of new imaging techniques, the deter-
39. mination of their prognostic value is needed. Few major adverse events may be expected when

examining a young group of adult patients with congenital heart defects. However, scoring these events over a five-year period and identifying real-time 3D echo-derived independent predictors of outcome would certainly strengthen the clinical use of real-time 3D echo. A limitation to this approach will be that by the time the results may be expected, newer ultrasound systems with better image quality will be available.

New applications

Imaging the right ventricle during cardiac surgery or percutaneous interventions can best be done using three-dimensional transesophageal echocardiography. So far no publications on the use of three-dimensional transesophageal echocardiography for RV assessment have been published. We have some experience and expect that applying this approach will result in a clearer definition of the RV inflow and outflow portions whilst the biggest challenge will be to incorporate the complete RV apex.

Three-dimensional deformation imaging

Currently, three-dimensional speckle tracking echocardiography has become available. Three-dimensional tracking of speckle patterns in high volume rate datasets will diminish the need for assumptions on the expected motion pattern by the tracking algorithm, and thereby increase the accuracy of measurements of RV deformation. In other words, measurements will be more accurate since the motion of speckle patterns does not only occur within the imaging plane, but also in the other directions. The standardization of the measurement planes of the basal, mid, and apical part of the RV free wall from a three-dimensional dataset will improve the reproducibility of the measurements.

Fusion of images by various techniques

Fusion of multiple imaging modalities will result in combining the benefits of different techniques. For example the assessment of cardiac shape or volumes by real-time 3D echo or CMR imaging may be combined with speckle tracking derived deformation parameters or Doppler measurements of flow patterns.

In addition, fusion of images can result in improved image quality. Szmigielski et al⁸³ assessed three-dimensional fusion echocardiography combining several real-time 3D echo-derived full-volumes from different transducer positions. In a cardiac phantom they found fused datasets to show an improved contrast-to-noise ratio, which is an indicator of image quality. In patients, a better endocardial border definition was established using fusion echocardiography compared with a single real-time 3D echo dataset. Yet, fusion of the datasets did not affect the absolute left ventricular volumes or EF.

1. CONCLUSIONS

2.

3. Using currently available real-time 3D echo results in widely applicable, accurate, and reproducible measurements of RV volumes and EF. There is still a lot to learn about the assessment and implications of RV (dys)function in adults with congenital heart disease. Understanding the uniqueness of normal and abnormal RV physiology combined with appropriate application of the available imaging techniques, such as real-time 3D echo, deformation imaging, and CMR imaging, will provide solutions to problems that challenge these patients and their caregivers.

9.

10.

11.

12.

13.

14.

15.

16.

17.

18.

19.

20.

21.

22.

23.

24.

25.

26.

27.

28.

29.

30.

31.

32.

33.

34.

35.

36.

37.

38.

39.

1. Redington AN. Right ventricular function. *Cardiol Clin.* 2002;20:341-9, v. 1.
2. Ou P, Iserin L, Raisky O, Vouhe P, Brunelle F, Sidi D, et al. Post-operative cardiac lesions after cardiac surgery in childhood. *Pediatr Radiol.* 2010;40:885-94. 2.
3. Warnes CA. The adult with congenital heart disease: born to be bad? *J Am Coll Cardiol.* 2005;46:1-8. 3.
4. Warnes CA. Jane Somerville. *Clin Cardiol.* 2008;31:183-4. 4.
5. Graham TP, Jr., Bernard YD, Mellen BG, Celermajer D, Baumgartner H, Cetta F, et al. Long-term outcome in congenitally corrected transposition of the great arteries: a multi-institutional study. *J Am Coll Cardiol.* 2000;36:255-61. 5.
6. Knauth AL, Gauvreau K, Powell AJ, Landzberg MJ, Walsh EP, Lock JE, et al. Ventricular size and function assessed by cardiac MRI predict major adverse clinical outcomes late after tetralogy of Fallot repair. *Heart.* 2008;94:211-6. 6.
7. Kilner PJ, Geva T, Kaemmerer H, Trindade PT, Schwitter J, Webb GD. Recommendations for cardiovascular magnetic resonance in adults with congenital heart disease from the respective working groups of the European Society of Cardiology. *Eur Heart J.* 2010;31:794-805. 7.
8. Mertens LL, Friedberg MK. Imaging the right ventricle-current state of the art. *Nat Rev Cardiol.* 2010. 8.
9. Jiang L, Levine RA, Weyman AE. Echocardiographic Assessment of Right Ventricular Volume and Function. *Echocardiography.* 1997;14:189-206. 9.
10. van den Bosch AE, Krenning BJ, Roelandt JR. Three-dimensional echocardiography. *Minerva Cardio-angi.* 2005;53:177-84. 10.
11. Vogel M, Gutberlet M, Ditttrich S, Hosten N, Lange PE. Comparison of transthoracic three dimensional echocardiography with magnetic resonance imaging in the assessment of right ventricular volume and mass. *Heart.* 1997;78:127-30. 11.
12. van der Zwaan HB, Helbing WA, McGhie JS, Geleijnse ML, Luijnenburg SE, Roos-Hesselink JW, et al. Clinical Value of Real-Time Three-Dimensional Echocardiography for Right Ventricular Quantification in Congenital Heart Disease: Validation With Cardiac Magnetic Resonance Imaging. *J Am Soc Echocardiogr.* 2010;23:134-40. 12.
13. Grewal J, Majdalany D, Syed I, Pellikka P, Warnes CA. Three-dimensional echocardiographic assessment of right ventricular volume and function in adult patients with congenital heart disease: comparison with magnetic resonance imaging. *J Am Soc Echocardiogr.* 2010;23:127-33. 13.
14. Iriart X, Montaudon M, Lafitte S, Chabaneix J, Reant P, Balbach T, et al. Right ventricle three-dimensional echography in corrected tetralogy of fallot: accuracy and variability. *Eur J Echocardiogr.* 2009;10:784-92. 14.
15. Khoo NS, Young A, Occlshaw C, Cowan B, Zeng IS, Gentles TL. Assessments of right ventricular volume and function using three-dimensional echocardiography in older children and adults with congenital heart disease: comparison with cardiac magnetic resonance imaging. *J Am Soc Echocardiogr.* 2009;22:1279-88. 15.
16. Niemann PS, Pinho L, Balbach T, Galuschky C, Blankenhagen M, Silberbach M, et al. Anatomically oriented right ventricular volume measurements with dynamic three-dimensional echocardiography validated by 3-Tesla magnetic resonance imaging. *J Am Coll Cardiol.* 2007;50:1668-76. 16.
17. Shimada YJ, Shiota M, Siegel RJ, Shiota T. Accuracy of right ventricular volumes and function determined by three-dimensional echocardiography in comparison with magnetic resonance imaging: a meta-analysis study. *J Am Soc Echocardiogr.* 2010;23:943-53. 17.
18. Sugeng L, Mor-Avi V, Weinert L, Niel J, Ebner C, Steringer-Mascherbauer R, et al. Multimodality Comparison of Quantitative Volumetric Analysis of the Right Ventricle. *JACC Cardiovasc Imaging.* 2010;3:10-8. 18.
19. Hoch M, Vasilyev NV, Soriano B, Gauvreau K, Marx GR. Variables influencing the accuracy of right ventricular volume assessment by real-time 3-dimensional echocardiography: an in vitro validation study. *J Am Soc Echocardiogr.* 2007;20:456-61. 19.

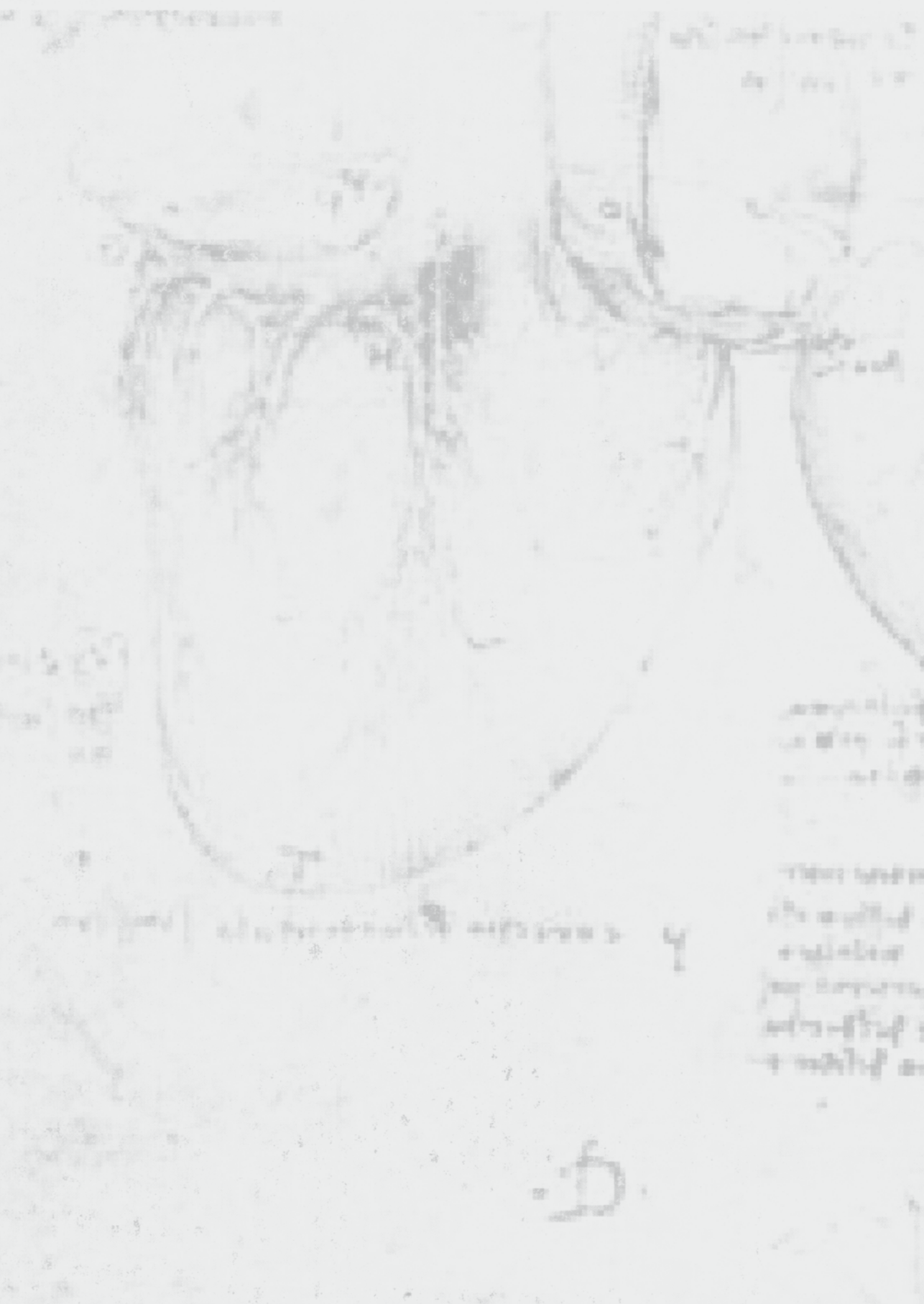
1.
2.
3.
4.
5.
6.
7.
8.
9.
10.
11.
12.
13.
14.
15.
16.
17.
18.
19.
20.
21.
22.
23.
24.
25.
26.
27.
28.
29.
30.
31.
32.
33.
34.
35.
36.
37.
38.
39.

1. 20. Mor-Avi V, Jenkins C, Kuhl HP, Nesser HJ, Marwick T, Franke A, et al. Real-time 3-dimensional echocardiographic quantification of left ventricular volumes: multicenter study for validation with magnetic resonance imaging and investigation of sources of error. *JACC Cardiovasc Imaging*. 2008;1:413-23.
2. 21. van den Bosch AE, Meijboom FJ, McGhie JS, Roos-Hesselink JW, Ten Cate FJ, Roelandt JR. Enhanced visualisation of the right ventricle by contrast echocardiography in congenital heart disease. *Eur J Echocardiogr*. 2004;5:104-10.
3. 22. Krenning BJ, Kirschbaum SW, Soliman OI, Nemes A, van Geuns RJ, Vletter WB, et al. Comparison of contrast agent-enhanced versus non-contrast agent-enhanced real-time three-dimensional echocardiography for analysis of left ventricular systolic function. *Am J Cardiol*. 2007;100:1485-9.
4. 23. van der Zwaan HB, Helbing WA, Boersma E, Geleijnse ML, McGhie JS, Soliman OI, et al. Usefulness of real-time three-dimensional echocardiography to identify right ventricular dysfunction in patients with congenital heart disease. *Am J Cardiol*. 2010;106:843-50.
5. 24. Maceira AM, Prasad SK, Khan M, Pennell DJ. Reference right ventricular systolic and diastolic function normalized to age, gender and body surface area from steady-state free precession cardiovascular magnetic resonance. *Eur Heart J*. 2006;27:2879-88.
6. 25. Alfakih K, Plein S, Thiele H, Jones T, Ridgway JP, Sivananthan MU. Normal human left and right ventricular dimensions for MRI as assessed by turbo gradient echo and steady-state free precession imaging sequences. *J Magn Reson Imaging*. 2003;17:323-9.
7. 26. Hudsmith LE, Petersen SE, Francis JM, Robson MD, Neubauer S. Normal human left and right ventricular and left atrial dimensions using steady state free precession magnetic resonance imaging. *J Cardiovasc Magn Reson*. 2005;7:775-82.
8. 27. Lorenz CH, Walker ES, Morgan VL, Klein SS, Graham TP, Jr. Normal human right and left ventricular mass, systolic function, and gender differences by cine magnetic resonance imaging. *J Cardiovasc Magn Reson*. 1999;1:7-21.
9. 28. Robbers-Visser D, Boersma E, Helbing WA. Normal biventricular function, volumes, and mass in children aged 8 to 17 years. *J Magn Reson Imaging*. 2009;29:552-9.
10. 29. Gopal AS, Chukwu EO, Iwuchukwu CJ, Katz AS, Toole RS, Schapiro W, et al. Normal values of right ventricular size and function by real-time 3-dimensional echocardiography: comparison with cardiac magnetic resonance imaging. *J Am Soc Echocardiogr*. 2007;20:445-55.
11. 30. Teo KS, Carbone A, Piantadosi C, Chew DP, Hammett CJ, Brown MA, et al. Cardiac MRI assessment of left and right ventricular parameters in healthy Australian normal volunteers. *Heart Lung Circ*. 2008;17:313-7.
12. 31. Tamborini G, Marsan NA, Gripari P, Maffessanti F, Brusoni D, Muratori M, et al. Reference values for right ventricular volumes and ejection fraction with real-time three-dimensional echocardiography: evaluation in a large series of normal subjects. *J Am Soc Echocardiogr*. 2010;23:109-15.
13. 32. Aune E, Baekkevar M, Rodevand O, Otterstad JE. The limited usefulness of real-time 3-dimensional echocardiography in obtaining normal reference ranges for right ventricular volumes. *Cardiovasc Ultrasound*. 2009;7:35.
14. 33. Kjaergaard J, Sogaard P, Hassager C. Quantitative echocardiographic analysis of the right ventricle in healthy individuals. *J Am Soc Echocardiogr*. 2006;19:1365-72.
15. 34. Luijnenburg SE, Robbers-Visser D, Moelker A, Vliegen HW, Mulder BJ, Helbing WA. Intra-observer and interobserver variability of biventricular function, volumes and mass in patients with congenital heart disease measured by CMR imaging. *Int J Cardiovasc Imaging*. 2010;26:57-64.
16. 35. Mor-Avi V, Sugeng L, Lindner JR. Imaging the forgotten chamber: is the devil in the boundary? *J Am Soc Echocardiogr*. 2010;23:141-3.
17. 36. Carabello BA. Evolution of the study of left ventricular function: everything old is new again. *Circulation*. 2002;105:2701-3.
18. 37. Greutmann M, Tobler D, Biaggi P, Mah ML, Crean A, Wald RM, et al. Echocardiography for assessment of regional and global right ventricular systolic function in adults with repaired tetralogy of Fallot. *Int J Cardiol*. 2010.
19. 38.
20. 39.

38. Scherptong RW, Mollema SA, Blom NA, Kroft LJ, de Roos A, Vliegen HW, et al. Right ventricular peak systolic longitudinal strain is a sensitive marker for right ventricular deterioration in adult patients with tetralogy of Fallot. *Int J Cardiovasc Imaging*. 2009;25:669-76. 1.
39. van der Hulst AE, Roest AA, Delgado V, Holman ER, de Roos A, Blom NA, et al. Relationship between temporal sequence of right ventricular deformation and right ventricular performance in patients with corrected tetralogy of Fallot. *Heart*. 2011;97:231-6. 2.
40. Solarz DE, Witt SA, Glascock BJ, Jones FD, Khoury PR, Kimball TR. Right ventricular strain rate and strain analysis in patients with repaired tetralogy of Fallot: possible interventricular septal compensation. *J Am Soc Echocardiogr*. 2004;17:338-44. 3.
41. Toyono M, Harada K, Tamura M, Yamamoto F, Takada G. Myocardial acceleration during isovolumic contraction as a new index of right ventricular contractile function and its relation to pulmonary regurgitation in patients after repair of tetralogy of Fallot. *J Am Soc Echocardiogr*. 2004;17:332-7. 4.
42. Salehian O, Burwash IG, Chan KL, Beauchesne LM. Tricuspid annular systolic velocity predicts maximal oxygen consumption during exercise in adult patients with repaired tetralogy of Fallot. *J Am Soc Echocardiogr*. 2008;21:342-6. 5.
43. Eyskens B, Weidemann F, Kowalski M, Bogaert J, Dymarkowski S, Bijmens B, et al. Regional right and left ventricular function after the Senning operation: an ultrasonic study of strain rate and strain. *Cardiol Young*. 2004;14:255-64. 6.
44. Vogel M, Derrick G, White PA, Cullen S, Aichner H, Deanfield J, et al. Systemic ventricular function in patients with transposition of the great arteries after atrial repair: a tissue Doppler and conductance catheter study. *J Am Coll Cardiol*. 2004;43:100-6. 7.
45. Bos JM, Hagler DJ, Silvillairat S, Cabalka A, O'Leary P, Daniels O, et al. Right ventricular function in asymptomatic individuals with a systemic right ventricle. *J Am Soc Echocardiogr*. 2006;19:1033-7. 8.
46. Chow PC, Liang XC, Cheung EW, Lam WW, Cheung YF. New two-dimensional global longitudinal strain and strain rate imaging for assessment of systemic right ventricular function. *Heart*. 2008;94:855-9. 9.
47. Pettersen E, Helle-Valle T, Edvardsen T, Lindberg H, Smith HJ, Smevik B, et al. Contraction pattern of the systemic right ventricle shift from longitudinal to circumferential shortening and absent global ventricular torsion. *J Am Coll Cardiol*. 2007;49:2450-6. 10.
48. Helbing WA, Luijnenburg SE, Moelker A, Robbers-Visser D. Cardiac stress testing after surgery for congenital heart disease. *Curr Opin Pediatr*. 2010;22:579-86. 11.
49. Goetschalckx K, Rademakers F, Bogaert J. Right ventricular function by MRI. *Curr Opin Cardiol*. 2010;25:451-5. 12.
50. Di Salvo G, Pacileo G, Rea A, Limongelli G, Baldini L, D'Andrea A, et al. Transverse strain predicts exercise capacity in systemic right ventricle patients. *Int J Cardiol*. 2010;145:193-6. 13.
51. Harada K, Toyono M, Yamamoto F. Assessment of right ventricular function during exercise with quantitative Doppler tissue imaging in children late after repair of tetralogy of Fallot. *J Am Soc Echocardiogr*. 2004;17:863-9. 14.
52. Winter MM, Scherptong RW, Kumar S, Bouma BJ, Tulevski I, Tops LF, et al. Ventricular response to stress predicts outcome in adult patients with a systemic right ventricle. *Am Heart J*. 2010;160:870-6. 15.
53. La Gerche A, Prior DL, Heidbuchel H. Clinical consequences of intense endurance exercise must include assessment of the right ventricle. *J Am Coll Cardiol*. 2010;56:1263; author reply -4. 16.
54. Pulver AF, Puchalski MD, Bradley DJ, Minich LL, Su JT, Saarel EV, et al. Safety and imaging quality of MRI in pediatric and adult congenital heart disease patients with pacemakers. *Pacing Clin Electrophysiol*. 2009;32:450-6. 17.
55. Grothues F, Moon JC, Bellenger NG, Smith GS, Klein HU, Pennell DJ. Interstudy reproducibility of right ventricular volumes, function, and mass with cardiovascular magnetic resonance. *Am Heart J*. 2004;147:218-23. 18.
56. Fratz S, Schuhsbaeck A, Buchner C, Busch R, Meierhofer C, Martinoff S, et al. Comparison of accuracy of axial slices versus short-axis slices for measuring ventricular volumes by cardiac magnetic resonance in patients with corrected tetralogy of fallot. *Am J Cardiol*. 2009;103:1764-9. 19.

1. 57. Moroseos T, Mitsumori L, Kerwin WS, Sahn DJ, Helbing WA, Kilner PJ, et al. Comparison of Simpson's method and three-dimensional reconstruction for measurement of right ventricular volume in patients with complete or corrected transposition of the great arteries. *Am J Cardiol.* 2010;105:1603-9.
- 2.
- 3.
4. 58. Bodhey NK, Beerbaum P, Sarikouch S, Kropf S, Lange P, Berger F, et al. Functional analysis of the components of the right ventricle in the setting of tetralogy of Fallot. *Circ Cardiovasc Imaging.* 2008;1:141-7.
- 5.
6. 59. Wald RM, Haber I, Wald R, Valente AM, Powell AJ, Geva T. Effects of regional dysfunction and late gadolinium enhancement on global right ventricular function and exercise capacity in patients with repaired tetralogy of Fallot. *Circulation.* 2009;119:1370-7.
- 7.
8. 60. Dupont MV, Dragean CA, Coche EE. Right ventricle function assessment by MDCT. *AJR Am J Roentgenol.* 2011;196:77-86.
- 9.
10. 61. Gao Y, Du X, Liang L, Cao L, Yang Q, Li K. Evaluation of right ventricular function by 64-row CT in patients with chronic obstructive pulmonary disease and cor pulmonale. *Eur J Radiol.* 2010.
11. 62. Plumhans C, Muhlenbruch G, Rapae A, Sim KH, Seyfarth T, Gunther RW, et al. Assessment of global right ventricular function on 64-MDCT compared with MRI. *AJR Am J Roentgenol.* 2008;190:1358-61.
12. 63. Muller M, Teige F, Schnapauff D, Hamm B, Dewey M. Evaluation of right ventricular function with multidetector computed tomography: comparison with magnetic resonance imaging and analysis of inter- and intraobserver variability. *Eur Radiol.* 2009;19:278-89.
13. 64. Coche E, Walker MJ, Zech F, de Crombrugge R, Vlassenbroek A. Quantitative right and left ventricular functional analysis during gated whole-chest MDCT: a feasibility study comparing automatic segmentation to semi-manual contouring. *Eur J Radiol.* 2010;74:e138-43.
14. 65. Savino G, Zwerner P, Herzog C, Politi M, Bonomo L, Costello P, et al. CT of cardiac function. *J Thorac Imaging.* 2007;22:86-100.
15. 66. Ou P, Celermajer DS, Calcagni G, Brunelle F, Bonnet D, Sidi D. Three-dimensional CT scanning: a new diagnostic modality in congenital heart disease. *Heart.* 2007;93:908-13.
16. 67. Geva T, Sandweiss BM, Gauvreau K, Lock JE, Powell AJ. Factors associated with impaired clinical status in long-term survivors of tetralogy of Fallot repair evaluated by magnetic resonance imaging. *J Am Coll Cardiol.* 2004;43:1068-74.
17. 68. Rutledge JM, Nihill MR, Fraser CD, Smith OE, McMahon CJ, Bezold LI. Outcome of 121 patients with congenitally corrected transposition of the great arteries. *Pediatr Cardiol.* 2002;23:137-45.
18. 69. Hraska V, Duncan BW, Mayer JE, Jr., Freed M, del Nido PJ, Jonas RA. Long-term outcome of surgically treated patients with corrected transposition of the great arteries. *J Thorac Cardiovasc Surg.* 2005;129:182-91.
19. 70. Piran S, Veldtman G, Siu S, Webb GD, Liu PP. Heart failure and ventricular dysfunction in patients with single or systemic right ventricles. *Circulation.* 2002;105:1189-94.
20. 71. Winter MM, Bouma BJ, Hardziyenka M, De Bruin-Bon RH, Tan HL, Konings TC, et al. Echocardiographic determinants of the clinical condition in patients with a systemic right ventricle. *Echocardiography.* 2010;27:1247-55.
21. 72. Forfia PR, Fisher MR, Mathai SC, Houston-Harris T, Hemnes AR, Borlaug BA, et al. Tricuspid annular displacement predicts survival in pulmonary hypertension. *Am J Respir Crit Care Med.* 2006;174:1034-41.
22. 73. van Wolferen SA, Marcus JT, Boonstra A, Marques KM, Bronzwaer JG, Spreeuwenberg MD, et al. Prognostic value of right ventricular mass, volume, and function in idiopathic pulmonary arterial hypertension. *Eur Heart J.* 2007;28:1250-7.
23. 74. Nath J, Demarco T, Hourigan L, Heidenreich PA, Foster E. Correlation between right ventricular indices and clinical improvement in epoprostenol treated pulmonary hypertension patients. *Echocardiography.* 2005;22:374-9.
- 24.
- 25.
- 26.
- 27.
- 28.
- 29.
- 30.
- 31.
- 32.
- 33.
- 34.
- 35.
- 36.
- 37.
- 38.
- 39.

75. Giusca S, Dambrauskaite V, Scheurwegs C, D'Hooge J, Claus P, Herbots L, et al. Deformation imaging describes right ventricular function better than longitudinal displacement of the tricuspid ring. *Heart*. 2010;96:281-8. 1.
 76. Ghio S, Gavazzi A, Campana C, Inserra C, Klersy C, Sebastiani R, et al. Independent and additive prognostic value of right ventricular systolic function and pulmonary artery pressure in patients with chronic heart failure. *J Am Coll Cardiol*. 2001;37:183-8. 2.
 77. de Groote P, Millaire A, Foucher-Hossein C, Nugue O, Marchandise X, Ducloux G, et al. Right ventricular ejection fraction is an independent predictor of survival in patients with moderate heart failure. *J Am Coll Cardiol*. 1998;32:948-54. 3.
 78. Zornoff LA, Skali H, Pfeffer MA, St John Sutton M, Rouleau JL, Lamas GA, et al. Right ventricular dysfunction and risk of heart failure and mortality after myocardial infarction. *J Am Coll Cardiol*. 2002;39:1450-5. 4.
 79. Antoni ML, Scherptong RW, Atary JZ, Boersma E, Holman ER, van der Wall EE, et al. Prognostic value of right ventricular function in patients after acute myocardial infarction treated with primary percutaneous coronary intervention. *Circ Cardiovasc Imaging*. 2010;3:264-71. 5.
 80. Macron L, Lim P, Bensaid A, Nahum J, Dussault C, Mitchell-Heggs L, et al. Single-beat versus multibeam real-time 3D echocardiography for assessing left ventricular volumes and ejection fraction: a comparison study with cardiac magnetic resonance. *Circ Cardiovasc Imaging*. 2010;3:450-5. 6.
 81. Shahgaldi K, Manouras A, Abrahamsson A, Gudmundsson P, Brodin LA, Winter R. Three-dimensional echocardiography using single-heartbeat modality decreases variability in measuring left ventricular volumes and function in comparison to four-beat technique in atrial fibrillation. *Cardiovasc Ultrasound*. 2010;8:45. 7.
 82. Soliman OI, Krenning BJ, Geleijnse ML, Nemes A, van Geuns RJ, Baks T, et al. A comparison between QLAB and TomTec full volume reconstruction for real time three-dimensional echocardiographic quantification of left ventricular volumes. *Echocardiography*. 2007;24:967-74. 8.
 83. Szmigielski C, Rajpoot K, Grau V, Myerson SG, Holloway C, Noble JA, et al. Real-time 3D fusion echocardiography. *JACC Cardiovasc Imaging*. 2010;3:682-90. 9.
10.
11.
12.
13.
14.
15.
16.
17.
18.
19.
20.
21.
22.
23.
24.
25.
26.
27.
28.
29.
30.
31.
32.
33.
34.
35.
36.
37.
38.
39.



Chapter 11

Summary - Samenvatting



1. SUMMARY

2.

3. Part 1: Echocardiography in congenital heart disease

4. In Chapter 1 a general introduction to the characteristics of the right ventricle is provided. Not
5. only basic information on right ventricular (RV) anatomy and function is given, but also the
6. various imaging techniques used for RV assessment, are described. Furthermore, the outline
7. of the thesis is given. A systematic review of the clinical value of echocardiographic imaging
8. modalities in patients with congenital heart disease is presented in Chapter 2 of this thesis.
9. Real-time three-dimensional echocardiography (real-time 3D echo) -derived measurements
10. were found to be more accurate for RV quantification than conventional two-dimensional
11. echocardiography-derived measurements in patients with tetralogy of Fallot, atrial septal
12. defects or systemic right ventricles. Doppler-based techniques measuring regional RV wall
13. motion velocities, strain, and strain rate showed a variable agreement with RV ejection fraction
14. (EF) by cardiac magnetic resonance (CMR) imaging, the reference technique for RV assessment..
15. In addition to the measurements suggested in the latest echocardiography and congenital
16. heart disease guidelines, we advised using real-time 3D echo for serial follow-up in patients
17. with congenital heart disease. In case of poor acoustic windows or if deterioration of RV
18. function is suspected based on echocardiographic measurements, CMR imaging remains the
19. indicated imaging technique. The use of all possible applications of real-time 3D echo in adult
20. congenital heart disease is described in Chapter 3. The assessment of RV volumes and EF is dis-
21. cussed, as well as the additional value of real-time 3D echo for imaging of cardiac morphology.
22. Illustrative examples of congenital abnormalities that are common in adults are described, and
23. implicate that the clinician does no longer have to reconstruct cardiac anatomy from multiple
24. two-dimensional images, but can have a realistic three-dimensional view.

25.

26. Part 2: Right ventricular acquisition, analysis, and clinical applications

27. In Chapter 4 the accuracy and reproducibility of real-time 3D echo were compared with conven-
28. tional two-dimensional echocardiographic measurements and CMR imaging in patients with
29. congenital heart disease and healthy controls. The participants underwent echocardiography
30. and CMR imaging and the results were compared. We found that real-time 3D echo improved
31. quantitative RV size and function assessment compared with two-dimensional echocardiog-
32. raphy alone. The reproducibility of real-time 3D echo was comparable to the two-dimensional
33. echocardiography-derived measurements on variability. Furthermore, receiver operating char-
34. acteristic curves revealed that real-time 3D echo-derived measurements were highly sensitive
35. and specific to identify RV dysfunction in patients with congenital heart disease. So, clinical
36. use of real-time 3D echo for RV quantification represents an additional value in RV assessment.
37. In Chapter 5 we investigated the test-retest variability of RV volume and EF measurements by
38. real-time 3D echo in patients with congenital heart disease and healthy controls. Conventional
39. reproducibility has been investigated extensively, but the test-retest variability, that more

closely represents everyday clinical use of the technique, was rarely examined. Two sonographers acquired three sequential RV datasets in each participant during one outpatient visit. The test-retest variability turned out to be good and, besides the practical nature of real-time 3D echo for RV volume and EF assessment, makes it a valuable technique for serial follow-up. Although it may be challenging to diminish all factors that influence serial echocardiographic examination, standardization of RV size and function measurements should be a goal to produce more interchangeable data.

In a clinical validation study including patients with a variety of congenital heart defects, we found real-time 3D echo to be feasible in about 80% of patients, as is described in Chapter 6. Furthermore, a good agreement was established between real-time 3D echo and CMR imaging. Compared with CMR imaging, real-time 3D echo resulted in smaller RV end-diastolic and end-systolic volumes. Importantly, the time needed for RV acquisition and analysis by real-time 3D echo was only some minutes and consequently much less than for CMR imaging. So, in the majority of unselected patients with complex congenital heart disease, real-time 3D echo provides fast and reproducible assessment of RV volumes and EF when using current commercially available hardware and software. In Chapter 7 we investigated the usefulness of real-time 3D echo to identify RV dysfunction in patients with congenital heart disease. First, we defined cut-off values for normal RV volumes and EF that were derived by CMR imaging in healthy controls. Thereafter, receiver operating characteristic curves were created in patients with various congenital heart diseases to obtain the sensitivity and the specificity of real-time 3D echo for identification of RV dysfunction. The best cut-off values predicting RV dysfunction based on real-time 3D echo were identified. Real-time 3D echo turned out to be a very sensitive tool to identify RV dysfunction in patients with congenital heart disease and could clinically be applied to rule out RV dysfunction or to identify patients whom may need further quantitative analysis of their RV function, for example using CMR imaging.

Part 3: Troubleshooting for right ventricular assessment

In Chapter 8 the potential sources of segmental volume differences between real-time 3D echo and CMR imaging were studied in patients with tetralogy of Fallot. As mentioned before in this summary, using real-time 3D echo results in smaller RV volumes compared with CMR imaging. Software that facilitates side by side comparison of echocardiographic and CMR-derived images, was applied. The differences found for RV volumes were caused by several sources related to either anatomical characteristics of the right ventricle or technological limitations of the used techniques. The main sources of RV volume differences between real-time 3D echo and CMR imaging were the RV anterior region which is poorly visualized by real-time 3D echo, the use of disc summation by CMR imaging, and the visualization and management of trabeculae. The understanding of this intermodality discordance will help to implement real-time 3D echo into clinical practice, assuming that consensus will be reached regarding a uniform methodology for contour delineation. Because the identification of the RV endocardial border

1. represents a crucial step in RV analysis, we investigated the value of using contrast on both RV
2. endocardial border visualization and quantification in Chapter 9. Non contrast-enhanced and
3. contrast-enhanced real-time 3D echo datasets were obtained to determine RV volumes and
4. EF. A 17-segment RV model was used to grade the endocardial border definition. Three image-
5. quality groups (good, fair, and uninterpretable) were identified. During contrast-enhanced 3D
6. echo, compared with non contrast-enhanced 3D echo, the number of segments with optimal
7. visualization of the endocardial border increased as well as the number of participants with
8. a good-quality echocardiogram. On the other hand, the RV outflow tract and inferior wall
9. appeared worse compared with non contrast-enhanced real-time 3D echo. Furthermore,
10. smaller RV volumes were found using contrast-enhanced real-time 3D echo compared with
11. non contrast-enhanced real-time 3D echo. The variability of the contrast-enhanced versus the
12. non contrast-enhanced real-time 3D echo images was not different. So, using echo contrast
13. does not provide the ultimate solution for poor RV visibility and quantification. At this moment,
14. it is not advised to use contrast-enhanced real-time 3D echo for RV analysis.

15. In Chapter 10 the findings of this thesis are evaluated. Results of our studies concerning
16. the assessment of RV size and function and the prognostic importance of RV function in
17. cardiac disease are discussed in the context of known literature on these topics. Furthermore,
18. future perspectives on the clinical role of real-time 3D echo-derived RV volumes and EF were
19. described.

20.
21.
22.
23.
24.
25.
26.
27.
28.
29.
30.
31.
32.
33.
34.
35.
36.
37.
38.
39.

1. **SAMENVATTING**

2.

3. Deel 1: Echocardiografie bij congenitale hartziekten

4. In Hoofdstuk 1 worden in de algemene introductie de karakteristieken van de rechter ventrikel
5. (RV) beschreven. Naast basisinformatie over RV anatomie en functie, komen ook de verschei-
6. dene beeldvormingstechnieken die gebruikt worden voor RV bepalingen aan bod. Verder is
7. een overzicht van de inhoud van dit proefschrift weergegeven. Een systematisch overzichts-
8. artikel betreffende de klinische waarde van echocardiografische beeldvormingsmodaliteiten
9. bij patiënten met congenitale hartziekten is weergegeven in Hoofdstuk 2. Hieruit bleken RV
10. metingen met behulp van real-time driedimensionale echocardiografie (3D echo) meer accu-
11. raat te zijn dan de gebruikelijke tweedimensionale echocardiografische metingen bij patiënten
12. de volgende specifieke congenitale hartziekten: tetralogie van Fallot, atrium septum defect en
13. systemische rechter ventrikel. De toepassing van Doppler echocardiografie, waarmee regionale
14. RV wandbewegingsnelheden, strain, en strain rate kunnen worden bepaald, resulteerde in
15. een wisselende overeenkomst met RV ejectiefractie (EF) op basis van cardiale magnetische
16. resonantie imaging (MRI), de referentietechniek voor bepaling van RV volumina en EF. Naast
17. de metingen die gedaan zouden moeten worden volgens de meest recente richtlijnen wat
18. betreft echocardiografie en wat betreft aangeboren hartafwijkingen, is het wenselijk om 3D
19. echo toe te passen voor seriële follow-up van patiënten met congenitale hartziekten. In het
20. geval van onvoldoende beeldvormingskwaliteit of als een achteruitgang van de RV functie
21. wordt vastgesteld op basis van echocardiografische metingen, is MRI de aangewezen techniek.
22. Het spectrum aan mogelijke toepassingen van 3D echo bij volwassenen met congenitale
23. hartziekten is beschreven in Hoofdstuk 3. De berekening van RV volumina en EF is becom-
24. mentarieerd, evenals de toegevoegde waarde van 3D echo voor het in beeld brengen van de
25. cardiale morfologie. Illustratieve voorbeelden van congenitale hartziekten die gezien worden
26. op de volwassenen leeftijd zijn beschreven. Dit impliceert dat de dokter niet langer de cardiale
27. anatomie in het hoofd hoeft te reconstrueren op basis van tweedimensionale afbeeldingen,
28. maar hij/ zij ziet zich direct geconfronteerd met een realistische driedimensionale afbeelding.

29.

30.

31. Deel 2: Rechter ventrikelacquisitie, -analyse en klinische toepassingen

32. In Hoofdstuk 4 worden de accuraatheid en reproduceerbaarheid van RV metingen op basis van
33. 3D echo vergeleken met conventionele tweedimensionale echocardiografie en MRI bij patiën-
34. ten met congenitale hartziekten en gezonde vrijwilligers. De geïncludeerde personen onder-
35. gingen elk de drie beeldvormingsonderzoeken en de resultaten hiervan werden met elkaar
36. vergeleken. We vonden dat 3D echo een toegevoegde waarde had wat betreft de accuraatheid
37. van de metingen ten opzichte van tweedimensionale echocardiografie, wanneer vergeleken
38. met MRI. De reproduceerbaarheid van de metingen op basis van 3D echo was vergelijkbaar
39. met die gebaseerd op tweedimensionale echocardiografie. Receiver operating characteristic

curves lieten zien dat metingen verkregen met 3D echo zeer sensitief en specifiek waren om RV disfunctie op te sporen bij patiënten met congenitale hartziekten. Kortom, klinisch gebruik van 3D echo voor de bepaling van de RV grootte en functie resulteert in een verbetering ten opzichte van het gebruik van tweedimensionale echocardiografie alleen. In Hoofdstuk 5 hebben we de test-retest variabiliteit onderzocht van RV volume en EF metingen gebaseerd op 3D echo bij patiënten met congenitale hartziekten en gezonde vrijwilligers. Conventionele reproduceerbaarheid was al uitgebreid onderzocht, maar de test-retest variabiliteit, die beter overeenkomt met de dagelijks klinische praktijk, was nog nauwelijks onderzocht. Twee echocardiografisten hebben drie opeenvolgende RV datasets opgenomen bij elke deelnemer tijdens een poliklinisch bezoek. De test-retest variabiliteit bleek goed te zijn en maakt dat 3D echo, naast de praktische aard van de techniek, een waardevolle techniek is voor seriële follow-up. Hoewel het moeilijk is om alle factoren uit te schakelen die van invloed zijn op seriële echocardiografische onderzoeken, zal standaardisatie van RV metingen een doel moeten zijn om data te verkrijgen die uitwisselbaar zijn tussen de verschillende afdelingen of ziekenhuizen.

In een klinische validatie studie bij patiënten met een verscheidenheid aan congenitale hartziekten vonden we dat 3D echo bij zo'n 80% van opeenvolgend geïnccludeerde patiënten kon worden toegepast, zoals beschreven is in Hoofdstuk 6. Verder werd een goede overeenkomst tussen RV volumina en EF op basis van 3D echo en MRI gevonden. In vergelijking met MRI waren de RV volumina die gemeten werden met 3D echo kleiner. Een belangrijke bevinding was dat de tijd die benodigd was om de rechter ventrikel in beeld te brengen en te analyseren, slechts enkele minuten bedroeg en dus veel korter is dan wanneer gebruik gemaakt wordt van MRI. Dus, bij de meerderheid van de ongeselecteerde patiënten met congenitale hartziekten, voorziet 3D echo in snelle en reproduceerbare metingen van RV volumina en EF indien gebruik gemaakt wordt van de huidige, commercieel beschikbare, hardware en software. In Hoofdstuk 7 hebben we de bruikbaarheid van 3D echo voor het vaststellen van RV disfunctie bij patiënten met congenitale hartziekten onderzocht. Eerst hebben we de normaalwaarden voor RV volumina en functie bepaald aan de hand van MRI waarden van gezonde vrijwilligers. Daarna hebben we gebruik gemaakt van receiver operating characteristic curves bij patiënten met congenitale hartziekten, om de sensitiviteit en de specificiteit van 3D echo voor het vaststellen van RV disfunctie te bepalen. We hebben de beste afkapwaarden die RV disfunctie op basis van 3D echo voorspelden, vastgesteld. 3D echo bleek een heel sensitieve methode te zijn om RV disfunctie bij patiënten met congenitale hartziekten te identificeren en kan klinisch toegepast worden om RV disfunctie uit te sluiten of om patiënten te identificeren die verdere kwantitatieve analyse van hun RV functie behoeven, door bijvoorbeeld gebruik te maken van MRI.

Deel 3: Probleemanalyse voor rechter ventrikel bepalingen

In Hoofdstuk 8 zijn de potentiële bronnen van volumeverschillen tussen 3D echo en MRI bestudeerd bij patiënten met tetralogie van Fallot. Zoals eerder in deze samenvatting genoemd, zijn de RV volumina berekend op basis van 3D echo kleiner dan die bepaald met MRI. Software die

1. een zij aan zij weergave van de 3D echo en MRI beelden mogelijk maakt, was voor deze studie
2. gebruikt. De verschillen die gevonden werden tussen de RV volumina bleken veroorzaakt te
3. zijn door verscheidene bronnen, die ofwel samenhangen met anatomische RV karakteristieken
4. ofwel met de technologische beperkingen van de gebruikte technieken. De belangrijkste
5. bronnen van verschillen tussen RV volumina op basis van 3D echo en MRI bleken de matige
6. afbeelding van het RV anterieure segment met 3D echo, het gebruik van de methode van disc
7. sommatie voor RV bepalingen met MRI en de afbeelding en hantering van trabekels. Begrip
8. van de verschillen tussen beide technieken zal de implementatie van 3D echo in de klinische
9. praktijk vergemakkelijken. Omdat het traceren van de RV endocardiale grens een cruciale stap
10. betreft in de RV analyse, hebben we de waarde van het gebruik van contrast onderzocht
11. op zowel de zichtbaarheid van de RV endocardiale grens en de RV bepalingen in Hoofdstuk
12. 9. 3D echo datasets met en zonder contrast werden opgenomen om RV volumina en EF te
13. bepalen. Een 17-segment RV model werd gebruikt om de definitie van de endocardiale grens
14. te graderen voor de verschillende RV segmenten. Drie groepen met een verschillende beeld-
15. vormingskwaliteit (goed, redelijk en niet te interpreteren) werden vastgesteld. Bij het gebruik
16. van contrast nam het aantal segmenten met een optimale afbeelding van de endocardial
17. grens toe alsook het aantal deelnemers met een goede kwaliteit echocardiogram. Echter bij
18. het bekijken van segmentale verschillen bleek juist dat de RV uitstroombaan en onderwand
19. slechter afgebeeld werden bij het gebruik van contrast. Verder werden kleinere RV volumina
20. gevonden bij de toepassing van contrast. De variabiliteit van de RV metingen op basis van 3D
21. echo verschilde niet. Dus, het gebruiken van contrast voorziet niet in de ultieme oplossing voor
22. matige RV beeldvorming en kwantificatie. Op dit moment is er geen indicatie om contrast toe
23. te passen bij toepassing van 3D echo voor RV bepalingen.

24. In Hoofdstuk 10 worden de bevindingen uit dit proefschrift geëvalueerd. De studieresultaten
25. betreffende de bepaling van RV grootte en functie met 3D echo en de prognostische betekenis
26. van RV functie bij cardiale ziekten, worden weergegeven binnen de context van bekende litera-
27. tuur. Verder worden ook de verwachtingen ten aanzien van toekomstige ontwikkelingen en de
28. klinische toepassing van 3D echo voor RV volumina en EF, beschreven.

29.

30.

31.

32.

33.

34.

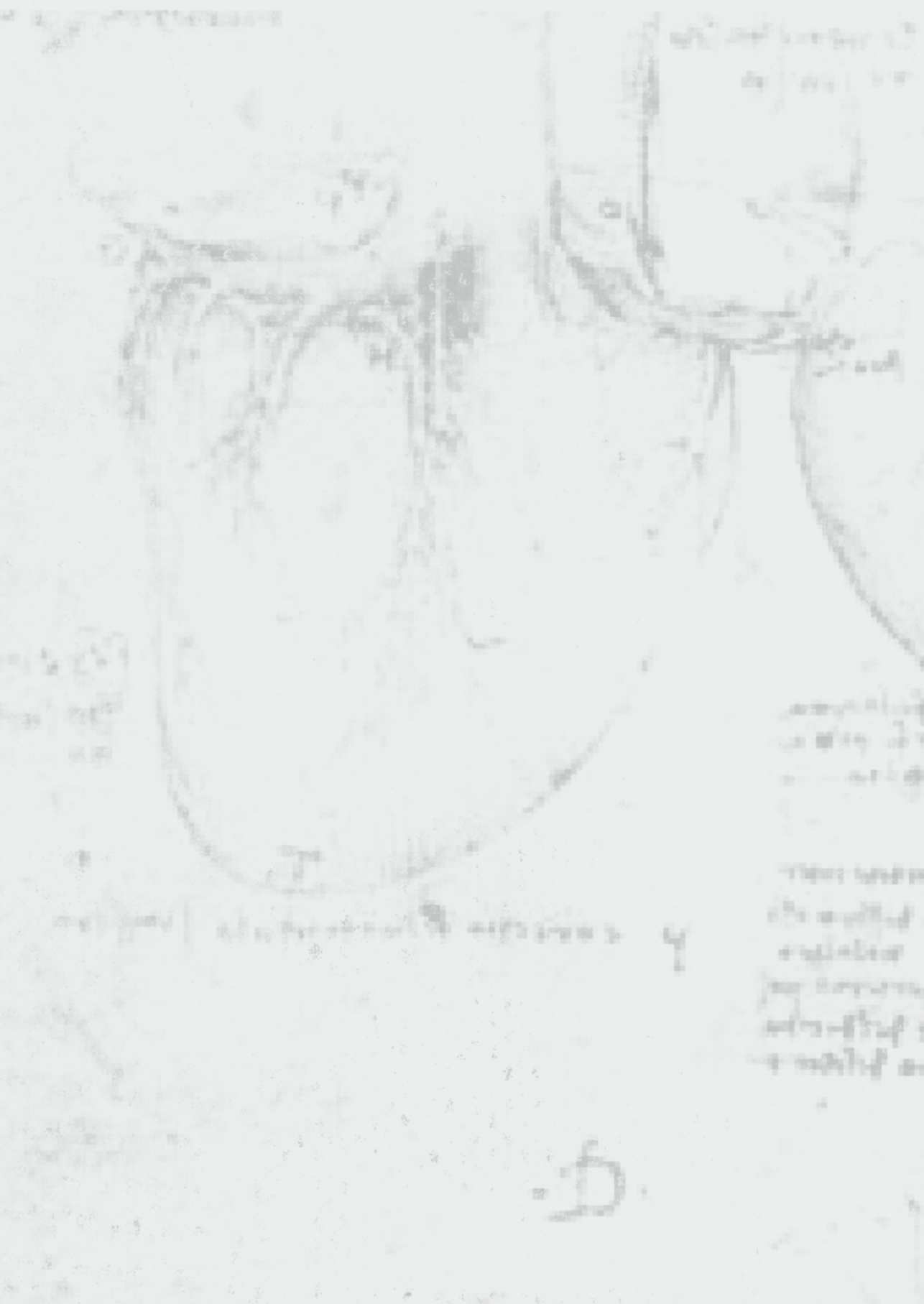
35.

36.

37.

38.

39.





List of publications

Abstracts

Related awards

PhD portfolio

About the author

Dankwoord

1. LIST OF PUBLICATIONS

- 2.
3. **1.** Soliman OI, Kirschbaum SW, van Dalen BM, **van der Zwaan HB**, Mahdavian Delavary B, Vletter WB, van Geuns RJ, Ten Cate FJ, Geleijnse ML. Accuracy and reproducibility of quantitation of left ventricular function by real-time three-dimensional echocardiography versus cardiac magnetic resonance. *Am J Cardiol.* 2008 Sep 15;102(6):778-83.
- 4.
- 5.
- 6.
7. **2.** Soliman OI, van Dalen BM, Nemes A, **van der Zwaan HB**, Vletter WB, ten Cate FJ, Theuns DA, Jordaens LJ, Geleijnse ML. Quantification of left ventricular systolic dyssynchrony by real-time three-dimensional echocardiography. *J Am Soc Echocardiogr.* 2009 Mar;22(3):232-9.
- 8.
- 9.
10. **3.** van Dalen BM, Soliman OI, Vletter WB, Kauer F, **van der Zwaan HB**, ten Cate FJ, Geleijnse ML. Feasibility and reproducibility of left ventricular rotation parameters measured by speckle tracking echocardiography. *Eur J Echocardiogr.* 2009 Jul;10(5):669-76.
- 11.
- 12.
13. **4.** van Dalen BM, Kauer F, Michels M, Soliman OI, Vletter WB, **van der Zwaan HB**, ten Cate FJ, Geleijnse ML. Delayed left ventricular untwisting in hypertrophic cardiomyopathy. *J Am Soc Echocardiogr.* 2009 Dec;22(12):1320-6.
- 14.
- 15.
16. **5.** van Dalen BM, Kauer F, Vletter WB, Soliman OI, **van der Zwaan HB**, Ten Cate FJ, Geleijnse ML. Influence of cardiac shape on left ventricular twist. *J Appl Physiol.* 2010 Jan;108(1):146-51.
- 17.
- 18.
19. **6.** van Dalen BM, Soliman OI, Kauer F, Vletter WB, **van der Zwaan HB**, Cate FJ, Geleijnse ML. Alterations in left ventricular untwisting with ageing. *Circ J.* 2010 Jan;74(1):101-8.
- 20.
21. **7.** **van der Zwaan HB**, Helbing WA, McGhie JS, Geleijnse ML, Luijnenburg SE, Roos-Hesselink JW, Meijboom FJ. Clinical value of real-time three-dimensional echocardiography for right ventricular quantification in congenital heart disease: validation with cardiac magnetic resonance imaging. *J Am Soc Echocardiogr.* 2010 Feb;23(2):134-40.
- 22.
- 23.
- 24.
25. **8.** Soliman OI, De Jong N, **Van Der Zwaan HB**, Galema TW, Vletter WB, Van Dalen BM, Schinkel AF, Ten Cate FJ, Geleijnse ML. Contrast echocardiography: mechanism of action, safety and clinical applications. *Minerva Cardioangiol.* 2010 Jun;58(3):343-55.
- 26.
- 27.
28. **9.** **van der Zwaan HB**, Helbing WA, Boersma E, Geleijnse ML, McGhie JS, Soliman OI, Roos-Hesselink JW, Meijboom FJ. Usefulness of real-time three-dimensional echocardiography to identify right ventricular dysfunction in patients with congenital heart disease. *Am J Cardiol.* 2010 Sep 15;106(6):843-50.
- 29.
- 30.
- 31.
32. **10.** **van der Zwaan HB**, Stoel MG, Roos-Hesselink JW, Veen G, Boersma E, von Birgelen C. Early versus late ST-segment resolution and clinical outcomes after percutaneous coronary intervention for acute myocardial infarction. *Neth Heart J.* 2010 Sep;18(9):416-22.
- 33.
- 34.
35. **11.** van Dalen BM, Caliskan K, Soliman OI, Kauer F, **van der Zwaan HB**, Vletter WB, van Vark LC, Ten Cate FJ, Geleijnse ML. Diagnostic value of rigid body rotation in noncompaction cardiomyopathy. *J Am Soc Echocardiogr.* 2011.
- 36.
- 37.
38. **12.** **van der Zwaan HB**, Geleijnse ML, Soliman OI, McGhie JS, Wiegers-Groeneweg EJA, Helbing WA, Roos-Hesselink JW, Meijboom FJ. Test-Retest Variability of Volumetric Right
- 39.

- Ventricular Measurements Using Real-Time Three-Dimensional Echocardiography. *J Am Soc Echocardiogr.* 2011. 1. 2.
- 13. van der Zwaan HB**, Geleijnse ML, McGhie JS, Boersma E, Helbing WA, Meijboom FJ, Roos-Hesselink JW. Right ventricular quantification in clinical practice: two-dimensional versus three-dimensional echocardiography compared with cardiac magnetic resonance imaging. *Eur J Echocardiogr.* 2011 3. 4. 5. 6.
- 14. van der Zwaan HB**, Roos-Hesselink JW, Boersma E, Helbing WA, Soliman OII, Geleijnse ML, Meijboom FJ. Right ventricular quantification in congenital heart disease: a systematic review on conventional and new echocardiographic techniques. Submitted. 7. 8. 9.
- 15. van der Zwaan HB**, Leung KYE, Soliman OII, van Burken G, Bosch JG, McGhie JS, Roos-Hesselink JW, Meijboom FJ, Geleijnse ML, Helbing WA. Sources of differences in volumetric right ventricular estimation using a 9-Segment model: real-time 3-dimensional echocardiography versus cardiac magnetic resonance imaging. Submitted. 10. 11. 12. 13.
- 16. van der Zwaan HB**, Gommans F, Geleijnse ML, McGhie JS, Meijboom FJ, van Dijk AP, Roos-Hesselink JW. Right Ventricular Visualization and Quantification by Using Contrast in Real-Time Three-Dimensional Echocardiography. Submitted. 14. 15. 16. 17. 18. 19. 20. 21. 22. 23. 24. 25. 26. 27. 28. 29. 30. 31. 32. 33. 34. 35. 36. 37. 38. 39.

1. ABSTRACTS

2.

3. Nederlandse Vereniging voor Cardiologie voorjaarscongres 2009, Amsterdam:

4. **1. van der Zwaan HB**, Helbing WA, McGhie JS, Geleijnse ML, Roos-Hesselink JW, Meijboom
5. FJ. Feasibility and accuracy of real-time 3-dimensional echocardiography for right ventri-
6. cular function in congenital heart disease: validation with cardiac magnetic resonance
7. imaging. Oral Presentation.

8.

9. Annual Congress of the European Society of Cardiology 2009, Barcelona, Spain:

10. **2. van der Zwaan HB**, Helbing WA, McGhie JS, Geleijnse ML, Roos-Hesselink JW, Meijboom
11. FJ. Feasibility and accuracy of real-time 3-dimensional echocardiography for right ventri-
12. cular function in congenital heart disease: validation with cardiac magnetic resonance
13. imaging. Oral Presentation.

14.

15. Nederlandse Vereniging voor Cardiologie najaarscongres 2009, Amsterdam:

16. **3. van der Zwaan HB**, Soliman Oll, Helbing WA, McGhie JS, Roos-Hesselink JW, Geleijnse ML,
17. Meijboom FJ. The ability of real-time 3-dimensional echocardiography to identify right
18. ventricular dysfunction in congenital heart disease. *Oral Presentation*.

19.

20. EuroEcho 2009, Madrid, Spain:

21. **4. van der Zwaan HB**, Soliman Oll, Helbing WA, McGhie JS, Roos - Hesselink JW, Geleijnse
22. ML, Meijboom FJ. The ability of real-time 3-dimensional echocardiography to identify
23. right ventricular dysfunction in congenital heart disease. *Poster Presentation*.

24.

25. Nederlandse Vereniging voor Cardiologie voorjaarscongres 2010, Papendal:

26. **5. van der Zwaan HB**, Leung KYE, Soliman Oll, van Burken G, Bosch JG, McGhie JS, Roos-
27. Hesselink JW, Geleijnse ML, Meijboom FJ, Helbing WA. Sources of differences in volumetric
28. right ventricular estimation using a nine-segment model: real-time three-dimensional
29. echocardiography and cardiac magnetic resonance imaging. *Poster Presentation*.

30.

31. Annual Congress of the European Society of Cardiology 2010, Stockholm, Sweden:

32. **6. van der Zwaan HB**, Helbing WA, Geleijnse ML, McGhie JS, Roos-Hesselink JW, Meijboom
33. FJ. Comparing right ventricular measurements in healthy Dutch volunteers with the cur-
34. rent guidelines. *Poster Presentation*.

35.

36. Nederlandse Vereniging voor Cardiologie najaarscongres 2010, Egmond aan Zee:

37. **7. van der Zwaan HB**, Geleijnse ML, McGhie JS, Boersma E, Helbing WA, Meijboom FJ, Roos-
38. Hesselink JW. Right ventricular quantification: two-dimensional versus three-dimensional
39. echocardiography as compared to cardiac magnetic resonance imaging. *Oral Presentation*.

EuroEcho 2010, Copenhagen, Denmark:	1.
8. van der Zwaan HB , Meijboom FJ, McGhie JS, Helbing WA, Geleijnse ML, Roos-Hesselink JW. Echocardiographic variables of right ventricular size and function in patients with congenital heart disease: comparison with cardiac magnetic resonance imaging <i>Moderated Poster Presentation</i> .	2. 3. 4. 5.
9. van der Zwaan HB , Leung KYE, Soliman OII, van Burken G, Bosch JG, McGhie JS, Roos-Hesselink JW, Geleijnse ML, Meijboom FJ, Helbing WA. Sources of differences in volumetric right ventricular estimation using a 9-segment model: real-time 3-dimensional echocardiography and cardiac magnetic resonance imaging. <i>Moderated Poster Presentation</i> .	6. 7. 8. 9. 10.
Annual Congress of the European Society of Cardiology 2011, Paris, France:	11.
10. van der Zwaan HB , Geleijnse ML, Soliman OII, McGhie JS, Wiegiers-Groeneweg EJA, Helbing WA, Roos-Hesselink JW, Meijboom FJ. Test-retest variability of volumetric right ventricular measurements using real-time three-dimensional echocardiography.	12. 13. 14.
11. van der Zwaan HB , Gommans F, Geleijnse ML, McGhie JS, Meijboom FJ, van Dijk AP, Roos-Hesselink JW. Right ventricular visualization and quantification using contrast using real-time three-dimensional echocardiography.	15. 16. 17. 18. 19. 20. 21. 22. 23. 24. 25. 26. 27. 28. 29. 30. 31. 32. 33. 34. 35. 36. 37. 38. 39.

AWARDS

- 1.
- 2.
3. - Price best oral presentation Congenital heart disease session "Nederlandse Vereniging voor Cardiologie voorjaarscongres 2009" (Feasibility and accuracy of real-time 3-dimensional echocardiography for right ventricular function in congenital heart disease: validation with cardiac magnetic resonance imaging)
- 4.
- 5.
- 6.
7. - Price best poster presentation Imaging session "Nederlandse Vereniging voor Cardiologie voorjaarscongres 2010" (Sources of differences in volumetric right ventricular estimation using a nine-segment model: real-time three-dimensional echocardiography and cardiac magnetic resonance imaging)
- 8.
- 9.
- 10.
11. - Price best oral presentation Heart failure session "Nederlandse Vereniging voor Cardiologie najaarscongres 2010" (Right ventricular quantification: two-dimensional versus three-dimensional echocardiography as compared with cardiac magnetic resonance imaging)
- 12.
- 13.
- 14.
- 15.
- 16.
- 17.
- 18.
- 19.
- 20.
- 21.
- 22.
- 23.
- 24.
- 25.
- 26.
- 27.
- 28.
- 29.
- 30.
- 31.
- 32.
- 33.
- 34.
- 35.
- 36.
- 37.
- 38.
- 39.

1. PHD PORTFOLIO SUMMARY

3. Summary of PhD training and teaching activities

Heleen B. van der Zwaan	PhD period: April 2008- Jan 2011
Erasmus MC Department: Cardiology	Promotor(s): Prof.dr. J.W. Roos-Hesselink;
Research School: Coeur	Prof.dr. W.A. Helbing
	Co-promotor: Dr. F.J. Meijboom

9. 1. PhD training

	Year	Workload (ECTS)
--	-------------	----------------------------

12. General academic skills

- Biomedical English Writing and Communication	2009	2.0
- Research Integrity		
- NWO Talent class "Branding Yourself"	2009	2.0
- NWO Talent class "Networking"	2010	0.5
	2010	0.5

18. Research skills

- Statistics "Classical Methods for Data-Analysis"	2008	5.7
--	------	-----

21. In-depth courses (e.g. Research school, Medical Training)

- Cardiac function and adaptation, Papendal		
- Coeur courses on congenital heart disease and cardiovascular imaging and diagnostics	2008 2009 - 2010	2.0 3.0

27. Presentations

28. Oral presentations

- Coeur courses on congenital heart disease, Erasmus MC Rotterdam	2009	0.3
- Nederlandse Vereniging voor Cardiologie voorjaarscongres, Amsterdam	2009	0.9
- Annual Congress of the European Society of Cardiology, Barcelona, Spain	2009	1.8
- 4th European Echocardiography Course on Congenital Heart Disease, Rotterdam	2009	1.5
- Nederlandse Vereniging voor Cardiologie najaarscongres, Amsterdam	2009	0.9

	Year	Workload (ECTS)	
- Congres Algemene Cardiologie, Davos, Switzerland	2010	1.2	1.
- Nederlandse Vereniging voor Cardiologie voorjaarscongres, Amsterdam	2010	0.9	2.
- Wetenschappelijke vergadering sectie Kindercardiologie, Nijmegen	2010	0.6	3.
- 44 th annual meeting Association for European Paediatric Cardiology, Innsbruck, Austria	2010	1.2	4.
- Three-Dimensional Echo Course, Rotterdam	2010	0.9	5.
- PhD day Coeur, Rotterdam	2010	0.6	6.
- Academic innovations in Grown-Up Congenital Heart Disease, Zeist	2010	0.6	7.
- Nederlandse Vereniging voor Cardiologie najaarscongres, Egmond aan Zee	2010	0.9	8.
- EuroEcho, Copenhagen, Denmark	2010	1.8	9.
- Interactieve echocursus voor gevorderden: aangeboren hartafwijkingen, Rotterdam	2011	0.6	10.
- Coeur course on congenital heart disease, Erasmus MC, Rotterdam	2011	0.3	11.
(Moderated) poster presentations			12.
- EuroEcho, Madrid, Spain	2009	1.5	13.
- Annual Congress of the European Society of Cardiology, Stockholm, Sweden	2010	1.8	14.
International conferences			15.
- Three-dimensional cardiac imaging in comparison, Berlin, Germany	2008	0.6	16.
- EuroEcho, Lyon, France	2008	1.2	17.
Seminars and workshops			18.
- Coeur research seminars and lectures	2008 – 2010	1.9	19.
Didactic skills			20.
- Course Teach the Teacher, Erasmus MC, Rotterdam	2008 – 2010	1.9	21.
			22.
			23.
			24.
			25.
			26.
			27.
			28.
			29.
			30.
			31.
			32.
			33.
			34.
			35.
			36.
			37.
			38.
			39.

1. **2. Teaching activities**2. **Lecturing**

3. - Patiënten voorlichtingsdag	2010	0.6
---------------------------------	------	-----

4. **Supervising practicals Erasmus MC**

5. - Keuze-onderwijs tweedejaars geneeskunde studenten	2009 – 2010	
--	-------------	--

6. - RISK onderwijs	2010	
---------------------	------	--

7. - Junior Med School	2010	
------------------------	------	--

8. - Minor onderwijs aangeboren hartafwijkingen	2010	
---	------	--

9.

10.

11.

12.

13.

14.

15.

16.

17.

18.

19.

20.

21.

22.

23.

24.

25.

26.

27.

28.

29.

30.

31.

32.

33.

34.

35.

36.

37.

38.

39.

1. ABOUT THE AUTHOR

2.

3. Heleen Berdina van der Zwaan was born on December 3rd, 1982 in Alkmaar, The Netherlands.

4. After graduating summa cum laude from secondary school in 2001 (VWO, Nature & Health, Erf-

5. gooiers College, Huizen), she started her medicine study at the Free University in Amsterdam.

6. During medical school, she worked in the Anatomy department, teaching to medicine- and

7. biomedical students. She was an active member of the “Jaar Vertegenwoordigers Commis-

8. sie” of the Free University. During the second year, her interest in cardiology was raised and

9. she chose to follow a special, optional program on Heart- and Vessel diseases. Furthermore,

10. she participated in a research project on ST-segment resolution and clinical outcomes after

11. percutaneous coronary intervention for acute myocardial infarction (head; Prof.dr. C.A. Visser).

12. In 2007 she graduated summa cum laude from medical school and began to work as a cardiol-

13. ogy resident at the Erasmus MC Thoraxcenter in Rotterdam. After three months, she started a

14. research project concerning right ventricular assessment using real-time 3D echo in patients

15. with congenital heart disease, under the supervision of Prof.dr. J.W. Roos-Hesselink, Prof.dr. W.A.

16. Helbing and Dr. F.J. Meijboom. April 2011 she started working in the internal medicine depart-

17. ment at the Sint Franciscus Gasthuis in Rotterdam for two years (head: A.P. Rietveld), as part of

18. her cardiology training. Afterwards she will work one year at the cardiology department of the

19. Albert Schweitzer Ziekenhuis in Dordrecht (head: Dr. M.J. Kofflard). Thereafter the cardiology

20. training will be continued at the Erasmus MC Thoraxcenter (head: Prof.dr. F. Zijlstra).

21.

22.

23.

24.

25.

26.

27.

28.

29.

30.

31.

32.

33.

34.

35.

36.

37.

38.

39.

1. DANKWOORD

2.

3. The secret of getting things done is to act! (Dante Alighieri)

4.

5. Bovenstaande uitspraak is wellicht een goede typering voor het promotietraject in algemene
6. zin; natuurlijk zijn er verscheidene mensen die de promovendus bijstaan, inspireren, uitdagen
7. en nieuwe inzichten verschaffen. Graag wil ik hierbij iedereen danken die een bijdrage heeft
8. geleverd aan de succesvolle totstandkoming van mijn proefschrift, waaronder alle patiënten
9. met aangeboren hartafwijkingen die hebben deelgenomen aan het onderzoek. De afronding
10. van dit promotietraject zal hopelijk het begin zijn van een mooie wetenschappelijke carrière.

11. In de eerste plaats gaat mijn dank uit naar mijn co-promotor, dr. F.J. Meijboom. Folkert,
12. wat een project en wat een bijzondere periode was dit! Jij vertrok uit het Erasmus MC toen
13. ik er begon. Het onderzoek maakte zijn dieptepunt door toen ik ermee startte, maar met de
14. nodige inspanningen mag het resultaat er nu echt zijn. Jij typeerde het omslagpunt in het
15. onderzoekstraject aan de hand van het 'Tipping point' beschreven door Malcolm Gladwell:
16. hoe kleine dingen een groot verschil kunnen maken. Vanaf een bepaald moment nam ons
17. onderzoeksproject een zeker vlucht en ontvingen we positieve commentaren van reviewers.
18. Ik dank je hartelijk voor het keer op keer kritisch bekijken van onze resultaten, je ideeën en je
19. bereidheid om alle manuscripten van gedetailleerd en helder commentaar te voorzien. Verder
20. ben ik je ook bijzonder dankbaar voor alle keren dat je mij de kans gegeven hebt om presenta-
21. ties te houden op congressen en symposia waardoor ik me verder heb kunnen bekwamen in
22. het presenteren en een leuk netwerk heb kunnen opbouwen.

23. Prof.dr. J.W. Roos-Hesselink, Jolien, tijdens één van onze gesprekken liet je me weten nooit
24. spijt gehad te hebben van dingen die je gedaan had. Het waren de dingen die je niet gedaan
25. had waar je achteraf wel eens spijt van hebt gehad. Ik geloof dat ik nu hetzelfde kan zeggen
26. aangaande dit onderzoek. Ik ben heel blij dat ik dit traject ingegaan ben. Niet alleen heb ik veel
27. van je kunnen leren op het gebied van aangeboren hartafwijkingen of het onderhouden van
28. een netwerk, maar ook heb je mij vakkundig mijn eerste rode piste afgeholpen! Dank voor je
29. motiverende gesprekken, het delen van je enthousiasme voor het werk en de fijne omgang.

30. Prof.dr. W.A. Helbing, Wim, hartelijk dank voor het medemogelijk maken van dit onderzoek-
31. sproject. Het voelt alsof ik in je voetsporen getreden ben: vijftien jaar geleden onderzocht jij
32. het gebruik van tweedimensionale echocardiografie voor de beoordeling van rechterven-
33. trikelkarakteristieken. In tegenstelling tot tweedimensionale echocardiografie, bleek juist
34. cardiale MRI, destijds een heel nieuwe techniek, een geschikte beeldvormingstechniek voor
35. rechterventrikelbeoordeling. Ik hoop dat je het idee met mij deelt dat de driedimensionale
36. echocardiografische benadering van toegevoegde waarde is voor de afbeelding van die inter-
37. essante rechterhartkamers.

38. Graag wil ik prof.dr. M.L. Simoons, prof.dr. L. Mertens en prof.dr.ir. A.F.W. van der Steen har-
39. telijk danken voor het plaatsnemen in de leescommissie en voor de kritische beoordeling van

mijn proefschrift. Professor Simoons, ik ben heel content met mijn keuze voor het Erasmus 1.
MC. Als co-assistent uit Amsterdam mocht ik bij u solliciteren waarbij u mij vragen stelde over 2.
het syndroom van Eisenmenger, vanwege mijn interesse voor de congenitale cardiologie. 3.
In mijn opinie vormt het Thoraxcentrum waaraan u zoveel jaren leiding hebt gegeven, een 4.
ontzettend uitdagende, stimulerende en faciliterende werkomgeving. Professor Mertens, ik 5.
vind het een eer dat u mij zult opponeren. Uw kennis over de echocardiografische benadering 6.
van de rechterventrikel is veelomvattend zoals blijkt uit de voordrachten die u de afgelopen 7.
jaren op verscheidene congressen hebt gegeven en die ik bij heb kunnen wonen. Onze 8.
onderzoeksgebieden, deformation imaging en driedimensionale echocardiografie, zullen zich 9.
wellicht binnen afzienbare tijd verenigen in driedimensionale speckle tracking. Professor Van 10.
der Steen, het is bijzonder dat iemand een professor in eerste instantie doet denken aan een 11.
stripfiguur. In ons geval bleek dat zo te zijn! Desalniettemin heb ik met plezier samengewerkt 12.
met verscheidene medewerkers van de Biomedial Engineering afdeling van wie ik veel heb 13.
mogen leren. 14.

Prof.dr. A.J. Bogers, dr. F.J. ten Cate en dr. A.P. van Dijk, vriendelijk bedankt voor het plaatsne- 15.
men in de grote leescommissie. Dr. Ten Cate, dank voor uw onaflatende belangstelling voor 16.
mijn onderzoek en het enthousiasme als ik opnieuw een prijs gewonnen had 'voor de echo 17.
afdeling'. Ik ben heel blij dat ik onder uw leiding ben begonnen aan de klinische opleiding tot 18.
cardioloog. Dr. Van Dijk, Arie, hartelijk dank voor de samenwerking aangaande het gebruik van 19.
echo contrast voor visualisatie van de rechterventrikel. Ik denk dat er een helder manuscript uit 20.
voortgekomen is. 21.

Jackie McGhie, zonder jouw bijzondere expertise, volhardendheid, Schotse optimisme en 23.
humor zouden we die bijzondere rechterventrikels nooit zo mooi in beeld gekregen hebben. Ik 24.
heb ontzettend plezierig met je samengewerkt: in eerste instantie was het ploeteren om tot de 25.
juiste wijze van opname en analyse te komen, maar met wat trial and error zijn we nu experts 26.
op het gebied van driedimensionale echocardiografie en rechterventrikels. We hebben onze 27.
expertise intussen met velen mogen delen in allerhande hands-on sessies op verscheidene 28.
congressen. Veel dank voor je betrokkenheid en ik stel voor dat we regelmatig fijn rode wijn 29.
gaan drinken op een Amsterdams (of Delfts, Rotterdams, ..) terras. 30.

Dr. M.L. Geleijnse, Marcel, dank voor de kritische evaluatie van mijn manuscripten. Het is wel 31.
aardig om te beseffen dat onze voorkeur aangaande hartkamers en politiek net gekruist is. Het 32.
is je ongetwijfeld bekend wat men zegt over jeugdigheid en links stemmen en de move naar 33.
rechts bij het ouder worden: misschien is er hoop! 34.

Wim Vletter, dank voor je acquisities op de vrijdagmiddagen in Jackie haar afwezigheid. Ik 35.
glimlach als ik bedenk dat je er een sport van maakte om die lastige pulmonalisklep in beeld 36.
te krijgen. Je hoopte hiermee indruk te maken op Jackie en zodoende uit te komen onder je 37.
wekelijkse kook- en/of stofzuigbeurten! Ellen Wiegers, heel fijn dat je bereid bent geweest 38.
om je de driedimensionale echocardiografische benadering van de rechterventrikel eigen te 39.

1. maken. Het heeft geleid tot een mooie publicatie. Ik verwacht dat je je met veel enthousiasme
2. zal mengen in de wetenschappelijke achtergronden van de echocardiografie. Willeke van der
3. Bent, zonder jouw bemoedigende woorden, lekkere muffins, humor en gezelligheid was mijn
4. promotietijd een stuk minder aangenaam geweest. Met name bij aanvang van het project heb
5. je me stevig bij de arm genomen en geweest waar ik zo ongeveer uit moest komen. Ik denk
6. dat het heel aardig gelukt is en dank je voor je inspanningen met betrekking tot de laatste
7. loodjes. René Frowijn, ietwat angstig kijk ik uit naar je serie boeken over de promovendi in
8. kamer Ba-302 door de jaren heen! Dank voor je onuitputtelijke geduld als ik weer eens tachtig
9. keer te vaak geklikt had of vieze vingers op het computerscherm maakte zonder dat het een
10. touchscreen was. Intussen heb je me geleerd hoe ik figuren omzet van Powerpoint, naar PDF,
11. naar Photoshop en weer terug, dus dat zal jou wat ontlasten. Kitty, Celeste en Tineke, fijn dat
12. ik altijd welkom was op jullie zonnige kamer en zo nu en dan eens fijn bij kon kletsen. Anja,
13. Debbie, Ellen, Linda, Lourus en Marianne, dank dat ik vaak eventjes snel voor mocht gaan om
14. kort een driedimensionaal echo te maken. Ik denk dat het nu aan jullie is: na al het onderzoek
15. naar het gebruik van driedimensionale echocardiografie in het Thoraxcentrum, moeten we
16. natuurlijk ook de eerste zijn die deze onderzoeksresultaten routinematig implementeren in de
17. dagelijkse, klinische realiteit. Ik heb er vertrouwen in dat dit bij jullie in goede handen zal zijn.
- 18.
19. Prof.dr. E. Boersma, Eric, hartelijk dank voor het meedenken bij moeilijk te duiden resultaten,
20. het kiezen van de juiste statistische tests bij bepaalde onderzoeksvragen en je heldere input
21. op mijn manuscripten.
22. Dr. J.G. Bosch, dr. K.Y.E. Leung en Gerard van Burken, Hans, Esther en Gerard, heel hartelijk
23. dank voor de plezierige samenwerking. Ik blijf het een zeer sterke kwaliteit van het Thoraxcen-
24. trum vinden dat er zulke korte lijnen bestaan tussen de klinische cardiologie en ingenieurs.
25. Doordat mijn achtergrond van die van jullie verschilt, heb ik veel mogen leren.
26. Graag wil ik de afdeling Radiologie hartelijk danken voor de gastvrije ontvangst bij het
27. vervaardigen van MRI scans. In het bijzonder wil ik dr. A. Moelker bedanken, Adriaan, fijn dat je
28. je inzichten aangaande MRI scans van de rechterventrikel hebt gedeeld en de supervisie van de
29. MRI scans bij de gezonde vrijwilligers op je wilde nemen. Ik verwacht dat de analysesoftware
30. voor kwantificatie van ventrikelvolumina op basis van MRI ook spoedig meer driedimensionaal
31. van aard zal zijn en daarmee sneller en eenvoudiger zal worden.
32. Lucia Jewbali en dr. L. M. van den Toorn wil ik danken voor hun samenwerking aangaande de
33. patiënten met pulmonale hypertensie. Ik denk dat jullie streven naar snelle en gestructureerde
34. diagnostiek bij patiënten met pulmonale hypertensie van groot belang is voor het welbevinden
35. van patiënten en een voorbeeld vormt van de moderne geneeskunde.
36. De kindercardiologen wil ik danken voor hun interesse in mijn onderzoek. Ik hoop van harte
37. dat driedimensionale echocardiografie een plaats zal vinden binnen de dagelijkse routine van
38. jullie afdeling.
- 39.

Dr. O.I.I. Soliman, Osama, during almost my complete PhD project you have been on my right- 1.
hand side. We shared not only ideas on ventricular quantification using three-dimensional 2.
echocardiography, but more importantly, we discussed life. Even though you insulted the right 3.
ventricle I worked on by calling it the wrong ventricle, that made you laugh all the time, in my 4.
new kitchen I will finally teach you how to cook penne all'arrabbiata. Dr. J.A. Schaar, Johannes, 5.
als een van mijn eerste kamergenoten heb ik, vaak met verbazing, genoten van al je levenswi- 6.
jsheden, enorme algemene kennis en scherpheid wat betreft onderzoek. Laura van Vark, wat 7.
hebben we een ontzettend gezellige, relaxte, goede tijd gehad in Ba-302. Ik vind het best heel 8.
bijzonder dat we eigenlijk vanaf onze start in het Erasmus MC fijn contact hebben en hoop dat 9.
dit zo blijft. Floris Kauer, van die tijd in Ba-302 maakte jij natuurlijk ook deel uit: er zullen talloze 10.
anekdotes blijven bestaan! Zeker de laatste maanden van mijn onderzoek, en daarmee ook 11.
de laatste maanden van jouw versnelde onderzoeksperiode, hebben we vooral hard gewerkt 12.
en ik hoop dat de resultaten daarvan zich snel voor je zullen openbaren in de vorm van mooie 13.
publicaties. Lotte de Groot, wat een energie heb jij vanaf het begin gestoken in het opzetten 14.
en includeren van patiënten voor je onderzoeksproject Hiervoor heb je chirurgen met de neus 15.
dezelfde kant op moeten krijgen, secretaresses moeten motiveren, patiënten bereid moeten 16.
vinden, en, niet in de laatste plaats, je co-promotor op het juiste spoor weten te krijgen. Ik ben 17.
er zeker van dat dit zal resulteren in iets moois. 18.

Dr E. Moltzer, Els, glansrijk ben je mij een aantal maanden geleden voorgegaan. Ik heb 19.
genoten van onze cuppu's samen en hoop dat we elkaar zo nu en dan tegenkomen om terug 20.
te kijken op onze bewogen promotietrajecten. Saskia Luijnenburg en Tirza Springeling, in de 21.
eerste plaats dank voor jullie hulp bij het includeren en scannen van de gezonde vrijwilligers. 22.
Hoewel jullie misschien nog niet helemaal overtuigd zijn van de superioriteit van echocardio- 23.
grafie ten opzichte van MRI (!), denk ik dat we heel plezierig hebben samengewerkt. De etentjes 24.
met elkaar moeten we in stand houden. Natuurlijk dank ik alle andere arts-onderzoekers van 25.
de Cardiologie evenals de arts-assistenten voor de fijne samenwerking en de onvergetelijk 26.
skiweekenden die het werkplezier zeker vergroot hebben. Dank aan de congenitale dokters 27.
en poli dokters voor de fijne werksfeer. Dank aan allen die als gezonde vrijwilligers hebben 28.
deelgenomen aan mijn onderzoek. 29.

Giske Biesbroek en Nynke Teeninga, wat fijn dat jullie mij tijdens mijn verdediging bij zullen 31.
staan! Gis, onze vriendschap bestaat al zo'n vijftien jaar en lijkt alle verhuizingen en veranderin- 32.
gen van werk vrijwel moeiteloos te doorstaan. Ik hoop dat er nu weer wat lucht komt en we 33.
elkaar vaker kunnen zien. Ik ben ontzettend benieuwd naar het verloop van jouw promotietra- 34.
ject en hoop dat we vaker samen reisjes kunnen plannen als één van ons een congres heeft! Nijn, 35.
sinds de introductieweek van geneeskunde hebben we elkaar in het vizier en in verscheidene 36.
theatervoorstellingen hebben we samen op de planken gestaan. Ik heb grote bewondering 37.
voor je doorzettingsvermogen om een lastig promotietraject tot een goed einde te brengen. 38.
Ik ben ervan overtuigd dat je er in zal slagen en hoop dat de weg naar kindergeneeskunde 39.

1. daarmee gelegd is. Verder hoop ik vooral op gezelligheid, theaters en terrasjes samen,
2. het werk.
3. Vera en Ties, wat een ontzettend warm welkom hebben jullie mij gegeven! Dank voor jullie
4. steun de afgelopen tijd, jullie interesse in mijn onderzoek en de onmisbare hulp bij het klussen
5. in ons nieuwe, mooie huis. Voorlopig zullen er even geen boekjes meer verschijnen van Bas' of
6. mijn hand, maar dat zal het aantal etentjes bij ons thuis en onze vrije tijd wellicht ten goede
7. komen.
8. Oop en Oom, het boek is nu eindelijk af! Ik heb ontzettend veel bewondering voor jullie
9. kracht en doorzettingsvermogen in de afgelopen periode. Nu vooruit met hopelijk nog heel
10. wat bijzondere momenten samen in het verschiep. Opa en oma, ik hoop van harte dat jullie er
11. de vijftiende bij kunnen zijn.
12. Lennart, leukerd, wat een heerlijke broer ben je! Ik kan ontzettend met je lachen en de
13. afgelopen periode heb ik veel aan je nuchtere kijk op het leven en je brede schouder gehad. Ik
14. ben trots op hoe je in het leven staat! Het is goed om te zien hoe je je weg binnen de fysiothera-
15. pie vindt en die master zal zeker van toegevoegde waarde zijn. Ik wens Es en jou heel veel geluk
16. en mooie momenten toe in jullie appartement in Haarlem waar ik lekker vaak langs zal komen,
17. zodat we naar het filmhuis en Fred kunnen.
18. Gijs en Cynthia, lieve pap en mam, wat een ongelooflijk jaar hebben we achter de rug!
19. Gelukkig bleek al snel dat we elkaar ook onder dergelijke, heftige omstandigheden heel nabij
20. konden zijn. De liefde die jullie voor elkaar voelen en waarin ik ben grootgebracht, maakt dat
21. ik me sterk voel. Dank voor jullie onuitputtelijke interesse en steun voor mijn studie, promoti-
22. etraject en al het andere in het leven. Ik heb mij altijd gestimuleerd gevoeld om het beste te
23. bereiken. Nu hoop ik dat we nog veel jaren van elkaar zullen genieten, mooie reisjes kunnen
24. maken en vooral ook de eens zo 'gewone' momenten intens met elkaar mogen beleven.
25. Sebas, liefste, dat geluk niet afhankelijk is van dingen buiten ons, maar van de manier waarop
26. wij de dingen zien, hebben we de afgelopen tijd ervaren. Ons prille samenzijn kreeg vorig jaar
27. onmiddellijk een vuurdoop, maar zoals jij eerder schreef, bestaat er tussen ons een diepe band
28. en unieke liefde. Jouw intelligentie, humor en optimisme maken elke dag bijzonder. Ik ben
29. ontzettend gelukkig dat we samen zoiets moois hebben. Onze beide promotietrajecten zijn
30. hierbij afgerond, en daarmee verdwijnt de directe aanleiding tot al dit moois, maar laten we
31. deze liefde een levenlang leven. Nu ons huis zover klaar is, mijn moeder dapper opkrabbelt, en
32. dit boek compleet is, moeten we wel op zoek naar een hobby: heb je een voorstel?!
- 33.
- 34.
- 35.
- 36.
- 37.
- 38.
- 39.

**ADDITIONAL FINANCIAL SUPPORT FOR THIS THESIS
WAS GENEROUSLY PROVIDED BY:**

Actelion Pharmaceuticals Nederland BV

AstraZeneca

Cardialysis

Erasmus University Rotterdam

Merck Sharp & Dohme B.V.

Philips Nederland B.V. / Healthcare

Siemens AG Healthcare Sector

TomTec Imaging Systems GmbH